

Function and Evolution of highly conserved head genes in the red flour beetle *Tribolium castaneum*

Dissertation submitted in partial fulfillment of the requirements for the degree of
“doctor rerum naturalium (Dr. rer. nat.)”
in the GGNB program “Molecular Biology of Development and Interaction between
Organisms”
of the Georg-August-University Göttingen

from

Nico Posnien

Heiligenstadt,
Germany

Göttingen, 2009

First Referee / Advisor: Prof. Dr. Gregor Bucher (University)
Second Referee: Prof. Dr. Andreas Wodarz (University)
Third Referee: Prof. Dr. Tomas Pieler (University)

Date of submission of the Dissertation: June 30th, 2009

Herewith I declare, that I prepared the Dissertation

"Function and Evolution of highly conserved head genes in the red flour beetle *Tribolium castaneum*"

on my own and with no other sources and aids than quoted.

Nico Posnien

Göttingen, June 30th, 2009

**Für
Anke & Mara**

Danksagung

An erster Stelle danke ich Herrn Prof. Dr. Gregor Bucher für die hervorragende Betreuung der Doktorarbeit! Ich danke ihm für die wissenschaftlichen Hilfestellungen, die die Arbeit stets vorangebracht und fokussiert haben. Im Speziellen möchte ich mich für das Vertrauen uneingeschränkt selbstständig arbeiten zu dürfen bedanken. Außerdem bedanke ich mich für die Möglichkeit an zahlreichen Tagungen teilzunehmen, bei denen ich meine Daten präsentieren, neue Impulse sammeln und Kollaborationen initiieren konnte. Und nicht zuletzt bedanke ich mich für unzählige Gespräche und die konstante Unterstützung abseits der Doktorarbeit!

Ich bedanke mich bei Herrn Prof. Dr. Ernst A. Wimmer für viele kritische Anmerkungen und Diskussionen im Bezug auf meine Arbeit. Desweiteren danke ich ihm für die Möglichkeiten an den Aktivitäten (Tagungen, Methodenkurse) des Marie Curie Research Training Networks (ZOONET) teilnehmen zu können.

Herrn Prof. Dr. Andreas Wodarz und Herrn Prof. Dr. Tomas Pieler danke ich für die fachlich unterstützende und unkomplizierte Aktivität in meinem Thesis Committee.

Ein besonderer Dank gilt Daniela Grossmann und Anna Gilles für die kritische Durchsicht der Arbeit.

Herzlichen Dank den Mitarbeitern und Mitarbeiterinnen der Abteilung Entwicklungsbiologie für die angenehme Arbeitsatmosphäre, die stete Hilfsbereitschaft und die vielen fachlichen und privaten Diskussionen und Gespräche. Ein Spezieller Dank geht dabei an das gesamte Labor 3: Anna Gilles, Daniela Grossmann, Hendrikje Hein, Katrin Kanbach, Sebastian Kittelmann, Nikolaus Koniszewski, Elke Küster, Inga Schild, Johannes Schinko (Danke für die unzähligen Laufstunden und Gespräche!) und Monique Weidner.

Der Neurogenese Gruppe der Abteilung Entwicklungsbiochemie, insbesondere Frank Nieber und Dr. Kristine Henningfeld, danke ich für die stete Unterstützung bei der Arbeit mit *Xenopus laevis*.

Außerdem bedanke ich mich bei meinen Eltern, meinem Bruder und meinen Freunden für ihre Unterstützung und ihre Anteilnahme an meiner Arbeit.

Und die wichtigsten Personen zum Schluss: Ich danke meiner (bald) Frau Anke und meiner Tochter Mara für die wundervolle Zeit und Unterstützung fernab der Arbeit! Eine bessere kleine Familie kann man sich nicht wünschen!

Table of content

1	Summary	9
2	Introduction	11
2.1	Evo-Devo and the search for the genetic core of urbilaterian development	11
2.2	Similarities of early establishment of the central nervous system in bilaterian animals	12
2.2.1	Establishment of neural tissue - the dorsal-ventral axis of the embryo	12
2.2.2	The conserved columnar genes further subdivide the dorsal-ventral axis of the neuroectoderm	12
2.2.3	The assignment of neural identity to cells in the neurogenic ectoderm is based on a similar molecular basis in Bilaterians	13
2.3	Patterning of the anterior-posterior axis in bilaterian animals	14
2.3.1	Patterning of the vertebrate neural plate and its implication on cranial placode and neural crest development	14
2.3.2	Patterning of the anterior region of bilaterian animals is governed by some highly conserved genes	17
2.3.3	The identity of tissue along the anterior-posterior axis is governed by the highly conserved Hox-genes in the posterior region	18
2.3.4	The involvement of Wnt-signaling in anterior-posterior axis formation seems to be conserved among Bilaterians	18
2.4	The internalization of the central nervous system differs in vertebrates and insects	19
2.5	Head development in insects	20
2.5.1	Head patterning in the fruit fly <i>Drosophila melanogaster</i>	20
2.5.2	Some unsolved problems concerning insect head development	22
2.6	The red flour beetle <i>Tribolium castaneum</i> as insect model for head development	23
2.7	Aims	25
3	Materials and Methods	26
3.1	Animals	26
3.2	Identification and cloning of candidate genes in <i>Tribolium</i>	26
3.3	Phylogenetic analysis	26
3.4	Fixation of embryos	27
3.5	Whole mount in situ hybridization	27
3.6	Knock down of gene function by RNA interference (RNAi)	28
3.6.1	Control experiments for RNAi procedure	29
3.6.2	Off-Target effects in RNAi experiments	29
3.7	Cuticle preparations	30
3.8	Documentation of cuticles and stained embryos	30

3.9	Interaction analysis in <i>Xenopus laevis</i>	30
4	Results	32
4.1	Analysis of highly conserved anterior patterning genes	32
4.1.1	Identification of the <i>Tribolium</i> orthologs	32
4.1.2	Expression of candidate genes in <i>Tribolium castaneum</i>	32
4.1.2.1	Genes with exclusive expression in the head anlagen	33
4.1.2.2	Genes with additional segmental expression - segment polarity genes	37
4.1.2.3	Other genes with additional segmental expression	40
4.1.2.4	Genes involved in vertebrate cranial placode development	44
4.1.3	A virtual expression map for early head patterning	46
4.1.4	Function of the candidate genes in epidermal development	46
4.1.4.1	Genes whose knock down leads to severe head patterning defects	47
4.1.4.2	Genes whose knock down leads to minor defects in the dorsal bristle pattern	51
4.1.5	Regulatory network of head patterning	52
4.1.5.1	Tc-optix/six3 represses the expression of Tc-wg/wnt1, Tc-otd1/otx and Tc-ey/pax6	53
4.1.5.2	Tc-tll/tlx is necessary for the establishment of specific cells in the anterior head lobes	57
4.1.5.3	Tc-eya, Tc-so/six1 and Tc-six4 form a regulatory network to establish the anterior most rim of the developing embryo	60
4.1.6	Analysis of six3 interactions in <i>Xenopus laevis</i>	63
4.2	Wnt-signaling in anterior patterning of <i>Tribolium castaneum</i>	65
4.2.1	<i>Tc-axin</i> is involved in anterior-posterior axis formation	65
4.2.2	The knock down of <i>Tc-axin</i> results in posteriorized embryos	69
4.3	Development of the intercalary segment	70
4.3.1	Delayed specification of the intercalary parasegment boundary	71
4.3.2	<i>Tc-labial</i> function is required for the formation of lateral parts of the head cuticle	73
4.3.3	Knock down of <i>Tc-lab</i> leads to loss of the intercalary segment	74
5	Discussion	77
5.1	Analysis of highly conserved anterior patterning genes	77
5.1.1	Subdivision of the anterior head and developmental units	77
5.1.1.1	Early subdivision of the anterior head	77
5.1.1.2	Identification of a signaling center in the <i>Tribolium</i> head	79
5.1.1.3	Genes involved in vertebrate cranial placode development pattern the anterior rim region of the <i>Tribolium</i> head	80
5.1.2	The regulatory network that governs the patterning of the <i>Tribolium</i> head	81
5.1.2.1	The hierarchy within the regulatory network	81
5.1.3	Testing hypotheses of regulatory interactions	84
5.1.3.1	Tc-optix/six3 establishes anterior-median tissue by repression of laterally expressed genes	84
5.1.3.2	Involvement of Tc-tll/tlx in the activation of Tc-rx and Tc-optix/six3	85

5.1.3.3	The potential placodal region is patterned by a regulatory network comprising Tc-eya, Tc-so/six1 and Tc-six4	85
5.1.3.4	Are the observed six3 interactions conserved in vertebrates?	86
5.1.4	Conservation of anterior patterning in bilaterian animals	88
5.1.4.1	The insect ocular/preocular region corresponds to the fore-and midbrain region of the vertebrate neural plate	90
5.1.4.2	Some late expression domains of <i>Tribolium</i> genes possess correlates in vertebrates	93
5.1.4.3	The insect head boundary (IHB) and the vertebrate mid-/hindbrain boundary (MHB) probably evolved from an anterior signaling center of the ancestor of Bilaterians	95
5.1.4.4	The <i>Tribolium</i> orthologs of some important neural plate patterning genes are not involved in the patterning of comparable regions in the beetle	98
5.1.4.5	Comparison of neural plate associated genes	99
5.1.4.6	Genes which are expressed in the prechordal plate of vertebrates are not conserved in their early function	104
5.2	Wnt-signaling in anterior patterning of <i>Tribolium castaneum</i>	105
5.2.1	Canonical Wnt-signaling is involved in an ancient mode of anterior-posterior patterning	105
5.3	Development of the intercalary segment	108
5.3.1	<i>Tc-labial</i> knock-down leads to loss of the intercalary segment rather than a transformation	108
5.3.2	Different patterning mechanism in the intercalary segment	109
5.3.3	The intercalary segment is required for lateral parts of the head	110
5.4	Outlook	110
6	References	112
7	Appendix	131
7.1	Supplementary Tables	131
7.2	Supplementary Figures (phylogenetic trees).	136
7.3	Abbreviations	141
8	Curriculum vitae	142

1 Summary

The anterior-posterior axis of all bilaterian animals is subdivided into a posterior region marked by the expression of highly conserved Hox-cluster genes and an anterior region free of them. Some highly conserved genes that are expressed in the anterior head are involved in anterior patterning of both vertebrates and insects. This suggests that basic principles of head development are shared throughout bilateria. However, a comprehensive comparison of genes involved in anterior patterning of insects and vertebrates is missing so far.

In order to identify more candidates of the highly conserved core of anterior bilaterian patterning genes, I systematically analyzed the expression and function of orthologs of vertebrate neural plate patterning genes in the red flour beetle *Tribolium castaneum*. Based on these results I hypothesized parts of an interaction network that might govern head development in *Tribolium*. Subsequently, I selected some of the proposed interactions and tested them directly, and could confirm most of them. Some of the interactions found in *Tribolium* were then tested in *Xenopus laevis* as a vertebrate model in order to gain insights into the conservation of the network. I find that the potential of *six3* to activate *pax6* and to repress *wnt1* might be conserved. The comparison of the expression patterns in *Tribolium* vertebrates reveals that the ocular/preocular region of the embryonic insect head is highly similar to the fore-/midbrain region of vertebrates. Furthermore, this comparison suggests that the last common ancestor of vertebrates and insects possessed an important signalling center in the anterior region.

The establishment of the anterior-posterior axis in vertebrates involves the action of canonical Wnt-signaling. Recent results from different arthropods suggest a conserved role of Wnt-signaling in the formation of posterior structures among Bilaterians.

To further substantiate the involvement of canonical Wnt-signaling in anterior-posterior axis formation of *Tribolium* I ectopically activated Wnt-signaling in the anterior head region by *Tc-axin* RNAi. These results show that ectopic early anterior Wnt-signaling leads to the posteriorization of the embryos, indicating that Wnt-signaling is indeed essential for proper anterior-posterior axis formation in *Tribolium*.

Additionally, to date some aspects of insect head development like the contribution of the intercalary segment to the head capsule remained enigmatic. Therefore, I analyzed the function of the intercalary marker *labial/Hox1* in *Tribolium*. The data show that loss of *Tc-labial/Hox1* leads to loss of the intercalary segment and that this segment gives rise to lateral parts of head cuticle.

2 Introduction

2.1 Evo-Devo and the search for the genetic core of urbilaterian development

Most animals on earth belong to the group of Bilateria, which are characterized by a bilateral symmetric body plan. Bilateria show an incredibly large variety of forms. The bilateral symmetric animals are divided into two main groups: the Protostomes comprising Nematodes, Arthropods, Annelids and Mollusks and the Deuterostomes comprising Echinoderms, Hemichordates and Chordates (Adoutte et al., 2000; Aguinaldo et al., 1997; Peterson and Eernisse, 2001). Most obviously, the Bilateria possess an anterior-posterior axis with an anterior region that is clearly distinguishable from the rest of the body. It contains the mouth, the eyes and the brain and in some taxa it is separated from the trunk by a neck region. The anterior region is often referred to as head. Although this term does not describe strictly homologous parts, I want to use it synonymously for the anterior region for the sake of simplicity. The head region comprises the major command center of the animal, where sensory input is processed in order to allow appropriate response to the environment. In order to achieve this complex task, the ectodermally derived nervous system is especially centralized in an anteriorly located brain. The more posterior part of the body is involved in additional functions like locomotion and reproduction (Ax, 1999; Westheide and Rieger, 1996).

Although Bilateria possess highly diverse morphologies, scientists in the research field which combines Evolution and Development (Evo-Devo) showed in the last 20 years that both the complement and sequences of many developmental genes are highly conserved. These findings in distant taxa indicate that the last common ancestor of the Bilateria, the so called Urbilateria, already possessed a complex set of developmental genes (“toolkit”) similar to recent representatives (e.g. Carroll, 2005; Carroll et al., 2005; De Robertis, 2008; Gilbert et al., 1996). One main task for Evo-Devo research is to identify genes with conserved function in order to gain insights into the nature of the regulatory gene network of the Urbilateria and thereby understand how changes in this “toolkit” lead to the observed diversity.

2.2 Similarities of early establishment of the central nervous system in bilaterian animals

The Evo-Devo approach revealed many similarities of early central nervous system development in bilaterian animals. Namely, the molecular basis for the distinction of neural and non-neural ectoderm is very similar among so far analyzed Bilaterians. Furthermore, the subdivision of the dorsal-ventral axis of the neural ectoderm is based on similar genes. Finally, conserved genes are involved in the establishment of neural identity within the neural ectoderm.

2.2.1 Establishment of neural tissue - the dorsal-ventral axis of the embryo

During early embryonic development of vertebrates and insects maternally provided factors are involved in the establishment of the dorsal-ventral axis of the embryo. As one consequence of these early events, the ectoderm becomes subdivided into a neurogenic and a non-neurogenic portion. The factors that are involved in this process are highly conserved from insects to vertebrates. The vertebrate *Bone morphogenic protein 4 (BMP4)* and its insect ortholog *decapentaplegic (dpp)* are required for non-neurogenic epidermal development of the ectoderm. Their function is antagonized by the action of *chordin* in vertebrates and *short gastrulation (sog)* in insects whose activity defines the neurogenic part of the ectoderm. However, due to an inversion of the dorsal-ventral axis in the chordate lineage, the neurogenic ectoderm of vertebrates is located on the dorsal side, whereas the central nervous system of non-chordates develops from the ventral region (for reviews see e.g. Arendt and Nubler-Jung, 1999; De Robertis et al., 2000; Urbach and Technau, 2008).

2.2.2 The conserved columnar genes further subdivide the dorsal-ventral axis of the neuroectoderm

Through the action of the so called columnar genes, the neuroectoderm of insects and vertebrates becomes further subdivided into three parallel, longitudinal domains on each side of the midline. Hence, neural precursor cells are specified within one of these three columns.

The ventral or medial column is marked by *ventral nerve cord defective (vnd)/nkx2.2*. The intermediate column is marked by the expression of *intermediate nerve cord defective (Richards et al.)/Gsh* and in the lateral column, *muscle segment homeodomain (msh)/Msx* is expressed (Buescher and Chia, 1997; Chu et al., 1998; Isshiki et al., 1997; Skeath, 1999; Weiss et al., 1998). Additionally, these genes have been shown to be expressed in conserved longitudinal domains in the red flour beetle *Tribolium castaneum* (Wheeler et al., 2003).

Although their early establishment is different from *Drosophila*, the vertebrate orthologs of the columnar genes are similarly involved in the dorsal-ventral patterning of the neural plate and subsequently within the neural tube (Arendt and Nubler-Jung, 1999; Cornell and Ohlen, 2000; Urbach and Technau, 2008; Wilson and Maden, 2005). Interestingly, it has been shown in the annelid *Platynereis dumerilii*, a lophotrochozoan protostome, that the dorsal-ventral axis of its ventral nerve cord is similarly patterned as in vertebrates and insects. Additionally, it has been shown that conserved neuron types develop from comparable regions along the dorsal-ventral axis (Denes et al., 2007), confirming a highly conserved principle of dorsal-ventral patterning in the nervous system.

2.2.3 The assignment of neural identity to cells in the neurogenic ectoderm is based on a similar molecular basis in Bilaterians

Another task of early neural patterning is similarly based on conserved mechanisms: the final separation of neuroectoderm from epidermal ectoderm.

The link between early dorsal-ventral axis specification, by which neural fate becomes determined, and the assignment of neural identity seems to be mediated by genes of the *sox*-family in *Drosophila* and vertebrates (Buescher et al., 2002; Mizuseki et al., 1998a; Mizuseki et al., 1998b; Sasai, 2001a; Sasai, 2001b).

In *Drosophila* the decision of what cell becomes a neuroblast is governed by the action of proneural *basic-helix-loop-helix (bHLH)* factors of the *achaete-scute (as-c)* complex that define a field of cells which have the potential to adopt a neural fate. By lateral inhibition by Delta/Notch signaling one cell is destined to become a neuroblast and to delaminate to undergo several asymmetric stem cell divisions (Campos-Ortega, 1995; Campos-Ortega, 1998; Dambly-Chaudiere and Vervoort, 1998; Technau et al., 2006; Wodarz and Huttner, 2003).

Similarly, vertebrate orthologs of *as-c* factors and components of the Delta/Notch pathway are expressed in the neural ectoderm. It has been shown that a well defined action of these factors is essential to regulate the balance between proliferation and differentiation (Ishibashi, 2004).

In summary, the early distinction of neural and non-neural ectoderm in so far analyzed Bilaterians is based on conserved genes and their interactions during dorsal-ventral axis formation. The dorsal-ventral axis of the neuroectoderm is patterned by the conserved columnar genes. Finally, also the establishment of neural identity is based on similar factors in vertebrates and insects. These findings suggest a monophyletic origin of bilaterian central nervous systems.

2.3 Patterning of the anterior-posterior axis in bilaterian animals

The central nervous systems of bilaterian animals are established by highly conserved signals. Also the early establishment of the anterior-posterior axis and the subsequent regional specification of the neural ectoderm seem to be based on conserved factors among Bilaterians.

2.3.1 Patterning of the vertebrate neural plate and its implication on cranial placode and neural crest development

As described above, the vertebrate neuroectoderm, the neural plate, requires the action of BMP4 antagonists in the dorsal ectoderm. These antagonists are released from the dorsal blastopore lip (De Robertis et al., 2000). In addition to dorsal-ventral axis formation, the dorsal blastopore lip is also involved in the patterning of the anterior-posterior axis within the neural plate.

This process is partly linked to the ingressing mesoderm during gastrulation. The first cells that pass the dorsal blastopore lip will later contribute to the so called pharyngeal mesendoderm or prechordal plate which underlies the anterior portion of the neural plate (e.g. Nieuwkoop, 1997; Ruiz i Altaba, 1993). One important gene that has been shown to promote these mesoderm movements is *gooseoid* (*gsc*). This gene is expressed in the early organizer and later marks the prechordal plate in so far analyzed vertebrates (Blum et al., 1992; Cho et al., 1991; Izpisua-Belmonte et al., 1993; Schulte-Merker et al., 1994; Stachel et al., 1993).

The prechordal plate secretes factors which inhibit Wnt-signals emitted from more posterior organizer derivatives. This antagonizing action results in a posterior to anterior gradient of Wnt-signals (Kiecker and Niehrs, 2001). The importance of posterior Wnt-signals has been shown by loss Wnt function, which results in posterior truncations (Galceran et al., 1999; Pinson et al., 2000; Takada et al., 1994). FGF factors were shown to provide the right condition for cells to respond to Wnt-signaling (Domingos et al., 2001). A retinoid acid (RA) gradient with highest concentration in the posterior region seems to be similarly involved in posterior specification of the neural plate (Cho and De Robertis, 1990; Dupe and Lumsden, 2001). Together, Wnt and RA signaling are required for pattern formation along the anterior-posterior axis in a concentration dependent manner. Among other genes, the activation of Hox-cluster genes depends on RA signals (Daftary and Taylor, 2006; Kessel, 1992; Kessel and Gruss, 1991).

However, the region anterior to the hindbrain lacks Hox-cluster gene expression (McGinnis and Krumlauf, 1992). The Wnt inhibitors from the prechordal plate provide a Wnt-signal-free surrounding in the anterior neural plate, which is further patterned by two important signaling centers, namely the zona limitans intrathalamica (zli) and the mid-/hindbrain boundary (MHB). This implies that patterning of the anterior region relies on different mechanisms and genes than posterior patterning.

The Wnt-signal-free anterior surrounding is necessary for the activation of anterior marker genes like *six3*, *otx2* and *bfl/foxg1* (Braun et al., 2003; Houart et al., 2002; Kiecker and Niehrs, 2001; McGrew et al., 1995; Niehrs, 1999). Contrary, higher Wnt-levels promote the activation of posterior neural plate markers like *irx3* (Braun et al., 2003). The interface between anterior *six3* and posterior *irx3* expression marks the boundary between the telencephalon (anterior forebrain) and the diencephalon (posterior forebrain). This boundary, the zona limitans intrathalamica, has been shown to possess signaling capabilities like the mid-/hindbrain boundary (see below) (Kiecker and Lumsden, 2004; Vieira et al., 2005).

The anterior hindbrain and the midbrain are mainly patterned by the action of an organizer region called istmic organizer or mid-/hindbrain boundary. It has been shown by several authors that the MHB possesses organizing properties, since a misplaced or absent MHB leads to severe patterning defects in adjacent tissues of the midbrain as well as in the hindbrain (Hidalgo-Sanchez et al., 2005; Wurst and Bally-Cuif, 2001). The MHB is defined by mutual repression of *otx2* and *gbx1/2* genes shortly after gastrulation. Subsequently, genes become active either exclusively in the mid- or hindbrain (*wnt1*, *fgf8*) or in domains overlapping the *otx2/gbx1/2* interface (*en1/2*, *pax2/5/8* and SP-factors). Together, these genes

are involved in a regulatory network that governs the development of adjacent brain regions (Griesel et al., 2006; Rhinn et al., 2005; Tallafuss et al., 2001; Wurst and Bally-Cuif, 2001). Another important function of the signals involved in neuroectoderm formation is the patterning of the neural plate associated tissue, the cranial placodes and neural crest. At the interface between the neural plate and the ventral epidermal ectoderm where high epidermal levels of BMP signals meet posterior neural Wnt and FGF signals, a special rim region is specified (Fig. 2.1). Depending on the environment, this rim region gives rise to either the neural crest in the posterior or the cranial placodes in the anterior region (Fig. 2.1) (Baker and Bronner-Fraser, 1997; Brugmann and Moody, 2005; Schlosser, 2006; Schlosser, 2008; Streit, 2007). The anterior rim ectoderm which gives rise to cranial placodes (the preplacodal ectoderm, PPE) is marked by genes of the *eyes absent* (*eya*) and *sine oculis homeobox* (*six1* and *six4*) family from early stages on (Schlosser and Ahrens, 2004). During further development the PPE becomes further subdivided and eventually the placodal cells delaminate from the ectoderm to form different cell types of sensory organs in the vertebrate head (Schlosser, 2006; Streit, 2004).

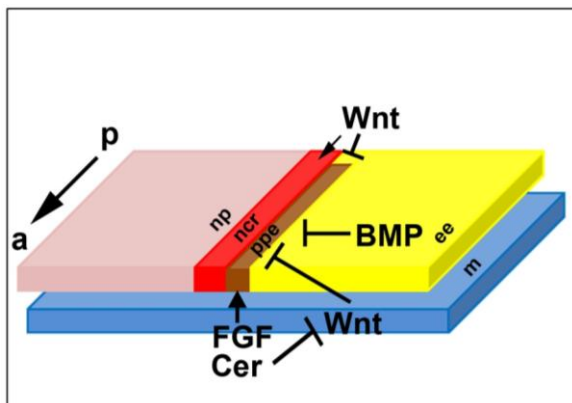


Fig. 2.1: Establishment of the preplacodal ectoderm (PPE).

The interface between the neural (np) and the epidermal ectoderm (ee) gives rise to neural crest tissue (ncr) and the preplacodal ectoderm (ppe). While posterior Wnt-signals in combination with epidermal BMP-signals promote the formation of neural crest tissue, Wnt-antagonists and FGF factors from the anterior mesoderm (m) promote the formation of the preplacodal ectoderm (PPE). The PPE gives rise to cranial sensory placodes. a-anterior, p-posterior (after Schlosser, 2008 and Streit, 2007)

In summary, the Wnt antagonists from the anterior non-neural regions are essential for the establishment of two signaling centers within the anterior neural ectoderm. These signaling centers themselves are involved in the anterior-posterior subdivision and subsequent specification of the anterior neural ectoderm. Also the specification of neural plate associated tissue, the cranial placodes and the neural crest, depends on the signals involved in dorsal-ventral and anterior-posterior axis patterning. More specifically, the anterior cranial placodes which develop from ectoderm adjacent to the neural plate depend on the anterior Wnt-signal-free surrounding.

2.3.2 Patterning of the anterior region of bilaterian animals is governed by some highly conserved genes

Experiments in mouse and *Drosophila* show, that *orthodenticle* (*otd/otx*) and *empty spiracles* (*ems/emx*) are essential for proper head and brain formation in these highly diverse organisms. More strikingly, *Drosophila otd* is partly able to rescue mouse *otx1* mutant phenotypes, indicating a deep conservation among Bilaterians (Fig. 2.2) (Acampora et al., 1998; Hirth and Reichert, 1999; Holland et al., 1992; Lichtneckert and Reichert, 2005). These findings suggest that the genes which are involved in early head patterning are similarly conserved as for example the Hox-genes in the posterior region (see below). This suggestion is substantiated by work on the Hemichordate *Saccoglossus kowalevskii*, a Deuterostome, in which the patterning of both the anterior-posterior and the dorsal-ventral axis is achieved by the same large set of genes as in higher Chordates, like fish, frogs, birds and mice. Moreover, these conserved genes are also expressed in comparable regions along the axes (Lowe, 2008; Lowe et al., 2006; Lowe et al., 2003). These data clearly indicate that the patterning of anterior structures is at least among Deuterostomes highly conserved.

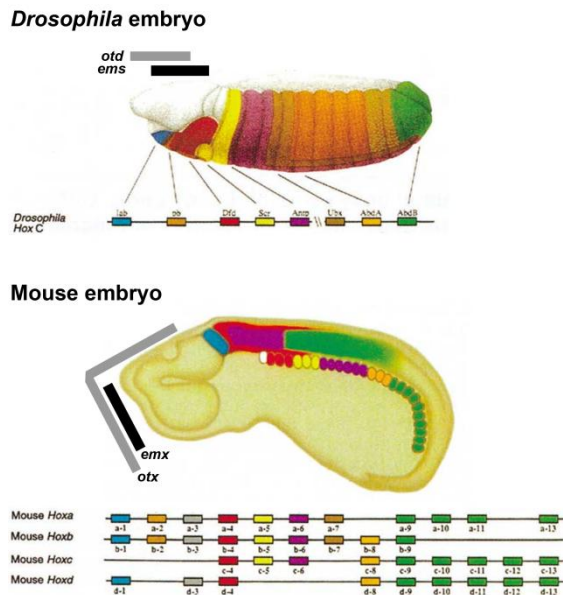


Fig. 2.2: Conserved anterior-posterior regions in insects and vertebrates.

The anterior to posterior expression of the Hox-cluster genes corresponds to their 3' to 5' organization within the chromosomal cluster. The genes of the Hox-cluster are expressed in specific regions along the anterior-posterior axis where they specify regional identity. The anterior region of *Drosophila* and mouse is free of genes of the Hox-cluster. Here some highly conserved genes like *otd/otx* and *ems/emx* are involved in regionalization.

Taken from (Carroll, 1995); *otd/otx* and *ems/emx* data extracted from (Holland et al., 1992)

Moreover, a growing number of publications show that also Protostomes and Deuterostomes are very similar based on some anterior patterning genes (e.g. Arendt et al., 2004; Tessmar-Raible et al., 2007; Urbach, 2007). However, a comprehensive comparison of genes involved in early anterior patterning is missing so far (see also chapter 2.5.1).

2.3.3 The identity of tissue along the anterior-posterior axis is governed by the highly conserved Hox-genes in the posterior region

The homeotic selector genes of the Hox-cluster (Hox-genes, Fig. 2.2) are present in all so far analyzed Bilaterians. They are involved in the specification of tissue identity along the anterior-posterior axis (Finnerty, 2003; Slack et al., 1993). Interestingly, the anterior-posterior order in which these genes are expressed is mimicked in the 3-prime to 5-prime order in which the genes are organized in a chromosomal cluster. This spatial collinearity is a common feature of Hox-genes in most Bilaterians (Favier and Dolle, 1997; Garcia-Fernandez, 2005; McGinnis and Krumlauf, 1992).

The most 3-prime located Hox gene *labial/Hox1* for example is also the most anterior expressed Hox gene in the fruit fly *Drosophila melanogaster* in which it is expressed in the intercalary segment (Diederich et al., 1989; Merrill et al., 1989). The same is true for other arthropods (Janssen and Damen, 2006). Also in vertebrates, *Hox1* is initially the anterior most expressed Hox-gene. It is expressed in the region of the rhombomeres 3/4 in the hindbrain (McNulty et al., 2005; Murphy and Hill, 1991; Sundin et al., 1990). Due to successive duplications and subsequent divergence of the entire Hox-cluster, vertebrates possess more than one paralog of a respective Hox gene (Prince and Pickett, 2002). Therefore it is necessary to abolish the action of all paralogs in order to analyze the function of a specific Hox gene in vertebrates. The loss of function of all three *Hox1/labial* genes in the frog *Xenopus laevis* results in the reduction of hindbrain and the loss of hindbrain associated neural crest derivatives (McNulty et al., 2005). The function of *Drosophila labial/Hox1*, however, is not that clear because loss of function results in head involution defects. Hence, it is difficult to distinguish between direct effects of loss of *Dm-labial/Hox1* function and secondary defects due to defective head involution (Diederich et al., 1989; Merrill et al., 1989).

2.3.4 The involvement of Wnt-signaling in anterior-posterior axis formation seems to be conserved among Bilaterians

Recent findings in a variety of protostomes started to shed light on the conservation of the role of Wnt-signaling in anterior-posterior axis formation. In the red flour beetle *Tribolium castaneum* and the spider *Achaearanea tepidariorum* it has been shown that loss of Wnt-signals results in posterior truncations (Bolognesi et al., 2008b; McGregor et al., 2008).

Furthermore, it has been shown in the cricket *Gryllus bimaculatus* that the expression of the posterior marker *caudal* depends on Wnt-signaling (Shinmyo et al., 2005). In planarians (Platyhelminthes), the regeneration of posterior structures depends on Wnt-signaling (Adell et al., 2009). These loss of function results indicate a conserved role of Wnt-signaling in posterior patterning (Martin and Kimelman, 2009). However, the effect of ectopic Wnt-signals in the anterior region of protostomes remains to be analyzed in different protostomes.

In conclusion, although the function of *labial/Hox1* in insects is still enigmatic, much is known about posterior patterning and the specification of tissue by the highly conserved Hox-genes. But so far no comprehensive comparison of genes involved in anterior patterning is available. Furthermore, loss of function experiments indicate that the involvement of Wnt-signaling in the formation of posterior structures could be conserved among Bilaterians. However, the effects of ectopic Wnt-signals in the anterior region of protostomes, have not been analysed.

2.4 The internalization of the central nervous system differs in vertebrates and insects

Although many early events in central nervous system development seem to be conserved among Bilaterians, the process of internalization of the neural ectoderm to form the ventral nerve cord in insects and the neural tube in vertebrates differs significantly.

The vertebrate neural plate is composed of a coherent sheet of neuroectodermal cells. Drastic morphological changes after gastrulation lead to the inward folding of the entire neural plate (neurulation). This process results in a neural tube which is covered by epidermal ectoderm and underlined by mesodermal derivatives of the organizer, the notochord (Schoenwolf and Smith, 1990).

In contrast, in insects the future neural and epidermal cells are located in one initially undistinguishable ectodermal cell layer. By the above described action of *achaete-scute* (*as-c*) factors and Delta/Notch signaling individual neural stem cells, the neuroblasts, are determined. The neuroblasts delaminate from the surface ectoderm to ingress into the embryo. Once the neuroblasts moved inside, they undergo several asymmetric cell divisions, by which they produce ganglion mother cells (GMC). The GMCs then divide once more to generate neurons and glia cells (Campos-Ortega, 1995; Technau et al., 2006; Wodarz and Huttner,

2003). Importantly, the former neighbors of the neuroblasts remain in the epithelium and later contribute to the epidermis that secretes the cuticle.

Hence, the vertebrate central nervous system develops from a coherent sheet of cells, whereas in insects, individual cells ingress to form the nervous system. This difference offers a great advantage for the analysis of conserved neural patterning genes. Therefore, the analysis of orthologs of vertebrate neural plate patterning genes in insects offers the opportunity to analyze neural and epidermal ectodermal patterning simultaneously, i.e. the easy to score cuticle defects will in many cases correlate to less accessible brain defects.

As an example, the anterior marker genes *otd/otx* and *ems/emx* are highly conserved with regard to their expression and function in vertebrates and insects. In vertebrates these two genes are expressed in the neural plate and solely involved in neural patterning. In *Drosophila* and *Tribolium*, both genes are expressed in the anterior embryonic head region, which is composed of both potential neural and epidermal ectodermal cells. Indeed, they affect both central nervous system and epidermal patterning (Acampora et al., 1998; Hirth and Reichert, 1999; Holland et al., 1992; Lichtneckert and Reichert, 2005; Schinko et al., 2008).

Since a comprehensive comparison of anterior patterning among Bilaterians is still missing, the analysis of vertebrate anterior patterning genes in an insect model will provide new insights into the degree of conservation of anterior patterning in bilaterian animals. Additionally, this approach can reveal new genes involved in anterior patterning in insects, which is actually an important task, because no comprehensive list of genes involved in head development of insects exists (see below).

2.5 Head development in insects

2.5.1 Head patterning in the fruit fly *Drosophila melanogaster*

The insect head is built by two major parts, each of which is formed by tissue derived from at least three embryonic segments. The posterior gnathal region (gnathocephalon) comprises three segments that bear the mouthparts, namely the labial (lb), maxillary (mx) and mandibular (md) segments (Fig. 2.3). The ganglia of these three segments are fused to form the suboesophageal ganglion of the brain (Dettner and Peters, 2003). The anterior pregnathal region (procephalon) is composed of the appendage-free intercalary segment (ic), the antennal (ant), the ocular segments (oc) and additional preantennal tissue (Fig. 2.3) (Rogers and

Kaufman, 1996; Rogers and Kaufman, 1997; Snodgrass, 1935). The intercalary ganglion represents the tritocerebrum, the antennal segment provides the deutocerebrum part and the neural cells of the preantennal region form the protocerebrum. Together these ganglia form the supraoesophageal ganglion of the brain (Dettner and Peters, 2003).

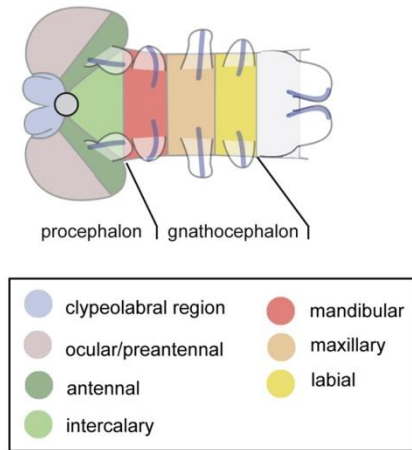


Fig. 2.3: Segmental organization of the embryonic insect head.

The embryonic insect head is composed of several segments. The gnathocephalon consists of three segments: the labial, the maxillary and the mandibular segment. The procephalon consists of two segments: the intercalary, the antennal segment. Anterior to the antennal segment an ocular/preantennal region exists. The median clypeolabral region comprises the insect upper lip (labrum) and the stomodeum.

(Taken from Posnien and Bucher, submitted)

In *Drosophila*, the patterning of the maxillary and labial segments occurs through the same segmentation cascade as in the trunk involving maternal morphogens, gap-, pair-rule and segment polarity genes (Ingham, 1988; Pankratz and Jackle, 1990; St Johnston and Nusslein-Volhard, 1992). The segment identity is specified by the action of homeotic selector genes of the Hox-cluster (Lawrence and Morata, 1994; Lewis, 1978; McGinnis and Krumlauf, 1992). In contrast, the pregnathal region is patterned in a different way, for instance without pair-rule function. In *Drosophila*, a set of so called head gap genes is required for proper pregnathal segment polarity gene expression (Cohen and Jurgens, 1990; Crozatier et al., 1999; Grossniklaus et al., 1994; Wimmer et al., 1997; Wimmer et al., 1993). The identity of these segments is specified largely independently from Hox-genes as the intercalary segment is the anterior most segment expressing a Hox-cluster gene, namely the *Hox1* ortholog *labial* (Diederich et al., 1989; Merrill et al., 1989; Nie et al., 2001). The mandibular segment represents the hinge region between the posterior and the anterior patterning system because this segment is patterned by both the posterior pair-rule genes and the anterior head gap genes (Vincent et al., 1997). Although some genes and interactions are known, a comprehensive list of genes involved in early patterning of the insect head does not exist so far.

2.5.2 Some unsolved problems concerning insect head development

One unsolved problem in insect head patterning concerns the formation of the insect head capsule. During early embryonic development, the gnathal segments and their appendages are formed in a row very similar to the more posterior trunk segments (Fig. 2.3). Later in development extensive morphogenetic movements occur that lead to the migration of mouthparts towards anterior where they end up surrounding the mouth opening. Both these ventral morphogenetic movements and the formation of the dorsal head capsule of the first larval instar have remained enigmatic. Although the segmental and parasegmental boundaries of arthropods (except for the disputed labral segment) are clearly defined in the embryo by adjacent expression of *engrailed* and *wingless*, it remains unclear where these borders are located in the fully developed head. Hence, it remains unclear what tissues exactly form dorsal or lateral portions of the head capsule in a typical insect head.

Especially the contribution of the intercalary segment to the larval cuticle is difficult to analyze since it has no landmarks like appendages that could be followed throughout development. Also the function of the intercalary marker *labial/Hox1* is difficult to analyze because in *Drosophila labial* mutants, head involution is defective which leads to several secondary defects which blur the direct effects (Diederich et al., 1989; Merrill et al., 1989). It has been suggested that the intercalary segment contributes to lateral and ventral regions of the larval pharynx (Rogers and Kaufman, 1997). Also the embryonic hypopharyngeal lobes have been assigned to the intercalary segment but also a mandibular origin has been proposed (Economou and Telford, 2009; Mohler et al., 1995).

Unfortunately, *Drosophila* is less well suited for studies on the development of the insect head for two main reasons. First, during late embryonic development the main head structures become internalized into the thorax by a process called head involution. Consequentially, the head becomes highly reduced, which hampers the analysis of the impact of head phenotypes significantly (Akam, 1989; Bucher and Wimmer, 2005; Jürgens et al., 1986; VanHook and Letsou, 2008; Younossi-Hartenstein et al., 1993). More specifically, the reduced head is poor in morphological markers which could be analyzed in order to detect head patterning defects. Many mutations lead to head involution defects. Hence, the cuticle phenotype is a mix of direct defects and secondary defects based on disturbed head involution. Second, *Drosophila* and other higher dipterans utilize a specific and derived system to establish the anterior portion of the embryo. This system is based on the maternally provided factor *bicoid* whose translation product forms an anterior to posterior gradient. The gradient provides positional

information along the anterior portion of the anterior-posterior axis. (Driever and Nusslein-Volhard, 1988a; Driever and Nusslein-Volhard, 1988b). However, so far it has been impossible to find *bicoid* orthologs in other insects than higher dipterans, suggesting that the original mechanism of anterior patterning was based on other genes (Brown et al., 2001; Stauber et al., 2002).

In conclusion, although from work in *Drosophila* much is known about anterior head patterning in insects, a comprehensive list of involved markers and their conservation among Bilaterians is still missing. Furthermore, specific questions like the contribution of head segments to the lateral and dorsal head capsule are difficult to answer by using *Drosophila* as model for head development.

2.6 The red flour beetle *Tribolium castaneum* as insect model for head development

For developmental studies the fruit fly *Drosophila melanogaster* is the most powerful insect model organism. For Evo-Devo approaches, however, *Drosophila* is not always the first choice, since several features are considered to be a highly derived adaption to a very short life cycle. One example for this is the long germband mode of embryogenesis, where segments become specified simultaneously in early blastodermal stages. In contrast, the red flour beetle *Tribolium castaneum* develops in a more insect typical short germband mode, in which posterior segments are added progressively from a posterior growth zone (Lynch and Desplan, 2003a; Lynch and Desplan, 2003b; McGregor, 2006; Peel et al., 2005). Hence, *Tribolium* possesses a more ancestral mode of early development and is therefore well suited to serve as model for Evo-Devo questions.

On the other hand, for studies on the development of the insect head, *Drosophila* is a rather poor model because head involution and lack of larval appendages, including mouthparts, hampers the analysis of early head development. In contrast, *Tribolium* possesses a fully developed larval head with well formed external mouthparts. Effects of manipulations of early embryonic patterning processes on head development are easily scored in larval stages (Bucher and Wimmer, 2005). Beside the more insect typical development and head formation, a robust reverse genetic method to knock down gene function is available (RNA interference, RNAi). The fact that the RNAi response is even transmitted systemically allows the

application of this method in every stage of development. Specifically, double stranded RNA (dsRNA) can be injected into pupal or adult stages and the RNAi effect is transmitted to the offspring, which can be obtained and analyzed in large numbers. And robust systemic RNAi in combination with the accessible genome is a powerful tool for candidate gene approaches and functional genome wide screens (Bucher et al., 2002; Bucher and Wimmer, 2005; Richards et al., 2008).

Alongside these benefits, more general features qualify *Tribolium* as an insect model organism. First, the beetles are easy to keep because they can be reared on normal flour without an additional water source. Second, one life cycle lasts around four weeks at 30°C. At this temperature the embryonic development is completed within 3-4 days. Hence, effects of applied RNAi can be analyzed in very short time. Third, the long lifespan of approximately three years simplifies the stock keeping procedure. Fourth, a comprehensive piggyBac based mutagenesis screen provided mutants affecting genes that are so far unknown developmental genes (Trauner et al., in preparation). And finally, various transgenic techniques are available, like heat-shock mediated misexpression and the recently established UAS/GAL4 system (Schinko and Bucher, personal communication). In conclusion, *Tribolium castaneum* is perfectly suited to study head development.

In recent years some progress in understanding head development in *Tribolium* has been made. Like in *Drosophila*, the formation of gnathal segments and the specification of their identity appear to rely in principle on the same mechanisms as in the trunk (Beeman et al., 1993; Brown et al., 2002; Choe and Brown, 2007; Choe et al., 2006; Maderspacher et al., 1998; Tomoyasu et al., 2005). For the patterning of the pregnathal region it has been shown that the head gap genes as known from *Drosophila* possess diverged functions in *Tribolium*. In contrast to its function in *Drosophila*, *Tc-orthodenticle1* (*Tc-otd1*) knock down affects all blastodermally established segments, indicating an early regionalization function. The later patterning function of *Tc-otd1* in the anterior head is similar to its *Drosophila* ortholog (Schinko et al., 2008; Schroder, 2003). *Tc-empty spiracles* (*Tc-ems*) function is restricted to the posterior ocular and anterior antennal region. And although expressed in the early mandibular segment, the knock down of *Tc-buttonhead* (*Tc-btd*) does not affect head development. In contrast to the findings in *Drosophila*, both *Tc-ems* and *Tc-btd* seem to be less important for early anterior head patterning (Schinko et al., 2008). Also in contrast to *Drosophila*, the gap gene *Tc-knirps* is essential for the development of the mandible and antennae in *Tribolium* (Cerny et al., 2008). Additionally, *Tc-labial/Hox1* has been shown to specifically mark the intercalary segment in *Tribolium* (Nie et al., 2001). This observation and

the comparison of other intercalary and mandibular marker genes (*cap'n'collar*, *cnc*; *knot*, *kn* and *crocodile*, *croc*) in *Tribolium* and *Drosophila* already helped to clarify the affinity of a *Drosophila* head specific structure (hypopharyngeal lobes) to the mandibular segment (Economou and Telford, 2009). Beside these findings, not much is known about the patterning of the head in *Tribolium*. More specifically, like in *Drosophila* a comprehensive list of genes involved in early head patterning is still missing.

2.7 Aims

Encouraged by the high degree of conservation of the anterior patterning genes *otd/otx* and *ems/emx* in vertebrates and insects, I aimed to identify more candidates of the highly conserved core of anterior bilaterian patterning genes. Therefore, I analyzed the expression and function of *Tribolium* orthologs of vertebrate neural plate patterning genes. If these genes are involved in the formation of comparable regions in insects and vertebrate, there is a high chance that they already belonged to the repertoire of anterior patterning genes of the urbilateria. If the orthologs of vertebrate neural plate genes are expressed in the embryonic head of *Tribolium*, they are very likely involved in the patterning of the epidermal as well as the neural ectoderm (see chapter 2.4). Hence, this candidate gene screen provides several new genes involved in anterior patterning in insects.

Based on the expression and function of the candidate genes, I formulated hypotheses on the hierarchy within the interaction network which governs head formation in *Tribolium*. In addition I hypothesized selected interactions, which I subsequently tested experimentally. Finally, I compared the *Tribolium* data to the corresponding vertebrate situation in order to gain insight into the conservation of the candidate genes among Bilaterians.

Since canonical Wnt-signaling seems to be involved in posterior patterning of insects and vertebrates, I aimed to test the effects of ectopic Wnt-signals in the anterior region of *Tribolium*.

Finally, I analyzed the function of *labial/Hox1* in *Tribolium* in order to reveal the contribution of the intercalary segment to the head capsule.

3 Materials and Methods

3.1 Animals

For the experiments the wild type *Tribolium castaneum* strain San Bernardino (Richards et al.) was used. The beetles were reared under standard conditions on full grain flour (Sokoloff, 1974).

3.2 Identification and cloning of candidate genes in *Tribolium*

Mouse protein sequences of the candidate genes (see Table S1) were obtained from the NCBI database (<http://www.ncbi.nlm.nih.gov/>). The search for potential *Tribolium* orthologs was performed using the Blast server of the Baylor College of Medicine (<http://www.hgsc.bcm.tmc.edu/blast/blast.cgi?organism=tcastaneum>).

mRNA of 0-48h staged embryos was isolated using the MicroPoly(A)Purist Kit (Ambion) and cDNA was synthesized by using the SMART PCR cDNA Synthesis Kit (ClonTech). Subsequently, based on the Blast analysis sequence specific primers were designed and gene fragments were isolated from cDNA by standard PCR. Cloning of the obtained fragments into plasmids was performed by using the TA Cloning Dual Promotor Kit (pCRII) (Invitrogen GmbH, Karlsruhe). The cloned fragments were sequenced by Macrogen (Korea) by using standard T7 (TAATACGACTCACTATAGG), SP6 (GATTTAGGTGACACTATAGA), M13 (GTAAAACGACGGCCAGTG) or M13R (GGAAACAGCTATGACCAT) primers.

In order to link the *Tribolium* orthologs to the corresponding vertebrate gene, the analyzed genes are always indicated with the *Tribolium* ortholog followed by the name of the vertebrate ortholog, in case this name is different (e.g. *Tc-otd1/otx*).

3.3 Phylogenetic analysis

In order to reveal the orthology of the cloned genes, the obtained sequences were analyzed by calculating phylogenetic trees. The sequences of the cloned genes were blasted against the entire available nucleotide collection using the tblastn algorithm of the NCBI database

(Altschul et al., 1997). Sequences of different search results from insects, vertebrate and if available from other groups were used for later tree calculation. Furthermore, the sequences of the cloned genes were blasted against the *Tribolium* nucleotide collection using the tblastn algorithm of the NCBI database. Each of the first three hits that were not identical to the initial sequence was used for tree calculation and was again blasted against the entire available nucleotide collection using the tblastn algorithm of the NCBI database. The first three hits of each these searches were used for the tree calculation.

All sequences obtained with the help this approach were aligned using the ClustalW algorithm of Mega 4 (Kumar et al., 2008; Tamura et al., 2007). The alignment was used as basis for the phylogenetic tree calculation in Mega 4 using the Neighbor-Joining method (Saitou and Nei, 1987). Specificities of the phylogenetic analysis were the following: The bootstrap consensus tree inferred from 10.000 replicates is taken to represent the evolutionary history of the analyzed genes (Felsenstein, 1985). Evolutionary distances were computed using the Poisson correction method (Zuckerandl and Pauling, 1965). All positions containing gaps and missing data were eliminated from the dataset (Complete deletion option). See Supplementary Figures for all phylogenetic trees. The phylogenetic relationship for the following genes are already published: *Tc-wnt11* and *Tc-wg/wnt1* (Bolognesi et al., 2008a), *Tc-otd1/otx* and *Tc-ems/emx* (Schinko et al., 2008), *Tc-ey/pax6* and *Tc-toy/pax6* (Yang et al., 2009a), *Tc-eya* (Yang et al., 2009b).

3.4 Fixation of embryos

Wild type and RNAi treated embryos were fixed between 0-48 h of development by using standard procedure (Marques-Souza et al., 2008). In contrast to the quoted reference, embryos were dechorionized in bleach solution two times for three minutes and the remaining embryos were passed through a 0.8 needle.

3.5 Whole mount in situ hybridization

Single (NBT/BCIP) and double in situ stainings (NBT/BCIP & FastRed or INT/BCIP) were performed for wild type and RNAi embryos as described (Wohlfrom et al., 2006). Staging of the embryos is based on *Tc-wg* expression. *Tc-wg* stripes were counted starting with the mandibular one, thus excluding the ocular and antennal *Tc-wg* domains.

3.6 Knock down of gene function by RNA interference (RNAi)

Templates for in vitro transcription were amplified from plasmids by PCR reaction using primers that contain the promoter for the T7 RNA polymerase. The dsRNA was produced by in vitro transcription using Megascript T7 kit (Ambion).

Parental and embryonic RNAi was performed as published previously by injecting female pupae and fertilized eggs at the early blastoderm stage (Bucher et al., 2002; Schinko et al., 2008). Because pupal injection of dsRNA of some genes leads to sterility, adult females were injected. They were cooled on ice and squeezed using entomology tweezers until they protruded their genitalia and were injected laterally. Lengths of gene fragments used for dsRNA synthesis are listed in Table 3.1 and 3.2. For the analysis of *Tc-labial/Hox1* a 1080bp fragment was used to synthesize dsRNA which was injected into pupae. The following concentrations were used for the RNAi experiments: pupal RNAi and adult RNAi: 2-4µg/µl; embryonic RNAi: 1-2µg/µl.

Table 3.1: Overview of the genes isolated in this work.

The used primer pairs are listed as well as the RNAi approach used for knocking down the respective gene. fw-forward, rev-reverse, eRNAi-embryonic RNAi, pRNAi-pupal RNAi, aRNAi-adult RNAi

Gene	Size	fw primer (5' - 3')	rev primer (5' - 3')	eRNAi	pRNAi	aRNAi
<i>Tc-ase</i>	737bp	CGTCAGTGTGGTATCCCCTC	GCTGTTCCCACCACTGCAT			
<i>Tc-axin1</i>	1070bp	TGCACGAGGCCCAAGCAC	CTTCGGGAGGCGTTCGG			X
<i>Tc-BarH</i>	731bp	CGTTTTCGCTCCTTTAACC	CAGGCACAAAAGTCGTATCC			
<i>Tc-chx</i>	787bp	GACAACTAGACAATCCAAAGACTTCTC	CTAGTCTCTGCATTGACCACCTCC			
<i>Tc-ci</i>	1351bp	GGATTTTCAAGCCGCTATGTCTGC	TGTAGCGCTTCGTGCAACCG		X	
<i>Tc-dbx</i>	489bp	ATGAGGAGCGGCGAAGGAAG	TTCTCCACTTCATTGCGCGG		X	
<i>Tc-Dll</i>	948bp	CACCATGTCGGGGGAGG	GTAACATAATCACTTCTTCAGTATT	X		
<i>Tc-eya</i>	1252bp	TACCCCAATCGTACTCAGC	GAAAAACGCCTCCTAGACC	X		
<i>Tc-fez</i>	561bp	CAAGCCCTCCATCGTGAC	GAATCGGAGGCGGAAGTAC		X	
<i>Tc-gsc</i>	703bp	GAAAACTGGCGGAAGTCAAA	CTCCTGCAGACATCCTCCTC		X	
<i>Tc-lim1</i>	1009bp	CGGTACAAAAGTGCCTGG	GAACTGGCCTTGTCTGTTCTG		X	
<i>Tc-munster</i>	827bp	TGCTTGTGAACATTTCCGT	GTCTCGCTCCTGTTATGCC		X	
<i>Tc-ptx</i>	946bp	ACACGCCGTCCTCCAC	GACAGCCCTGCCGAAGAC		X	
<i>Tc-scro</i>	837bp	TTGAGTCCCAAGCATCATC	GATTGTTGGGTGCGAGATG		X	
<i>Tc-six3</i>	839bp	AACTCCGCGAGCTGACTC	CGAGTGGAAAGCCCTTACTG	X	X	
<i>Tc-six4</i>	966bp	AAGTCGGCGGAAAGAAC	CTAAATTTATGGTACTTGATAATCCG		X	
<i>Tc-slp</i>	1142bp	CCGCTTGTGAAAAATCTCATTGTG	TCCATGTTGAAGCCTTGCTG			
<i>Tc-so</i>	892bp	CGGGAATGCTTGAAGTTTGCTC	CTGTACAAGGCCTGGTAGTCGT			X
<i>Tc-wnt11</i>	961bp	GCTTTTCGATTCGTGGTTGTC	CCGCAGCACAAATGACGACA			

Table 3.2: Overview of other genes used in this work.

The RNAi approach used for knocking down the respective gene is listed.
eRNAi-embryonic RNAi, pRNAi-pupal RNAi, aRNAi-adult RNAi

Gene	Size	Source	eRNAi	pRNAi	aRNAi
<i>Tc-ems</i>	888bp	Johannes Schinko			
<i>Tc-ey</i>	860bp	Markus Friedrich		X	
<i>Tc-hh</i>	1148bp	Evgenia Ntini			
<i>Tc-irx</i>	350bp	Fakrudin Bashasab			X
<i>Tc-otd1</i>	1116bp	Johannes Schinko			
<i>Tc-rx</i>	395bp	Fakrudin Bashasab		X	
<i>Tc-tll</i>	1600bp	Reinhard Schröder		X	
<i>Tc-toy</i>	859bp	Markus Friedrich		X	
<i>Tc-wg</i>	1700bp	?			

3.6.1 Control experiments for RNAi procedure

A comprehensive negative control for pupal RNAi was performed by either only sticking the needle into the pupae or injecting water, injection buffer or dsRNA for tGFP. All controls showed no significant effects on the development of the offspring.

3.6.2 Off-Target effects in RNAi experiments

RNAi acts through small interfering RNAs with 21 nucleotides (nt) length (Filipowicz, 2005). Potentially, long dsRNAs as used in the presented experiments may contain small stretches of sequence identical to other genes. The observed phenotype could then be a mixture of effects produced predominantly by the gene of interest but with a minor contribution of the off-target. In order to test if the performed RNAi experiments resulted in off-target effects, the respective sequences were blasted against the *Tribolium* genome (Blast server of <http://beetlebase.org/>). Most obtained off-target sequences were shorter than 21 nt. The exceptions are listed in Table. 3.3. The number of nucleotides of specific target sequences was correlated to the number of nucleotides of off-target sequences of 21 nt length or longer. The fact that the RNAi effects of these experiments are based on 17 to 72 times more specific 21 nucleotides indicates that the observed effects are specific. Additionally, the off-target sequences were assigned to the respective genes (Table 3.3). Of note, *Tc-tll* which was used for interaction analyses in addition to the cuticle screen possesses one off-target sequence which does not affect a predicted gene. Hence, it is very likely that the observed results for *Tc-tll* RNAi are specific for the function of this gene.

Table 3.3: Off-target effects for the performed RNAi experiments.

The number of specific nucleotides (nt) corresponds to the length of the respective cDNA clone. The number of off-target nucleotides corresponds to the sum of nucleotides in stretches larger than 21 nt. The ratio of specific nt and off-target nt shows that the experiments are based on X times more specific 21 nucleotides. The off-target sequences are part of the listed genes.

Gene	specific nt	off-target nt	specific nt/off-targets nt	off-target genes
<i>Tc-ci</i>	1351	44	30,70	<i>Tc-KRAB box and zinc finger, C2H2 type domain containing protein Mm-PR domain containing 9 (Prdm9)</i>
<i>Tc-toy</i>	859	23	37,35	<i>Tc-pox meso</i>
<i>Tc-scro</i>	837	48	17,44	<i>Tc-gbx2</i> <i>Tc-similar to AGAP000484-PA</i>
<i>Tc-rx</i>	395	21	18,81	<i>Tc-ptx</i>
<i>Tc-dbx</i>	489	23	21,26	<i>Tc-similar to AGAP000484-PA</i>
<i>Tc-munster</i>	827	45	18,38	<i>Dm-ladybird early</i> <i>Tc-similar to protease S51 alpha-aspartyl dipeptidase</i>
<i>Tc-ill</i>	1600	22	72,73	no gene prediction

3.7 Cuticle preparations

First instar wild type and RNAi larvae were dechorionized and incubated in lactic acid/Hoyer's medium (1:1) at 65 °C overnight (Bucher and Klingler, 2004).

3.8 Documentation of cuticles and stained embryos

Wild type and *Tc-scro/nkx2.1* RNAi cuticles were documented using the Zeiss LSM 510 as described (Wohlfrom et al., 2006). All other cuticles were documented by recording 50-100 planes using a Zeiss Axioplan 2 microscope. With the help of the ImageProPlus software (Version 6.2; MediaCybernetics) deconvolution was performed with the “No Neighbour” method followed by a “Z Projection” (“Max Intensity”) using ImageJ (version 1.40g). Embryos stained by in situ hybridization were prepared free from the yolk and documented with a Zeiss Axioplan 2 microscope and the ImageProPlus software (Version 6.2; MediaCybernetics).

3.9 Interaction analysis in *Xenopus laevis*

The full length cDNA for *Xsix3* was isolated from a cDNA pool kindly provided by Frank Nieber by using the following primers: fwd: 5'- CGGAATTCATGGTGTTTCAGGTCCCCTC -3' (*EcoRI*); rev: 5'-CGCTCGAGTCATACGTCACATTCAGAGTCAC-3' (*XhoI*). The

attached restriction sites allowed the directed cloning into the *EcoRI/XhoI* site of the pCS2+ expression vector. The vector was linearized by *Acc65I* digestion and subsequently mRNA was synthesized by using the mMESSAGE mMACHINE SP6 kit (Ambion, Austin). For knock down of *Xsix3* a previously published and tested antisense morpholinos was ordered: 5'-ACCTGAACACCATGGGATGGCCGG-3' (Gene Tools) (Gestri et al., 2005). The Digoxigenin labeled probes for in situ hybridization were synthesized from plasmids kindly provided by the Department of Developmental Biochemistry (Prof. Tomas Pieler). The plasmids were linearized and in vitro transcription was performed by using the DIG-RNA-labeling Kit (Roche, Mannheim) (see Table. 3.4).

Table 3.4: Genes used for in situ hybridization in *Xenopus laevis*.

Gene	Enzyme for linearization	RNA polymerase for in vitro transcription
Xnkx2.1	NotI	T7
Xotx	NotI	T7
Xpax6	NotI	T7
Xttl	EcoRI	T7
Xwnt1	HindIII	SP6

Xenopus laevis embryos were obtained by HCG induced egg laying and in vitro fertilization. The embryos were dejellied in 2% cysteine (pH 8.0) and washed and cultured in 0.1X MBS until the two cell stage. One of the two blastomeres was injected either with the *Xsix3* mRNA or the morpholino. As a lineage tracer 50 pg β -Gal mRNA was coinjected. The injected embryos were again cultured until the early neurula stage (Nieuwkoop and Faber, 1967) and then they were fixed in MEMFA. The spatial expression patterns were determined by whole mount in situ hybridization (Harland, 1991). The stained embryos were documented with the Leica Fluoreszenz Stereomikroskop MZ16FA and the ImageProPlus software (Version 6.2; MediaCybernetics).

4 Results

4.1 Analysis of highly conserved anterior patterning genes

4.1.1 Identification of the *Tribolium* orthologs

In order to identify genes involved in head patterning, I performed a candidate gene screen based on situ hybridization and RNAi.

I identified 27 candidate genes involved in vertebrate neural plate patterning from the literature (Table S1). The phylogenetic analysis revealed that three genes are not found in the genomes of *Tribolium* and *Drosophila* (*Dmbx1/Atx*, *Vax1*, *Hesx1/Rpx*). The remaining 24 of these candidates possess orthologs in *Tribolium* and *Drosophila*. This led to a set of 24 genes that I investigated in more detail.

4.1.2 Expression of candidate genes in *Tribolium castaneum*

Some of the candidates have been described before with respect to the segmentation process or eye patterning, but an exact analysis for the head has been missing so far.

I analyzed the expression patterns of 24 candidate genes including counterstaining with *Tc-wg/wnt1* in order to identify the exact time and region of their activity. Of these, only *Tc-BarH*, *Tc-wnt11* and *Tc-mun/arf* are not expressed in the head anlagen throughout embryonic development (not shown). 21 genes are expressed in the embryonic head at some stage. They fall into roughly three groups based on spatial expression features. The first set of eight genes is almost exclusively expressed in the embryonic head (*Tc-otd1/otx*, *Tc-optix/six3*, *Tc-tll/tlx*, *Tc-lim1/5*, *Tc-scro/nkx2.1*, *Tc-gsc*, *Tc-rx* and *Tc-fez*). The nine genes of the second group show segmentally reiterated domains in addition to the head expression (*Tc-hh/shh*, *Tc-wg/wnt1*, *Tc-ci/gli3*, *Tc-mirr/irx*, *Tc-ems/emx*, *Tc-slp2/bf1*, *Tc-ey/pax6*, *Tc-dbx* and *Tc-ptx/pitx*). The transcripts of the third set of four genes mark the rim of the head lobes (*Tc-eya*, *Tc-Dll/Dlx*, *Tc-so/six1* and *Tc-six4*). Some genes show mixed aspects that are mentioned in the corresponding paragraph.

A comprehensive list of all genes including the complete names and functional domains of the coded proteins is depicted in Table S1.

4.1.2.1 Genes with exclusive expression in the head anlagen

These genes show exclusive expression in the head. Some candidates also possess additional expression features in later stages (e.g. expression in the appendages). But these are clearly independent of the initial head expression domains.

Tc-otd1/otx (Schinko et al., 2008; Schroder, 2003) is already provided maternally in a broad domain which gets rapidly restricted to the anterior head region (Fig. 4.1A). Throughout embryonic development *Tc-otd1/otx* positive cells are located mainly in the lateral head lobes (Fig. 4.1B-E). At the 5-8 *wg*-stripe stage a ventral midline domain of *Tc-otd1/otx* arises de novo (black arrowhead in Fig. 4.1C-E).

Tc-optix/six3 has no maternal contribution. Expression starts at the anterior pole of the egg (not shown). Slightly later, the expression retracts from the pole and a ventral triangle shaped domain becomes visible (Fig. 4.1F). The anterior border of this domain corresponds to the anterior most embryonic tissue at blastodermal stage (Steinmetz, Posnien et al., unpublished). At early germ band stages *Tc-optix/six3* is expressed anterior to and separated from the ocular *Tc-wg/wnt1* domain (Fig. 4.1G). At the 5-8 *wg*-stripe stage the expression resolves into three distinct regions. A median domain marks the prospective labral/stomodaeal region (black arrowhead in Fig. 4.1H), whereas two lateral domains are located in the anterior most head lobes (arrow in Fig. 4.1H). At later stages expression in the larval eye anlagen (open arrowhead in Fig. 4.1I,J) and in three 2-3 cell-clusters in the mandibular segment is detectable (stars in Fig. 4.1J).

Tc-tll/tlx (Schroder et al., 2000) expression starts at the posterior pole at early blastodermal stages (arrow in Fig. 4.1K). Expression in the head is first detectable at blastodermal/germ band transition anterior to the ocular *Tc-wg/wnt1* domain (Fig. 4.1L). At the same time the posterior domain disappears (Schroder et al., 2000). During germ band elongation the *Tc-tll/tlx* expression expands in accompany with the formation of the head lobes and finally covers large parts of them (Fig. 4.1M-O).

Tc-lim1/5 is first detectable at an early germ band stage covering the ocular *Tc-wg/wnt1* stripe and 2-4 cell rows posterior to it (Fig. 4.1P). At the 5-8 *wg*-stripe stage expression is restricted to the anterior part of the antennal parasegment, framed by the antennal and ocular *Tc-wg/wnt1* domains (Fig. 4.1Q). At later stages this antennal expression condenses and finally

marks a few cells between the ventral part of the ocular *Tc-wg/wnt1* domain and the antennae (open arrowhead in Fig. 4.1R,S). Furthermore, de novo expression domains in the proximal part of the developing appendages (arrow in Fig. 4.1R,S) and in specific ventral cells arise at the elongated germ band stage (black arrowhead Fig. 4.1S).

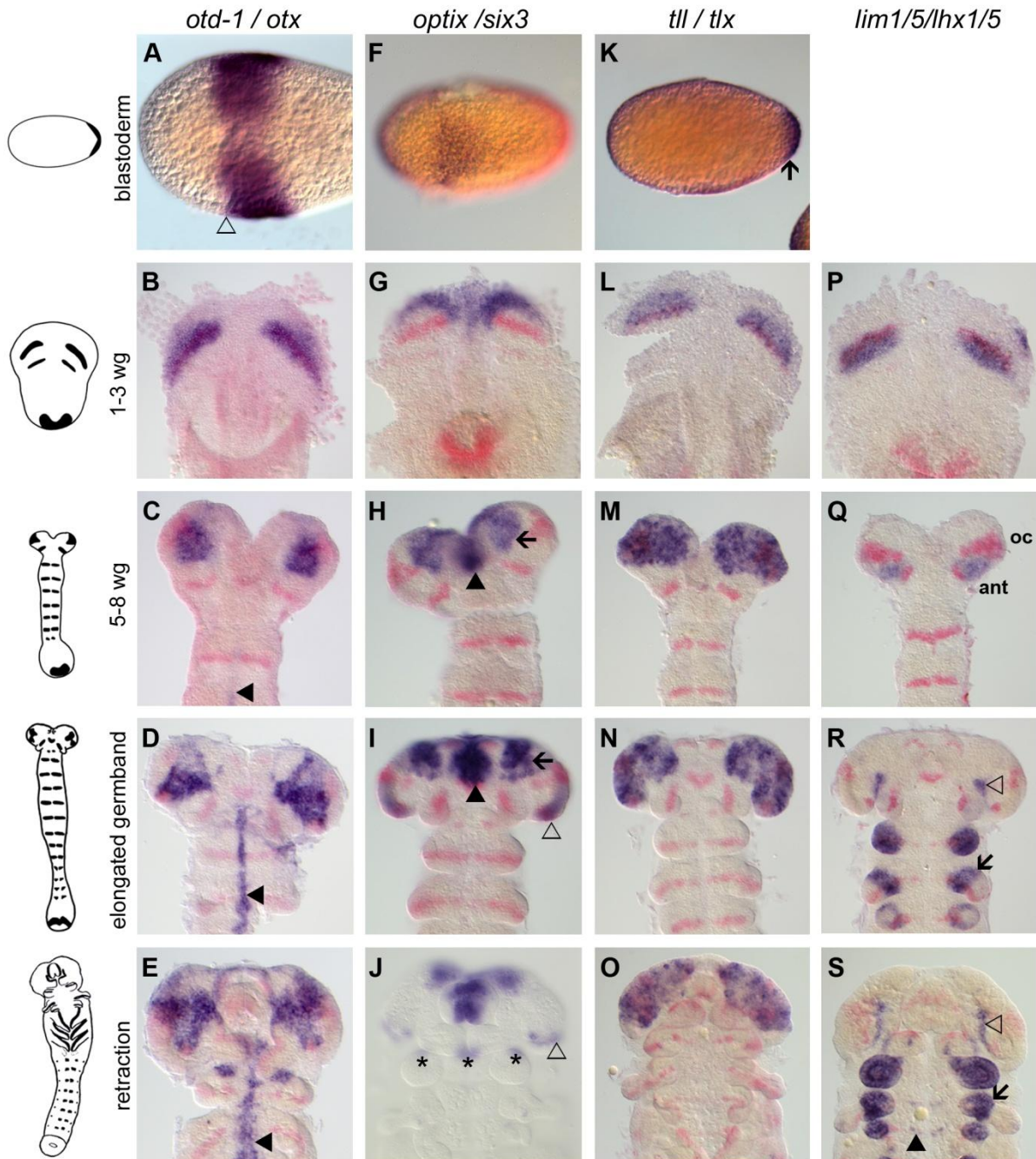


Fig. 4.1: Expression of early genes with exclusive domains in the embryonic head.

The respective candidate gene is stained in blue. *Tc-wg/wnt1* is stained in red. The blastodermal stages (A, F, K) are oriented with anterior to the left. The heads of germ band stages are oriented with anterior to the top. The stage to which the heads belong is schematically depicted on the left side.

Expression of *Tc-otd1/otx* (A-E). At late blastodermal stages *Tc-otd1/otx* transcripts are located in the anterior portion of the embryonic tissue (A; the open arrowhead marks the anterior border of the embryonic tissue). At

the 1-3 *wg*-stripe stage *Tc-otd1/otx* is co-expressed with the ocular *Tc-wg/wnt1* domain (B). During germ band elongation a de novo expression in the ventral midline is detectable (arrowhead in C-E). Expression of *Tc-optix/six3* (F-J). In blastoderms *Tc-optix/six3* transcripts are visible in a triangle shaped domain in the anterior embryonic region (F). At the 1-3 *wg*-stripe stage *Tc-optix/six3* transcripts cover large parts of the head anterior to the ocular *Tc-wg/wnt1* domain (G). During germband elongation the expression in the head becomes more complex (H-J): Expression is detectable in a median stomodeal/labral domain (arrowhead in H,I), a lateral domain (arrow in H,I) and in a latero-ventral domain (open arrowhead in I,J). At retraction stages additional expression in the mandibular segment arises (stars in J). Expression of *Tc-tll/tlx* (K-O). At late blastodermal stages *Tc-tll/tlx* transcripts are located at the posterior pole (arrow in K). From early germ band stage on *Tc-tll/tlx* expression covers the entire anterior head lobes (L-O). Expression of *Tc-lim1/5* (P-S). At the 1-3 *wg*-stripe stage *Tc-lim1/5* is expressed in the region of the ocular *Tc-wg/wnt1* domain and in some cells more posterior of it (P). At the 5-8 *wg*-stripe stage transcripts are located between the ocular (oc in Q) and the antennal (ant in Q) *Tc-wg/wnt1* domains. At later stages *Tc-lim1/5* is expressed in a small patch of cells between the antennae and the ocular region (open arrowheads in R,S) and in the proximal parts of developing appendages (arrows in R,S). At retraction stages de novo expression arises in the ventral region (arrowhead in S).

A is taken from Schinko et al., 2008.

The first *Tc-scro/nkx2.1* transcripts are visible at a 2-3 *wg*-stripe stage in a faint small patch of cells adjacent to the gastrulating mesoderm (arrow in Fig. 4.2A and Handel et al., 2005 for mesoderm location). These spot like domains broaden first posteriorly and subsequently laterally to end up as two triangle shaped domains that are connected in the stomodeal region (Fig. 4.2B). During germ band elongation the anterior part of the *Tc-scro/nkx2.1* positive region fuses to form a contiguous domain which covers the stomodeal and clypeolabral part of the median head (Fig. 4.2C). Outside of this median part, expression arises in some lateral cells (black arrowhead in Fig. 4.2C). Additionally, some cells in the lateral ocular region start to express *Tc-scro/nkx2.1* (open arrowhead in Fig. 4.2C). In retracting embryos *Tc-scro/nkx2.1* is expressed in the distal labrum (arrow in Fig. 4.2D), the stomodeum, an anterior median domain in the head lobes (black arrowhead in Fig. 4.2D) and in the optic lobe anlagen (open arrowhead in Fig. 4.2D) (see Fig. 3 in Yang et al., 2009b for location of the optic lobe anlagen).

Tc-gsc expression starts in early germ bands posterior to the ocular *Tc-wg/wnt1* stripe (open arrowhead in Fig. 4.2E). This domain laterally broadens to become a wedge shaped domain overlapping the ocular *Tc-wg/wnt1* domain extending 2-3 cell rows posteriorly (Fig. 4.2F). At the elongated germ band stage the *Tc-gsc* expression dissolves into a bean like domain covering the tissue between the ventral part of the ocular *Tc-wg/wnt1* and the outgrowing antennae (black arrowhead in Fig. 4.2G). In addition, some stomodeal cells start to express *Tc-gsc* de novo (arrow in Fig. 4.2G). At late stages transcripts are located in lateral parts of the head lobes (black arrowheads in Fig. 4.2H) and in the stomodeum (arrow in Fig. 4.2H).

Tc-rx expression is first detectable at a 5 *wg*-stripe stage. The transcripts are located in a patch of anterior cells (Fig. 4.2I). This initial domain then resolves into two domains, one anterior (black arrowhead in Fig. 4.2J) and a smaller one more posterior (open arrowhead in Fig. 4.2J).

These cells continuously express *Tc-rx* and can be found in the anterior head lobes during germ band retraction (black and open arrowheads in Fig. 4.2K). Shortly before the germ band is fully elongated an additional expression is observed in the labrum (arrow in Fig. 4.2K).

The onset of *Tc-fez* expression is observed at the 5-6 *wg*-stripe stage. Initially, some cells adjacent to the ocular *Tc-wg/wnt1* domain are *Tc-fez* positive (open arrowhead in Fig. 4.2L). This domain elongates laterally (not shown). The lateral part of the *Tc-fez* expression further expands and finally covers the whole posterior region of the head lobes (black arrowhead in Fig. 4.2M,N). In contrast, the median domain seems to stay located in its position, finally ending up in the anterior median part of the head lobes (arrow in Fig. 4.2M,N).

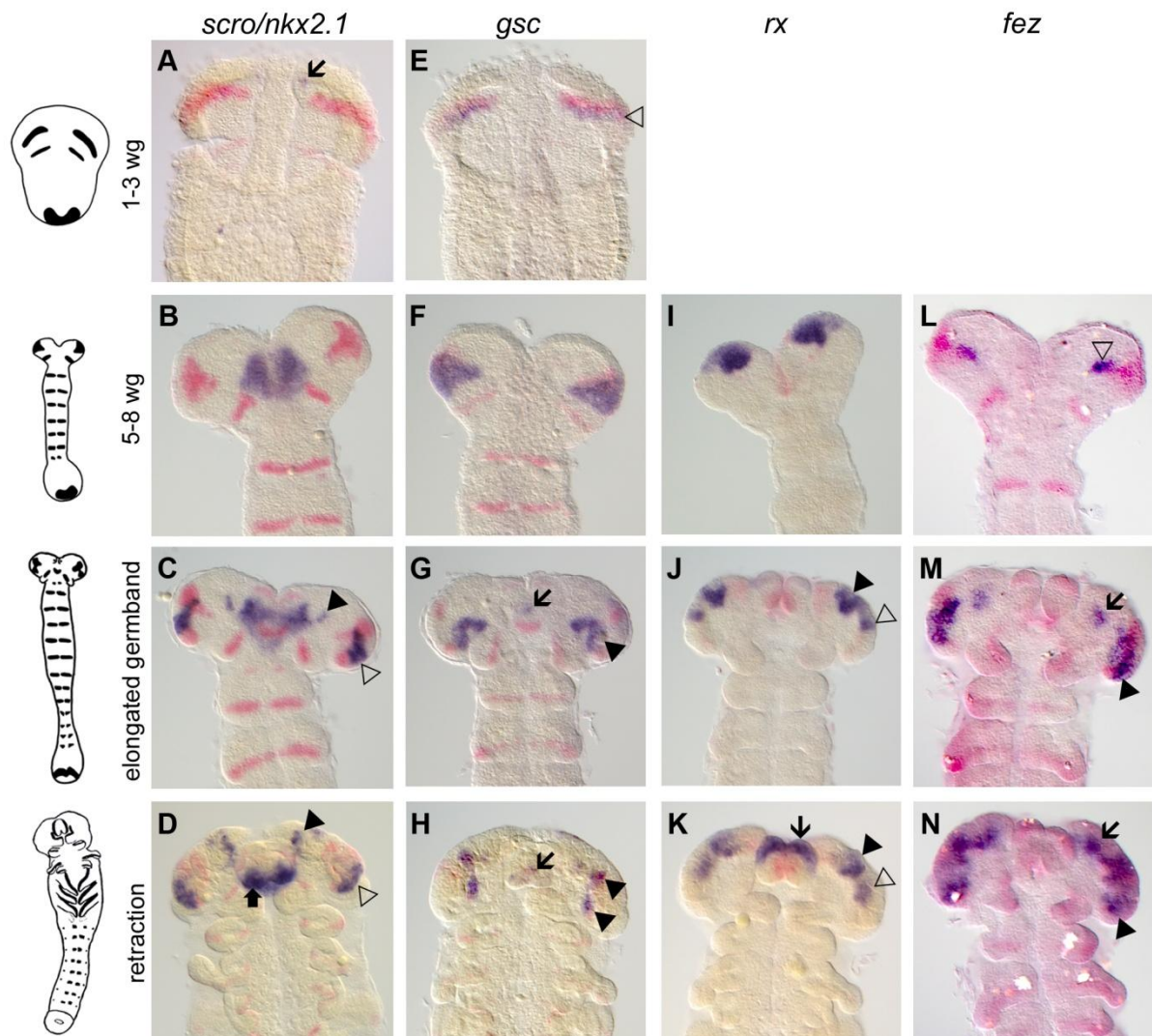


Fig. 4.2: Expression of genes with exclusive domains in the embryonic head.

The respective candidate gene is stained in blue. *Tc-wg/wnt1* is stained in red. In I-K *Tc-optix/six3* is stained in red. The heads of germ band stages are oriented with anterior to the top. The stage to which the heads belong is schematically depicted on the left side.

Expression of *Tc-scro/nkx2.1* (A-D). Expression starts at the 1-3 *wg*-stripe stage in a small domain anterior to the ocular *Tc-wg/wnt1* domain (arrow in A). During germ band elongation *Tc-scro/nkx2.1* transcripts are active in

the median stomodeal/labral region (B-D). In elongated germ bands and during retraction additional domains are visible: a small patch of cells anterior to the median region (arrowheads in C,D), a domain in the ventral ocular region (open arrowhead in C,D) and expression in the labrum (bulky arrow in D). Expression of *Tc-gsc* (E-H). At the 1-3 *wg*-stripe stage *Tc-gsc* transcripts are visible posterior to the ocular *Tc-wg/wnt1* domain (open arrowhead in E). At the 5-8 *wg*-stripe stage expression covers the ocular region (F). During germ band elongation the expression is detectable in a bean like domain between the antennae and the ocular region (arrowhead in G). This domain becomes separated at retraction stages (arrowheads in H). De novo expression of *Tc-gsc* arises in the stomodeum (arrows in G,H). Expression of *Tc-rx* (I-K). At the 5-8 *wg*-stripe stage *Tc-rx* transcripts are located in the anterior head lobes (I). This domain becomes distinguishable in an anterior part (arrowheads in J,K) and a posterior part (open arrowheads in J,K) during elongation. At retraction stages de novo expression arises in the labrum (arrow in K). Expression of *Tc-fez* (L-N). At the 5-8 *wg*-stripe stage *Tc-fez* is expressed in the region median to the ocular *Tc-wg/wnt1* domain (open arrowhead in L). During later stages two domains are distinguishable: one anterior median domain (arrows in M,N) and one lateral coular domain (arrowhead in M,N).

4.1.2.2 *Genes with additional segmental expression - segment polarity genes*

Tc-hh/shh (Farzana and Brown, 2008) starts to be expressed at late blastodermal stages as a stripe in the anterior region of the embryonic portion of the blastoderm (open arrowhead in Fig. 4.3A). In addition, the posterior most region is also *Tc-hh/shh* positive (Fig. 4.3A). At early germ band stages *Tc-hh/shh* is expressed in the ocular region posterior to the ocular *Tc-wg/wnt1* stripe (Fig. 4.3B). Ventrally, this stripe bends and extends anteriorly (black arrowhead in Fig. 4.3B). This median domain becomes associated with the stomodeum from germ band elongation onwards (Farzana and Brown, 2008) (black arrowhead in Fig. 4.3C-E). In the ocular region, *Tc-hh/shh* expressed is retained until late retraction stages (arrow in Fig. 4.3C-E).

Tc-wg/wnt1 (Nagy and Carroll, 1994) shows initial head expression at late blastodermal stages when the embryonic tissue is clearly distinguishable from the extra-embryonic tissue (not shown). The first stripes arise in the ocular region (open arrowhead in Fig. 4.3G) and later in the mandibular segment (black arrowhead in Fig. 4.3G). During elongation expression arises in the ventral stomodeum (star in Fig. 4.3I) and in the dorsal labrum (Posnien et al., accepted for publication) (black arrow in Fig. 4.3I,J). The expression in the antennal and intercalary stripes is delayed compared to the more posterior expression (antennal stripe is marked by white arrowhead in Fig. 4.3H,I and chapter 4.3.1). With ongoing germ band elongation, the ocular domain expands giving rise to a triangle shaped expression (open arrowhead in Fig. 4.3H) that gets subsequently separated in the elongated germ band stage (open arrowheads in Fig. 4.3I). The posterior part of this domain segregates with the optic lobe anlage (open arrowhead “ola” in Fig. 4.3J) whereas the anterior part marks anterior eye lobe tissue (open arrowhead “elo” in Fig. 4.3J) and a more median region of the head lobe

(open arrowhead “m” in Fig. 4.3J) (assignment of the ocular domains based on Liu and Friedrich, 2004).

The first *Tc-ci/gli3* (Farzana and Brown, 2008) transcripts are detectable at early germ band stages in the complete anterior part of the future head lobes posteriorly covering the ocular *Tc-wg/wnt1* domain (open arrow in Fig. 4.3K). The ventrally located prospective mesoderm (arrow in Fig. 4.3K) is free of *Tc-ci/gli3* expression. During germ band elongation, the anterior head domain gives rise to a wedge shaped expression which covers the ocular *Tc-wg/wnt1* region and additional anterior tissue (open arrowhead in Fig. 4.3L). The broad posterior domains are located in the posterior compartment of each parasegment (stars in Fig. 4.3L). In the course of development, this ocular domain undergoes numerous changes leading to a complex pattern of *Tc-ci/gli3* expression in the region of the labrum (black arrowhead in Fig. 4.3M), the anterior median head lobe and the lateral eye lobe tissue (open arrowheads in Fig. 4.3M). In retracting embryos transcripts are detectable in a wedge shaped domain in the lateral head (open arrowhead in Fig. 4.3N). Further, there are *Tc-ci/gli3* positive cells in the labrum (black arrowhead in Fig. 4.3N).

In *Drosophila* *Dm-mirror* is considered to be a segment polarity gene (McNeill et al., 1997; Urbach and Technau, 2003). In *Tribolium* *Tc-mirr/irx* transcripts are located in the anterior portion of each segment, suggesting a similar function (Fig. 4.3O-R). *Tc-mirr/irx* expression starts at around the 2-3 *wg*-stripe stage in the anterior-median part of the embryo (arrow in Fig. 4.3O) and in 1-2 segmental stripes (stars in Fig. 4.3O). The anterior most domain remains in contact with the stomodeal region during germ band elongation (arrow in Fig. 4.3P). In elongated embryos and at subsequent stages, *Tc-mirr/irx* expression is still visible in the stomodeum (arrow in Fig. 4.3Q,R). Additional cells in the ventral portion of the head lobes are *Tc-mirr/irx* positive (open arrowhead in Fig. 4.3Q,R).

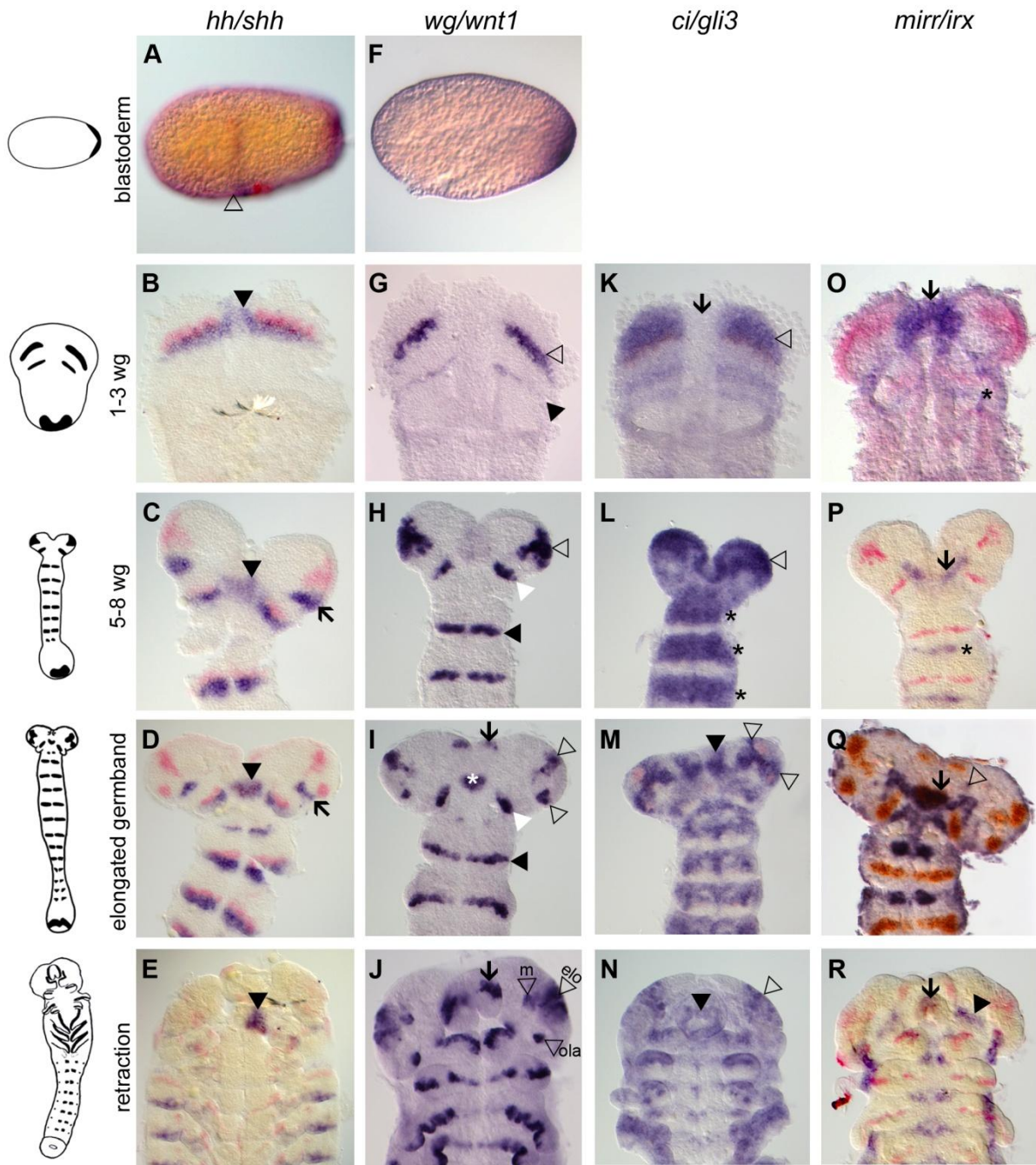


Fig. 4.3: Expression of segment polarity genes in the embryonic head.

The respective candidate gene is stained in blue. *Tc-wg/wnt1* is stained in red. The blastodermal stages (A, F) are oriented with anterior to the left. The heads of germ band stages are oriented with anterior to the top. The stage to which the heads belong is schematically depicted on the left side.

Expression of *Tc-hh/shh* (A-E). At late blastodermal stages *Tc-hh/shh* transcripts are located in the anterior portion of the embryonic tissue (open arrowhead in A). At the 1-3 *wg*-stripe stage *Tc-hh/shh* is expressed posterior to the ocular *Tc-wg/wnt1* domain and in some ventral cells (arrowhead B). This ventral expression is later connected to the stomodeum region (arrowheads in C-E) (Farzana and Brown, 2008). The ocular *Tc-hh/shh* domain stays active posterior to the ocular *Tc-wg/wnt1* domain (arrows in C-E). Expression of *Tc-wg/wnt1* (F-J). In blastoderms *Tc-wg/wnt1* transcripts are visible at posterior pole (F). At the 1-3 *wg*-stripe stage *Tc-wg/wnt1* transcripts are visible in an ocular (open arrowhead in G) and in a mandibular stripe (arrowhead in G). At the 5-8 *wg*-stripe stage the ocular domain becomes triangle shaped (open arrowhead in H) and expression in an antennal stripe arises (white arrowhead in H). During germ band elongation the ocular domain splits up (open arrowheads in I) until three domains are visible: a median domain (“m” in J), an eye lobe domain (“elo” in J) and a ventral optic lobe expression (“ola” in J). In elongated germ bands expression in the labrum (arrow in I,J) and in the stomodeum (star in I) arises. Expression of *Tc-ci/gli3* (K-N). At the 1-3 *wg*-stripe stage *Tc-ci/gli3* transcripts are

visible in the anterior-lateral head region (open arrowhead in K) while the median part of the embryo stays free of expression (arrow in K). During germ band elongation and during retraction *Tc-ci/gli3* stays active in the ocular lateral head lobes (open arrowheads in L-M). The expression in the trunk marks the posterior part of each parasegment (stars in L). Additionally, expression becomes visible in the labrum (arrowhead in M,N). Expression of *Tc-mirr/irx* (O-R). At the 1-3 *wg*-stripe stage *Tc-mirr/irx* is expressed in the anterior-median region (arrow in O) and in a posterior stripe (star in O). The initial anterior-median domain stays connected to the stomodeal region throughout embryonic development (arrows in P-R). Additionally, some cells in the ventral head lobes express *Tc-mirr/irx* (open arrowhead in Q and arrowhead in R).

4.1.2.3 Other genes with additional segmental expression

In addition to the segment polarity genes I analyzed some candidate genes that are expressed in the head and show additional segmental domains in different stages and processes of development.

The pair-rule and segment polarity gene *Tc-slp/bf1* is involved in segmentation in *Tribolium* (Choe and Brown, 2007; Choe and Brown, 2009; Choe et al., 2006). First expression is visible very early in the anterior part of the prospective embryonic tissue of a blastodermal staged embryo (star in Fig. 4.4A). At the 1-3 *wg*-stripe stage the initial expression covers the ocular *Tc-wg/wnt1* domain and some more posteriorly located cell rows (star in Fig. 4.4B). During germ band elongation this stripe splits into domains in the antennal segment (bulky arrow in Fig. 4.4C-E) and in the ocular region (open arrowhead in Fig. 4.4C). Additionally, some more anterior cells median to the ocular region become also *Tc-slp/bf1* positive (arrow in Fig. 4.4C), suggesting that the initial stripe splits into an antennal and an ocular part. Whereas the antennal part of this expression is retained, the ocular portion undergoes several changes. Namely, this domain splits into an anterior (arrow in Fig. 4.4C) and a posterior band comprising 2-3 cell rows (open arrowhead in Fig. 4.4C). The posterior band expands into the ocular region and finally undergoes the same anterior-posterior splitting as the *Tc-wg/wnt1* domain (open arrowheads in Fig. 4.4D,E). In the meantime the anterior band gets separated ending up in some anterior-median cells lateral to the labrum (arrows in Fig. 4.4D,E). During germ band retraction, several cells in the anterior head lobes and the antennal segment express *Tc-slp/bf1* (Fig. 4.4E). In addition, with the first morphological sign of outgrowth the labrum starts to express *Tc-slp/bf1* de novo (black arrowheads in Fig.4.4D,E).

Tc-ems/emx (Schinko et al., 2008) starts to be expressed in the late blastoderm as a stripe (open arrowhead in Fig. 4.4F). This stripe is located posterior to the ocular *Tc-wg/wnt1* expression at early germ band stages (open arrowhead in Fig. 4.4G). This domain remains active in the posterior ocular segment and the anterior antennal segment throughout embryonic development (open arrowhead in Fig. 4.4H,I). Additionally, a small patch of cells

median to the antennal, starts to express *Tc-ems/emx* de novo in elongated germ bands (black arrowhead in Fig. 4.4I). In retracting embryos a band of 1-2 cells in width reaches from the proximal antennae towards anterior (black arrowhead in Fig. 4.4J). It is not clear if this expression can be ascribed to the de novo domain mentioned above. In addition to the head expression, *Tc-ems/emx* becomes visible in successive segmental patches of lateral cells with ongoing elongation (arrow in Fig. 4.4I,J).

In *Tribolium* two orthologs of *pax6* exist, *Tc-ey* and *Tc-toy* (Yang et al., 2009a). Here I show the expression of *Tc-ey/pax6* (Fig. 4.4K-O) and mention some features of *Tc-toy/pax6* expression (Yang et al., 2009a and not shown). *Tc-ey/pax6* is first expressed at late blastodermal stages in the anterior portion of the embryonic tissue (star in Fig. 4.4K). In early elongating germ bands the transcripts are visible in an ocular stripe (star in Fig. 4.4L). This stripe broadens posteriorly leading to a wedge shaped lateral expression domain (star in Fig. 4.4M). Until this stage both *pax6* orthologs show similar expression, although *Tc-toy/pax6* seems to be expressed more anterior (not shown). With progressing germ band elongation, the wedge shaped *Tc-ey/pax6* domain gets increasingly complex, finally covering the whole lateral eye lobe tissue (star in Fig. 4.4N) and some cells in the anterior-median and median region of head lobes (arrowheads in Fig. 4.4N). The same is true for *Tc-toy/pax6* expression (Yang et al., 2009a and not shown). From the 8 *wg*-stripe stage onwards *Tc-ey/pax6* positive cells are visible anterior to the ocular *Tc-wg/wnt1* domain. These cells belong to the segmental pattern (Fig. 4.4N,O). This segmental expression includes domains in the antennal segment (open arrowhead in Fig. 4.4N,O) and median to the eye lobe tissue (black arrowhead in Fig. 4.4N,O). In contrast, the segmental expression of *Tc-toy/pax6* is restricted to more posterior segments (not shown). In retracting germ bands, both *pax6* orthologs are expressed in several spots in the anterior head lobes and in the larval eye primordium (arrow in Fig. 4.4O) (Yang et al., 2009a).

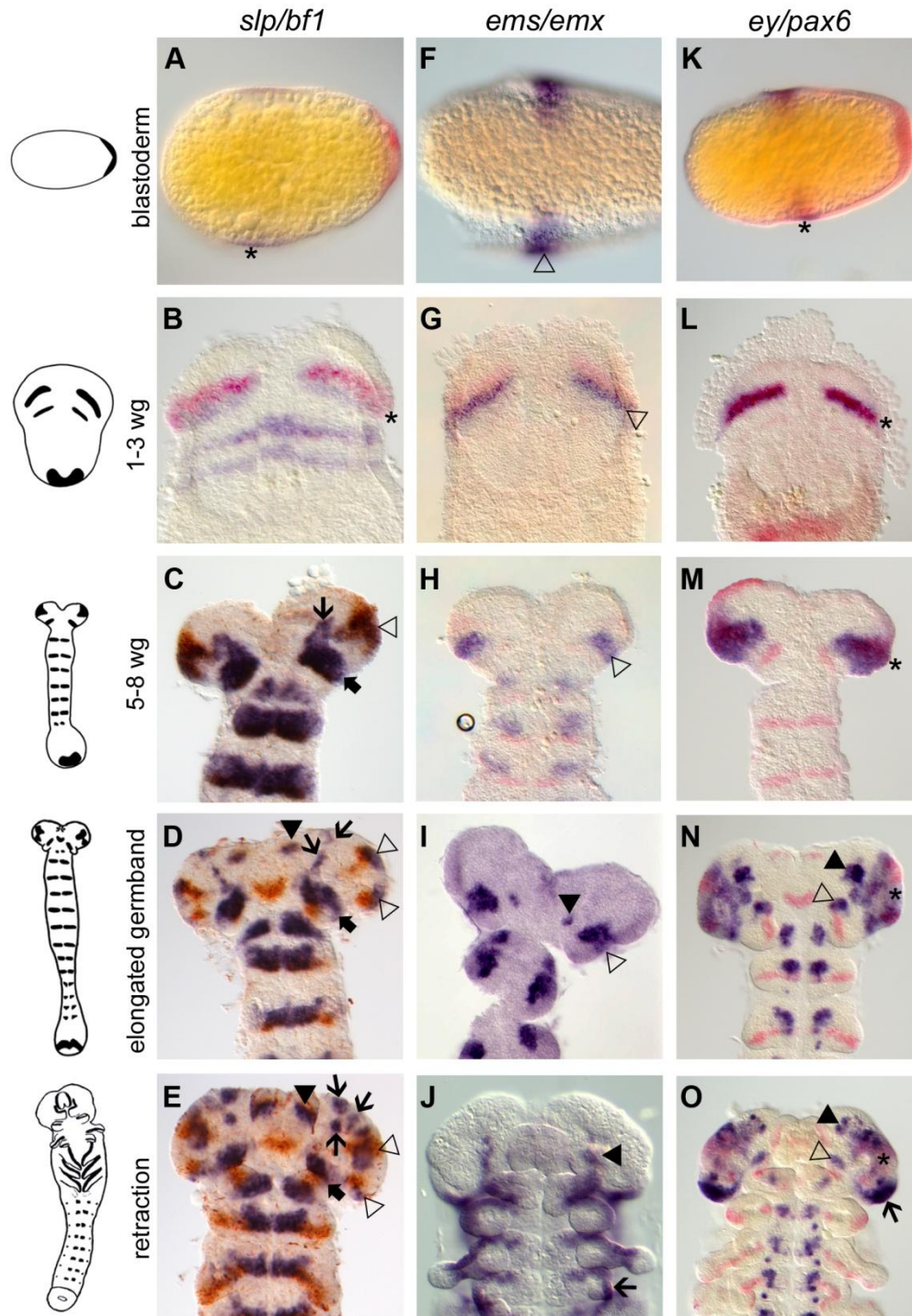


Fig. 4.4: Expression of other genes with segmental contribution.

The respective candidate gene is stained in blue. *Tc-wg/wnt1* is stained in red. The blastodermal stages (A, F, K) are oriented with anterior to the left. The heads of germ band stages are oriented with anterior to the top. The stage to which the heads belong is schematically depicted on the left side.

Expression of *Tc-slp/bf1* (A-E). At late blastodermal stages *Tc-slp/bf1* transcripts are located in the anterior portion of the embryonic tissue (star in A). This expression is located in the region of the ocular *Tc-wg/wnt1* domain and posterior to it at the 1-3 *wg*-stripe stage (star in B). This initial stripes splits into an anterior-medial portion (arrows in C-E), a lateral ocular domain (open arrowheads in C-E) and an antennal domain (bulky arrow in C-E). From elongated germ band stages on, expression in the labrum is detectable (arrowheads in D,E). Expression of *Tc-ems/emx* (F-J). In blastoderms *Tc-ems/emx* transcripts are visible in a broad stripe (open arrowhead in F). At the 1-3 *wg*-stripe stage *Tc-ems/emx* transcripts are detectable posterior to the ocular *Tc-wg/wnt1* domain (open arrowhead in G). During germband elongation the expression in the head stays active

Results

between the ocular and the antennal *Tc-wg/wnt1* domains (open arrowheads in H,I). At later stages an additional expression in the ventral posterior head lobes is visible (arrowheads in I,J). Lateral segmental expression domains are visible at later stages (arrow in J). Expression of *Tc-ey/pax6* (K-O). At late blastodermal stages *Tc-ey/pax6* transcripts are located in the anterior portion of the embryonic tissue (star in K). This initial expression stays active in the ocular region throughout embryonic development (stars in L-O). De novo expression domains arise in the ventral region of each segment during germ band elongation (N). The anterior domains of this segmental expression correspond to an anterior-median domain (arrowheads in N,O) and an antennal domain (open arrowhead in N,O). In retracting embryos the anterior-median domains becomes more complex (arrowhead in O). The ventral part of the ocular expression becomes more dominant during retraction (arrow in O).

F is taken from Schinko et al., 2008.

Tc-dbx expression starts at late elongation stages in single cells near the ventral midline (arrows in Fig. 4.5A) and in a patch of cells which are located medially between the anterior and posterior ocular *Tc-wg/wnt1* domain (black arrowhead in Fig. 4.5A). At retracting germ band stages *Tc-dbx* positive cells are detectable in three spots in the head lobes (open arrowheads in Fig. 4.5B) and in spots along the ventral nervous system (arrows in Fig. 4.5B). First *Tc-ptx/pitx* transcripts are detectable at late elongation stages in single segmental cells along the anterior posterior axis (arrows in Fig. 4.5C,D). One small spot is found in the antennal segment (open arrowhead in Fig. 4.5C,D) and one in the anterior head lobe (black arrowhead in Fig. 4.5C,D). This expression does not change until embryonic-larval transition (see Fig. 4.5D for retraction stage).

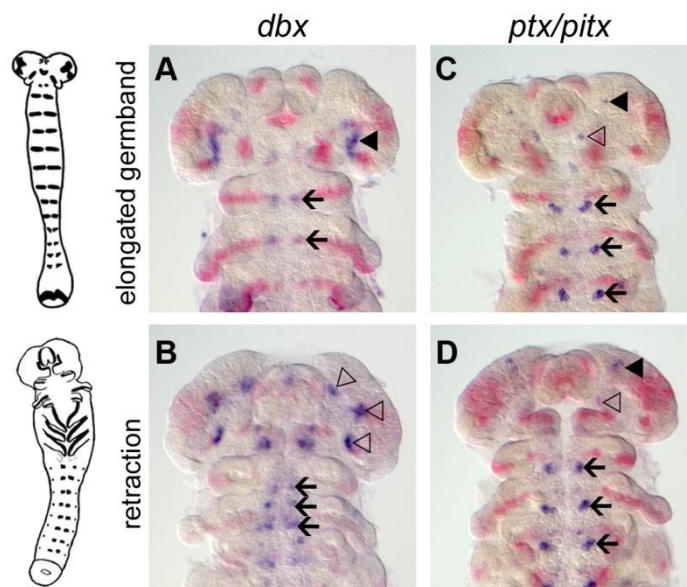


Fig. 4.5: Expression of genes that are active only late during embryonic development.

The respective candidate gene is stained in blue. *Tc-wg/wnt1* is stained in red. The heads of germ band stages are oriented with anterior to the top. The stage to which the heads belong is schematically depicted on the left side. Expression of *Tc-dbx* (A,B). At elongated germ band stages *Tc-dbx* is expressed in a bean like domain between the antennae and the ocular region (arrowhead in A) and in segmental ventral domains (arrows in A). During retraction three small domains are visible in the head lobes (open arrowheads in B). The ventral segmental pattern seems to become more complex during retraction (arrows in B). Expression of *Tc-ptx/pitx* (C,D). *Tc-*

ptx/pitx transcripts are detectable in an anterior (arrowheads in C,D) and a posterior (open arrowhead in C,D) spot in the head lobes. Additionally, segmental cell clusters on both sides of the ventral midline are *Tc-ptx/pitx* positive.

4.1.2.4 Genes involved in vertebrate cranial placode development

Tc-eya is first expressed at blastodermal stages (Yang et al., 2009b). In early germ bands the lateral rim of the future head lobes (arrow in Fig. 4.6A) and median cells of the future stomodeum express *Tc-eya* (star in Fig. 4.6A). Throughout embryonic development, *Tc-eya* expression is retained in the stomodeum (star in Fig. 4.6B-D). The expression at the rim of the head lobes becomes more prominent during early elongation (arrow in Fig. 4.6B). At fully elongated germ band stages the rim-domain is separated in two distinguishable domains, one anterior-median lateral to the labrum (black arrowhead in Fig. 4.6C) and a more posterior one in the lateral eye lobe tissue (open arrowhead in Fig. 4.6C). This distinction is more obvious in retracting embryos, when the posterior domain clearly marks the larval eye anlagen (open arrowhead in Fig. 4.6D) and the anterior domain is still located in the anterior-median head lobe (black arrowhead in Fig. 4.6D). In addition to the head domains, *Tc-eya* possesses complex segmental expression features (Fig. 4.6B-D).

Tc-Dll/Dlx (Beermann et al., 2001) is first expressed at early germ band stages at the lateral rim of the future head lobes like *Tc-eya* and *Tc-so/six1* (black arrowhead in Fig. 4.6E). As elongation proceeds, this initial domain expands to cover the lateral rim of the eye lobe tissue (black arrowhead in Fig. 4.6F). Around the same time, de novo expression in the budding antennae becomes evident (open arrowhead in Fig. 4.6F). Subsequently, *Tc-Dll/Dlx* is expressed in all developing appendages (arrows in Fig. 4.6G), except the mandibles (arrow “m” in Fig. 4.6G). At elongated germ band stages *Tc-Dll/Dlx* is still active in the eye lobe tissue (black arrowheads in Fig. 4.6G), but possesses an additional domain in the anterior head lobe (bulky arrow in Fig. 4.6G). During retraction, expression in the head lobes is not detectable anymore (Fig. 4.6H). However, the expression data of Beermann et al., 2001 still shows transcripts in the lateral head lobes at late stages.

Tc-so/six1 (Yang et al., 2009b) is expressed highly similar to *Tc-eya*. Therefore, I only describe the differences here. First, the onset of *Tc-so/six1* expression is slightly later (Fig. 4.6I). Second, at elongated germ band stages, the anterior domain fades and finally disappears (black arrowhead in Fig. 4.6J), whereas the expression in the lateral eye lobe tissue is retained (open arrowhead in Fig. 4.6J). Third, in retracting embryos less cells of the anterior head lobes are *Tc-so/six1* positive (Fig. 4.6K).

Tc-six4 expression starts at the 5-8 *wg*-stripe stage in two small anterior cell clusters (Fig. 4.6L). During further elongation this domain expands, finally covering the anterior-median rim of the head lobes (Fig. 4.6M). This expression remains detectable throughout embryonic development (Fig. 4.6N). Note that this *Tc-six4* domain marks the same tissue as the anterior portion of *Tc-eya* expression (compare black arrowheads in Fig. 4.6C and Fig. 4.6M). Furthermore, *Tc-six4* positive cells are the ones which switch off *Tc-so/six1* at elongated germ band stages (compare black arrowheads in Fig. 4.6J and Fig. 4.6M).

The segmental expression in addition to the head domains of *Tc-eya* and *Tc-so/six1* would also allow integrating these genes into the group of genes with additional segmental expression. Accordingly, *Tc-Dll/Dlx* and *Tc-six4* could be grouped with the genes with exclusive expression in the head. But in all four cases the unique expression at the rim of the head lobes and their involvement in vertebrate placode formation clearly justifies the introduction of an own group.

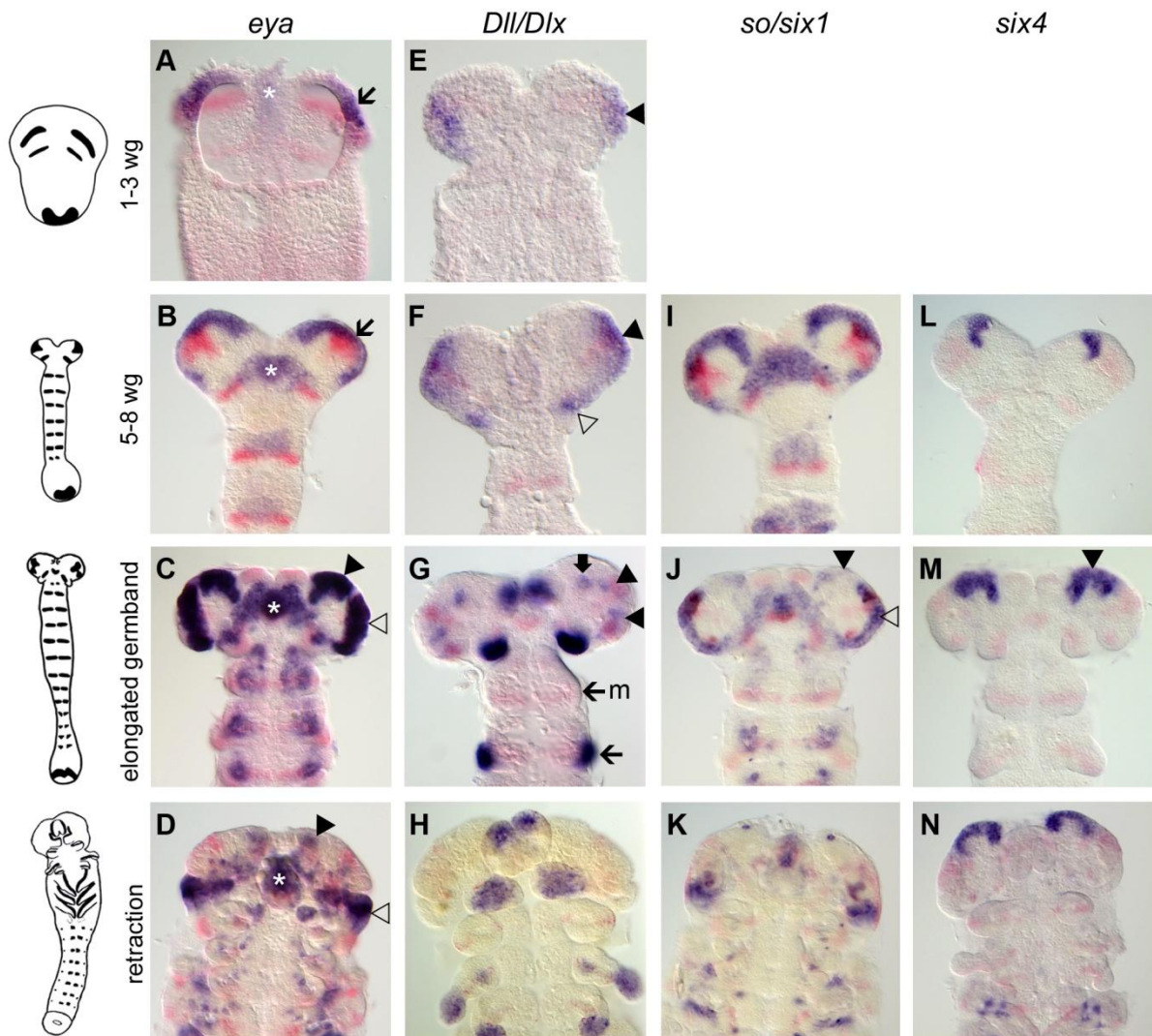


Fig. 4.6: Expression of genes involved in vertebrate cranial placode development

The respective candidate gene is stained in blue. *Tc-wg/wnt* is stained in red. The heads of germ band stages are oriented with anterior to the top. The stage to which the heads belong is schematically depicted on the left side. Expression of *Tc-eya* (A-D). At the 1-3 *wg*-stripe stage expression of *Tc-eya* covers the lateral rim of the future head (arrow in A) and in a median domain (star in A). The median domain is later located in the median stomodeal region (stars in B-D). The expression of *Tc-eya* in the lateral rim region expands to cover the entire rim of the head lobes at the 5-8 *wg*-stripe stage (arrow in B). At later stages the rim expression is subdivided into an anterior part (arrowhead in C,D) and a posterior ocular domain (open arrowhead in C,D). Expression of *Tc-Dll/Dlx* (E-H). *Tc-Dll/Dlx* transcripts are detectable in the lateral region of the head lobes (arrowheads in E,F). From germ band elongation on *Tc-Dll/Dlx* marks the distal portions of the developing appendages (open arrowhead in F marks the antennal expression; arrows in G mark the maxillary expression). Note that the mandibles are free of *Tc-Dll/Dlx* expression (“m”-arrow in G). In the anterior head *Tc-Dll/Dlx* is expressed in an anterior-median domain (bulky arrow in G) and in the lateral ocular region (arrowheads in G). Expression of *Tc-so/six1* (I-K). The expression of *Tc-so/six1* is very similar to the one of *Tc-eya*. One major difference is the loss of expression in the anterior rim region (arrowhead in J), while the lateral ocular domain (open arrowhead in J) stays active. Expression of *Tc-six4* (L-N). *Tc-six4* is expressed in the anterior rim region of the head lobes throughout embryonic development (e.g. arrowhead in M).

4.1.3 A virtual expression map for early head patterning

The double staining of the before described genes with *Tc-wg/wnt1* allows to create a virtual expression map for different stages of development. To that end, similar aged embryos were “morphed” to standard embryos based on both expression of *Tc-wg/wnt1* and morphology of the head lobes. This has been done for different stages. Then the analyzed expression patterns of the respective stages were documented with respect to the standard embryos. This allows to map the relative position of all combinations of expression patterns in multiple “virtual staining” (Fig. 5.3 and Fig. 5.4). This map can either be used to formulate hypotheses on interactions of the analyzed genes (see chapter 4.1.5) or to comprehensively compare the *Tribolium* expression data to the corresponding vertebrate situation (see chapter 5.1.4).

4.1.4 Function of the candidate genes in epidermal development

Based on the fact that neural and epidermal ectoderm arises from the same epithelium, several genes have been shown to be required for *Drosophila* epidermal and neural head formation and for vertebrate neural plate patterning (see chapter 2.4) (Dalton et al., 1989; Finkelstein and Boncinelli, 1994; Finkelstein and Perrimon, 1990; Reichert and Simeone, 2001; Wieschaus et al., 1984; Yu et al., 1994). Hence, it is likely that the candidate genes of my screen are involved in epidermal ectoderm patterning.

In order to figure out if the candidate genes are indeed involved in the patterning and formation of the epidermal ectoderm, I performed RNAi knock down experiments for the

candidate genes. Subsequently I analyzed the heads of first instar larvae for cuticle defects, since epidermal cells of the ectoderm secrete the cuticle (Dettner and Peters, 2003). In *Tribolium* a large set of markers exists to identify head phenotypes. Ventral defects are visible through abnormally formed gnathal appendages. Dorsal defects can be identified by analyzing a set of dorsal bristles and setae (Schinko et al., 2008). Interestingly, I find defects of essentially two main groups. Several genes result in severe defects after RNAi, leading to different levels of malformations of the whole head capsule (*Tc-ci/gli3*, *Tc-slp/bf1*, *Tc-eya*, *Tc-optix/six3*, *Tc-ey/pax6/Tc-toy/pax6* double knock down, *Tc-lim1/5*, *Tc-scro/nkx2.1*, *Tc-rx* and *Tc-six4*). The phenotypes of *Tc-otd1/otx* and *Tc-ems/emx* also belong to this group, but they are already described elsewhere (Schinko et al., 2008). The knock down of another set of genes leads only to mild defects with an affected dorsal bristle pattern without overall defects in the head capsule (*Tc-ey/pax6* and *Tc-toy/pax6* single knock down, *Tc-so/six1*, *Tc-dbx*, *Tc-ptx/pitx*, *Tc-mirr/irx*, *Tc-mun/arx*, *Tc-fez*, *Tc-gsc*, *Tc-tll/tlx* and *Tc-Dll/dlx*). First I focus on genes that result in severe head phenotypes upon RNAi because they are very likely crucial for early head patterning. Subsequently, I will mention some specific aspects of the weak defects.

4.1.4.1 Genes whose knock down leads to severe head patterning defects

Tc-ci/gli3 RNAi interferes with segmentation of the entire embryo (Farzana and Brown, 2008). The head phenotypes range from the total loss of the head (9,1%, n=11) to the loss and malformation of gnathal segments (90,9%; Fig. 4.7C). Note that the labrum is only affected in 18,2% of analyzed larvae. Hence, the gnathal segments are more sensitive to *Tc-ci/gli3* RNAi than the labrum. If accessible, the dorsal bristle pattern was analyzed. This shows mainly the disruption of the vertex setae (Fig. 4.7C' and Table S2).

Knock down of *Tc-slp/bf1* typically leads to the loss of gnathal segments and even-numbered trunk segments (Choe and Brown, 2007) (70%, n=10; Fig. 4.7D). Although the antennae are present, they are shorter and buckled compared to the wild type (Fig. 4.7D). I also observed weaker phenotypes with two pairs of legs and gnathal appendages which show features of maxillary or labial palps (30% and not shown). In addition to the observed ventral defects, the median part of the vertex, the bell row and the maxilla escort bristles are affected after *Tc-slp/bf1* RNAi (Fig. 4.7D' and Table S2).

In Yang et al., 2009b a broad role of *Tc-eya* in head patterning has been mentioned, but not shown. RNAi against *Tc-eya* leads to the loss of the complete dorsal head capsule, including

the labrum and the antennae, in 46,2% of the analyzed cuticles (n=13) (Fig. 4.7E). The ventral part of the head, represented by the gnathal appendages, seems unaffected (Fig. 4.7E). However, in some of these larvae the mouthparts are highly reduced (not shown). These could be secondary effects due to the loss of large portions of dorsal head tissue. In weaker phenotypes, where the dorsal head is still present, the analysis of the bristle pattern reveals that the lateral portion of the head capsule is most sensitive to the RNAi effect (Fig. 4.7E' and Table S2).

Tc-optix/six3 knock down leads to the loss of the labrum and clypeolabral parts of the anterior head capsule (Posnien et al., accepted for publication) (100%, n=16; Fig. 4.7F). In line with the loss of anterior median cuticle, the anterior vertex seta and the anterior vertex bristle are missing (Fig. 4.7F' and Table S2). In addition, the median part of the dorsal head cuticle displays an undefined pattern of additional bristles and setae (Fig. 4.7F' and Table S2).

The single knock down experiments for *Tc-ey/pax6* and *Tc-toy/pax6* only revealed bristle pattern defects (see below and Fig. 4.8B and Fig. 4.8G). In eye development both genes act synergistically (Yang et al., 2009a). Therefore I performed double knock down experiments. In double RNAi cuticles the whole head capsule is reduced in size. Especially the junction between the posterior head and the thorax is affected (Fig. 4.7G). All dorsal and lateral bristles, except the anterior vertex and the labrum quartet, are affected after double RNAi (Fig. 4.7G' and Table S2). The comparison to single RNAi experiments reveals a 1,4 to 6 fold increase of the penetrance of bristle pattern defects using the same concentration of dsRNA (Table S3). This implies that the two *Tribolium pax6* orthologs act synergistically in head patterning.

The most obvious phenotype of *Tc-lim1/5* RNAi larvae is a compacted and shortened head (16,7%, n=12; Fig. 4.7H). Despite their presence, the head appendages are mostly malformed. For example, the mandibles appear more roundish and the tips of the antennae are missing (41,7%; Fig. 4.7H). The labrum seems to be unaffected (not shown). Corresponding to the defects in appendages, the anterior and median maxilla escort bristles fail to form (Fig. 4.7H' and Table S2). In 20,8% (n=12 times two halve sides) of the larvae no bell row is observed (Fig. 4.7H' and Table S2), suggesting that the shortened heads may be a consequence of missing tissue in this posterior region of the head capsule.

Tc-scro/nkx2.1 RNAi results in an obvious labrum phenotype (73%, n=15) (Fig. 4.7I). In 60% of the analyzed larvae the labrum fails to fuse (Fig. 4.7I). Some weaker phenotypes show proximally fused labral limbs, whereas the distal portion is unfused (13,3%; not shown). The bristle pattern remains more or less unaltered after RNAi. Only the anterior vertex bristle,

which probably belongs to the clypeolabral region, is lost in some larvae (Fig. 4.7I' and Table S2). Interestingly, the labrum quartet bristles are unaltered, although the labrum remains unfused (Fig. 4.7I' and Table S2).

In *Tc-rx* knock down larvae the labrum is narrower than in wild type larvae, which leads to a widened space between the labrum and the antennae (25%, n=8; Fig. 4.7J). In accordance with this observation, the clypeus bristles of the labrum quartet is lost in more than half of the analyzed RNAi larvae (Fig. 4.7J' and Table S2). Additionally, the antenna basis bristle and the median maxilla escort seta is sensitive to *Tc-rx* knock down (Fig. 4.7J' and Table S2). *Tc-six4* RNAi leads to minor defects in the clypeolabral region between the labrum and the antennae (100%, n=8; Fig. 4.7K). On the level of the dorsal bristle pattern, the posterior vertex bristle and antenna basis bristle of the vertex are affected after *Tc-rx* knock down (Fig. 4.7K' and Table S2).

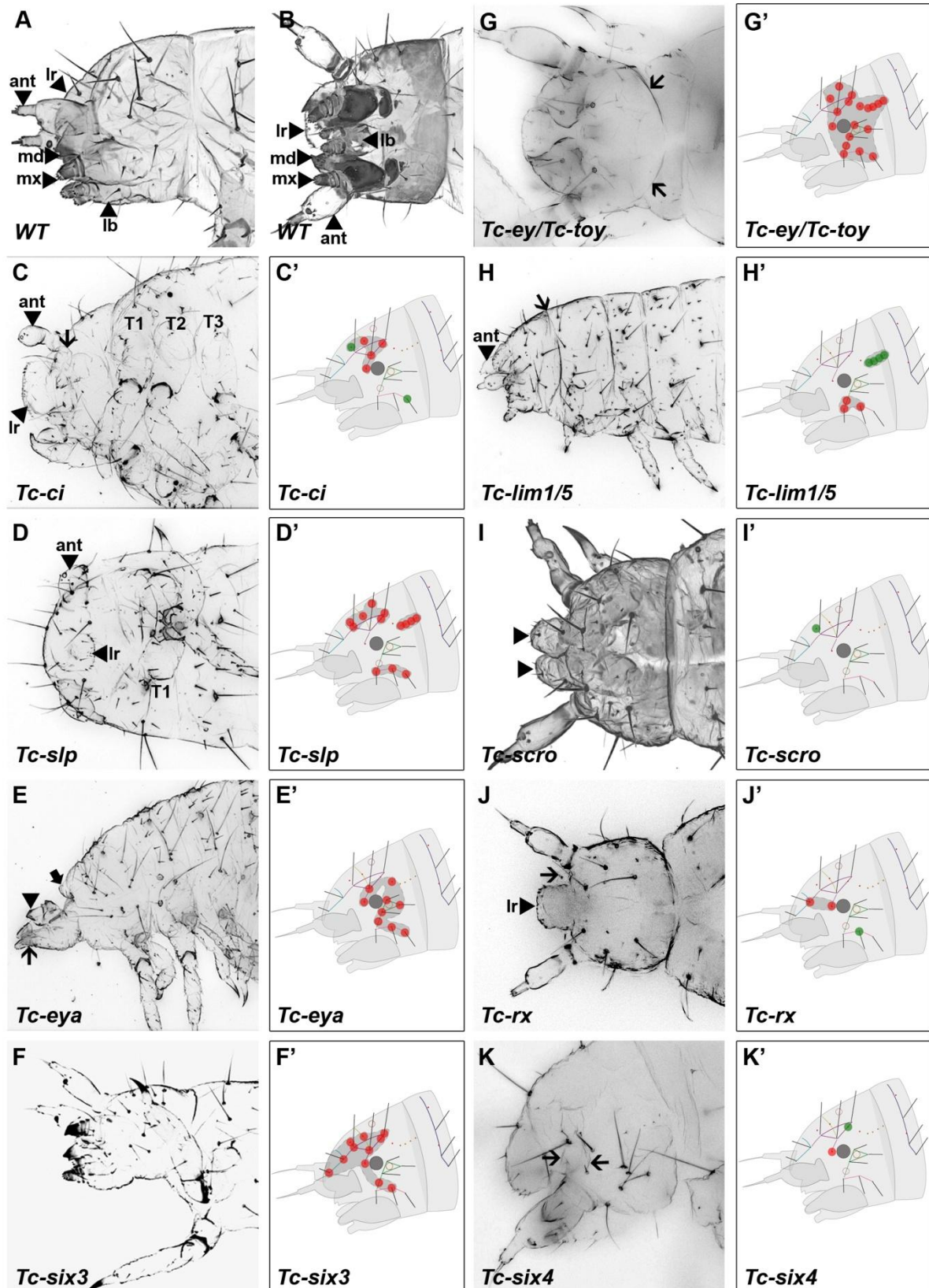


Fig. 4.7: Genes whose knock down results in severe defects in larval cuticles.

Larval head cuticles (C-K) and schematic representations of bristle pattern defects are depicted (C'-K'). All larval heads are oriented with the anterior to the left. The bristle pattern defects are described in the text. See Fig. 4.8 for a legend of the bristle pattern analysis.

Lateral view of a wild type larval head cuticle (A). Ventral view of a wild type larval head cuticle (B). Phenotype of *Tc-ci/gli3* RNAi (C) with affected antennae, remnants of a gnathal appendage (arrow in C) and a

normal labrum. In *Tc-slp/bfl* RNAi cuticles (D) only T1, affected antennae and a reduced labrum are visible. Even numbered segments and the the gnathal segments are missing. *Tc-eya* RNAi results in the loss of dorsal tissue (E). Remaining structures are mandible like (arrowhead) and maxilla like (arrow) appendages and remnants of the dorsal cuticle (bulky arrow). In *Tc-optix/six3* RNAi larvae anterior median tissue including the labrum is missing (F). After *Tc-ey/pax6* and *Tc-toy/pax6* double knock down the entire posterior head region is free of bristles (G). Further, the posterior transition between head and thorax is affected (arrows in G). *Tc-lim1/5* RNAi results in shortened head capsules and malformed appendages (H, the arrow marks the interface between head and thorax). In *Tc-scro/nkx2.1* RNAi larvae the labrum remains unfused (I, the arrowheads mark the two individual labrum parts). *Tc-rx* knock down results in an enlarged distance between the labrum and the antennae (arrow in J). This could be due to a narrower labrum (J). After *Tc-six4* RNAi the region between the labrum and the antennae is affected (the arrows point to folds in this region, K).
ant-antenna, lb-labium, lr-labrum, md-mandible, mx-maxilla, T1-first thoracic segment, T2-second thoracic segment, T3-third thoracic segment

4.1.4.2 Genes whose knock down leads to minor defects in the dorsal bristle pattern

Phenotypes that are restricted to defects in the dorsal bristle pattern are shown in Fig. 4.8 and Table S2. Some genes only show lateral bristle pattern defects (gena triplet and maxilla escort) upon RNAi (*Tc-dbx*, *Tc-ey/pax6* and *Tc-gsc*; Fig. 4.8A,B,C). Knock down of some candidates only leads to dorsal bristle pattern defects (bell row and vertex) (*Tc-ptx/pitx*, *Tc-mirr/irx* and *Tc-Dll/Dlx*; Fig. 4.8D,E,F). Some genes are responsible for more global bristle pattern defects (*Tc-toy/pax6*, *Tc-so/six1*, *Tc-fez* and *Tc-tll/tlx*; Fig. 4.8G,H,J,K).

For *Tc-mun/arg* I was not able to observe expression during early development (two independent probes were used for in situ hybridization). But I cloned this gene from embryonic cDNA (0-48h), showing that it is indeed expressed at these stages. Therefore I injected *Tc-mun/arg* dsRNA. Interestingly, the knock down results in a significant loss of bristles (Fig. 4.8I). This suggests that the expression might start very late in stages which were not analyzed. Another explanation could be that the endogenous expression level of *Tc-mun/arg* is below the detection sensibility.

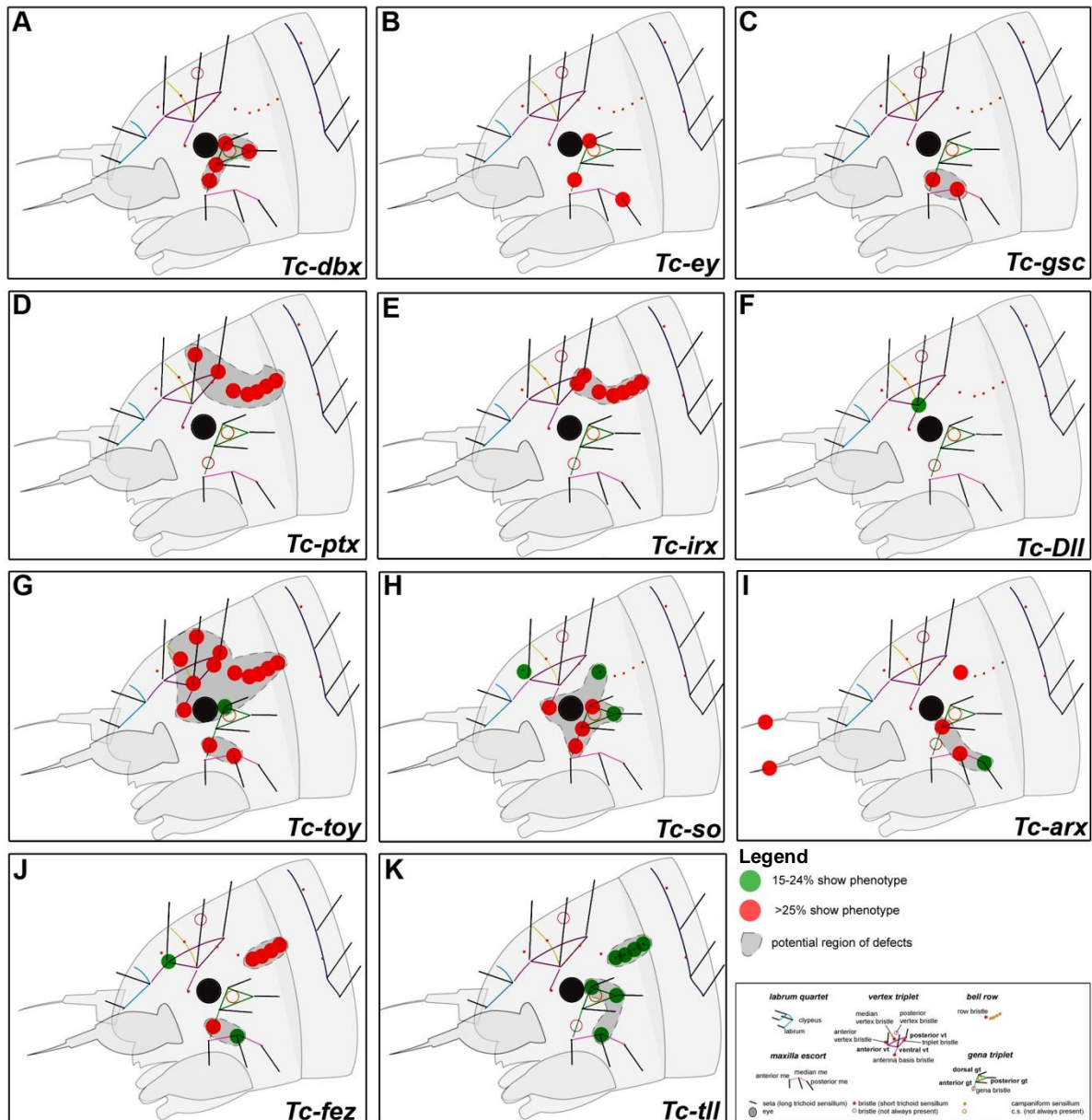


Fig. 4.8: Genes whose knock down results in minor defects in larval cuticles.

Schematic representations of bristle pattern defects are depicted. All larval heads are oriented with the anterior to the left. Assumed that not only the bristles itself are affected after RNAi, but also the tissue surrounding them, one can predict a potential region of defects (grey fields).

The knock down of *Tc-dbx* (A), *Tc-ey/pax6* (B) or *Tc-gsc* (C) affects the formation of lateral bristles. RNAi against *Tc-ptx/pitx* (D), *Tc-mirr/irx* (E) or *Tc-Dll/Dlx* (F) mainly affects dorsal bristles. And the knock down of *Tc-toy/pax6* (G), *Tc-so/six1* (H), *Tc-mun/arx* (I), *Tc-fez* (J) and *Tc-tll/tlx* (K) results in more global bristle pattern defects.

The legend for the wild type bristle pattern is taken from Schinko et al., 2008.

4.1.5 Regulatory network of head patterning

The comprehensive expression and RNAi analysis provides the possibility to identify those genes that most likely play important roles in the early patterning network of the head. In

order to find these genes I formulated hypotheses on potential interactions, which are based on the expression data, the virtual expression map and the RNAi results.

4.1.5.1 Tc-optix/six3 represses the expression of Tc-wg/wnt1, Tc-otd1/otx and Tc-ey/pax6

Based on expression and function, *Tc-optix/six3* appears to be an upstream regulator of median head tissue. First, *Tc-optix/six3* marks the anterior pole of the embryo from very early stages on, suggesting an important role in early specification of anterior tissue. Second, *Tc-optix/six3* expression is restricted to the anterior most region of the developing embryo and shows no segmental contribution, indicating a specific role in head patterning (see Fig. 4.1F-J for expression). Third, the knock down of *Tc-optix/six3* affects only a very specific portion of the larval head (see Fig. 4.7F,F' for RNAi phenotype), suggesting a function in the formation of a specific region rather than global involvement as seen for *Tc-otd1/otx* (Schinko et al., 2008) and *Tc-axin* (see chapter 4.2). And finally, a role of *optix/six3* in head patterning in *Drosophila* has not been described.

I hypothesized that *Tc-optix/six3* could repress the expression of *Tc-wg/wnt1*, *Tc-otd1/otx*, *Tc-ey/pax6* and *Tc-rx* because these genes are expressed in non overlapping domains lateral and posterior to *Tc-optix/six3* (compare expression domains in Fig. 5.3). *Tc-scro/nkx2.1* and *Tc-tll/tlx* become active in the *Tc-optix/six3* positive region when its expression is already established (compare expression domains in Fig. 5.3). Hence, *Tc-optix/six3* could be an activator for these genes. In the future visual system *Tc-optix/six3* and *Tc-ey/pax6* are co-expressed, suggesting that *Tc-optix/six3* might be involved in *Tc-ey/pax6* regulation there. I performed pRNAi for *Tc-optix/six3* and subsequently detected the expression of the above mentioned genes.

The expression of *Tc-wg/wnt1* is massively expanded in *Tc-optix/six3* RNAi embryos (Fig. 4.9A,A',B,B'). This expansion is already obvious at early germ band stages when *Tc-wg/wnt1* transcripts are detectable in the median parts of the embryo (compare Fig. 4.9A to A'). In fully elongated germ bands this expansion becomes more prominent because the whole median region of the embryo is *Tc-wg/wnt1* positive after *Tc-optix/six3* RNAi (compare Fig. 4.9B to B').

Also the expression of *Tc-otd1/otx* is altered after *Tc-optix/six3* knock down (Fig. 4.9C,C',D,D'). Instead of only the ocular region, the whole early head lobes express *Tc-otd1/otx* after *Tc-optix/six3* knock down (compare Fig. 4.9C to C'). At elongated germ band

stages the wild type domain appears with strongest expression whereas the median ectopic region of expression is weaker (compare Fig. 4.9D to D').

The expression patterns of *Tc-rx*, *Tc-tll/tlx* and *Tc-scro/nkx2.1* are unchanged after *Tc-optix/six3* knock down (not shown; Fig. 4.9E).

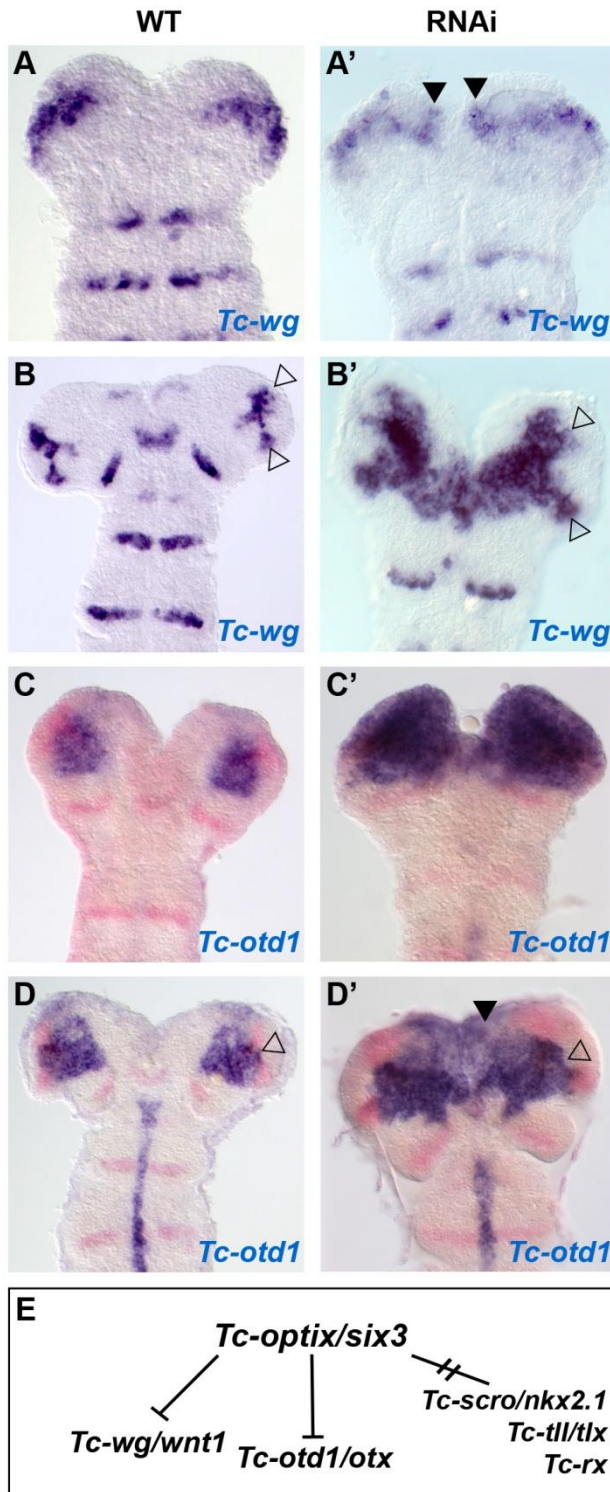


Fig. 4.9: Effects of *Tc-optix/six3* RNAi on *Tc-wg/wnt1* and *Tc-otd1/otx* expression.

Tc-wg/wnt1 and *Tc-otd1/otx* are stained in blue. The *Tc-otd1/otx* marked embryos are double stained with *Tc-wg/wnt1* in red. The heads are oriented with anterior to the top.

Expression of *Tc-wg/wnt1* in wild type embryos (A,B) and in *Tc-optix/six3* RNAi embryos (A',B'). At early stages the knock down of *Tc-optix/six3* results in a median expansion of the ocular *Tc-wg/wnt1* stripe (arrowheads in A' mark the ectopic expression). This expansion is also clearly detectable in later stages (B'; open arrowheads mark the same lateral domains in B and B'). Expression of *Tc-otd1/otx* in wild type embryos (C,D) and in *Tc-optix/six3* RNAi embryos (C',D'). The early expression domain of *Tc-otd1/otx* is massively expanded after *Tc-optix/six3* RNAi (C'). At later stages it is possible to distinguish between the original expression of *Tc-otd1/otx* (open arrowhead in D and D') and the ectopic median expression (arrowhead in D') after *Tc-optix/six3* RNAi. The results are summarized in E.

The effect of *Tc-optix/six3* RNAi on *Tc-ey/pax6* varies depending on the domain (Fig. 4.10). At early germ band elongation stages the *Tc-ey/pax6* domain is heavily expanded towards the midline (compare Fig. 4.10A to A'; the arrow marks ectopic expression in Fig. 4.10A'). But the domains in the anterior-median head lobes are missing or indistinguishable from the expanded ocular domain (compare Fig. 4.10A to A'; the bulky arrow marks anterior-median domain in Fig. 4.10A). At slightly later stages, when the *Tc-ey/pax6* expression is more complex, it is obvious that *Tc-optix/six3* RNAi leads to ectopic expression in the median region (compare Fig. 4.10B to B'). Based on the relative location of the counterstained gene *Tc-dachshund* (*Tc-dac*) to *Tc-ey/pax6* the anterior-median domain of *Tc-ey/pax6* is missing after *Tc-optix/six3* RNAi (compare Fig. 4.10B to B'; bulky arrow marks anterior-median domain in Fig. 4.10B). Additionally, the lateral portion of the ventral ocular domain shows reduced *Tc-ey/pax6* expression in RNAi embryos (compare arrowheads in Fig. 4.10B to B'). Note that *Tc-optix/six3* is expressed in this region (open arrowhead in Fig. 4.11I,J). A similar expression pattern of *Tc-ey/pax6* is also evident at later stages (compare Fig. 4.10C to C'). Again, ectopic expression in the median region is observed (compare Fig. 4.10C to C'; the arrow marks ectopic expression in Fig. 4.10C'). As described above, the anterior-median domain is lost and the ventro-lateral ocular domain is reduced after *Tc-optix/six3* RNAi (compare arrowheads in Fig. 4.10C and C').

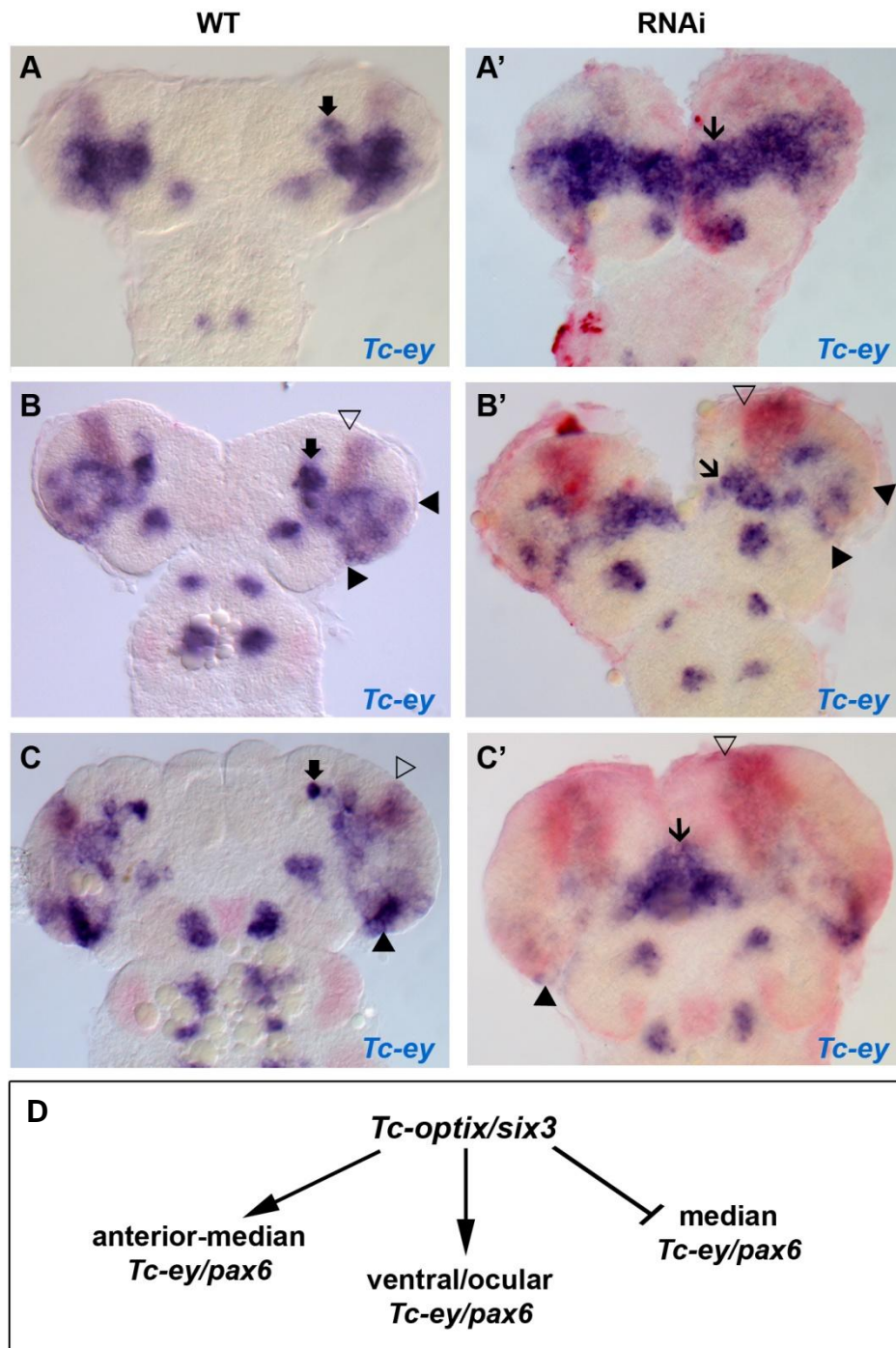


Fig. 4.9: Effects of *Tc-optix/six3* RNAi on *Tc-ey/pax6* expression.

Tc-ey/pax6 is stained in blue. The embryos are double stained with *Tc-dachshund* in red. The heads are oriented with anterior to the top.

Expression of *Tc-ey/pax6* in wild type embryos (A,B,C) and in *Tc-optix/six3* RNAi embryos (A',B',C'). At early stages the knock down of *Tc-optix/six3* results in a median expansion of the ocular *Tc-ey/pax6* domain (arrow in A'). This ectopic median expression is also clearly detectable in later stages (arrows in B',C'). The anterior-medial domain of *Tc-ey/pax6* (marked by the bulky arrow in A-C) is not detectable anymore after *Tc-optix/six3* (A'-C') RNAi. The ventral ocular *Tc-ey/pax6* expression is highly reduced after *Tc-optix/six3* RNAi (arrowheads in B and B' demarcate the ocular region; arrowheads in C and C' mark the ventral ocular region of older stages). The open arrowheads in B,B',C and C' mark the anterior border of the *Tc-dachshund* counterstaining. The results are summarized in D. (Taken from Hein, 2007, Diploma thesis).

In summary, I show extensive expansions towards the anterior midline after *Tc-optix/six3* pRNAi for *Tc-wg/wnt1* and *Tc-otd1/otx*. This implies that *Tc-optix/six3* is involved in the negative regulation of these genes (Fig. 4.9E). Similarly, *Tc-optix/six3* is needed to repress *Tc-ey/pax6* in the median region. In the development of the visual system however, *Tc-optix/six3* seems to be involved in the activation of *Tc-ey/pax6* expression. Importantly, *Tc-optix/six3* is essential for the establishment of *Tc-ey/pax6* positive cells in the anterior-median (Fig. 4.10D).

4.1.5.2 Tc-tll/tlx is necessary for the establishment of specific cells in the anterior head lobes

The expression screen shows that many candidates mark specific sub-regions in the anterior head. *Tc-tll/tlx* expression covers the entire anterior head anlagen from early stage on (Fig. 4.1L-O), indicating that it might be a general activator of anterior genes. As candidates to test this hypothesis I chose *Tc-optix/six3* and *Tc-rx*. *Tc-rx* expression is lying within the *Tc-tll/tlx* domain and becomes activated after *Tc-tll/tlx* expression is already detectable, suggesting an activating function. *Tc-optix/six3* is active long before *Tc-tll/tlx*. But the first observable *Tc-optix/six3* domain is the median stomodeal/labral one. The lateral domains in the head lobes arise after the expression of *Tc-tll/tlx*. Therefore I hypothesized that these lateral *Tc-optix/six3* domains depend on *Tc-tll/tlx* activity. In order to test these two hypotheses, I performed pRNAi for *Tc-tll/tlx* and subsequently analyzed the expression of *Tc-rx* and *Tc-optix/six3*.

Upon *Tc-tll/tlx* pRNAi *Tc-rx* expression is reduced (Fig. 4.11A,A',B,B'). More specifically, at early elongation stages the part of expression which reaches median into the head lobes in wild type embryos is not detectable anymore (compare Fig. 4.11A to A'). At later stages only one part of the expression domain remains active (Fig. 4.11B'). Although it is unclear which part is missing, residual expression on the right side of the knock down embryo suggests that the anterior domain of *Tc-rx* expression is more sensitive to *Tc-tll/tlx* pRNAi (compare black arrowhead in Fig. 4.11B to B').

Tc-optix/six3 expression is similarly reduced after *Tc-tll/tlx* knock down (Fig. 4.11C,C',D,D'). Whereas the median labral and stomodeal domain is unchanged, the lateral domain of early embryos is massively reduced (Fig. 4.11C and C'). In late embryos, large parts of the lateral *Tc-optix/six3* domains, including a few separated posterior cells, are missing after *Tc-tll/tlx* pRNAi (Fig. 4.11D and D').

In all analyzed embryos some cells maintain their respective expression. It is not possible to fully exclude that the remaining expression domains are due to incomplete knock down. Control experiments are required to show the complete knock down. In any case, the results indicate that *Tc-tll/tlx* is involved in the activation of *Tc-rx* and *Tc-optix/six3* (Fig. 4.11E).

Tc-tll/tlx RNAi only results in mild defects in epidermal development (Fig. 4.8K). It could therefore be involved in neural patterning rather than epidermal patterning. In *Drosophila* it has been shown that *Dm-tll* is essential for the formation of specific neuroblasts in the future anterior protocerebrum (Younossi-Hartenstein et al., 1997). Therefore I checked if *Tc-rx* and *Tc-optix/six3* are indeed expressed in a region, in which neuroblasts are formed. The double labeling of *Tc-optix/six3* and the neural precursor marker *Tc-asense* (*Tc-ase*) shows a clear overlap of the expression (Fig. 4.11F). Considering that *Tc-rx* directly abuts *Tc-optix/six3* expression posteriorly (Fig. 4.11G), I conclude by comparing *Tc-ase* and *Tc-rx* expression that neuroblasts also arise from *Tc-rx* positive tissue (compare Fig. 4.11F and G). The co-expression of *Tc-ase* with *Tc-optix/six3* and most likely with *Tc-rx* in the region which is also affected after *Tc-tll/tlx* RNAi suggests, that *Tc-tll/tlx* might be essential for the activation of neural precursor cells in this region.

In summary, I show that *Tc-tll/tlx* is necessary for the establishment or maintenance of *Tc-optix/six3* and *Tc-rx* positive cells which could contribute to anterior protocerebral neuroblasts.

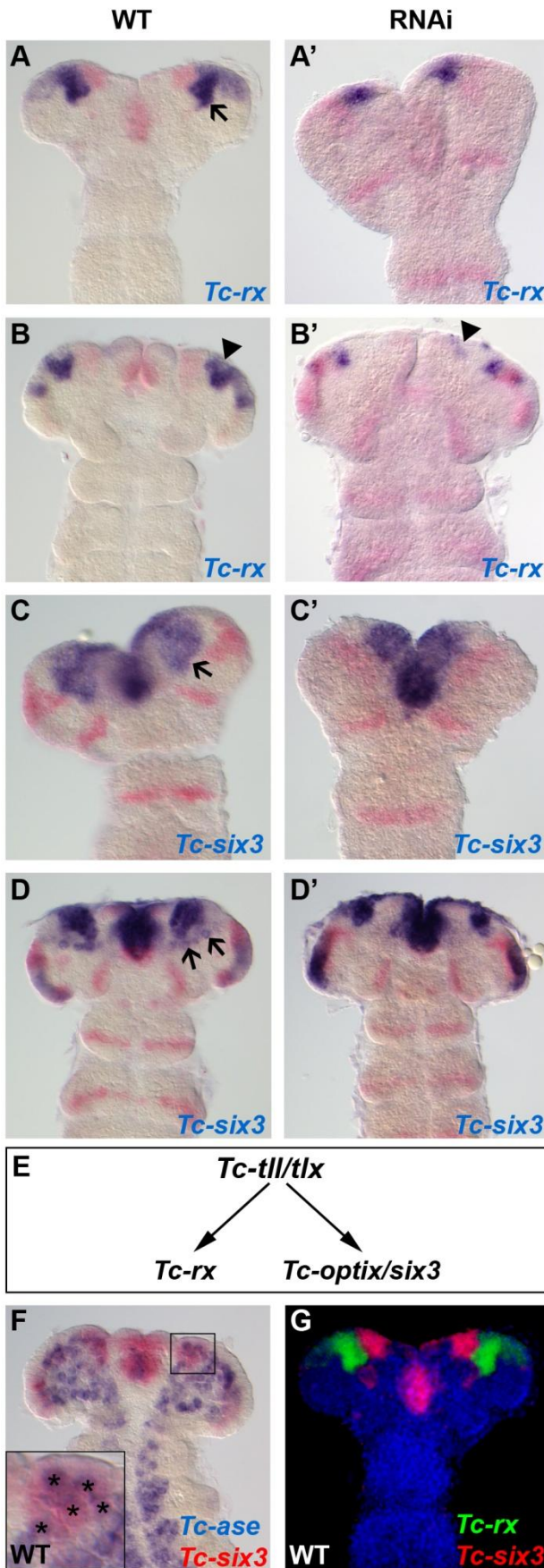


Fig. 4.11: Effects of *Tc-tll/tlx* RNAi on *Tc-rx* and *Tc-optix/six3* expression.

Tc-rx and *Tc-optix/six3* are stained in blue (A-D, A'-D'). The embryos in A and B are double stained with *Tc-optix/six3* in red. The embryos in A'-D' and C,D are double stained with *Tc-wg/wnt1*. The embryo in F is stained for *Tc-ase* (blue) and *Tc-optix/six3* (Richards et al.). The embryo in G is stained for *Tc-rx* (Younossi-Hartenstein et al.) and *Tc-optix/six3* (Richards et al.). The heads are oriented with anterior to the top.

Expression of *Tc-rx* in wild type embryos (A,B) and in *Tc-optix/six3* RNAi embryos (A',B'). At early stages the knock down of *Tc-optix/six3* results in reduced expression of *Tc-rx* (A'). Affected cells are most likely located in a more median region of the *Tc-rx* domain (arrow in A). The arrowheads in B and B' mark the same domains. Expression of *Tc-optix/six3* in wild type embryos (C,D) and in *Tc-tll/tlx* RNAi embryos (C',D'). After *Tc-tll/tlx* RNAi median located *Tc-optix/six3* positive cells (arrows in C,D) are lost (C'D'). The RNAi results are summarized in E. *Tc-optix/six3* positive cells coexpress the neural precursor marker *Tc-ase* (stars in F). *Tc-rx* expression posteriorly abuts *Tc-optix/six3* expression (G).

4.1.5.3 Tc-eya, Tc-so/six1 and Tc-six4 form a regulatory network to establish the anterior most rim of the developing embryo

The vertebrate *eya/six1/six4* genes are involved in patterning cranial placodes at the anterior rim of the neural plate (Schlosser, 2006; Schlosser and Ahrens, 2004). In *Tribolium* *Tc-eya*, *Tc-so/six1* and *Tc-six4* show a similar expression at the rim of the embryonic head lobes (see Fig. 4.6). Whereas *Tc-six4* exclusively marks the anterior most rim region, the other two genes are expressed additionally in the lateral eye lobe tissue and in the stomodeal region. A function of *Tc-eya* and *Tc-so/six1* in visual system development has been shown for *Tribolium* (Yang et al., 2009b). However, the relationship of these genes within the anterior portion of the head lobes has not been studied. The dynamic expression profile in combination with large overlapping domains of the three mentioned genes in the anterior region suggests that they regulate each other during early development. Based on the expression profiles I hypothesize that *Tc-eya* is involved in the activation of *Tc-six4* and *Tc-so/six1*, whereas the latter two repress each other (see also Fig. 5.3D).

Tc-eya is expressed from early stages on (see Fig. 4.6A-D). *Tc-so/six1* expression follows the one of *Tc-eya* in largely overlapping domains (see Fig. 4.6I-J). This suggests a function of *Tc-eya* in establishing *Tc-so/six1*. Indeed, the knock down of *Tc-eya* via aRNAi leads to strong reduction of *Tc-so/six1* (compare Fig. 4.12A to C and B to D). In strongly affected embryos, the expression of *Tc-so/six1* is completely absent (not shown). Hence, *Tc-eya* is essential for the establishment of *Tc-so/six1* expression.

At late elongating germ band stages the expression of *Tc-so/six1* starts to disappear in the anterior rim region (Fig. 4.6J). Slightly earlier, the expression of *Tc-six4* starts in this region (Fig. 4.6L,M). This relationship suggests that *Tc-six4* represses *Tc-so/six1* activity in the anterior head. Indeed, *Tc-six4* knock down leads to ectopic anterior *Tc-so/six1* expression at late embryonic stages (compare black arrowheads in Fig. 4.12E,F to B). The embryo in Fig. 4.12E corresponds to the one shown as wild type control (Fig. 4.12B). The embryo in Fig. 4.12F represents a later stage. In the wild type situation, I never observed anterior *Tc-so/six1* expression in embryos older than the one shown in Fig. 4.12B. My results show that *Tc-so/six1* in the anterior rim region is repressed by *Tc-six4* activity.

Finally, I wanted to know how *Tc-six4* expression is established. *Tc-so/six1* is expressed prior to *Tc-six4* in the anterior rim region. Therefore I analyzed *Tc-six4* expression in *Tc-so/six1* aRNAi embryos. *Tc-six4* expression is reduced after *Tc-so/six1* knock down (compare Fig. 4.12G' to G and H' to H). The remaining expression could be due to incomplete knock down.

Another hypothesis would be that *Tc-so/six1* alone is not sufficient to activate *Tc-six4* expression. Since *Tc-eya* and *Tc-so/six1* are expressed simultaneously in the anterior rim region prior to *Tc-six4* onset, it is rather possible that both genes have a redundant function activating *Tc-six4*.

My data shows that *Tc-eya*, *Tc-so/six1* and *Tc-six4* act together in a hierarchical regulatory network to establish the anterior rim of the head lobes (Fig. 4.12I).

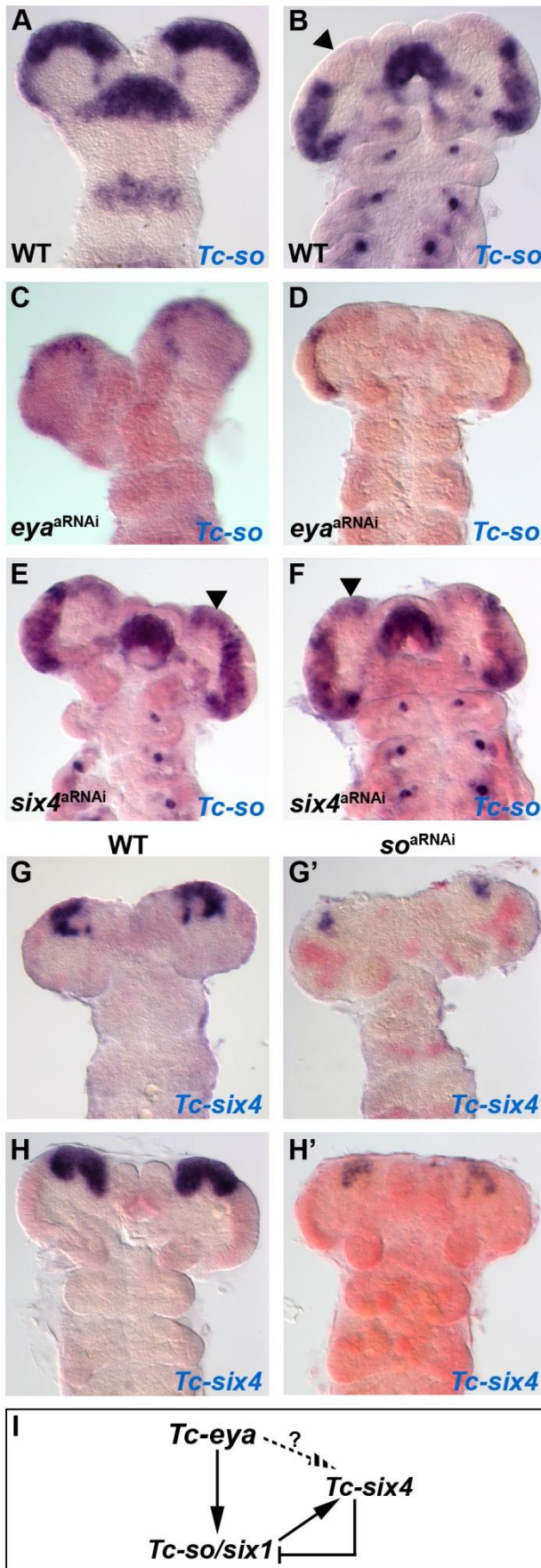


Fig. 4.12: Regulatory interactions of *Tc-eya*, *Tc-so/six1* and *Tc-six4*.

Tc-so/six1 and *Tc-six4* are stained in blue. The embryos are double stained with *Tc-wg/wnt1* in red. The heads are oriented with anterior to the top. Wild type expression of *Tc-so/six1* in an early elongating germ band and in a retracting germ band (A,B). The anterior-medial region is free of *Tc-so/six1* expression at retraction stages (arrow in B). After *Tc-eya* RNAi the expression of *Tc-so/six1* is reduced (C,D). The knock down of *Tc-six4* results in ectopic anterior-medial expression of *Tc-so/six1* (arrowheads in E,F). Wild type stains of *Tc-six4* (G,H). The knock down of *Tc-so/six1* results in reduced expression of *Tc-six4* (G' and H' for two different stages). The results are summarized in I.

4.1.6 Analysis of *six3* interactions in *Xenopus laevis*

The candidates for my screen were chosen because of their involvement in vertebrate neural plate patterning and their expression is conserved to a large degree (see discussion and Fig. 5.3). Therefore, I also wanted to test if the interactions I found in *Tribolium* might be conserved. In order to gain first insights into the conservation of specific interactions, I decided to analyze the *six3* interaction which I observed in *Tribolium* in *Xenopus laevis* as vertebrate model. I cloned the complete ORF of the *Xenopus laevis* *Xsix3* gene and synthesized mRNA for overexpression studies (Gestri et al., 2005). Furthermore, I used antisense morpholinos to analyze loss of function effects (Gestri et al., 2005, Gene Tools). I injected one blastomere of 2-cell stages and subsequently observed expression of the *Xenopus* genes *Xotx2*, *Xpax6*, *Xwnt1*, *Xtlx* and *Xnkx2.1*.

The expression patterns of *Xotx2*, *Xtlx* and *Xnkx2.1* remained unchanged after the above mentioned manipulations (not shown).

The overexpression of *Xsix3* leads to the expansion of *Xpax6* expression in the injected halve side (Fig. 4.13A-C). Contrary, the knock down of *Xsix3* results in reduced *Xpax6* expression domains in the injected halves (Fig. 4.13D-F). Hence, *Xsix3* is involved in the activation of *Xpax6* in the anterior region of the neural plate. This relationship of both genes is similar to the one observed for the anterior-median and ventro-lateral ocular *Tc-ey/pax6* domain. However, no repressive effect of *Xsix3* on *Xpax6* like in early *Tribolium* embryos was detectable in the stages I analyzed.

Similarly, the loss of *Xsix3* function leads to a significant reduction of *Xwnt1* expression (Fig. 4.13H). The overexpression of *Xsix3* leads to contradicting results, namely the same percentage of *Xwnt1* expansion and reduction (Fig. 4.13G shows an embryo with expanded expression). These preliminary results suggest that *Xsix3* is involved in *Xwnt1* regulation.

In Fig. 4.13I the results for *Xpax6* and *Xwnt1* are quantified and summarized.

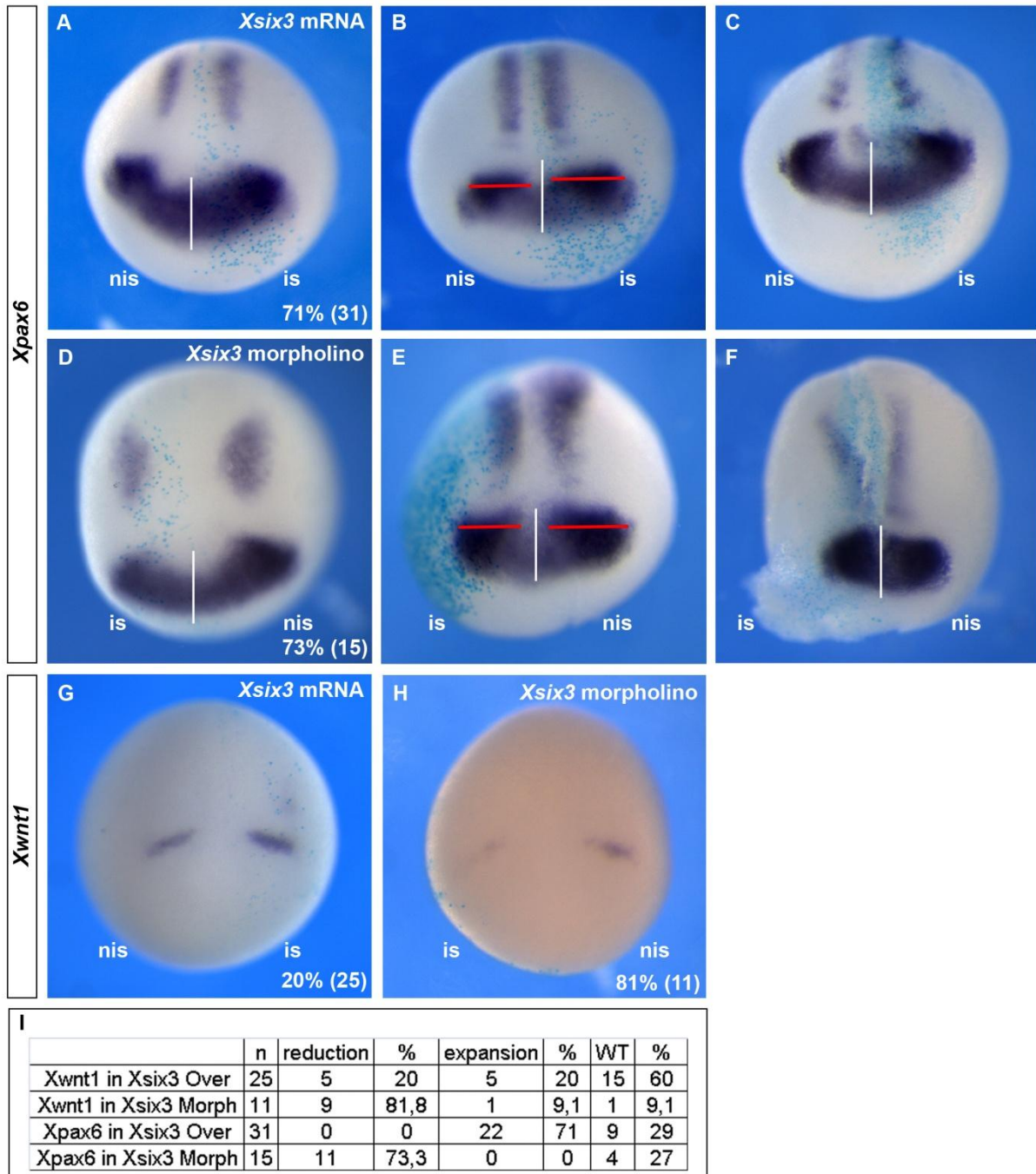


Fig. 4.13: *six3* interactions in *Xenopus laevis*.

Frontal views of *Xenopus laevis* embryos between stage 11 and 13.5 (Nieuwkop and Faber, 1967). Dorsal is oriented to the top. Embryos were stained for *Xpax6* (Garcia-Fernandez) and *Xwnt1* (G,H). The turquoise color in the embryos represents the injected site (is). The white bars in A-F indicate the midline. The percentage of embryos showing the respective phenotype is given in the lower right corner with the number of scored embryos in brackets.

The overexpression of *Xsix3* results in an expansion of *Xpax6* expression (A-C, compare red bars in C). Contrary, the knock down of *Xsix3* results in reduced expression of *Xpax6* (D-F, compare red bars in E). The overexpression of *Xsix3* results in the same number of embryos with expanded and reduced *Xwnt1* expression (I). The embryo shown in G is one with expanded expression of *Xwnt1* in the injected side after *Xsix3* overexpression. The knock down of *Xsix3* results in a reduction of *Xwnt1* expression (H). A quantification of the results is depicted in I.

is-injected site, nis-non injected site, Over-overexpression, Morph-knock down via morpholino

4.2 Wnt-signaling in anterior patterning of *Tribolium castaneum*

In vertebrates, canonical Wnt-signaling is involved in the patterning of the anterior-posterior axis within the neural plate. High levels of Wnt-signals in the posterior region are needed to activate posterior marker genes like the Hox-genes. Contrary, in order to establish anterior brain structures, canonical Wnt-signaling has to be blocked by Wnt-antagonists (Kiecker and Niehrs, 2001). Recent results from *Tribolium* and from the spider *Achaearanea tepidariorum* indicate that Wnt-signaling is similarly involved in the formation of posterior regions in arthropods (Bolognesi et al., 2008b; McGregor et al., 2008). However, the question remains if the requirement of a Wnt-free region for an anterior fate is similarly conserved in arthropods. Therefore, I aimed to analyze the effects of ectopically activated Wnt-target genes in the anterior region of *Tribolium* embryos.

4.2.1 *Tc-axin* is involved in anterior-posterior axis formation

In order to test if canonical Wnt-signaling is involved in the anterior-posterior axis formation I knocked down *Tc-axin*. Within the canonical Wnt-pathway, Axin is incorporated in the β -catenin destruction complex, which degrades β -catenin in the absence of Wnt-signals. When extracellular Wnt-signals are present, the destruction complex becomes inhibited. Hence, β -catenin is not degraded and is able to activate the transcription of target genes (Logan and Nusse, 2004). The knock down of *Tc-axin* therefore leads to a β -catenin accumulation due to a functionless destruction complex. As a consequence, Wnt-target genes are ectopically activated, mimicking an ectopic expression of Wnt-signals.

I knocked down *Tc-axin* via aRNAi and analyzed cuticles of first instar larvae. I injected 1,5 μ g/ μ l and 4,0 μ g/ μ l of the dsRNA and observed the same phenotypes in both independent experiments. The results shown here are based on the results of the 4,0 μ g/ μ l injection. Consecutive egg collections showed that the RNAi effect decreases over time. In the first three collections I only observed empty egg shells after clearing (E in Fig. 4.15A), indicating that in the most strongly affected phenotypes the embryos die before secreting a cuticle. The fourth to sixth collections were done 6.5, 7.5 and 19.5 days after injection. In these collections I observed severely affected larval cuticles (C in Fig. 4.15A) and increasingly also wild type larvae (WT in Fig. 4.15A). The affected larvae were analyzed in more detail and were assigned to three groups based on the severity of the effect, although I observed all

intermediate phenotypes from strong to weak. The strongest phenotypes only possess 2-4 posterior abdominal segments with remnants of the hind gut sticking out (P in Fig. 4.15B and Fig. 4.14B). In the next group, cuticles possess all abdominal segments and one to all three thoracic segments (T in Fig. 4.15B and Fig. 4.14C). The weakest phenotypes show head structures in addition to abdomen and thorax (H in Fig. 4.15B and Fig. 4.14D). According to the fact that the RNAi effect becomes weaker over time, I observed more weak phenotypes after 19.5 days post injection than after 6.5 days post injection (Fig. 4.14B). These results indicate that anterior structures are more sensitive to *Tc-axin* RNAi than posterior ones.

I also analyzed the heads of the weakly affected larvae to substantiate this notion (Fig. 4.15C). Indeed I found that the labrum, as the anterior most located appendage, is more often absent after *Tc-axin* RNAi than the posterior most mouthpart, the labium (Fig. 4.15C). Finally, I examined the bristle pattern of the larvae which possess all mouthparts and a relatively normal head capsule. I found that all dorsal (bell row and vertex) and labrum-associated bristles are affected after *Tc-axin* RNAi (Fig. 4.14E and Table S4). The lateral bristles seem to be less sensitive to the knock down, since the gena triplet setae are, if at all, only weakly affected. Furthermore, two of the three maxilla escord setae are frequently lost or misplaced after RNAi.

Based on the “bend and zipper” model (Posnien and Bucher, submitted), the anterior most embryonic tissue participates in the formation of the dorsal head capsule. Hence, the severely affected dorsal bristle pattern suggests that even in very weak phenotypes, the anterior most tissue is most sensitive to *Tc-axin* knock down.

In summary, my data shows that the knock down of *Tc-axin*, and thereby the up-regulation of Wnt-targets, leads to dose-dependent loss of anterior structures like in vertebrates.

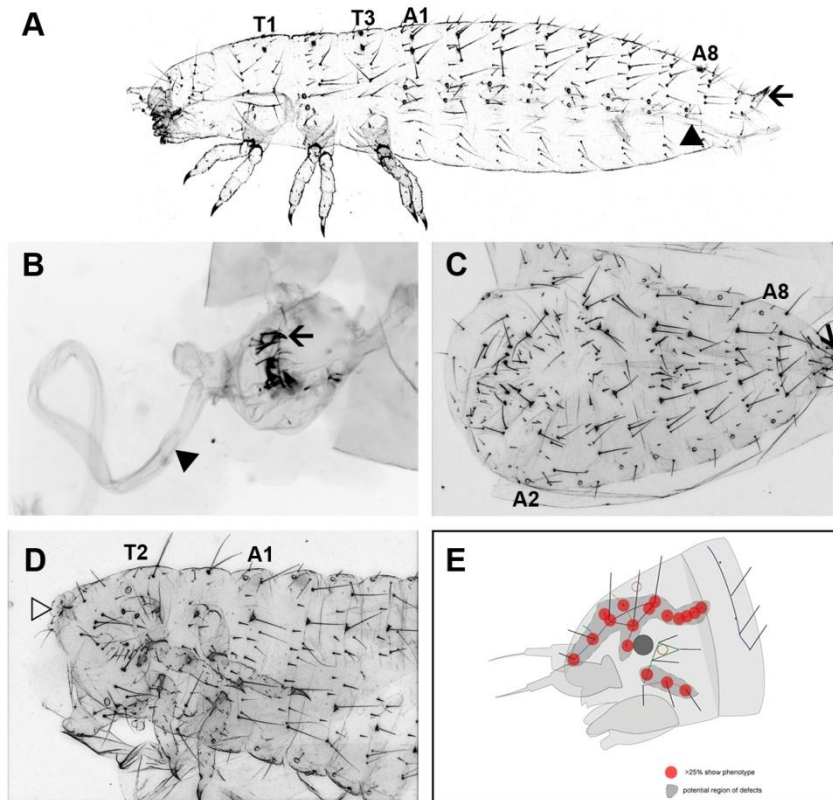


Fig. 4.14: *Tc-axin* RNAi results in anterior truncation of first instar larvae.

First instar larval cuticles (A-D) and a schematic representation of bristle pattern defects are depicted (E). All larvae are oriented with the anterior to the left. The bristle pattern defects are described in the text. See Fig. 4.8 for a legend of the bristle pattern analysis.

Lateral view of a wild type larval cuticle (A). The hindgut is marked by the arrowhead in A. The urogomphi are marked by the arrow in A. The strongest cuticle phenotypes after *Tc-axin* RNAi only consist of posterior cuticle structures (the arrow in B marks the urogomphi) and the hindgut sticking out of it (arrowhead in B). Intermediate phenotypes develop nearly a full abdomen (C, the arrow marks the urogomphi). Weakly affected larvae possess thoracic segments and highly reduced head structures (open arrowhead in D). Even weaker phenotypes develop a head. In these heads nearly all lateral and dorsal bristle are missing, after *Tc-axin* RNAi (E).

A- abdominal segments, T- thoracic segments

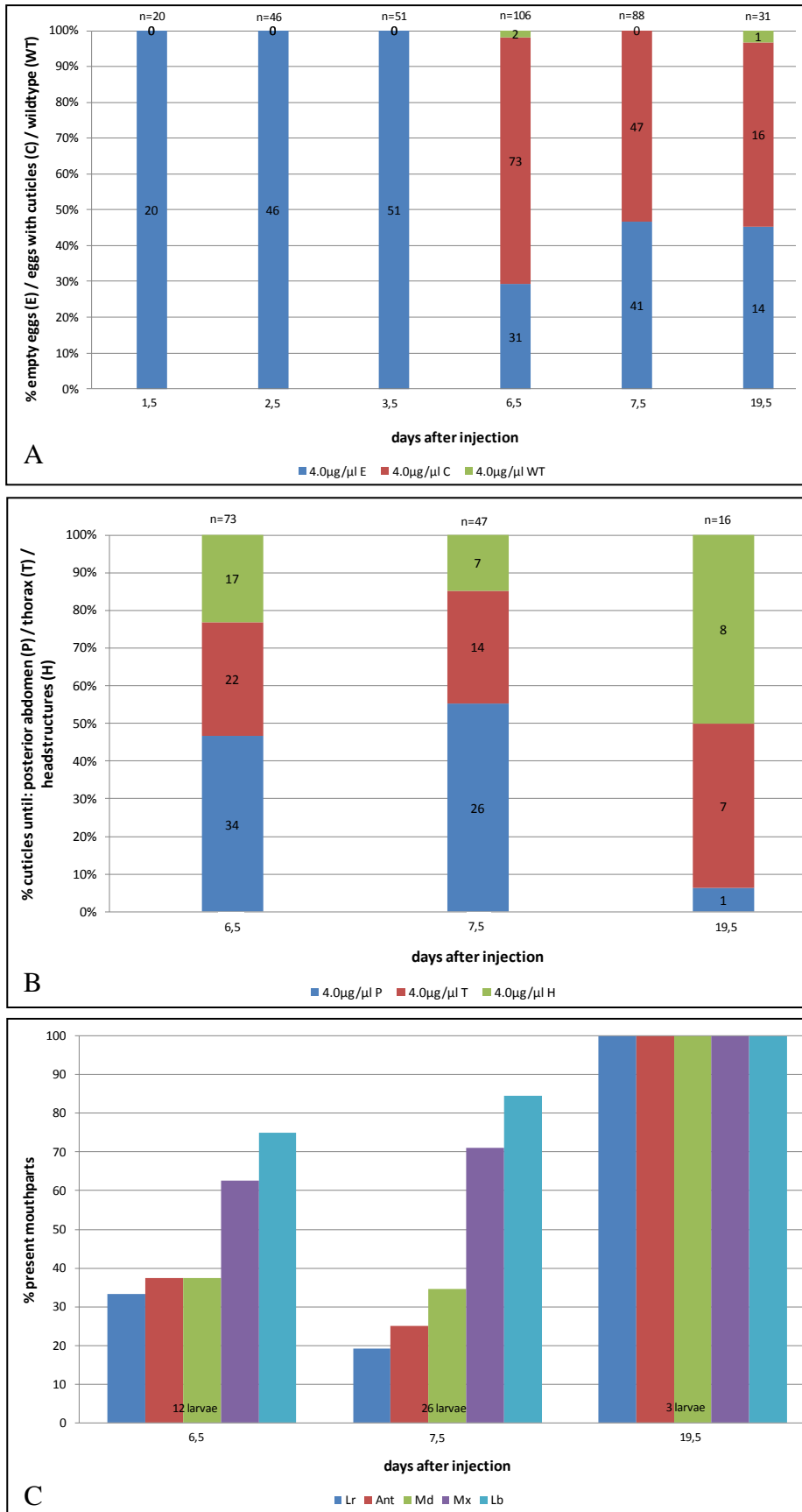


Fig. 4.15: Quantification of the anterior truncations after *Tc-axin* RNAi.

In the first 3.5 days after injection of adult beetles with *Tc-axin* dsRNA only empty egg shells (E in A). 6.5, 7.5 and 19.5 days after injection severely affected larval cuticles were observed (C in A). Also some wild type larvae were scored (WT in A). Some of the affected larvae (6.5, 7.5 and 19.5 days after injection) only

possess 2-4 posterior abdominal segments with remnants of the hind gut sticking out (P in B). Some cuticles possess all abdominal segments and one to all three thoracic segments (T in B). The weakest phenotypes show head structures in addition to abdomen and thorax (H in B). In the weakly affected larvae with head structures the anterior head regions like the labral region are more sensitive to *Tc-axin* RNAi than the more posterior ones (C).

Ant-antenna, Lb-labium, Lr-labrum, Md-mandible, Mx-maxilla

4.2.2 The knock down of *Tc-axin* results in posteriorized embryos

In order to further characterize the observed *Tc-axin* RNAi phenotypes, I analyzed embryos of different stages after knock down. Since Wnt-signaling promotes posterior fate in *Tribolium* and vertebrates (Bolognesi et al., 2008b; Niehrs, 1999), I investigated the expression of the posterior marker *Tc-caudal* (*Tc-cad*) in RNAi embryos (Copf et al., 2004; Schulz et al., 1998). The comparison of RNAi embryos to wild types clearly shows that *Tc-cad*, which is normally restricted to the posterior growth zone, is ectopically expressed throughout the embryo (Fig. 4.16C',D'). This expansion is already observable at early blastoderm stages (compare Fig. 4.16A,B to A',B'). Beside this altered expression pattern, I observed severe morphological changes of the embryo. For example, no signs of segmentation and no appendages are detectable (Fig. 4.16D'). In some embryos it is even impossible to distinguish between anterior and posterior, since no head lobes are visible (Fig. 4.16D'). In some cases with probably weak RNAi effects I still observe head lobes, which interestingly remain free of *Tc-cad* expression (arrow in Fig. 4.16C').

In the above mentioned embryos I detected *Tc-wg/wnt1* transcripts in addition to *Tc-cad*, by applying double in situ hybridization. Interestingly, the *Tc-wg/wnt1* expression remains active after RNAi in the most anterior and posterior parts of the embryos (Fig. 4.16C',D'). In contrast, all other *Tc-wg/wnt1* stripes are not detectable anymore, which is in accordance to the loss of segmental features (see above).

This work was performed in collaboration with Renata Bolognesi and Sue Brown. Their results confirm my findings by including *Tc-deformed/Hox4*, *Tc-AbdA/Hox8* and *Tc-wnt8* as posterior marker genes in RNAi embryos (see chapter 5.2.1).

In summary, the ectopic expression of *Tc-cad* after *Tc-axin* RNAi shows that ectopic Wnt-signaling results in posteriorized embryos like in vertebrates.

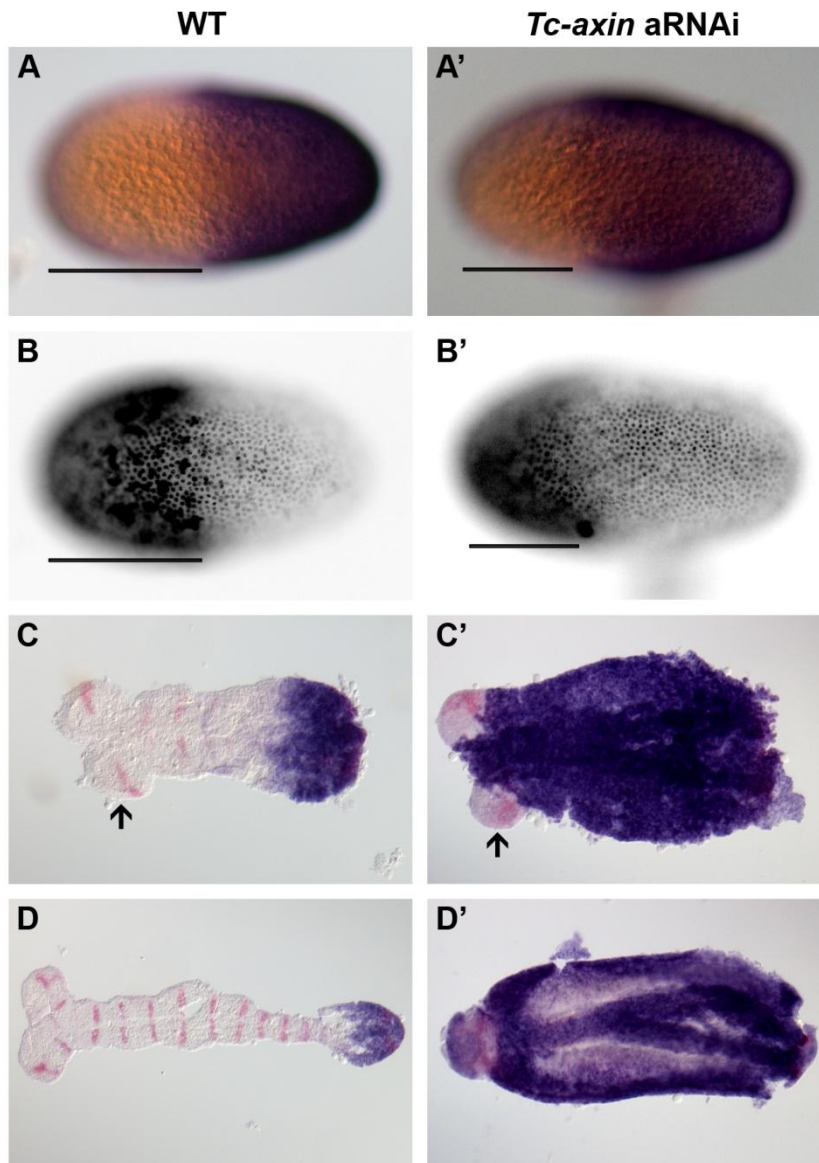


Fig. 4.16: *Tc-axin* RNAi results in posteriorized embryos.

Tc-cad is stained in blue. The embryos are double stained with *Tc-wg/wnt1* in red. The embryos are oriented with anterior to the left.

Tc-cad staining in wild type embryos (A-D) and in *Tc-axin* aRNAi embryos (A'-D'). B and B' are inverted DAPI pictures of the embryos as in A and A'. The darker anterior region corresponds to the *Tc-cad* free part of the egg where the fluorescent signal is not quenched. At blastoderm stages an anterior expansion of *Tc-cad* is detectable after *Tc-axin* RNAi (compare black bars which mark the *Tc-cad* free region in A,B and A'B'). *Tc-cad* is restricted to the posterior growth zone in wild type germ band embryos (C,D). After *Tc-axin* RNAi massive expansions of *Tc-cad* are visible (compare C,D and C',D'). While the head lobes in the early germ band are free of *Tc-cad* expression (arrows in C and C' mark the head lobes) the entire embryo in D' is *Tc-cad* positive. It is not possible to stage the embryo in D' because no segmental markers are visible. It is also not possible to clearly distinguish between anterior and posterior in this embryo (D').

4.3 Development of the intercalary segment

In order to properly interpret defects in head cuticles after RNAi it is necessary to determine what parts of the head are formed by which segments. Specifically, it has remained unclear to

what parts of the larval head cuticle the intercalary segment contributes to. The anterior most Hox-gene *labial/Hox1* (*lab/Hox1*) is specifically expressed in the intercalary segment (Diederich et al., 1989; Merrill et al., 1989; Nie et al., 2001). So far, the function of *labial* remained unclear because loss of function in *Drosophila* leads to head involution defects and therefore results in several secondary defects (Diederich et al., 1989; Merrill et al., 1989). Since analysis of head development in *Tribolium* is not hampered by morphological constraints, I used RNAi knock down of *Tc-lab* to investigate its function and to reveal the contribution of the intercalary segment to the head cuticle.

4.3.1 Delayed specification of the intercalary parasegment boundary

I first searched for segmentally expressed genes which mark different parts of the intercalary segment. I analyzed the expression of *Tc-slp1*, *Tc-wg*, *Tc-hh* and *Tc-mirror/irx* and the late marker *Tc-ey/pax6* (Choe and Brown, 2007; Choe et al., 2006; Farzana and Brown, 2008; McNeill et al., 1997; Nagy and Carroll, 1994). In all segments, the posterior boundary is marked by the expression of *Tc-hh* (Fig. 4.17C-C'' and Fig. 4.18H) (Farzana and Brown, 2008). Anteriorly adjacent, *Tc-wg* is expressed, although this domain is narrower than the *Tc-hh* expression (Fig. 4.17C'-C'') (Nagy and Carroll, 1994). *Tc-slp1* expression covers the *Tc-wg* domain but extends both anteriorly and to some extent also posteriorly, overlapping the anterior most *Tc-hh* expressing cells (Fig. 4.17D-D'' and Fig. 4.18G) (Choe et al., 2006). Also anterior to *Tc-wg*, but overlapping only slightly, I found *Tc-ey/pax6* expression in the region of the ventral neuroectoderm (Fig. 4.17F-F'' and Fig. 4.18F). And finally, I found *Tc-mirror/irx* expression at the anterior boundary of each segment (Fig. 4.17B-B'' and Fig. 4.18E) as also shown for *Drosophila* (McNeill et al., 1997). In contrast to other segments, intercalary *Tc-mirror/irx* additionally marks median cells, reaching posteriorly to the mandibular segment boundary (white arrowhead in Fig. 4.18E). Note the unique morphology of the intercalary segment: whereas the posterior border marked by *Tc-hh* and *Tc-wg* is perpendicular to the body axis, the anterior border marked by *Tc-mirror/irx* is parallel to the antennal parasegment boundary which is turned outwards with respect to the posterior trunk segments.

A detailed temporal analysis of the expression of these marker genes shows that formation of the intercalary parasegment boundary is strongly delayed compared to the adjacent antennal and mandibular parasegment boundaries (see *Tc-wg*, *Tc-hh* and *Tc-slp1* in Fig. 4.17G). The

Tc-engrailed stripe appears approximately at the same stage as *Tc-hh* (Brown et al., 1994). However, the intercalary/mandibular boundary is prefigured pretty early by adjacent expression of *Tc-cnc* and *Tc-lab* and marked by *Tc-col/knot* expression which suggests a crucial role of these genes in intercalary segment formation also in *Tribolium* (Economou and Telford, 2009; Mohler et al., 1995; Seecoomar et al., 2000). Interestingly, the delay also affects the anterior portion of the mandibular segment as shown by *Tc-mirror/irx* expression.

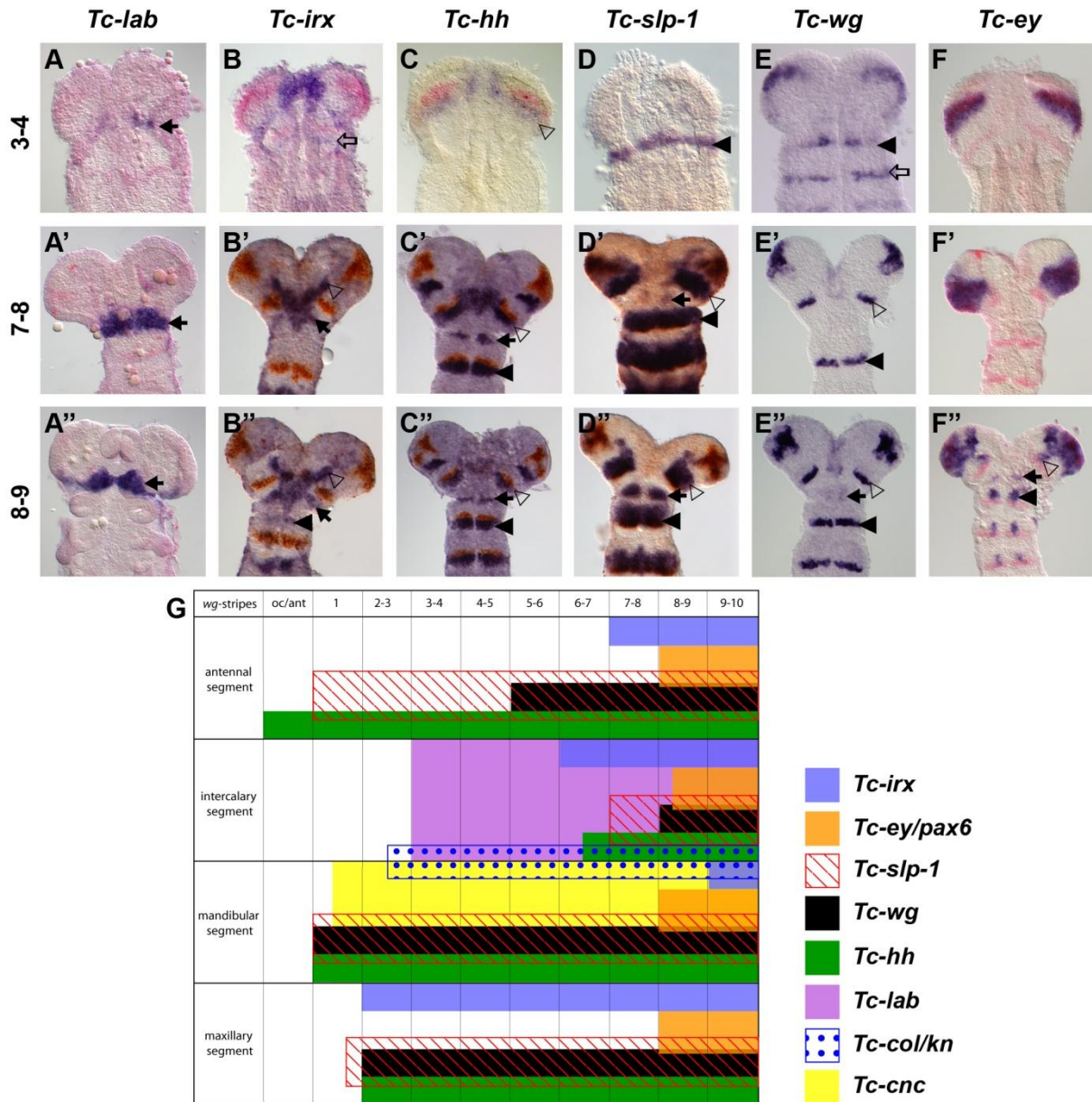


Fig. 4.17: Temporal analysis of marker gene expression in the intercalary segment.

Marker gene expression (blue staining in all pictures) in embryonic heads is shown at three different time points of development (3-4 *wg*-stripe stage, 7-8 *wg*-stripe stage and 8-9 *wg*-stripe stage). Anterior is oriented to the top. The counterstaining in red or brown represents *Tc-wg* transcripts (except A-A'' and E-E''). A) The first indication for the intercalary segment becomes evident by the first *Tc-lab* expressing cells at a 3-4 *wg*-stripe stage (black arrow). A'-A'') *Tc-lab* stays expressed in the intercalary segment until germ band elongation (black arrows). B) At the 3-4 *wg*-stripe stage the only segmental *Tc-mirror/irx* expression is found in the maxilla (open

arrow). B') At the 5-6 *wg*-stripe stage the first sign of intercalary *Tc-mirror/irx* expression becomes visible (black arrow) parallel to the antennal *Tc-wg* stripe (open arrowhead). B'') Only late at the 9 *wg*-stripe stage the mandibular *Tc-mirror/irx* expression arises (black arrowhead). C) In early germ band stages *Tc-hh* is expressed in an ocular-antennal stripe (open arrowhead; see also Farzana and Brown, 2008). Slightly later mandibular expression becomes evident (not shown). C'-C'') From the 6-7 *wg*-stripe stage on *Tc-hh* transcripts can be detected in the intercalary segment (black arrow) and the adjacent antennal (open arrowhead) and mandibular segment (black arrowhead). D) *Tc-slp1* is first expressed in a broad mandibular stripe (black arrowhead; see also Choe and Brown, 2007). D') At a 7-8 *wg*-stripe stage weak *Tc-slp1* expression becomes visible in the intercalary segment (black arrow). In the antennal (open arrowhead) and the mandibular segment (black arrowhead) *Tc-slp1* is strongly expressed. D'') Slightly later the intercalary *Tc-slp1* domain becomes clearly visible (black arrow). E) *Tc-wg* expression is already established in the mandibular (black arrowhead) and the maxillary segment (open arrow). E') At the 5-6 *wg*-stripe stage *Tc-wg* expression starts in the antennal segment (open arrowhead). E'') Only late at a 8-9 *wg*-stripe stage first signs of intercalary *Tc-wg* expression (black arrow) become evident between the antennal (open arrowhead) and the mandibular domain (black arrowhead). F-F') Throughout early germ band stages no segmental *Tc-ey/pax6* expression can be detected. F'') At the 8 *wg*-stripe stage segmental *Tc-ey/pax6* expression is observed in the antennal (open arrowhead), mandibular (black arrowhead) and subsequent segments. The intercalary *Tc-ey/pax6* expression (black arrow) is only slightly delayed. G) Schematic representation of temporal aspects of marker gene expression in the antennal, intercalary, mandibular and maxillary segments. Note that width and position of the bars reflect their location in the embryonic segments. Intercalary *Tc-engrailed* is not shown but appears at a similar stage as *Tc-hh* (7 *wg*-stripe stage; Brown et al. 1994). *Tc-cnc* and *Tc-col* are based on Economou and Telford, 2009.

4.3.2 *Tc-labial* function is required for the formation of lateral parts of the head cuticle

Tc-labial is the anteriormost gene of the Hox-cluster and marks the entire intercalary segment in *Tribolium* (Fig. 4.18A-D), other insects and the corresponding second antenna in crustaceans (Abzhanov and Kaufman, 1999). I extended the previously described pattern (Nie et al., 2001) to embryos undergoing retraction and surprisingly found expression domains of *Tc-lab* in the roof of the stomodeum (white arrowhead in Fig. 4.18D) and the roof of the proctodeum (the latter has also been found in *Drosophila*, not shown). The intercalary domain elongates during retraction and eventually becomes split into a median domain and a domain located in the lateral head lobes (black arrow in Fig. 4.18D). These domains appear to be separated by the mandible which is moving anterior with respect to the stomodeum. In the latest stainable embryonic stages the median *Tc-lab* domain becomes undetectable.

In order to reveal the contribution of the intercalary segment to the larval head cuticle, I knocked down the *Tribolium Hox1* ortholog *Tc-lab*. I examined the head bristle pattern of both halve sides of 10 larvae (for a description of the wild type pattern see Schinko et al., 2008). In none of these 20 independently analyzed halve sides could I observe any indication for a homeotic transformation. Rather, a set of bristles is missing: the posterior gena triplet bristle (80%), the dorsal gena triplet bristle (20%), the median maxilla escort bristle (70%) and the posterior maxilla escort bristle (100%) (Fig. 4.18I' and Table S5). Assuming that not only the bristles themselves are missing, but also surrounding tissue, a large portion of the lateral head is lost after *Tc-lab* RNAi.

4.3.3 Knock down of *Tc-lab* leads to loss of the intercalary segment

In order to understand the genesis of the cuticle phenotype, I examined the set of marker genes in the RNAi background. I concentrated on late elongation stages (between 10 and 14 *wg*-stripes) for the spatial analysis since at this stage the intercalary segment is well established. After knock down of *Tc-lab* I found a complete loss of intercalary *Tc-hh*, *Tc-wg*, *Tc-slp1* and *Tc-ey/pax6* expressions (compare black arrows in Fig. 4.18F-H to F'-H'). The anterior marker *Tc-mirror/irx* is only partly deleted. The *Tc-mirror/irx* expression that runs parallel to the antennal *Tc-wg* stripes (see white arrow in Fig. 4.18E) probably corresponds to the expression in the other segments and marks the corresponding anterior region of the intercalary segment. This domain is reduced in extension and intensity (compare white arrows in Fig. 4.18E to E'). The median domain, in contrast, appears unaffected (white arrowheads in Fig. 4.18E and E'). In compliance with the loss of marker gene expression, the mandibular *Tc-mirror/irx* domain is shifted anteriorly after RNAi and touches the median domain (black arrowheads in Fig. 4.18E and E'). The antennal and mandibular parasegment boundaries appear not to be affected by *Tc-lab* knock down. In conclusion, my data show that the knock down of *Tc-lab* leads to the loss of most of the intercalary segment and parts of the lateral head cuticle, rather than to a transformation (summarized in Fig. 4.18J). This finding contradicts the classical view that all gnathal segments contribute to the dorsal head cuticle like trunk segments to the dorsal trunk (Snodgrass, 1935; Weber, 1966).

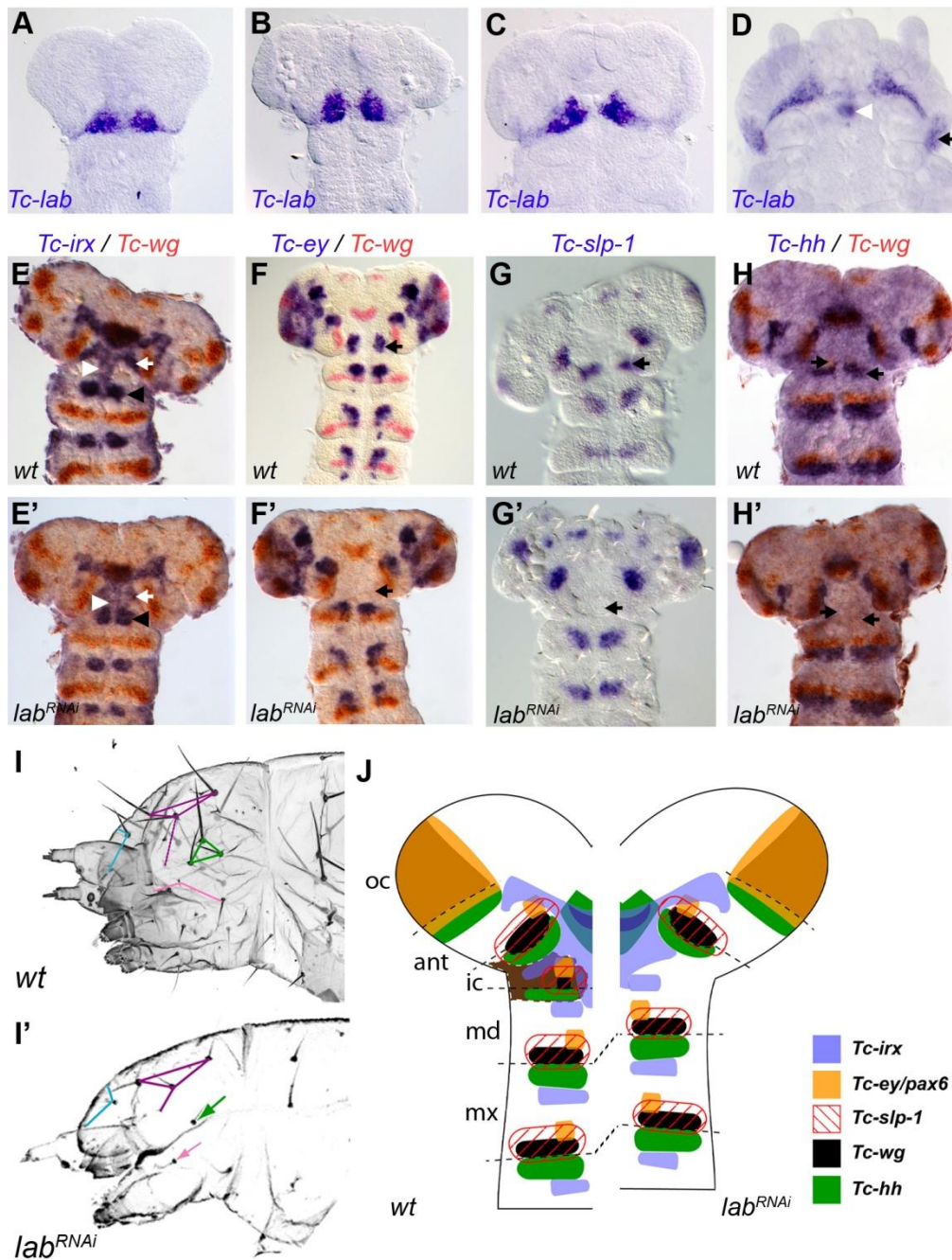


Fig. 4.18: Effects of *Tc-lab* RNAi on the intercalary segment.

A-C) Expression of *Tc-lab* marks the intercalary segment throughout embryonic development. D) At late stages, this domain elongates and splits into median triangle shaped stripes and a lateral expression domain (black arrow). The forward moving mandible is located where the domain splits. In addition, *Tc-lab* expression arises de novo in the stomodeum roof (white arrowhead). E-H) Wild type expression patterns of *Tc-mirror/irx* (E), *Tc-ey/pax6* (F), *Tc-slp1* (G) and *Tc-hh* (H). The white arrow in E and the black arrows in F-H indicate the respective intercalary expression. The anterior (left) black arrow in H marks the expression domain of *Tc-wg*. E'-H') Expression patterns of *Tc-mirror/irx* (E'), *Tc-ey/pax6* (F'), *Tc-slp1* (G') and *Tc-hh* (H') in *Tc-lab* RNAi embryos. The black arrows in F'-H' indicate the loss of the respective intercalary expression domain. The anterior (left) black arrow in H' marks the loss of the *Tc-wg* intercalary domain. E') The white arrow indicates the reduced expression domain of intercalary *Tc-mirror/irx*. Note that the median *Tc-mirror/irx* domain (white arrowheads) appears to be unaffected after *Tc-lab* RNAi. Additionally, the mandibular *Tc-mirror/irx* domain is shifted anteriorly after *Tc-lab* RNAi (compare black arrowheads in E and E'). I) A wild type head cuticle in a lateral view with the bristle pattern marked by coloured lines according to Schinko et al. 2008. At each angle, one seta is located. The lines and triangles help to identify the setae but do not reflect morphological or developmental units. purple: "vertex triplet"; green: "gena triplet"; pink "maxilla escort"; blue: "labrum quartet".

Results

I') The *Tc-lab* RNAi cuticles lack several bristles that mark the lateral portion of the head. Of the three “maxilla escort bristles” only one is left after RNAi (pink arrow). The same is true for the “gena triplet” (the green arrow points to the remaining bristle). J) Schematic representation of the *Tc-lab* RNAi results. The region which is lost after *Tc-lab* RNAi is marked in brown colour in the wild type.

oc: ocular region, ant: antennal, ic: intercalary, md-mandibular, mx: maxillary parasegment boundaries, respectively.

5 Discussion

5.1 Analysis of highly conserved anterior patterning genes

So far no comprehensive search for genes involved in the development of the Hox-free pregnathal head in protostomes has been performed. Therefore I aimed to identify important genes of head development by focusing on candidates that are active in vertebrates and insects. This approach identified a highly conserved core of anterior patterning genes. Below I will discuss the following aspects of the candidate gene screen.

First, the comprehensive expression analysis of the candidate genes presented in this work enables me to formulate hypotheses on the subdivision of the embryonic head. Additionally, it enables to identify developmental units of the head (chapter 5.1.1).

Second, hypotheses on the regulatory network that underlies the formation of the insect head can be formulated. More specifically, based on temporal expression aspects and the RNAi data it is possible to identify genes that are likely upstream in the hierarchy of this network (early expression, strong effects in RNAi). Accordingly, genes involved in more downstream processes can be identified (late expression, weak effects after RNAi) (chapter 5.1.2.1). Furthermore, spatial expression aspects enable me to hypothesize specific genetic interactions within the network (chapter 5.1.3).

And third, I gained first insights into the degree of conservation of anterior patterning by comparing the *Tribolium* data to the corresponding vertebrate situation (chapter 5.1.4).

5.1.1 Subdivision of the anterior head and developmental units

5.1.1.1 Early subdivision of the anterior head

The presented extensive expression analysis provides a large set of marker genes for different parts of the embryonic head. This data allows me to conclude that the Hox-free pregnathal head of *Tribolium* is subdivided into essentially three regions.

The antennal segment is specifically marked by the expression of *Tc-ems/emx* and *Tc-lim1/5* from early stages on (Fig. 5.1). The ocular region is distinguishable from the other head regions by specific expression of *Tc-otd1/otx*, *Tc-gsc*, *Tc-ey/pax6* and *Tc-fez* (Fig. 5.1). The

head lobes anterior to the ocular region are marked by activity of *Tc-optix/six3* and *Tc-rx* (Fig. 5.1). In addition to these region specific genes, the observed subdivision is in part confirmed by the activity of segmentally expressed genes. Namely, the genes essential for proper segmentation of the embryo (segment polarity: *Tc-wg/wnt1*, *Tc-hh/shh*, *Tc-ci/gli3*, *Tc-en*, *Tc-mirr/irx*; segment polarity/pair-rule: *Tc-slp/bf1*) (see Brown et al., 1994 for *Tc-en* data) are expressed in domains in the antennal and ocular region as in all posterior segments.

It is worth to note, that in addition to the above mentioned subdivision along the anterior-posterior axis, the median stomodeal/labral region is specifically marked by the expression of *Tc-scro/nkx2.1* from early stages on. Other genes like *Tc-optix/six3*, *Tc-eya*, *Tc-so/six1* and *Tc-mirr/irx* also possess large expression domains in this region in addition to their lateral domains. And *Tc-cap 'n' collar* (*Tc-cnc*) and *Tc-crocodile* (*Tc-croc*) also mark the stomodeal/labral region from early stages on (Economou and Telford, 2009). These expression profiles indicate that the median tissue might be a separate subunit of the developing head.

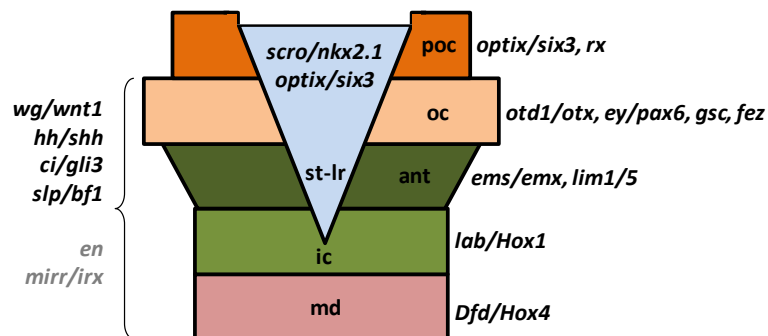


Fig. 5.1: Subdivision of the anterior head in *Tribolium castaneum*.

The mandibular and the intercalary segment are marked by genes of the Hox-cluster. The region anterior to the intercalary segment is free of genes of the Hox-cluster. The subdivision of this region is based on the expression of genes which mark specific regions (right side) and genes which are expressed segmentally (left side). *en* and *mirr/irx* are depicted in grey because they are only late or not expressed in the ocular region. md-mandibular segment, ic-intercalary segment, ant-antennal segment, oc-ocular region, poc-preocular region, st-lr-stomodeal/labral region

During stages later than the 5-8 *wg*-stripe stage, most of the expression profiles become more complex with additional domains (e.g. *Tc-otd1/otx*, *Tc-optix/six3*, *Tc-ey/pax6* and *Tc-slp/bf1*) or they become restricted to small patches of cells (e.g. *Tc-lim1/5* and *Tc-gsc*). This observation suggests that the subdivision of the anterior head is already established by the end of the 5-8 *wg*-stripe stage.

In summary, based on the expression of the analyzed candidate genes it is possible to subdivide the prenatthal region of the embryonic *Tribolium* head into three regions: the

antennal segment as the posterior most, the ocular region and the anterior most preocular region.

5.1.1.2 Identification of a signaling center in the *Tribolium* head

The expression data indicates that the ocular parasegment boundary possesses signaling center capabilities in the anterior *Tribolium* head.

At the 0-3 *wg*-stripe stage, the ocular parasegment boundary is already established in terms of adjacent expression of the morphogens *Tc-wg/wnt1* and *Tc-hh/shh* (Fig. 4.3B and Fig. 5.2). The ocular parasegment boundary is the first and anterior most one to be established. The analysis of head genes with respect to this boundary reveals that many genes have clear borders in this region at this early stage. Whereas *Tc-ci/gli3*, *Tc-tll/tlx*, *Tc-otd1/otx* and *Tc-ey/pax6* possess large posteriorly abutting domains (Fig. 5.2), *Tc-slp/bf1*, *Tc-gsc*, *Tc-lim1/5* and *Tc-ems/emx* are expressed posterior to or within the ocular region (Fig. 5.2). While the expression patterns mature (e.g. 5-8 *wg*-stripe stage) many genes still have their expression boundaries in this region (see Fig. 5.3). The posterior borders of anteriorly expressed genes like *Tc-otd1/otx* and *Tc-tll/tlx* coincide with the posterior part of the ocular region. On the other hand the expression domains of more posteriorly expressed genes like *Tc-ems/emx* and *Tc-lim1/5* abut this region from posterior. Some genes are specifically expressed within the ocular region (*Tc-gsc* and *Tc-ey/pax6*).

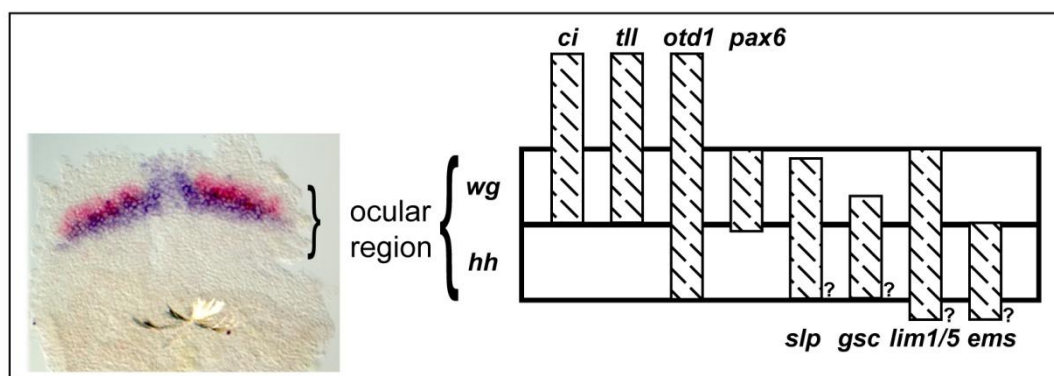


Fig. 5.2: The ocular parasegment boundary possesses signaling capabilities.

Adjacent *Tc-wg/wnt1* (Richards et al.) and *Tc-hh/shh* (blue) expression are the first indication of the ocular parasegment boundary (left side). Other early expressed genes possess either their posterior or their anterior border in this region (right side). The question marks indicate unclear posterior borders. The scheme on the right side is based on the respective gene expressions at the 1-3 *wg*-stripe stage.

Furthermore, it has been shown that the initially widespread blastodermal expression domains of *Tc-otd1/otx* retract from the anterior and/or posterior pole to finally end up in the region of the forming ocular parasegment boundary (Schinko et al., 2008). Moreover, this signaling center corresponds in position to the mid-/hindbrain boundary (MHB) in vertebrates (see chapter 5.1.4.3).

In summary, adjacent ocular expression of *Tc-wg/wnt1* and *Tc-hh/shh* appears to mark a region with an essential early role in anterior head patterning. Therefore, I call this region insect head boundary (IHB).

5.1.1.3 Genes involved in vertebrate cranial placode development pattern the anterior rim region of the Tribolium head

The spatial expression profile of the *Tribolium eya/six1/six4* genes shows that the rim region of the head lobes is subdivided into an anterior-median domain and a more posterior-lateral one.

Tc-eya and *Tc-so/six1* mark the rim of the head lobes from early stages on (Fig. 4.6 and Fig. 5.3D). *Tc-six4* is only active in the anterior-median portion of this rim region, while *Tc-Dll/Dlx* is restricted to more posterior portion of the lateral rim throughout early development (Fig. 4.6 and Fig. 5.3D). The posterior portion of the rim region is involved in visual development (Yang et al., 2009b). However, the anterior-median *Tc-six4* positive part has not been described so far.

Since some of the above mentioned genes are expressed in mutually exclusive domains around the head lobes, I propose that the rim region is subdivided into two individual developmental units: the anterior-median *Tc-six4* positive region and the more posterior-lateral ocular portion of the rim marked by *Tc-so/six1* and *Tc-Dll/Dlx*.

Vertebrate *eya* and *six1/4* genes mark the preplacodal ectoderm from early stages on. Based on their similar expression in *Tribolium*, the *Tc-six4* positive anterior-median rim region is likely to be homologous and will be called potential placodal region in the following chapters (see chapter 5.1.4.5 for further discussion).

5.1.2 The regulatory network that governs the patterning of the *Tribolium* head

Here I will discuss how the expression data and the RNAi results of my work can be used to shed first light on the regulatory network that governs head patterning in *Tribolium*. First, I will formulate hypotheses on the hierarchy of the analyzed genes within this network. Second, I will discuss specific interactions which I analyzed in order to test some predicted interactions.

5.1.2.1 The hierarchy within the regulatory network

Temporal expression aspects and the results of the RNAi screen provide a large dataset to formulate hypotheses on the hierarchy of the analyzed genes. I propose that there exist essentially four levels (Table 5.1).

Assumed that early expressed genes with strong effects in the RNAi analysis possess early functions in the formation of the *Tribolium* head, I hypothesize that *Tc-otd1/otx* and *Tc-optix/six3* are upstream to all the other analyzed genes in the network, because both genes are already active at very early blastodermal stages (“early regionalization” in Table 5.1). The next level is composed of genes whose expression starts when embryonic and extra-embryonic tissue is already distinguishable. These genes are most likely still involved in the subdivision of the head into broad domains (“regionalization” in Table 5.1). The further subdivision into smaller developmental units is then governed by genes whose expression in the head starts during early germ band elongation (“further subdivision” in Table 5.1). Finally, some genes start to be expressed only late during germ band elongation. These candidates are more likely involved in the specification of specific cell types within a given developmental subunit rather than regionalization (“specification of specific cells” in Table 5.1). Since all analyzed genes are expressed until the end of embryonic development, it is very likely that early involved genes possess also functions in more advanced stages and processes.

Table 5.1: The hierarchy of the analyzed gene during head development.

The hierarchy is based on the respective gene expression and the strength of the RNAi defects (see text for a detailed discussion).

	early regionalization	regionalization	further subdivision	specification of specific cells
<i>Tc-otd1/otx</i>				
<i>Tc-optix/six3</i>				
<i>Tc-tll/tlx</i>				
<i>Tc-ey/pax6</i>				
<i>Tc-toy/pax6</i>				
<i>Tc-gsc</i>				
<i>Tc-eya</i>				
<i>Tc-so/six1</i>				
<i>Tc-Dll/Dlx</i>				
<i>Tc-ems/emx</i>				
<i>Tc-lim1/5</i>				
<i>Tc-scro/nkx2.1</i>				
<i>Tc-mirr/irx</i>				
<i>Tc-hh/shh</i>				
<i>Tc-wg/wnt1</i>				
<i>Tc-ci/gli3</i>				
<i>Tc-slp/bf1</i>				
<i>Tc-en</i>				
<i>Tc-fgf8</i>				
<i>Tc-rx</i>				
<i>Tc-fez</i>				
<i>Tc-six4</i>				
<i>Tc-dbx</i>				
<i>Tc-ptx/pitx</i>				
<i>Tc-arx</i>				

Tc-otd1/otx and *Tc-ems/emx* based on RNAi data from Schinko et al., 2008 and expression in this work

Tc-wg/wnt1 based on RNAi data from Posnien et al., accepted for publication and expression in this work

Tc-hh/shh based on RNAi data from Farzana and Brown, 2008 and Posnien et al., accepted for publication and expression in this work

Tc-fgf8 based on late expression in the head from Beermann and Schröder, 2008

Tc-en based on late expression in the ocular region from Brown et al., 1994

Tc-arx based on RNAi from this work, no expression data available

Based on this hierarchy one would assume that top level candidates that are early involved in the establishment of broad domains result in severe phenotypes upon loss of function. Accordingly, genes that start to be expressed later during development in more restricted regions most likely lead to milder defects after knock down of the respective gene. Hence, it is possible to test the hypotheses on the hierarchy by analyzing RNAi phenotypes.

Indeed, I found this prediction largely fulfilled: severely affected cuticles show malformed head capsules and head appendages, whereas weaker phenotypes are characterized by an abnormal dorsal and lateral bristle pattern. But does the phenotype of a given gene reflect its position within the network?

Tc-optix/six3 and *Tc-otd1/otx* as the two most upstream genes result in severely affected head after RNAi (Fig. 4.7F,F' and Schinko et al., 2008; Schroder, 2003 for *Tc-otd1/otx*). The

knock down of genes of the next level within the network also results in severe head phenotypes. For example RNAi against the segmentation genes *Tc-ci/gli3* and *Tc-slp/fl* leads to the loss of whole head segments (Fig. 4.7C) (Choe and Brown, 2007; Farzana and Brown, 2008). Similarly, entire head segments are missing after *Tc-wg/wnt1* and *Tc-hh/shh* RNAi (Posnien et al., accepted for publication). *Tc-eya* that is widely expressed in the embryonic head, leads to the loss of the complete dorsal head (Fig. 4.7E). *Tc-ey/pax6* and *Tc-toy/pax6* together are expressed in large portions of the embryonic head. This matches the globally affected larval heads after double knock down (Fig. 4.7G,G'). The labrum and median tissue associated phenotype of *Tc-scro/nkx2.1* is consistent with the expression of this gene in the labral/stomodeal region (Fig. 4.7I). Similarly, the affected gnathal appendages in *Tc-lim1/5* RNAi larvae can be explained by the expression of this gene in the proximal part of the growing limb buds (Fig. 4.7H). *Tc-ems/emx* RNAi results in malformed antennae (Schinko et al., 2008). These observations clearly place these genes on the top of the regulatory network. However, the knock down of some genes only results in relatively mild defects, although more severe defects could be assumed based on large and early expression domains in the developing head (e.g. *Tc-ey/pax6*, *Tc-toy/pax6*, *Tc-so/six1* and *Tc-tll/tlx*). In the case of *Tc-ey/pax6* and *Tc-toy/pax6* this could be explained by redundant functions, since both genes are expressed in largely overlapping domains. This idea is supported by the fact that the double knock down of these two genes results in an enhanced strength of the phenotype, suggesting synergistic action (Table S3). A similar redundancy or synergy of the *Tribolium pax6* genes has been shown for their role in eye development (Yang et al., 2009a). Redundancy could also be envisaged for *Tc-so/six1*, which is co-expressed with *Tc-eya* in the head. The relatively mild cuticle phenotype of *Tc-tll/tlx* (Fig. 4.8K) could either be due to an incomplete knock down or alternatively, that its main role is restricted to nervous system development like in *Drosophila* (Younossi-Hartenstein et al., 1997). Control experiments have to show whether *Tc-tll/tlx* knock down is efficient.

The knock down of genes like *Tc-mirr/irx*, *Tc-fez*, *Tc-ptx/pitx* and *Tc-dbx* also result in mild defects (Fig. 4.8), which is in line with their downstream location within the proposed regulatory network. I also observed bristle pattern defects for *Tc-mun/arf* RNAi although no transcripts have been detectable so far (Fig. 4.8I). The main affected region is located lateral in the head capsule. These defects could be related to a function of this gene in larval eye development, since the *Drosophila* gene *Dm-mun/Pph13* is expressed in the Bolwig organs (the larval eyes) (Goriely et al., 1999). Because this expression in *Drosophila* starts late during germ band retraction (Goriely et al., 1999) it is very likely that I could not detect the

expression in *Tribolium* because late stages have not been included. Therefore, based on the potential late expression and the mild defects after RNAi, this gene most likely belongs to tissue or cell specific factors.

In summary, the expression data and the RNAi results provide a comprehensive basis to formulate hypotheses on the hierarchy within the regulatory network that patterns the early *Tribolium* head.

5.1.3 Testing hypotheses of regulatory interactions

5.1.3.1 *Tc-optix/six3* establishes anterior-median tissue by repression of laterally expressed genes

Of the early acting genes, *Tc-optix/six3* specifically marks the anterior region of the developing head. This expression suggests an important function of this gene in the anterior-median head.

I showed that upon *Tc-optix/six3* RNAi the expression domains of *Tc-wg/wnt1*, *Tc-otd1/otx* and *Tc-ey/pax6* are heavily expanded (Fig. 4.9 and Fig. 4.10). These findings imply that *Tc-optix/six3* governs the patterning of the anterior-median region of the *Tribolium* embryo by the repression of more posteriorly and laterally expressed genes. By this *Tc-optix/six3* probably prevents anterior-median tissue from adopting a posterior fate. The early onset of expression at the anterior pole of the embryo and the complete loss of anterior-median tissue in RNAi larvae further argue for such an important role of *Tc-optix/six3*.

On the other hand, *Tc-optix/six3* is also essential for the activation of the anterior-median and the ocular *Tc-ey/pax6* domains, indicating that *Tc-optix/six3* also governs the expression of genes within the anterior region. Since the anterior-median and the ocular domain of *Tc-ey/pax6* are established relatively late, it is possible that the early establishment of the anterior-median region by *Tc-optix/six3* provides the proper surrounding for its later activation function.

How can such a dual role be explained? One key to this double life are very likely co-factors of *six3*. The repressive effects were shown to be due to physical interaction with transcriptional repressors of the *groucho* family (Kobayashi et al., 2001; Lopez-Rios et al., 2003; Zhu et al., 2002). Therefore, it would be interesting to analyze *groucho* orthologs in

Tribolium to test if the repression capabilities of *Tc-optix/six3* are based on interaction with these co-factors.

In summary, I could show that *Tc-optix/six3* very likely orchestrates the formation of the anterior-median head by repressing posterior genes. After this region is established, *Tc-optix/six3* also functions as activator of late *Tc-ey/pax6* domains. Some aspects of *six3* function seem to be conserved in vertebrates (see chapter 5.1.3.4 for discussion).

5.1.3.2 Involvement of *Tc-tll/tlx* in the activation of *Tc-rx* and *Tc-optix/six3*

The expression of *Tc-tll/tlx* in the entire head lobes suggests a general activation role of *Tc-tll/tlx* in the anterior head. I tested this hypothesis and found reduced expression domains of *Tc-rx* and *Tc-optix/six3* after *Tc-tll/tlx* RNAi (Fig. 4.11). Compared to the large expression domain that covers the whole head lobes, this relatively minor defect is unexpected. There are hints that *Tc-tll/tlx* is difficult to knock out completely (Sebastian Kittelmann, personal communication). In line with *Drosophila* where *tll* is involved in posterior patterning (Pignoni et al., 1990; Strecker et al., 1988), I also found posterior truncations. I only analyzed embryos which showed posterior patterning defects in addition to altered expression of *Tc-optix/six3* and *Tc-rx*. This implies that the phenotypes that I describe have been knocked down successfully, but may represent hypomorphic phenotypes.

In conclusion, *Tc-tll/tlx* is required for the establishment of *Tc-optix/six3* and *Tc-rx* positive cells in the anterior head lobes.

5.1.3.3 The potential placodal region is patterned by a regulatory network comprising *Tc-eya*, *Tc-so/six1* and *Tc-six4*

The data on *Tc-eya*, *Tc-so/six1* and *Tc-six4* interactions represents first insight in how the potential placodal region in *Tribolium* is patterned during embryonic development (Fig. 4.12). Based on my results *Tc-eya* would be on top of this cascade activating *Tc-so/six1* and probably *Tc-six4* (Fig. 4.12I). However, it is quite unlikely that *Tc-eya* alone is sufficient to activate *Tc-so/six1*, since EYA factors lack DNA-binding domains. It has been shown that they physically interact with SO/SIX1 and DAC (dachshund) factors (Chen et al., 1997; Pignoni et al., 1997). Furthermore, a specific interaction of EYA2 and SIX4 has been shown (Ohto et al., 1999). The co-expression with these factors suggests a similar situation in

Tribolium development. In mouse *eyal* knock-out mutants no *six1* transcripts are detectable in some placodal regions, suggesting a similar function of *eyal* in mouse development (Xu et al., 1999; Zheng et al., 2003). The combined action of *Tc-eya* and *Tc-so/six1* (in this work shown for *Tc-so/six1*) in *Tc-six4* activation is very likely since both genes are co-expressed prior *Tc-six4* expression. In turn *Tc-eya* and *Tc-six4* could cooperate in repressing *Tc-so/six1* expression in the anterior rim region. Whether this repression is direct or achieved by activation of other repressors remains unclear. Together, these observations show that the anterior rim region is patterned by combined action of *eya/six* genes in *Tribolium*.

To further expand this network the involvement of *Dll/Dlx*, *dac* and *sox2/3* genes should be investigated. *Tc-dac* is transiently expressed in the anterior-lateral head lobes where it probably functions in demarcating the posterior border of the potential placodal region (Yang et al., 2009b). *Tc-Dll/Dlx* is expressed in the rim of the head lobes (Fig. 4.6E-H) and in vertebrate placode development *Dlx5* has been shown to upregulate *six4* in the preplacodal region (McLarren et al., 2003). Finally, *sox2* and *sox3* are capable of activating *eyal* expression and are involved in later specification events of placodal development (Koster et al., 2000; Schlosser et al., 2008). The *Drosophila* gene *soxN* (*soxNeuro*) is expressed in the central nervous system from early stages on (Cremazy et al., 2000; Overton et al., 2002). Preliminary data from *Tribolium* shows that *Tc-soxN* is similarly expressed in the nervous system, and more specifically also in the anterior rim region (Franck Simonnet, personal communication).

5.1.3.4 Are the observed *six3* interactions conserved in vertebrates?

Since the candidate genes for the screen were chosen because of their involvement in vertebrate neural plate patterning, I also aimed to compare the interactions of *six3* from *Tribolium* to vertebrates.

In vertebrates, *six3* is also a crucial factor in patterning the anterior most region of the neural plate, since forebrain and craniofacial development is severely affected in mutants (Conte et al., 2005; Jean et al., 1999; Lagutin et al., 2003; Lopez-Rios et al., 1999; Zuber et al., 1999).

One key function of *six3* in early forebrain development is the anterior repression of Wnt-signals from posterior parts of the brain. For example, without the repression of *wnt1*, anterior brain regions become posteriorized (Lagutin et al., 2003; Lavado et al., 2008). My manipulation of *Xenopus laevis* *Xsix3* results at least in part in opposing effects on *Xwnt1* (Fig. 4.13). The low number of analyzed embryos and the contradictory results for the

overexpression show that more data is required to draw a final conclusion. However, the similar situation in mice, sea urchin (Lagutin et al., 2003; Lavado et al., 2008; Wei et al., 2009) and *Tribolium*, suggests that the repression of Wnt-signaling in the anterior region is a conserved role of *six3* in Bilaterians.

Interactions of *six3* with *pax6* have extensively been analyzed in optic development of different vertebrates. In this process *six3* acts as an activator (Bernier et al., 2000; Carl et al., 2002; Liu et al., 2006; Loosli et al., 1999; Zuber et al., 2003). I showed that this is also the case in anterior neural plate patterning in my *Xenopus* interaction experiments (Fig. 4.13). However, the *Xenopus* data contradicts data from mouse, where *pax6* expression expands into anterior brain regions in slightly older *six3* mutants (Lagutin et al., 2003). These findings suggest different roles of vertebrate *six3* genes in different processes. In *Tribolium* the early *Tc-ey/pax6* expression is repressed by *Tc-optix/six3*, whereas the later anterior-median domain depends on expression of *Tc-optix/six3*. Since the early domain is not comparable to vertebrate *pax6* expression (see chapter 5.1.4.2.1), this represents a novel interaction with respect to an expression that is unique to *Tribolium* or insects. However, the requirement of *Tc-optix/six3* for the establishment of the anterior-median *Tc-ey/pax6* domain could be a conserved function of *six3*, because this domain shows similarities to the anterior *pax6* expression in vertebrates (see chapter 5.1.4.2.1 for further discussion). Hence, *six3* might be involved in the activation of anterior *pax6* expression among Bilaterians.

An anterior expansion of *otx* expression has been shown in mouse *six3* mutants (Lagutin et al., 2003). Conversely, upon *Xsix3* overexpression an unaltered *Xotx2* expression has been reported within the eye field transcription factors (Zuber et al., 2003). This is supported by my *Xenopus* experiments where neither overexpression nor knock down of *Xsix3* results in altered *Xotx2* expression. In *Tribolium* *Tc-otd1/otx* expression is clearly expanded after *Tc-optix/six3* RNAi, arguing for repressive effect of *Tc-optix/six3* on *Tc-otd1/otx*. This is in line with the mouse data. The impact of *six3* on *otx* in *Xenopus* has to be re-examined in order to allow a statement on the conservation of their relationship. But at least based on the comparison of *Tribolium* and mouse, *six3* seems to be involved in the repression of *otd/otx* from the anterior region of the head.

My results show that *six3* is an ancient factor capable of establishing the anterior most tissue by functioning as an activator of *pax6* genes and as a repressor of *wnt1* and *otx* genes. However, more vertebrate models have to be analyzed in order to draw conclusions on the conservation of the entire network.

In summary, the candidate gene screen allows me to formulate hypotheses on interactions within the regulatory network of *Tribolium* head development. The first tests of these hypotheses are encouraging because many of the assumed interactions were confirmed. A judgment on the conservation of these genes with vertebrates is not possible at that stage because the vertebrate data are in some cases not identical. Some interactions like the activating effect of *six3* on *pax6* however, seem to be conserved. This encourages to further pursue this approach.

5.1.4 Conservation of anterior patterning in bilaterian animals

Since the initial selection of the candidate genes is based on expression in the vertebrate neural plate, I want to compare the *Tribolium* expression profiles to the corresponding vertebrate situation. This comparison shows that a large set of genes is involved in the formation of similar anterior regions in insects and vertebrates, indicating that the anterior most region of bilaterian animals was similarly patterned in the bilaterian ancestor (Fig. 5.3). As a representative of the vertebrate neural plate I chose an early 4-6 somite stage mouse neural plate (Rubenstein and Shimamura, 1997). However, the respective expression patterns are extracted from different vertebrate models (see Table S6 for a comprehensive reference list). In order to reduce inaccuracies based on temporal expression changes I focused on the following stages for the respective expression profiles: embryonic day 7-8.5 (mouse), 8-12 hours post fertilization (zebrafish), stage 11-14 (*Xenopus laevis*, stages after Nieuwkoop and Faber, 1967) and HH4-7.5 (chick, stages after Hamburger and Hamilton, 1992). All these stages span late gastrulation and early neurulation events. For *Tribolium* I depict three stages of development. The 5-8 *wg*-stripe stage marks the onset of neural precursor gene expression (Nikolaus Koniszewski, personal communication). Hence, in this stage the first distinction between epidermal and neural cell fate becomes obvious by the expression of *Tc-ase*. Furthermore, I show the elongated germ band stage since the segregation of neural from epidermal tissue should be finished by the end of this stage (Hartenstein et al., 1987). Finally, I depict candidate gene expression in retraction stages to show tissue specific expression features in a differentiating surrounding.

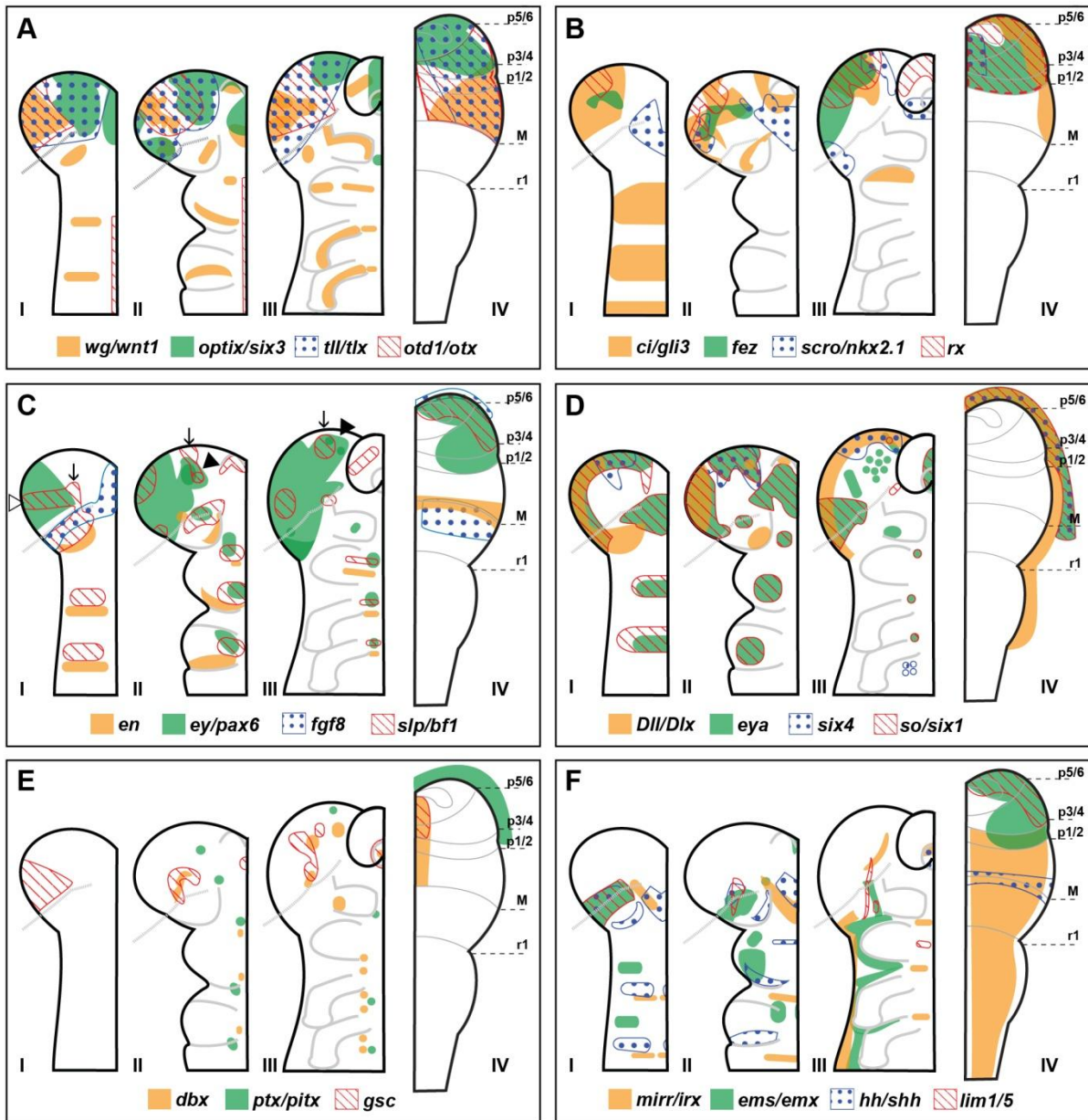


Fig. 5.3: Comparison of the candidate gene expression in *Tribolium* and vertebrates.

Comprehensive schematic representation of the candidate gene expression patterns in *Tribolium* (I-III in A-F) and in vertebrates (IV in A-F). See text for a detailed description of the depicted *Tribolium* stages and discussion. The expression patterns for the vertebrate genes are extracted from different vertebrate models (see Table S6 for a comprehensive reference list) and depicted in a mouse neural plate at a 4-6 somite stage. Dashed expression borders indicate unclear domains. The gray dashed lines in the *Tribolium* head indicate the approximate border between the ocular region (future protocerebrum) and the antennal segment (future deutocerebrum) (based on posterior border of *Tc-hh/shh* expression). Therefore, the gray dashed line roughly marks the location of the IHB. The *Tribolium fgf8* expression is based on Beermann and Schröder, 2008. The *Tribolium en* expression is based on Brown et al., 1994. The *Tribolium Dll* expression at late stages (D III) is based on Beermann et al., 2001.

p1/2-prosomeres 1 and 2 of the forebrain, p3/4-prosomeres 3 and 4 of the forebrain, p5/6-prosomeres 5 and 6 of the forebrain, M-midbrain, r1-rhombomere 1 of the hindbrain, open arrowhead in C I-ocular *Tc-slp/bf1* domain, arrow in C I - C III-anterior-medial *Tc-slp/bf1* domain, arrowhead in C II and C III-anterior-medial *Tc-ey/pax6* domain

5.1.4.1 The insect ocular/preocular region corresponds to the fore-and midbrain region of the vertebrate neural plate

First I summarize the expression of eight genes, which are active in the anterior head of *Tribolium* in similar patterns as in the vertebrate neural plate (Fig. 5.4; Fig. 5.3A-B).

5.1.4.1.1 six3 and otd/otx genes subdivide the anterior region that is defined by the expression of tll/tlx genes in vertebrates and insects

The expression of *Tc-optix/six3* and *Tc-otd1/otx* starts very early and together these two genes mark most of the head lobes (Fig. 5.4A and Fig. 5.3A). *Tc-optix/six3* is expressed anterior to *Tc-otd1/otx*. The early onset of expression implies an early function in anterior head regionalization. The mouse *otd* orthologs *otx1* and *otx2* are expressed in the fore- and midbrain region of the neural plate. The anterior most part of the neural plate is free of *otx1/2* expression. *otx2* knock out in mice leads to the loss of the whole rostral neuroectoderm, including the fore-, mid- and anterior hindbrain (Acampora et al., 1995; Rubenstein and Shimamura, 1997; Simeone et al., 1992a). Mouse *six3* is expressed from early stages on in the anterior most parts of the developing nervous system. In neural plate stages, expression covers the future forebrain (tel- and diencephalon) (Oliver et al., 1995). *six6* is a *six3* paralog in vertebrates. *six3* and *six6* expression is largely overlapping in early neural plate stages of different vertebrate models. *six3* knock-out mice lack the anterior forebrain (Conte et al., 2005; Jean et al., 1999; Lagutin et al., 2003; Lopez-Rios et al., 1999; Zuber et al., 1999). Hence, in *Tribolium* as well as in the vertebrate neural plate, both genes are expressed in a conserved non-overlapping anterior to posterior order in the anterior region of the neural ectoderm (Fig. 5.4A). Furthermore, both genes are involved in early regionalization of the anterior ectoderm.

Expression of *Tc-tll/tlx* is detectable in the entire anterior region only slightly after *Tc-otd1/otx* and *Tc-optix/six3* and overlaps both genes (Fig. 5.3A and Fig. 5.4A). Also the *tll* ortholog *tlx* is expressed in the anterior most part of the neural plate covering most of the *six3* and *otx* expression. Later during development, expression is found in the future fore-and midbrain region (Hollemann et al., 1998; Kitambi and Hauptmann, 2007; Monaghan et al., 1995; Yu et al., 1994). Hence, *tll/tlx* genes show conserved expression in the anterior part of the ectoderm overlapping *six3* and *otd/otx* in *Tribolium* and vertebrates. Beside this early

expression, *tll/tlx* genes are probably involved in the formation of similar brain regions. The loss of vertebrate *tlx* genes does not result in large brain defects. But a rather small part of the brain, the limbic system, that is involved learning and memory, is affected in mutant mice (Monaghan et al., 1997; Roy et al., 2002; Stenman et al., 2003; Zhang et al., 2008). In *Drosophila* the development of the mushroom bodies as part of the brain depends on *Dm-tll* function (Kurusu et al., 2009). Interestingly, it has been proposed that the hippocampus as part of the mammalian limbic system shares functional features with the insect mushroom bodies (Farris, 2008; Mizunami et al., 1998). Hence, it would be interesting to figure out if *Tc-tll/tlx* is also involved in mushroom body development in *Tribolium*.

5.1.4.1.2 fez, scro/nkx2.1 and rx genes also mark comparable anterior regions in Tribolium and in vertebrates

The onset of *Tc-fez*, *Tc-scro/nkx2.1* and *Tc-rx* expression clearly starts later than the before mentioned genes. In addition, these three genes are specifically expressed in more restricted patterns within the head lobes. *Tc-fez* and *Tc-rx* mark small patches of cells in the anterior-dorsal head lobes. Their expression domains partly overlap in later stages of development. *Tc-scro/nkx2.1* transcripts are mainly detectable in ventral part of the head lobes (Fig. 5.4B). *fezf1* and *fezf2*, the mouse orthologs of *fez*, are early markers of the forebrain and the olfactory system (Hashimoto et al., 2000; Hirata et al., 2006; Hirata et al., 2004; Jeong et al., 2007; Matsuo-Takasaki et al., 2000; Shimizu and Hibi, 2009). The vertebrate *rx* genes *rx1*, *rx2* and *rx3* are expressed in parts of the anterior neural plate which gives rise to the forebrain and the retina (Chuang et al., 1999; Mathers et al., 1997). Both genes cover overlapping regions in the neural plate like in *Tribolium*. The mouse gene *nkx2.1* is expressed in the anterior-median part of the neural plate (Shimamura et al., 1995), which corresponds to the expression found in *Tribolium*.

5.1.4.1.3 The wg/wnt1 and ci/gli3 genes have conserved expression in the heads of insects and vertebrates

Tc-wg/wnt1 expression in the head is restricted to the ocular region of the head lobes (Fig. 5.4A). *Tc-ci/gli3* head expression similarly covers the ocular region, but additionally marks more anterior cells (Fig. 5.4B). The vertebrate *wg* ortholog *wnt1* is expressed in the early

midbrain region. Loss of function experiments show that midbrain development is severely affected upon loss of *wnt1* expression (McMahon et al., 1992; Rowitch and McMahon, 1995). The *ci* ortholog *gli3* is expressed in the dorsal part of the anterior brain regions. In absence of *gli3* expression dorsal parts of the telencephalon fail to develop properly (Aoto et al., 2002; Hebert and Fishell, 2008; Theil et al., 1999; Tole et al., 2000). *Tc-ci/gli3* and *Tc-wg/wnt1* are expressed in comparable patterns in the anterior region of insects and vertebrates. In addition, both genes possess additional segmental expression and functions in other processes than head patterning (Fig. 5.4B) (Bolognesi et al., 2008b; Farzana and Brown, 2008; Ober and Jockusch, 2006; Oppenheimer et al., 1999). The same was described for their vertebrate orthologs. The vertebrate *wnt1* gene is also posteriorly active in the spinal cord in later stages of development. But the expression is restricted to the central nervous system (Echelard et al., 1994; McMahon et al., 1992). Since *ci/gli* genes are involved in mediating *hedgehog* signaling, the vertebrate *gli3* plays also crucial roles in other developmental processes like skeletal development, somitogenesis and neural tube patterning (Borycki et al., 2000; Lebel et al., 2007; Mo et al., 1997; Walterhouse et al., 1993). Hence, both genes possess additional functions in more posterior tissue in *Tribolium* and during vertebrate development. However, it is very unlikely that these posterior expression domains are homologous. In summary, the anterior expression domains of *wg/wnt1* and *ci/gli3* might be a conserved feature in vertebrates and insects, while the posterior domains very likely evolved independently.

In conclusion, these eight genes show expression patterns with similar locations and relative positions in *Tribolium* and vertebrates (Fig. 5.4). Strikingly, most of these eight genes are exclusively expressed in the head of *Tribolium*. This implies an ancient head specific function of these genes in patterning the anterior ectoderm. More specifically, it suggests that the ocular/preocular region of insects and the vertebrate fore-/midbrain evolved from the same structure in the last common ancestor.

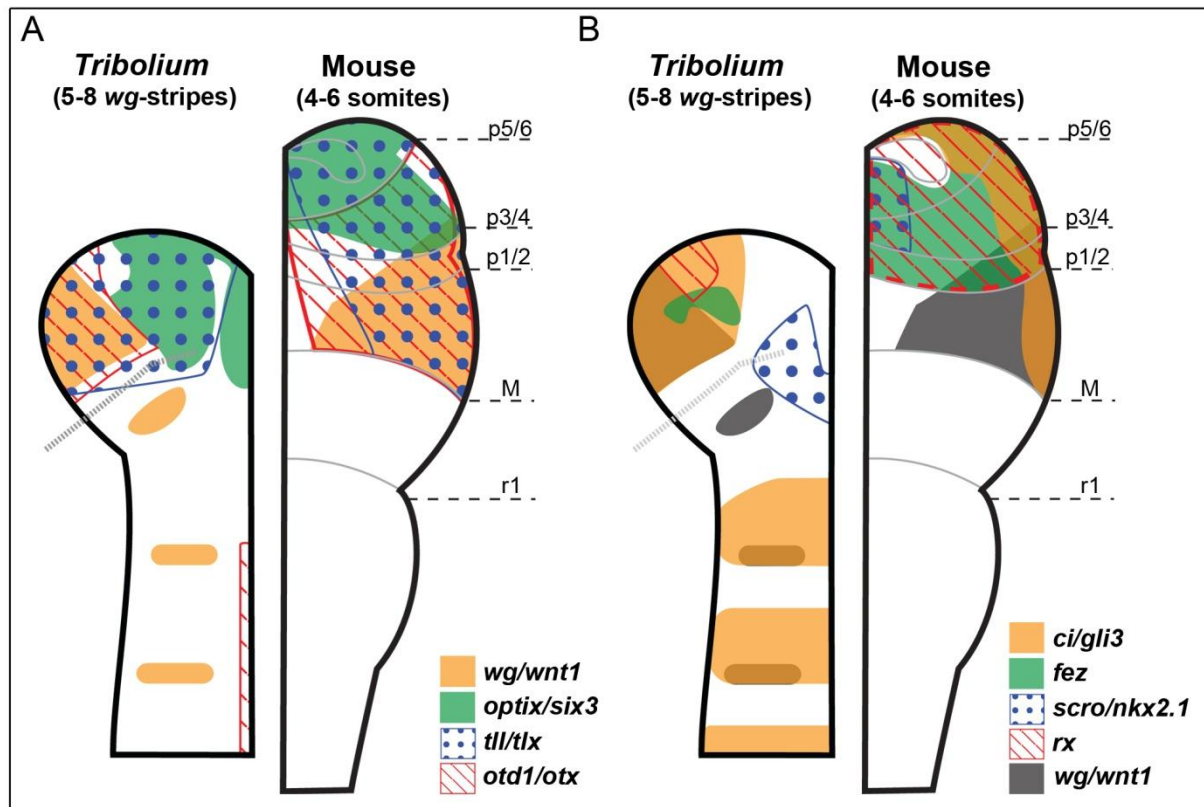


Fig. 5.4: Comparison of the ocular and preocular region in *Tribolium* to the fore-/midbrain region in vertebrates.

Comprehensive schematic representation of the candidate gene expression patterns in *Tribolium* (I-III in A-F) and in vertebrates (IV in A-F). For *Tribolium* a 5-8 wg-stripe stage is depicted. The expression patterns for the vertebrate genes are extracted from different vertebrate models (see Table S6 for a comprehensive reference list) and depicted in a mouse neural plate at a 4-6 somite stage. Dashed expression borders indicate unclear domains. The gray dashed lines in the *Tribolium* head indicate the approximate border between the ocular region (future protocerebrum) and the antennal segment (future deutocerebrum) (based on posterior border of *Tc-hh/shh* expression). Therefore, the gray dashed line roughly marks the location of the IHB. See text for a detailed and discussion.

p1/2-prosomeres 1 and 2 of the forebrain, p3/4-prosomeres 3 and 4 of the forebrain, p5/6-prosomeres 5 and 6 of the forebrain, M-midbrain, r1-rhombomere 1 of the hindbrain

5.1.4.2 Some late expression domains of *Tribolium* genes possess correlates in vertebrates

Here I discuss four genes whose late expression aspects can be compared to the corresponding vertebrate situation.

5.1.4.2.1 Late aspects of Tc-ey/pax6 and Tc-slp/bf1 may be conserved, while the early expression in the ocular region has no vertebrate correlate

Tc-ey/pax6 is expressed in the dorsal-posterior part of the head lobes at early elongation stages, largely overlapping with *Tc-wg/wnt1*. This early expression is connected to the formation of the optic system. Later, anterior-median located domains arise that are located anterior to the ocular *Tc-wg/wnt1* domain (arrowheads in Fig. 5.3C). In vertebrates, *pax6* is expressed in the dorsal forebrain region of the neural plate anterior to the *wnt1* domain (compare Fig. 5.3A IV to Fig. 5.3C IV). The loss of *pax6* function leads to severe patterning defects of the forebrain (Schmahl et al., 1993; Shimamura and Rubenstein, 1997; Stoykova et al., 1996; Warren and Price, 1997). Apparently, the expression of *Tc-ey/pax6* in the eye anlagen cannot be homologized to the vertebrate expression. The anterior-median expression, however, is similarly arranged with respect to *Tc-slp/bf1*, *Tc-optix/six3* and *Tc-rx* as *pax6* in vertebrates. Hence, *pax6* is expressed in the anterior ectoderm in *Tribolium* and in vertebrates. The segmental *Tc-ey/pax6* expression of later stages implies a function in the formation of specific cells in the ventral nerve cord. A later function in more posterior parts of the central nervous system has also been shown for vertebrates. Here *pax6* controls the establishment and the identity of specific motor neurons and ventral interneurons of the spinal cord (Ericson et al., 1997; Goulding et al., 1993). However, it is questionable if the posterior expression domains of vertebrates and insects can be homologized.

Early *Tc-slp/bf1* expression covers the posterior portion of the ocular region. This domain has no correlate in vertebrates (open arrowhead in Fig. 5.3C). During germ band elongation and finally in retraction, additional anterior cells become *Tc-slp/bf1* positive (arrow in Fig. 5.3C). This anterior expression in *Tribolium* is consistent with mouse and rat *bf1* expression in the whole early telencephalon anlagen (Shimamura et al., 1995; Tao and Lai, 1992).

5.1.4.2.2 Tc-en and Tc-fgf8 also possess late expression aspects that are consistent with the corresponding vertebrate expression

Tc-en is not expressed in the anterior head region at early stages of development (Fig. 5.3C). However, during germ band elongation expression is observed in a small domain of the posterior ocular region, the so called head spot (Brown et al., 1994). This restricted expression in insects appears to be a derived state, because in onychophorans, the respective ocular stripe

is fully developed (Eriksson et al., 2009 and Eriksson, personal communication). The mouse orthologs *en1* and *en2* are expressed in the region of the mid-/hindbrain boundary during early neural plate stages. The importance for the mid-/hindbrain boundary establishment of *en1* has been shown by its early deletion in *en1* mutant mice. In accordance with the *Tribolium* expression in more posterior tissue, mouse *en1* is also expressed along the hindbrain and spinal cord, in somites and in ventral ectoderm of the limb buds (Davidson et al., 1988; Davis et al., 1991; Davis and Joyner, 1988; McMahon et al., 1992; Wurst et al., 1994). Again, it is highly unlikely that these posterior expression domains are homolog. The ocular expression domain in insects, however, is probably comparable to the vertebrate MHB expression.

Tc-fgf8 is expressed in the stomodeal region of the early elongating embryo. Slightly later, expression arises within the lateral head lobes in a broad stripe (Fig. 5.3C) (Beermann and Schroder, 2008). This stripe is located posterior to the ocular *Tc-wg/wnt1* domain not abutting it (not shown). In mouse and zebrafish the *fgf8* gene is expressed in the region of the mid-/hindbrain boundary, anteriorly abutting *wnt1* (Crossley and Martin, 1995; Hidalgo-Sanchez et al., 1999; Reifers et al., 1998; Wurst and Bally-Cuif, 2001). Hence, in both vertebrates and insects, *fgf8* is expressed posterior to the anterior *wnt1* domain, although the direct abutting to *wnt1* is not conserved in *Tribolium*.

The four discussed genes possess late expression domains in the ocular/preocular region in *Tribolium* which have correlates in the vertebrate fore-/midbrain region. However, the late establishment of these domains in *Tribolium* argues against an involvement in early patterning in contrast to the corresponding vertebrate orthologs.

5.1.4.3 The insect head boundary (IHB) and the vertebrate mid-/hindbrain boundary (MHB) probably evolved from an anterior signaling center of the ancestor of Bilaterians

As discussed before, the embryonic ocular/preocular region of *Tribolium* is highly similar to the fore-/midbrain region of the vertebrate neural plate (see above). I also showed that the posterior portion of the ocular region (IHB) possesses signaling capabilities (see chapter 5.1.1.2). Interestingly, an important developmental boundary has been shown to separate the midbrain from the hindbrain in vertebrates. This so called mid-/hindbrain boundary (MHB) or isthmus organizer is already established in early neural plate stages (Martinez, 2001; Wurst and Bally-Cuif, 2001).

The first sign of the MHB becomes evident shortly after gastrulation by adjacent *otx2* and *gbx1/2* expression. The positioning of the anterior *otx2* and the posterior *gbx1/2* expression is at least in part mediated by Wnt-signaling (Rhinn et al., 2005; Wurst and Bally-Cuif, 2001). Subsequently, *wnt1* expression becomes restricted to the future midbrain, while *fgf8* expression is active in the hindbrain. At the same time *en1/2*, *pax2/5/8* and SP-factors (*sp8* in mouse, *bts1* in zebrafish) are active in a region overlapping the *otx2/gbx1/2* interface. Involved in a regulatory network, all these genes orchestrate the maintenance of the MHB and the formation of the adjacent mid- and hindbrain regions (Griesel et al., 2006; Tallafuss et al., 2001; Wurst and Bally-Cuif, 2001).

Based on the co-expression of *Tc-wg/wnt1*, *Tc-otd1/otx* and *Tc-tll/tlx* in the early *Tribolium* embryonic head, the region anterior to the IHB resembles the midbrain part of the MHB in vertebrates. The early onset of *Tc-wg/wnt1* expression suggests the involvement of Wnt-signaling in the positioning of the IHB, like in the MHB. Also other genes with expression in the vertebrate MHB region are expressed in similar regions in vicinity to the IHB. The transient *Tc-en* (Brown et al., 1994) and *Tc-fgf8* expression (Beermann and Schroder, 2008) in the IHB region suggests similar roles of these genes in IHB and MHB patterning. Also the Sp-factor, *Tc-buttonhead* is transiently expressed in the antennal region and in the lateral head lobes, most likely posterior and anterior to the IHB (Schinko et al., 2008). However, the expression of *Tc-unplugged* (*gbx* ortholog) and *Tc-pax2* and *Tc-pox-neuro* (*pax2/5/8* related genes) remains to be analyzed. Furthermore, preliminary functional experiments in *Tribolium* suggest that the core genetic interactions that establish the MHB are not conserved (Franck Simonnet, personal communication). It is worth to note that even within the chordates these features seem not to be strictly conserved (Holland and Holland, 1999; Wada and Satoh, 2001).

Support for the similarities of the IHB and the MHB comes from *Drosophila*, where later stages of embryonic development (stage 10/11) have been analyzed with respect to MHB-specific marker genes in early neuroblasts (Urbach, 2007). Based on the location of *Drosophila* *Otd* and *Dm-unplugged/gbx*, Urbach placed the “MHB” into the region of the future anterior deutocerebrum. Whereas the ventral portion of this “MHB” coincides with the proto-/deutocerebrum boundary, the dorsal part is shifted posteriorly into the deutocerebrum. However, this dorsal posterior shift is only based on two *Dm-unplugged/gbx* positive neuroblasts (Urbach, 2007). Hence, the late expression of *Dm-unplugged/gbx* seems not as important in the “MHB” region as the vertebrate ortholog in the MHB. Therefore, based on the activity of *Drosophila* *Otd* in the posterior most part of the ocular region at late embryonic

stages the proposed “MHB” region in *Drosophila* resembles the early IHB in *Tribolium*. However, more marker genes have to be analyzed in *Tribolium* (*unplugged/gbx*, *pax2/5/8*) in later embryonic stages.

It is worth to note that an alternative MHB-like region has been proposed in *Drosophila* based on late expression of *Dm-otd/otx*, *Dm-unpg/gbx* and *Dm-pax2/5/8* genes (in stage 13/14). This boundary has been placed between the deutocerebrum and the tritocerebrum (Hirth et al., 2003; Reichert, 2005). However, the *Tribolium* IHB data supports the location of a signaling center between the proto-/deutocerebral region.

One characteristic of the vertebrate MHB is the mitogenic effect of *wnt1* expression on midbrain cells. It has been observed that the *wnt1* positive dorsal-posterior midbrain region undergoes prolonged proliferation. Furthermore, the MHB shows very high proliferation potential. Instead of a growing MHB region, the new cells seem to get incorporated into either the midbrain or the hindbrain (Martinez, 2001). In *Tribolium* I observed that after the establishment of the IHB at early germ band stages, the head lobes start to form. Connected to this, the ocular *Tc-wg/wnt1* expression expands from a stripe to a triangle shaped domain. It is noteworthy that the dorsal part of this domain comprises significantly more cells than the ventral part (Fig. 4.3H) (Nagy and Carroll, 1994). It is possible that the head lobes, at least in part, form by unsymmetrical growth of the dorsal *Tc-wg/wnt1* positive ocular region. By applying BrdU labeling, Phospho-Histon H3 staining or in vivo imaging it would be possible to elucidate if this growth is due to extensive cell proliferation or alternatively to cell movements. Both the IHB and the MHB seem to induce growth of adjacent tissue, with involvement of *wnt1*.

In conclusion, the expression profile of the *Tribolium* IHB region in early embryonic stages is similar to the expression profile of the corresponding orthologs in the vertebrate MHB. Both regions are located posterior to an anterior region that seems to be similarly conserved: the ocular/preocular region of *Tribolium* and the vertebrate fore-/midbrain region, respectively. In the vicinity of both regions, extensive growth of tissue occurs, indicating that both are involved in promoting cell proliferation.

In summary, I showed that based on shared expression features, embryonic location and developmental aspects the *Tribolium* IHB and the vertebrate MHB are very likely homologous brain boundaries. This implies that the last common ancestor of all bilaterian animals already possessed a signaling center in a comparable region. The observed

differences, like *hh/shh* expression in the IHB region and the potentially minor importance of *unplugged/gbx* in insects, may reflect different adaptation in both lines.

5.1.4.4 The *Tribolium* orthologs of some important neural plate patterning genes are not involved in the patterning of comparable regions in the beetle

Some of the important vertebrate neural plate patterning genes are not conserved in their early function in *Tribolium*.

Vertebrate *emx* genes are essential for proper forebrain development. According to this function, they are expressed in the dorsal telencephalon anlage in early neural plate stages (Fig. 5.3F) (Qiu et al., 1996; Simeone et al., 1992b; Yoshida et al., 1997). Vertebrate *emx* genes are also expressed and functionally involved in the olfactory system (Bishop et al., 2003; Cecchi and Boncinelli, 2000; Mallamaci et al., 1998; Shinozaki et al., 2002; Simeone et al., 1992a; Simeone et al., 1992b). The expression of *Tc-ems/emx* in the antennal segment is not compatible with an early patterning function in the anterior brain. In *Drosophila* it has been shown that many sense organs, including those for olfactory sensing arise from the antennal segment. Consistent with this data, *Dm-ems* is involved in postembryonic development of the olfactory system (Lichtneckert et al., 2008). These observations suggest that *Tc-ems/emx* is similarly involved in the formation of the olfactory system. Hence, the involvement in the olfactory system development, but not in early neural plate patterning, seems to be a conserved feature of *ems/emx* expression and function.

Vertebrate *shh* is active in the dorsal foregut and serves as a signal that governs the patterning of the ventral forebrain (Fig. 5.3F) (Echelard et al., 1993; Ericson et al., 1995). The segmental staining of *Tc-hh/shh* has no counterpart in vertebrates, including its domain in the IHB. However, it is in addition expressed in two ventral domains that develop into the stomodeum from early stages on (Farzana and Brown, 2008). Potentially, this early *Tc-hh/shh* domain could provide ventral signals similar to vertebrates. However, this potential signal does not work along the entire body axis in contrast to vertebrates. Therefore, the important function of *shh* in patterning the ventral neural ectoderm is not highly conserved in *Tribolium* but could be present in the anterior region.

Vertebrate *irx* genes are involved in various patterning processes of the neural plate (Fig. 5.3F). In early development they establish the neural plate by Wnt-mediated *Bmp4* repression (*irx1* and *irx2*) and activation of proneural genes (Cavodeassi et al., 2001; Gomez-Skarmeta et al., 2001). Later, *irx* genes are involved in the dorso-ventral and anterior-posterior subdivision

of the neuroectoderm. In the anterior-posterior axis *irx* genes are posteriorly expressed, with a different anterior border for each representative. The anterior border of *irx2* lies at the mid-/hindbrain boundary (MHB), *irx1* has its anterior most expression at the fore/midbrain border and *irx3* reaches into the forebrain (Glavic et al., 2002). *Tc-mirr/irx* has its anterior most expression in the ventral IHB region (Fig. 5.3F). Based on the high similarities of the IHB and the MHB (see chapter 5.1.4.3), the *Tc-mirr/irx* expression would resemble the one of vertebrate *irx2*. And indeed, a recent phylogenetic analysis shows that the insect *mirror* genes belong to *irx2/5/6/4* group of vertebrate genes (Kerner et al., 2009). In dorsal-ventral axis patterning *irx* genes are essential for the specification of interneurons in the ventral spinal cord (Briscoe et al., 2000). Since *Tc-mirr/irx* remains active in small ventral clusters of the nerve cord, a similar function is possible. However, it is obvious that the wide-ranging early patterning functions of vertebrate *irx* genes are not conserved in *Tribolium*.

Lim1/5 (*lhx1/5*) genes are essential for fore- and midbrain development in vertebrates, as shown in loss-of-function studies. Correspondingly, the expression has been described to be located in large portions of the fore- and midbrain region (Fig. 5.3F) (Peng and Westerfield, 2006; Shawlot and Behringer, 1995; Sheng et al., 1997; Toyama et al., 1995). The expression of *Tc-lim1/5* in the antennal region in *Tribolium* argues against a similar function in patterning the anterior part of the brain. It has to be determined by functional analyses if the early expression in the IHB region might influence anterior brain formation. In retraction stages *Tc-lim1/5* gets activated in a segmental pattern close to the ventral midline, suggesting an involvement in specifying cells in the nerve cord. Involvement of the *Drosophila lim1* gene in motor- and interneuron formation substantiates this suggestion (Lilly et al., 1999). This late function would be a conserved feature since vertebrate *lim1/5* genes are also active in distinct sets of motor- and interneurons in the spinal cord (Pillai et al., 2007; Tsuchida et al., 1994).

In summary, the vertebrate orthologs of *Tc-ems/emx*, *Tc-hh/shh*, *Tc-mirr/irx* and *Tc-lim1/5* are essential for proper neural development. In *Tribolium* these genes possess no early function in corresponding neural regions comparable to vertebrates. However, some late and tissue specific aspects may be conserved.

5.1.4.5 Comparison of neural plate associated genes

The high conservation of genes involved in vertebrate neural plate patterning implies that neural plate associated genes might be similarly conserved. Therefore, I will discuss the

comparison of vertebrate genes expressed developing cranial placodes (*eya*, *so/six1*, *six4*, *Dll/Dlx*) to their *Tribolium* orthologs.

5.1.4.5.1 *The potential placodal region is patterned like the vertebrate preplacodal ectoderm (PPE)*

The vertebrate orthologs of *Tc-eya*, *Tc-so/six1*, *Tc-six4* and *Tc-Dll/Dlx* are crucial key factors in the development of cranial placodes. Cranial placodes develop from the preplacodal ectoderm (PPE), a tissue that is located at the interface between the neural ectoderm of the neural plate and the epidermal ectoderm. According to this, the above mentioned genes are expressed in ectodermal cells surrounding the anterior neural plate (Fig. 5.3D) (reviewed in Baker and Bronner-Fraser, 1997; Brugmann and Moody, 2005; Schlosser, 2006). *Dlx* genes are essential for the positioning of the PPE and its demarcation from adjacent neural and epidermal ectoderm (Bhattacharyya et al., 2004; Esterberg and Fritz, 2009; McLarren et al., 2003; Solomon and Fritz, 2002; Woda et al., 2003). Vertebrate *six1*, *six4* and *eya* genes are known as panplacodal markers because they are expressed in nearly all PPE and placodal cells throughout development (Schlosser and Ahrens, 2004). *six1* and *eya* were shown to regulate the switch between neural progenitor proliferation and neural differentiation in a dose-dependent manner. This switch is achieved by *soxB1* (*sox2/3*) regulation (Schlosser et al., 2008). Corresponding to this, it has been shown that medaka *sox3* is similarly expressed in the neuroectoderm and in all placodes prior to placode formation (Koster et al., 2000). *Tc-eya* and *Tc-so/six1* are expressed at the rim of the head lobes from early stages on. *Tc-Dll/Dlx* shows early transient expression in this region, while *Tc-six4* gets activated in the anterior rim region during germ band elongation (Fig. 5.3D). Since the lateral part of the rim expression segregates with the optic anlagen (Yang et al., 2009b), I will concentrate on the anterior rim region for the comparison. Note that the *Tribolium soxB1* ortholog *Tc-soxNeuro* is expressed in the anterior head anlagen from early blastodermal stages on (Franck Simonnet, personal communication).

Since I found co-expression of *six/eya/Dll* genes as well as *sox2/3* genes in the anterior rim region of *Tribolium* and in the vertebrate PPE, the possibility arises that *Tribolium* might possess placodal-like structures. This potential placodal region is marked by the expression of *Tc-six4* at the anterior rim of the head lobes.

5.1.4.5.2 *The potential placodal region in Tribolium possesses features of the hypophyseal placode in vertebrates*

The vertebrate PPE gives rise to a variety of sensory organs and cell types. Whereas the PPE is marked by the expression of only few genes, the specific cranial placodes possess a rather unique gene expression profile (Baker and Bronner-Fraser, 1997; Brugmann and Moody, 2005; Schlosser, 2006). Thus, the question arises to which type of vertebrate cranial placode the potential placodal region in *Tribolium* corresponds. Since the *Tc-six4* positive region marks the anterior most portion of the *Tribolium* head, the anterior most located hypophyseal placode and the olfactory placode are good candidates (Baker and Bronner-Fraser, 1997; Brugmann and Moody, 2005; Schlosser, 2006). The hypophyseal placode gives rise to parts of the neuroendocrine system. In most vertebrates the hypophyseal placode gets integrated into the stomodeum roof to form an evagination, the so called Rathke's Pouch, that fuses with a similar evagination of the diencephalon floor. Rathke's Pouch (hypophyseal placode) gives rise to the non neural part of the pituitary (adenohypophysis) and the diencephalon floor contributes to its neural part (neurohypophysis) (Baker and Bronner-Fraser, 1997; Kardong, 1998). The olfactory placode contributes to the formation of the olfactory system (Baker and Bronner-Fraser, 1997; Schlosser, 2006). Both placodes share a large set of transcription factors (*six1*, *six4*, *eya*, *Dlx*, *pax6*, *six3/6*, *otx2*, *ptx*, *sox2/3*, *bf1*). During embryonic development the expression code of each placode becomes distinguishable by the specific expression of *ptx* and *lhx3* in the hypophyseal placode and *sox9* and *emx2* in the olfactory placode (Baker and Bronner-Fraser, 1997; Schlosser, 2006). In *Tribolium* embryos, I found expression of all shared genes in the *Tc-six4* positive region at some stage (only at early germ band stages: *Tc-so/six1* and *Tc-Dll/Dlx*; at late retraction stages: *Tc-six4*, *Tc-eya*, *Tc-ey/pax6*, *Tc-optix/six3*, *Tc-otd1/otx*, *Tc-ptx/ptx*, *Tc-soxNeuro/soxB1* and *Tc-slp/bf1*) (Fig. 5.3A-E, *Tc-soxNeuro*, Frank Simonnet, personal communication). *Tc-ems/emx* is never active in the potential placodal region (Fig. 4.4F-J). The *sox9* ortholog in *Drosophila* (*Dm-sox100B*, *Dm-soxE*) is involved in testis, gut and malpighi tubule formation, but has never been shown to be expressed in the head anlagen (DeFalco et al., 2003; Hui Yong Loh and Russell, 2000). This implies that none of the specific olfactory placode markers is expressed in the potential placodal region in insects. On the other hand, I showed *Tc-ptx/ptx* expression in the late *Tc-six4* region (Fig. 5.3D III). The vertebrate *ptx* genes are important for the formation of the pituitary as part of the vertebrate neuroendocrine system (Lamonerie et al., 1996; Lanctot et al., 1997; Pommereit et al., 2001; Szeto et al., 1999; Tremblay et al., 1998). Additionally, in

Drosophila it has been shown that the *lhx3* ortholog *Dm-lim3* is expressed in a cluster of anterior brain cells adjacent to the pharynx at the end of retraction (De Velasco et al., 2004; Thor et al., 1999). However, the actual *Tc-lim3/lhx3* expression remains to be confirmed.

Together, based on the expression profile of the *Tc-six4* positive region, I conclude that the potential placodal region in *Tribolium* possesses features of the hypophyseal placode.

5.1.4.5.3 The potential placodal region in Tribolium might be involved in the development of the neuroendocrine system

Similar to the vertebrate hypophyseal placode, the *Tc-six4* positive region appears to contribute to neuroendocrine system development: I found that *Tc-chx* is expressed in the *Tc-six4* positive region (not shown) that is an early marker for the developing Pars Intercerebralis (PI) in *Drosophila*. This is an important neurosecretory brain center that innervates a neurosecretory gland, the corpus cardiacum (cc) (de Velasco et al., 2007; Hartenstein, 2006). Several authors already pointed out that the PI/cc of insects and the hypothalamus/pituitary of vertebrates share developmental, structural and functional features (Nassel, 2002; Veelaert et al., 1998). In line with this, a high degree of conservation of bilaterian neurosecretory systems has been discussed (Hartenstein, 2006; Tessmar-Raible, 2007; Tessmar-Raible et al., 2007).

Also the relative location of the involved tissue during development substantiates an involvement of the *Tc-six4* positive region in the development of the neuroendocrine system. For example, in *Drosophila* the cc develops from a region between the median protocerebrum and the future foregut, suggesting that PI and cc develop from adjacent tissue (De Velasco et al., 2004). Similarly, the vertebrate hypophyseal placode arises directly adjacent to the future hypothalamus (Couly and Le Douarin, 1990; Eagleson and Harris, 1990). In *Tribolium* the median *Tc-six4* positive region with its potential to contribute to neuroendocrine development and the developing stomodeum are in direct vicinity over a long period of embryonic development. This implies that the precursors of the neuroendocrine system in *Tribolium* are mainly located in the anterior-median region of the developing head. However, it remains unclear which specific part of the neuroendocrine system arises from the *Tc-six4* positive region. Cell tracking systems will be needed to address these important open questions.

5.1.4.5.4 *Development of parts of the neuroendocrine system from a placodal like region could be ancestral to bilaterian animals*

In 1983 Northcutt and Gans published their “New Head” theory that essentially proposes that the derived features of the vertebrate body plan are based on the appearance of cranial placodes and the neural crest tissue in the vertebrate stem group (Northcutt and Gans, 1983). Hence, cranial placodes were long considered to be vertebrate specific structures (Shimeld and Holland, 2000). In recent years, however, molecular data from tunicates, which are non-vertebrate chordates, suggest that parts of the neuroendocrine system of those animals develops from a region that is marked by *six1/4* and *eya* genes (Boorman and Shimeld, 2002; Christiaen et al., 2002; Mazet et al., 2005). My data from a protostome model indicate that the *Tc-six4* positive potential placodal region in *Tribolium* could give rise to parts of the neuroendocrine system. Hence, in insects, tunicates and in vertebrates, parts of the neuroendocrine system develop from a region that is patterned by *eya*, *six1* and *six4* genes. This suggests that the formation of parts of neuroendocrine system from a region with a genetic code similar to vertebrate cranial placodes is a common bilaterian feature (Fig. 5.5).

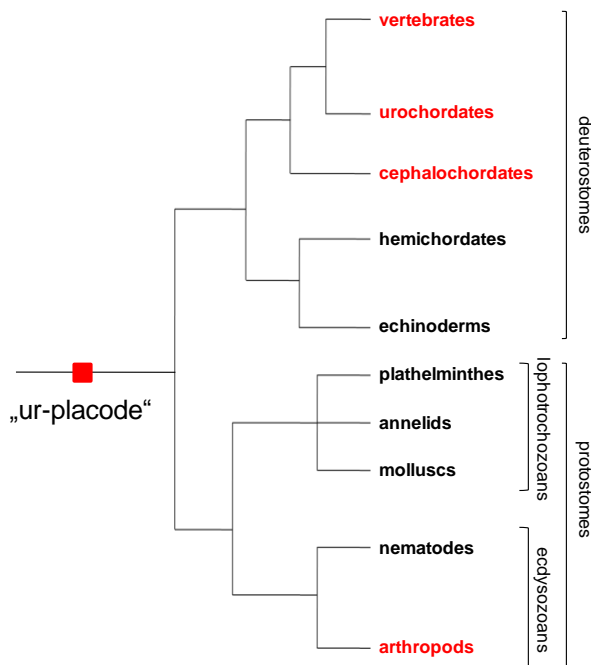


Fig. 5.5: Evolution of cranial placode development.

Cranial placodes were long thought to be vertebrate specific structures. But placodal like structures have also been found in urochordates (tunicates) and in cephalochordates (Mazet et al., 2005; Schlosser, 2005). My data indicates that the *Tc-six4* positive anterior region of the head possesses features of the hypophyseal placode of vertebrates. This suggests that neuroendocrine tissue arose from a region patterned like cranial placodes (“ur-placode”) in the last common ancestor of chordates and insects. See text for a detailed discussion.

5.1.4.6 Genes which are expressed in the prechordal plate of vertebrates are not conserved in their early function

All neural plate associated genes mentioned above are expressed at the rim of the neural plate. Another important tissue for neural plate patterning is the prechordal plate, that underlies the anterior neural ectoderm (Nieuwkoop, 1999). The vertebrate genes *gsc* and *dbx* are expressed in this tissue. A comparison to the corresponding *Tribolium* orthologs shows that the early patterning functions of these genes are not conserved. However, some late and tissue specific aspects are probably conserved (Fig. 5.3E).

At neural plate stages *gsc* is a marker for the prechordal plate. This tissue is an endomesodermal derivative of the gastrulation organizer (Spemann's organizer) that is located in the foregut roof underlying the anterior neural plate. The prechordal plate organizer is an important signaling center for forebrain patterning (Artinger et al., 1997; Belo et al., 1998; Gritsman et al., 2000; Pera and Kessel, 1997; Schneider and Mercola, 1999; Schulte-Merker et al., 1994; Steinbeisser and De Robertis, 1993). Similar to vertebrate *gsc*, the insect *gsc* genes seem to become active in cells of the foregut. These cells start to invaginate to form the stomatogastric nervous system (Hahn and Jackle, 1996). In *Tribolium* we also found a foregut-related expression of *Tc-gsc* (Fig. 4.2G,H). This expression is most likely connected to the formation of the stomatogastric nervous system. The expression of *Tc-gsc* in the early head lobes has no correlate in vertebrates. This early anterior expression might be a unique function of *gsc* in insects, since *Drosophila* also possesses *Dm-gsc* positive cells in the anterior head region (Hahn and Jackle, 1996). It has been suggested that *gsc* genes might be involved in the induction of cell fate changes or adhesion processes rather than the specification of cell fates (Goriely et al., 1996). In accordance with this it has been shown in vertebrates that *gsc* is essential to promote gastrulation movements (Blum et al., 1992; Cho et al., 1991; Izpisua-Belmonte et al., 1993; Schulte-Merker et al., 1994; Stachel et al., 1993). Interestingly, the head lobes are prone to drastic morphogenetic movements during head capsule formation (Posnien and Bucher, submitted). Thus, *Tc-gsc* could function there to promote the cellular changes underlying these movements. A conserved role in nervous system patterning is not found.

The early expression of vertebrate *dbx* orthologs is diverse. The zebrafish and frog *dbx* genes are expressed in an early anterior domain in the region of the forebrain and in a posterior domain along the spinal cord (Fjose et al., 1994; Gershon et al., 2000). In zebrafish the forebrain expression seems to be located in the prechordal plate underlying the neural plate

rather than in neural tissue (Fjose et al., 1994). The anterior domain in *Xenopus* is only transiently active (Gershon et al., 2000). The mouse *dbx* ortholog possesses no early domain. Expression in the fore-midbrain region arises late during development in mouse. But the spinal cord expression seems to be conserved among vertebrates (Lu et al., 1992; Shoji et al., 1996). In the spinal cord, *dbx* genes are involved in the *shh*-dependent formation of specific interneuron types (Gribble et al., 2007; Pierani et al., 1999). The late onset of *Tc-dbx* expression shows that no early function of this gene is evident in *Tribolium*. This is consistent with the data from mouse *dbx*. But the segmental expression of *Tc-dbx* suggests a role in the formation of specific cells in the ventral nerve cord. This is substantiated by the fact that *dbx* is expressed in specific neurons in another protostome, the annelid *Platynereis dumerilii* (Denes et al., 2007).

In summary, my data show that genes which possess early functions in neural plate associated regions only share late and specific aspects with the corresponding *Tribolium* orthologs.

5.2 Wnt-signaling in anterior patterning of *Tribolium castaneum*

5.2.1 Canonical Wnt-signaling is involved in an ancient mode of anterior-posterior patterning

I showed that *Tc-axin* is essential for proper embryonic anterior-posterior axis formation. Apparently, Wnt target genes have to be down-regulated in order to establish anterior structures. Additionally, embryos with ectopic Wnt-targets are posteriorized as shown by the anterior expansion of the posterior marker *Tc-cad* and the observation that in some cases both terminal regions exhibit posterior like characteristics (e.g. no head lobes). Additional support for the posteriorization comes from other experiments on *Tc-axin*. For example *Tc-wnt8* that is expressed in two cells clusters in the posterior growth zone in wild type embryos (Bolognesi et al., 2008a), becomes activated in two to four cell clusters in the prospective anterior region after *Tc-axin* RNAi (Renata Bolognesi, personal communication). Furthermore, the anterior gnathal segment specific Hox-gene *Tc-deformed/Hox4* (Brown et al., 1999) is absent in *Tc-axin* RNAi embryos (Renata Bolognesi, personal communication). In line with this, the posterior abdomen-specific Hox-gene *Tc-abdominal-A/Hox8* is expressed throughout the embryo after *Tc-axin* knock down (Renata Bolognesi, personal communication). These results strongly support a posteriorization of anterior tissue upon *Tc-*

axin RNAi. It is worth to note that the loss of *axin* function in zebrafish leads to the loss of the anterior telencephalon due to expansion of posterior diencephalon derivatives (Heisenberg et al., 2001).

Since the embryos are posteriorized, the question arises why I only found truncated larval cuticles rather than larvae with two posterior endings. The answer to this question probably lies in the severity of the phenotypes I observed. The fact that I found all intermediate phenotypes indicates that the RNAi effect is dose dependent. In the first three days after injection no cuticles were formed, indicating that the most severe phenotypes are not even capable of producing a proper cuticle. However, these egg collections were also used for in situ hybridization to analyze the strongest defects on embryonic level. The larvae that secreted a cuticle and which I analyzed might already represent weaker phenotypes with some residual *Tc-axin* activity. This would lead to some degree of Wnt-signaling repression, which probably results in incomplete transformation of the anterior region towards a posterior fate. This intermediate tissue might have degraded subsequently, whereas the correctly patterned posterior portion remained intact. Hence, the strong potentially bi-caudal phenotypes do not secrete a cuticle and the weaker phenotypes result in cuticles with degraded anterior tissue.

How is Wnt-signaling capable of directing an anterior fate? Based on the data presented so far and preliminary results regarding the effect of *Tc-axin* RNAi on *Tc-otd1* (see below) I propose the following working model (Fig. 5.6): Wnt-signals (Wnt1, Wnt8 and WntA) which are expressed at the posterior pole from early stages on (Bolognesi et al., 2008a) form a posterior to anterior gradient. In the posterior region of the *Tribolium* embryo this Wnt-signal activates *Tc-cad* and thereby a posterior fate is established. This is shown by the overexpression of *Tc-cad* after *Tc-axin* RNAi. In line with this assumption, *Tc-cad* expression is highly down-regulated if Wnt-signals are abolished (*Tc-porcupine* (involved in the secretion of Wnt-ligands) or *Tc-arrow* (LRP co-receptor ortholog) RNAi; not shown and Renata Bolognesi, personal communication). The Cad Protein might directly or indirectly restrict *Tc-otd1* to the anterior region. *Tc-otd1* in turn could be involved in the repression of *Tc-cad*. This is supported by data from the wasp *Nasonia vitripennis* where *cad* is derepressed after *otd* RNAi (Olesnicky et al., 2006). *Tc-zen1* represses *Tc-otd1* in the anterior extra embryonic region (van der Zee et al., 2005). Since *Tc-otd1* expression is reduced in some of the analyzed *Tc-axin* RNAi embryos (not shown), I propose that a Wnt-signaling/*Tc-cad* free surrounding is required for zygotic *Tc-otd1* expression (Fig. 5.6) (McGregor, 2006; Schroder, 2003).

This model suggests that *Tc-axin* is crucial for the establishment of an anterior Wnt-target/*Tc-cad* free region, which in turn provides the basis for anterior *Tc-otd1* expression.

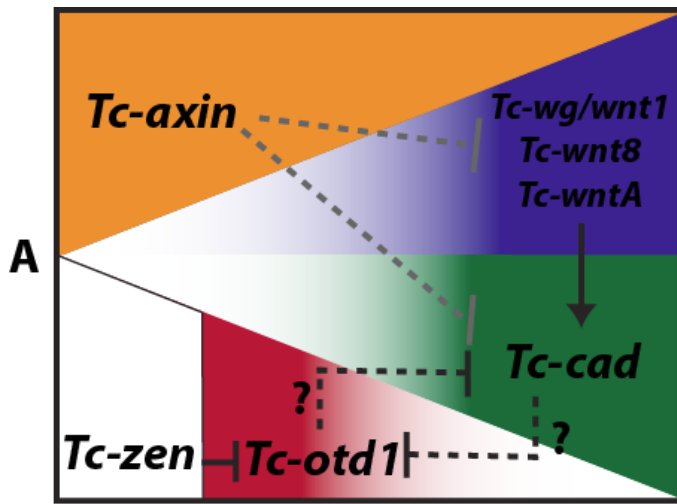


Fig. 5.6: Summary and working model for the analysis of Wnt-signaling in *Tribolium*.

The *Tc-axin* RNAi results show that an anterior Wnt-signal-free region is essential for proper development of anterior structures. The gray dashed lines indicate that *Tc-axin* function is needed in order to provide the anterior Wnt-signal-free region. In this region *Tc-otd1* becomes (zygotically) activated. *Tc-zen1* from extra-embryonic tissue restricts *Tc-otd1* to the future embryonic region. Wnt-signals in the posterior region are involved in the activation of *Tc-caudal* and therefore promote posterior fate. *Tc-caudal* and *Tc-otd1* might act through mutual repression. See text for a detailed discussion.

Interestingly, the loss of *Dm-axin* function (maternal and zygotic) does not result in severe anterior-posterior patterning defects in *Drosophila*. The phenotypes rather lack segmental denticle belts, resulting in naked larval cuticles (Hamada et al., 1999; Willert et al., 1999). These observations suggest that Wnt-signaling is not involved in the initial patterning of the anterior-posterior axis in *Drosophila*. Higher dipterans rather possess a very specialized and unique system composed of maternally provided and gradient-forming factors, namely *Dm-bicoid* (anterior) that regulates *Dm-caudal* translation (posterior) (Rivera-Pomar et al., 1996). This system initially patterns the anterior-posterior axis. However, the anterior specifying gene *bicoid* is not present in other insects (Brown et al., 2001; Stauber et al., 2002). Interestingly, several studies show that *otd* has the potential to be the ancient anterior master regulator for two main reasons. First, *otd* is provided maternally in insects other than *Drosophila*, indicating an early function (Lynch et al., 2006; Schetelig et al., 2008; Schinko et al., 2008; Schroder, 2003). And second, the knock down of *otd* in *Tribolium* and the wasp *Nasonia vitripennis* leads to the loss of large anterior regions, indicating a similar role to *bicoid* in *Drosophila* (Lynch et al., 2006; Schinko et al., 2008; Schroder, 2003).

The results on *Tc-axin* presented here suggest an additionally involved mechanism, namely the prerequisite of a Wnt-target free anterior region, that might act upstream of *Tc-otd1* to activate and restrict its expression in the head anlagen. Furthermore, these results show that the involvement of Wnt-signaling in anterior-posterior axis formation in *Tribolium* is highly similar to the vertebrate situation. The derived mode of *Drosophila* development has probably

hampered the identification of vertebrate-like involvement of Wnt-signaling in early axis formation.

It would be interesting to analyze the function and expression of *axin* in other insects in order to confirm the proposed ancient role of Wnt-signaling in anterior-posterior axis formation.

5.3 Development of the intercalary segment

5.3.1 *Tc-labial* knock-down leads to loss of the intercalary segment rather than a transformation

I showed that major parts of the embryonic intercalary segment fail to develop upon knock down of *Tc-lab* function as indicated by the loss of *Tc-hh*, *Tc-wg*, *Tc-slp1* and *Tc-ey/pax6* expression. The lack of intercalary tissue is confirmed by the mandibular *Tc-mirror/irx* domain which is shifted anteriorly in *Tc-lab* RNAi embryos. Also expression of the anterior marker *Tc-mirror/irx* is reduced at the lateral parts of the intercalary segment. However, some anterior median *Tc-mirror/irx* remains expressed. Interestingly, also *Tc-lab* expression does not cover median tissues at this stage (Fig. 4.18B,C) which might render them insensitive to *Tc-lab* RNAi. An alternative explanation is that this aspect of *Tc-mirror/irx* expression depends on signals that emanate from the adjacent stomodeum that is unaltered in its expression of the morphogens *Tc-wg* and *Tc-hh*. In this scenario, this aspect of *Tc-mirror/irx* expression would be independent from intercalary signals.

labial belongs to the group of homeotic selector genes (Hox) which specify the identity of specific body regions in all animals, including the insects *Drosophila* (Lawrence and Morata, 1994; Lewis, 1978; McGinnis and Krumlauf, 1992) and *Tribolium* (Beeman et al., 1993; Brown et al., 2002; Tomoyasu et al., 2005). Typically, members of the highly conserved Hox-gene cluster show different levels of segmental transformations upon loss of function or gain of function in a wide array of arthropods (Akam, 1998; Angelini et al., 2005; Copf et al., 2006; Hughes and Kaufman, 2000). However, the observed transformations are based on the expansion of anteriorly expressed Hox-genes, rather than specific effects of the lost Hox-gene. This is based on a phenomenon called “posterior prevalence” that describes the fact that posterior Hox genes repress the expression of more anterior ones (Hafen et al., 1984; Lufkin et al., 1991; McGinnis and Krumlauf, 1992; Struhl and White, 1985). Given the fact that *labial/Hox1* is the anterior most expressed Hox-gene it is not surprising that *labial/Hox1*

mutants in *Drosophila* do not show transformations because no anterior Hox-gene can substitute for its expression. Mutations in *Dm-labial* result in head involution defects which make interpretations difficult (Akam, 1989; Jürgens et al., 1986; Merrill et al., 1989). The loss of several cuticular structures in the larval head was thought to arise mostly secondarily as consequence of defective head involution. Two defects, however, correlate with embryonic *labial* expression in *Drosophila*: First, the fusion of the mandibular/maxillary lobe with the procephalic lobe does not occur. Second, *labial* expressing cells in the procephalic lobe fail to assimilate into the dorsal pouch (Merrill et al., 1989). In the light of my findings the former phenotype could be due to a loss of intercalary tissue between the mandibular/maxillary and the procephalic lobes. This would lead to the lack of fusion and the observed enlarged distance of these lobes (see Fig. 3B in Merrill et al., 1989). The similarity in both insects suggests that the establishment and/or maintenance of the intercalary segment might be a conserved function of *labial* within insects.

5.3.2 Different patterning mechanism in the intercalary segment

labial is the only Hox-gene expressed in the pregnathal head region that is patterned differently from the trunk (Cohen and Jurgens, 1990; Crozatier et al., 1999) and the segment polarity genes show different interactions in each of the pregnathal segments (Gallitano-Mendel and Finkelstein, 1997). My temporal expression analysis in *Tribolium* embryos shows that the intercalary parasegment boundary is established only late during germ band elongation (Fig. 4.17) which is in accordance with data in other insects (Rogers and Kaufman, 1996). This analysis also shows that *Tc-lab* is expressed in early germ band stages (3-4 *wg*-stripe stage) long before the first segmental marker becomes evident at a 6-7 *wg*-stripe stage (*Tc-mirror/irx*, Fig. 4.17B',G). The expression of other segmental markers is even more delayed (Fig. 4.17G). This implies that *Tc-lab* already operates in a tissue that is still unspecified in terms of parasegmental organization. Interestingly, not only the intercalary parasegment boundary but also the adjacent portions of the mandibular parasegment lag behind. Mandibular *Tc-mirror/irx* expression is first observed in a 9-10 *wg*-stripe stage whereas the posterior compartment of this segment is established much earlier – actually, it is the first trunk parasegment boundary to be specified (Fig. 4.17C,D). Apparently, the establishment of the intercalary parasegment boundary is required for patterning the anterior mandibular segment.

5.3.3 The intercalary segment is required for lateral parts of the head

I showed that the intercalary segment is required for the embryonic formation of lateral head cuticle (gena). This is in line with the analysis of temperature sensitive alleles in adult flies which has revealed defects in the postgena of adult flies (Merrill et al., 1989). The unexpected lateral location can probably be explained in the light of the drastic morphogenetic movements during head formation: In early embryonic development the gnathal mouthparts are specified well posterior to the mouth opening but later migrate anteriorly to end up in a circle around the mouth (Rogers and Kaufman, 1997; Snodgrass, 1935; Weber, 1966). The intercalary segment initially separates gnathal appendages from the mouth opening and is somehow split by the anterior movement of the mouthparts. My results indicate that the appendages split the intercalary segment and push parts of it laterally. This is supported by the expression of *Tc-lab* in late embryos: The *Tc-lab* domains become split where the mandible is located, indicating that the forward movement of the mandible is causative (Fig. 4.18D). This conclusion is based on the assumption that the expression of *Tc-labial* does not migrate over tissues, i.e. the observed split of *Tc-labial* expression reflects the split of intercalary tissue and that the cuticular defects are not due to secondary effects. The contribution of the median domain of the split *Tc-labial* expression to the head epidermis remains unclear. It could be involved in tritocerebrum formation as in *Drosophila* (Hirth et al., 2001).

5.4 Outlook

I identified a large set of genes whose expression indicates an involvement in processes reaching from anterior patterning to tissue and cell specific functions. Based on the expression and epidermal function of these genes I hypothesized interactions which I subsequently tested. The fact that most of these proposed interactions were confirmed shows that this is an adequate approach to reveal the network underlying anterior head patterning. Hence, more interactions should be tested. Additionally, a comprehensive comparison of interactions in insects and vertebrates will uncover the core interactions of the anterior bilaterian patterning network. Potential differences within this network might probably help to explain the diversity among Bilaterians.

In addition to this candidate gene approach, an unbiased search for new genes involved in anterior patterning of insects is needed. This could be achieved through mutagenesis screens

and genome wide RNAi screens. Both approaches are currently running or planned in *Tribolium*. The genes identified by these approaches should then be integrated into the network. Furthermore, these genes could be analyzed in vertebrates in order to expand the list of potentially conserved genes.

The analysis of the gene functions shown in this work is restricted on epidermal ectoderm patterning. Since early head patterning genes in insects are also potentially involved in neural development, the importance of the so far identified genes for neural development should be analyzed. In order to gain insight into the development of the *Tribolium* brain a variety of transgenic lines is needed, in which different parts of the larval brain are specifically marked. The genes identified in this work provide first candidates for such an approach. Once these lines are established, the effects of loss of function of early patterning genes on larval brain development can be scored. In line with this approach, it would be interesting to show whether the potential placodal region of *Tribolium* is really involved in the formation of the neuroendocrine system.

The data presented in this work indicates that an important signaling center (IHB) is involved in early head patterning. A comprehensive analysis of the IHB is needed to substantiate its importance for head development.

And finally, this work further substantiates the importance of canonical Wnt-signaling in the establishment of the anterior-posterior axis in *Tribolium*. It would be interesting to figure out how early Wnt-signaling is connected to other processes in anterior-posterior patterning.

6 References

- Abzhanov, A. and Kaufman, T. C.** (1999). Homeotic genes and the arthropod head: expression patterns of the labial, proboscipedia, and Deformed genes in crustaceans and insects. *Proc Natl Acad Sci U S A* **96**, 10224-9.
- Acampora, D., Avantaggiato, V., Tuorto, F., Barone, P., Reichert, H., Finkelstein, R. and Simeone, A.** (1998). Murine Otx1 and Drosophila otd genes share conserved genetic functions required in invertebrate and vertebrate brain development. *Development* **125**, 1691-702.
- Acampora, D., Mazan, S., Lallemand, Y., Avantaggiato, V., Maury, M., Simeone, A. and Brulet, P.** (1995). Forebrain and midbrain regions are deleted in Otx2^{-/-} mutants due to a defective anterior neuroectoderm specification during gastrulation. *Development* **121**, 3279-90.
- Adell, T., Salo, E., Boutros, M. and Bartscherer, K.** (2009). Smed-Evi/Wntless is required for beta-catenin-dependent and -independent processes during planarian regeneration. *Development* **136**, 905-10.
- Adoutte, A., Balavoine, G., Lartillot, N., Lespinet, O., Prud'homme, B. and de Rosa, R.** (2000). The new animal phylogeny: reliability and implications. *Proc Natl Acad Sci U S A* **97**, 4453-6.
- Aguinaldo, A. M., Turbeville, J. M., Linford, L. S., Rivera, M. C., Garey, J. R., Raff, R. A. and Lake, J. A.** (1997). Evidence for a clade of nematodes, arthropods and other moulting animals. *Nature* **387**, 489-93.
- Akam, M.** (1989). Hox and HOM: homologous gene clusters in insects and vertebrates. *Cell* **57**, 347-9.
- Akam, M.** (1998). Hox genes in arthropod development and evolution. *Biol Bull* **195**, 373-4.
- Altschul, S. F., Madden, T. L., Schaffer, A. A., Zhang, J., Zhang, Z., Miller, W. and Lipman, D. J.** (1997). Gapped BLAST and PSI-BLAST: a new generation of protein database search programs. *Nucleic Acids Res* **25**, 3389-402.
- Angelini, D. R., Liu, P. Z., Hughes, C. L. and Kaufman, T. C.** (2005). Hox gene function and interaction in the milkweed bug *Oncopeltus fasciatus* (Hemiptera). *Dev Biol* **287**, 440-55.
- Aoto, K., Nishimura, T., Eto, K. and Motoyama, J.** (2002). Mouse GLI3 regulates Fgf8 expression and apoptosis in the developing neural tube, face, and limb bud. *Dev Biol* **251**, 320-32.
- Arendt, D. and Nubler-Jung, K.** (1996). Common ground plans in early brain development in mice and flies. *Bioessays* **18**, 255-9.
- Arendt, D. and Nubler-Jung, K.** (1999). Comparison of early nerve cord development in insects and vertebrates. *Development* **126**, 2309-25.
- Arendt, D., Tessmar-Raible, K., Snyman, H., Dorresteijn, A. W. and Wittbrodt, J.** (2004). Ciliary photoreceptors with a vertebrate-type opsin in an invertebrate brain. *Science* **306**, 869-71.
- Artinger, M., Blitz, I., Inoue, K., Tran, U. and Cho, K. W.** (1997). Interaction of goosecooid and brachyury in *Xenopus* mesoderm patterning. *Mech Dev* **65**, 187-96.
- Ax, P.** (1999). Das System der Metazoa - Ein Lehrbuch der phylogenetischen Systematik. Stuttgart-Jena-Lübeck-Ulm: Gustav Fischer Verlag.
- Baker, C. V. and Bronner-Fraser, M.** (1997). The origins of the neural crest. Part I: embryonic induction. *Mech Dev* **69**, 3-11.
- Beeman, R. W., Stuart, J. J., Brown, S. J. and Denell, R. E.** (1993). Structure and function of the homeotic gene complex (HOM-C) in the beetle, *Tribolium castaneum*. *Bioessays* **15**, 439-44.

- Beermann, A., Jay, D. G., Beeman, R. W., Hulskamp, M., Tautz, D. and Jurgens, G.** (2001). The Short antennae gene of *Tribolium* is required for limb development and encodes the orthologue of the *Drosophila* Distal-less protein. *Development* **128**, 287-97.
- Beermann, A. and Schroder, R.** (2008). Sites of Fgf signalling and perception during embryogenesis of the beetle *Tribolium castaneum*. *Dev Genes Evol* **218**, 153-67.
- Belo, J. A., Leyns, L., Yamada, G. and De Robertis, E. M.** (1998). The prechordal midline of the chondrocranium is defective in Goosecoid-1 mouse mutants. *Mech Dev* **72**, 15-25.
- Bernier, G., Panitz, F., Zhou, X., Hollemann, T., Gruss, P. and Pieler, T.** (2000). Expanded retina territory by midbrain transformation upon overexpression of Six6 (Optx2) in *Xenopus* embryos. *Mech Dev* **93**, 59-69.
- Bhattacharyya, S., Bailey, A. P., Bronner-Fraser, M. and Streit, A.** (2004). Segregation of lens and olfactory precursors from a common territory: cell sorting and reciprocity of Dlx5 and Pax6 expression. *Dev Biol* **271**, 403-14.
- Bishop, K. M., Garel, S., Nakagawa, Y., Rubenstein, J. L. and O'Leary, D. D.** (2003). Emx1 and Emx2 cooperate to regulate cortical size, lamination, neuronal differentiation, development of cortical efferents, and thalamocortical pathfinding. *J Comp Neurol* **457**, 345-60.
- Blum, M., Gaunt, S. J., Cho, K. W., Steinbeisser, H., Blumberg, B., Bittner, D. and De Robertis, E. M.** (1992). Gastrulation in the mouse: the role of the homeobox gene goosecoid. *Cell* **69**, 1097-106.
- Bolognesi, R., Beermann, A., Farzana, L., Wittkopp, N., Lutz, R., Balavoine, G., Brown, S. J. and Schroder, R.** (2008a). *Tribolium* Wnts: evidence for a larger repertoire in insects with overlapping expression patterns that suggest multiple redundant functions in embryogenesis. *Dev Genes Evol* **218**, 193-202.
- Bolognesi, R., Farzana, L., Fischer, T. D. and Brown, S. J.** (2008b). Multiple Wnt genes are required for segmentation in the short-germ embryo of *Tribolium castaneum*. *Curr Biol* **18**, 1624-9.
- Boncinelli, E., Gulisano, M. and Broccoli, V.** (1993). Emx and Otx homeobox genes in the developing mouse brain. *J Neurobiol* **24**, 1356-66.
- Boorman, C. J. and Shimeld, S. M.** (2002). Pitx homeobox genes in *Ciona* and amphioxus show left-right asymmetry is a conserved chordate character and define the ascidian adeno-hypophysis. *Evol Dev* **4**, 354-65.
- Borycki, A., Brown, A. M. and Emerson, C. P., Jr.** (2000). Shh and Wnt signaling pathways converge to control Gli gene activation in avian somites. *Development* **127**, 2075-87.
- Braun, M. M., Etheridge, A., Bernard, A., Robertson, C. P. and Roelink, H.** (2003). Wnt signaling is required at distinct stages of development for the induction of the posterior forebrain. *Development* **130**, 5579-87.
- Briscoe, J., Pierani, A., Jessell, T. M. and Ericson, J.** (2000). A homeodomain protein code specifies progenitor cell identity and neuronal fate in the ventral neural tube. *Cell* **101**, 435-45.
- Brown, S., Fellers, J., Shippy, T., Denell, R., Stauber, M. and Schmidt-Ott, U.** (2001). A strategy for mapping bicoid on the phylogenetic tree. *Curr Biol* **11**, R43-4.
- Brown, S., Holtzman, S., Kaufman, T. and Denell, R.** (1999). Characterization of the *Tribolium* Deformed ortholog and its ability to directly regulate Deformed target genes in the rescue of a *Drosophila* Deformed null mutant. *Dev Genes Evol* **209**, 389-98.
- Brown, S. J., Patel, N. H. and Denell, R. E.** (1994). Embryonic expression of the single *Tribolium* engrailed homolog. *Dev Genet* **15**, 7-18.
- Brown, S. J., Shippy, T. D., Beeman, R. W. and Denell, R. E.** (2002). *Tribolium* Hox genes repress antennal development in the gnathos and trunk. *Mol Phylogenet Evol* **24**, 384-7.

- Brugmann, S. A. and Moody, S. A.** (2005). Induction and specification of the vertebrate ectodermal placodes: precursors of the cranial sensory organs. *Biol Cell* **97**, 303-19.
- Bucher, G. and Klingler, M.** (2004). Divergent segmentation mechanism in the short germ insect *Tribolium* revealed by giant expression and function. *Development* **131**, 1729-40.
- Bucher, G., Scholten, J. and Klingler, M.** (2002). Parental RNAi in *Tribolium* (Coleoptera). *Curr Biol* **12**, R85-6.
- Bucher, G. and Wimmer, E. A.** (2005). Beetle a-head. *B.I.F. Futura* **20**, 164-169.
- Buescher, M. and Chia, W.** (1997). Mutations in *lottchen* cause cell fate transformations in both neuroblast and glioblast lineages in the *Drosophila* embryonic central nervous system. *Development* **124**, 673-81.
- Buescher, M., Hing, F. S. and Chia, W.** (2002). Formation of neuroblasts in the embryonic central nervous system of *Drosophila melanogaster* is controlled by *SoxNeuro*. *Development* **129**, 4193-203.
- Campos-Ortega, J. A.** (1995). Genetic mechanisms of early neurogenesis in *Drosophila melanogaster*. *Mol Neurobiol* **10**, 75-89.
- Campos-Ortega, J. A.** (1998). The genetics of the *Drosophila* *achaete-scute* gene complex: a historical appraisal. *Int J Dev Biol* **42**, 291-7.
- Camus, A., Davidson, B. P., Billiards, S., Khoo, P., Rivera-Perez, J. A., Wakamiya, M., Behringer, R. R. and Tam, P. P.** (2000). The morphogenetic role of midline mesendoderm and ectoderm in the development of the forebrain and the midbrain of the mouse embryo. *Development* **127**, 1799-813.
- Carl, M., Loosli, F. and Wittbrodt, J.** (2002). *Six3* inactivation reveals its essential role for the formation and patterning of the vertebrate eye. *Development* **129**, 4057-63.
- Carroll, S. B.** (1995). Homeotic genes and the evolution of arthropods and chordates. *Nature* **376**, 479-85.
- Carroll, S. B.** (2005). *Endless Forms Most Beautiful: The New Science of Evo Devo and the Making of the Animal Kingdom*. New York: W.W. Norton.
- Carroll, S. B., Grenier, J. K. and Weatherbee, S. D.** (2005). *From DNA to Diversity: Molecular Genetics and the Evolution of Animal Design*. Malden, Mass Blackwell Scientific.
- Cavodeassi, F., Modolell, J. and Gomez-Skarmeta, J. L.** (2001). The Iroquois family of genes: from body building to neural patterning. *Development* **128**, 2847-55.
- Cecchi, C. and Boncinelli, E.** (2000). *Emx* homeogenes and mouse brain development. *Trends Neurosci* **23**, 347-52.
- Cerny, A. C., Grossmann, D., Bucher, G. and Klingler, M.** (2008). The *Tribolium* ortholog of *knirps* and *knirps*-related is crucial for head segmentation but plays a minor role during abdominal patterning. *Dev Biol* **321**, 284-94.
- Chen, R., Amoui, M., Zhang, Z. and Mardon, G.** (1997). *Dachshund* and *eyes absent* proteins form a complex and function synergistically to induce ectopic eye development in *Drosophila*. *Cell* **91**, 893-903.
- Cho, K. W., Blumberg, B., Steinbeisser, H. and De Robertis, E. M.** (1991). Molecular nature of Spemann's organizer: the role of the *Xenopus* homeobox gene *gooseoid*. *Cell* **67**, 1111-20.
- Cho, K. W. and De Robertis, E. M.** (1990). Differential activation of *Xenopus* homeobox genes by mesoderm-inducing growth factors and retinoic acid. *Genes Dev* **4**, 1910-6.
- Choe, C. P. and Brown, S. J.** (2007). Evolutionary flexibility of pair-rule patterning revealed by functional analysis of secondary pair-rule genes, paired and sloppy-paired in the short-germ insect, *Tribolium castaneum*. *Dev Biol* **302**, 281-94.
- Choe, C. P. and Brown, S. J.** (2009). Genetic regulation of *engrailed* and *wingless* in *Tribolium* segmentation and the evolution of pair-rule segmentation. *Dev Biol* **325**, 482-91.

- Choe, C. P., Miller, S. C. and Brown, S. J.** (2006). A pair-rule gene circuit defines segments sequentially in the short-germ insect *Tribolium castaneum*. *Proc Natl Acad Sci U S A* **103**, 6560-4.
- Christiaen, L., Burighel, P., Smith, W. C., Vernier, P., Bourrat, F. and Joly, J. S.** (2002). Pitx genes in Tunicates provide new molecular insight into the evolutionary origin of pituitary. *Gene* **287**, 107-13.
- Chu, H., Parras, C., White, K. and Jimenez, F.** (1998). Formation and specification of ventral neuroblasts is controlled by vnd in *Drosophila* neurogenesis. *Genes Dev* **12**, 3613-24.
- Chuang, J. C., Mathers, P. H. and Raymond, P. A.** (1999). Expression of three Rx homeobox genes in embryonic and adult zebrafish. *Mech Dev* **84**, 195-8.
- Cohen, S. M. and Jurgens, G.** (1990). Mediation of *Drosophila* head development by gap-like segmentation genes. *Nature* **346**, 482-5.
- Colombo, E., Galli, R., Cossu, G., Geetz, J. and Broccoli, V.** (2004). Mouse orthologue of ARX, a gene mutated in several X-linked forms of mental retardation and epilepsy, is a marker of adult neural stem cells and forebrain GABAergic neurons. *Dev Dyn* **231**, 631-9.
- Conte, I., Morcillo, J. and Bovolenta, P.** (2005). Comparative analysis of Six 3 and Six 6 distribution in the developing and adult mouse brain. *Dev Dyn* **234**, 718-25.
- Copf, T., Rabet, N. and Averof, M.** (2006). Knockdown of spalt function by RNAi causes de-repression of Hox genes and homeotic transformations in the crustacean *Artemia franciscana*. *Dev Biol* **298**, 87-94.
- Copf, T., Schroder, R. and Averof, M.** (2004). Ancestral role of caudal genes in axis elongation and segmentation. *Proc Natl Acad Sci U S A* **101**, 17711-5.
- Cornell, R. A. and Ohlen, T. V.** (2000). Vnd/nkx, ind/gsh, and msh/msx: conserved regulators of dorsoventral neural patterning? *Curr Opin Neurobiol* **10**, 63-71.
- Couly, G. and Le Douarin, N. M.** (1990). Head morphogenesis in embryonic avian chimeras: evidence for a segmental pattern in the ectoderm corresponding to the neuromeres. *Development* **108**, 543-58.
- Cremazy, F., Berta, P. and Girard, F.** (2000). Sox neuro, a new *Drosophila* Sox gene expressed in the developing central nervous system. *Mech Dev* **93**, 215-9.
- Crossley, P. H. and Martin, G. R.** (1995). The mouse Fgf8 gene encodes a family of polypeptides and is expressed in regions that direct outgrowth and patterning in the developing embryo. *Development* **121**, 439-51.
- Crozatier, M., Valle, D., Dubois, L., Ibnsouda, S. and Vincent, A.** (1999). Head versus trunk patterning in the *Drosophila* embryo; collier requirement for formation of the intercalary segment. *Development* **126**, 4385-94.
- Daftary, G. S. and Taylor, H. S.** (2006). Endocrine regulation of HOX genes. *Endocr Rev* **27**, 331-55.
- Dalton, D., Chadwick, R. and McGinnis, W.** (1989). Expression and embryonic function of empty spiracles: a *Drosophila* homeo box gene with two patterning functions on the anterior-posterior axis of the embryo. *Genes Dev* **3**, 1940-56.
- Dambly-Chaudiere, C. and Vervoort, M.** (1998). The bHLH genes in neural development. *Int J Dev Biol* **42**, 269-73.
- Davidson, D., Graham, E., Sime, C. and Hill, R.** (1988). A gene with sequence similarity to *Drosophila* engrailed is expressed during the development of the neural tube and vertebrae in the mouse. *Development* **104**, 305-16.
- Davis, C. A., Holmyard, D. P., Millen, K. J. and Joyner, A. L.** (1991). Examining pattern formation in mouse, chicken and frog embryos with an En-specific antiserum. *Development* **111**, 287-98.
- Davis, C. A. and Joyner, A. L.** (1988). Expression patterns of the homeo box-containing genes En-1 and En-2 and the proto-oncogene int-1 diverge during mouse development. *Genes Dev* **2**, 1736-44.

- De Robertis, E. M.** (2008). Evo-devo: variations on ancestral themes. *Cell* **132**, 185-95.
- De Robertis, E. M., Larrain, J., Oelgeschlager, M. and Wessely, O.** (2000). The establishment of Spemann's organizer and patterning of the vertebrate embryo. *Nat Rev Genet* **1**, 171-81.
- de Velasco, B., Erelik, T., Shy, D., Sclafani, J., Lipshitz, H., McInnes, R. and Hartenstein, V.** (2007). Specification and development of the pars intercerebralis and pars lateralis, neuroendocrine command centers in the *Drosophila* brain. *Dev Biol* **302**, 309-23.
- De Velasco, B., Shen, J., Go, S. and Hartenstein, V.** (2004). Embryonic development of the *Drosophila* corpus cardiacum, a neuroendocrine gland with similarity to the vertebrate pituitary, is controlled by *sine oculis* and *glass*. *Dev Biol* **274**, 280-94.
- DeFalco, T. J., Verney, G., Jenkins, A. B., McCaffery, J. M., Russell, S. and Van Doren, M.** (2003). Sex-specific apoptosis regulates sexual dimorphism in the *Drosophila* embryonic gonad. *Dev Cell* **5**, 205-16.
- Denes, A. S., Jekely, G., Steinmetz, P. R., Raible, F., Snyman, H., Prud'homme, B., Ferrier, D. E., Balavoine, G. and Arendt, D.** (2007). Molecular architecture of annelid nerve cord supports common origin of nervous system centralization in bilateria. *Cell* **129**, 277-88.
- Deschet, K., Bourrat, F., Ristoratore, F., Chourrout, D. and Joly, J. S.** (1999). Expression of the medaka (*Oryzias latipes*) *Ol-Rx3* paired-like gene in two diencephalic derivatives, the eye and the hypothalamus. *Mech Dev* **83**, 179-82.
- Dettner, K. and Peters, W.** (2003). *Lehrbuch der Entomologie*. Heidelberg-Berlin: Spektrum Akademischer Verlag.
- Dickinson, A. and Sive, H.** (2007). Positioning the extreme anterior in *Xenopus*: cement gland, primary mouth and anterior pituitary. *Semin Cell Dev Biol* **18**, 525-33.
- Diederich, R. J., Merrill, V. K., Pultz, M. A. and Kaufman, T. C.** (1989). Isolation, structure, and expression of *labial*, a homeotic gene of the Antennapedia Complex involved in *Drosophila* head development. *Genes Dev* **3**, 399-414.
- Domingos, P. M., Itasaki, N., Jones, C. M., Mercurio, S., Sargent, M. G., Smith, J. C. and Krumlauf, R.** (2001). The Wnt/beta-catenin pathway posteriorizes neural tissue in *Xenopus* by an indirect mechanism requiring FGF signalling. *Dev Biol* **239**, 148-60.
- Driever, W. and Nusslein-Volhard, C.** (1988a). The bicoid protein determines position in the *Drosophila* embryo in a concentration-dependent manner. *Cell* **54**, 95-104.
- Driever, W. and Nusslein-Volhard, C.** (1988b). A gradient of bicoid protein in *Drosophila* embryos. *Cell* **54**, 83-93.
- Dupe, V. and Lumsden, A.** (2001). Hindbrain patterning involves graded responses to retinoic acid signalling. *Development* **128**, 2199-208.
- Dutta, S., Dietrich, J. E., Aspöck, G., Burdine, R. D., Schier, A., Westerfield, M. and Varga, Z. M.** (2005). *pitx3* defines an equivalence domain for lens and anterior pituitary placode. *Development* **132**, 1579-90.
- Eagleson, G. W. and Harris, W. A.** (1990). Mapping of the presumptive brain regions in the neural plate of *Xenopus laevis*. *J Neurobiol* **21**, 427-40.
- Echelard, Y., Epstein, D. J., St-Jacques, B., Shen, L., Mohler, J., McMahon, J. A. and McMahon, A. P.** (1993). Sonic hedgehog, a member of a family of putative signaling molecules, is implicated in the regulation of CNS polarity. *Cell* **75**, 1417-30.
- Echelard, Y., Vassileva, G. and McMahon, A. P.** (1994). Cis-acting regulatory sequences governing Wnt-1 expression in the developing mouse CNS. *Development* **120**, 2213-24.
- Economou, A. D. and Telford, M. J.** (2009). Comparative gene expression in the heads of *Drosophila melanogaster* and *Tribolium castaneum* and the segmental affinity of the *Drosophila* hypopharyngeal lobes. *Evol Dev* **11**, 88-96.
- El-Hodiri, H. M., Qi, X. L. and Seufert, D. W.** (2003). The *Xenopus arx* gene is expressed in the developing rostral forebrain. *Dev Genes Evol* **212**, 608-12.

- Ericson, J., Muhr, J., Placzek, M., Lints, T., Jessell, T. M. and Edlund, T.** (1995). Sonic hedgehog induces the differentiation of ventral forebrain neurons: a common signal for ventral patterning within the neural tube. *Cell* **81**, 747-56.
- Ericson, J., Rashbass, P., Schedl, A., Brenner-Morton, S., Kawakami, A., van Heyningen, V., Jessell, T. M. and Briscoe, J.** (1997). Pax6 controls progenitor cell identity and neuronal fate in response to graded Shh signaling. *Cell* **90**, 169-80.
- Eriksson, B. J., Tait, N. N., Budd, G. E. and Akam, M.** (2009). The involvement of engrailed and wingless during segmentation in the onychophoran *Euperipatoides kanangrensis* (Peripatopsidae: Onychophora) (Reid 1996). *Dev Genes Evol* **219**, 249-64.
- Esterberg, R. and Fritz, A.** (2009). *dlx3b/4b* are required for the formation of the preplacodal region and otic placode through local modulation of BMP activity. *Dev Biol* **325**, 189-99.
- Farris, S. M.** (2008). Structural, functional and developmental convergence of the insect mushroom bodies with higher brain centers of vertebrates. *Brain Behav Evol* **72**, 1-15.
- Farzana, L. and Brown, S. J.** (2008). Hedgehog signaling pathway function conserved in *Tribolium* segmentation. *Dev Genes Evol* **218**, 181-92.
- Favier, B. and Dolle, P.** (1997). Developmental functions of mammalian Hox genes. *Mol Hum Reprod* **3**, 115-31.
- Felsenstein, J.** (1985). Confidence limits on phylogenies: An approach using the bootstrap. *Evolution* **39**, 783-791.
- Filipowicz, W.** (2005). RNAi: the nuts and bolts of the RISC machine. *Cell* **122**, 17-20.
- Finkelstein, R. and Boncinelli, E.** (1994). From fly head to mammalian forebrain: the story of *otd* and *Otx*. *Trends Genet* **10**, 310-5.
- Finkelstein, R. and Perrimon, N.** (1990). The orthodenticle gene is regulated by bicoid and torso and specifies *Drosophila* head development. *Nature* **346**, 485-8.
- Finnerty, J. R.** (2003). The origins of axial patterning in the metazoa: how old is bilateral symmetry? *Int J Dev Biol* **47**, 523-9.
- Fjose, A., Izpisua-Belmonte, J. C., Fromental-Ramain, C. and Duboule, D.** (1994). Expression of the zebrafish gene *hlx-1* in the prechordal plate and during CNS development. *Development* **120**, 71-81.
- Friocourt, G., Poirier, K., Rakic, S., Parnavelas, J. G. and Chelly, J.** (2006). The role of ARX in cortical development. *Eur J Neurosci* **23**, 869-76.
- Galceran, J., Farinas, I., Depew, M. J., Clevers, H. and Grosschedl, R.** (1999). Wnt3a^{-/-} like phenotype and limb deficiency in Lef1^(-/-)Tcf1^(-/-) mice. *Genes Dev* **13**, 709-17.
- Gallitano-Mendel, A. and Finkelstein, R.** (1997). Novel segment polarity gene interactions during embryonic head development in *Drosophila*. *Dev Biol* **192**, 599-613.
- Garcia-Fernandez, J.** (2005). The genesis and evolution of homeobox gene clusters. *Nat Rev Genet* **6**, 881-92.
- Gershon, A. A., Rudnick, J., Kalam, L. and Zimmerman, K.** (2000). The homeodomain-containing gene *Xdbx* inhibits neuronal differentiation in the developing embryo. *Development* **127**, 2945-54.
- Gestri, G., Carl, M., Appolloni, I., Wilson, S. W., Barsacchi, G. and Andreatzoli, M.** (2005). Six3 functions in anterior neural plate specification by promoting cell proliferation and inhibiting *Bmp4* expression. *Development* **132**, 2401-13.
- Gilbert, S. F., Opitz, J. M. and Raff, R. A.** (1996). Resynthesizing evolutionary and developmental biology. *Dev Biol* **173**, 357-72.
- Glavic, A., Gomez-Skarmeta, J. L. and Mayor, R.** (2002). The homeoprotein *Xiro1* is required for midbrain-hindbrain boundary formation. *Development* **129**, 1609-21.
- Gomez-Skarmeta, J., de La Calle-Mustienes, E. and Modolell, J.** (2001). The Wnt-activated *Xiro1* gene encodes a repressor that is essential for neural development and downregulates *Bmp4*. *Development* **128**, 551-60.

- Gomez-Skarmeta, J. L., Glavic, A., de la Calle-Mustienes, E., Modolell, J. and Mayor, R.** (1998). Xiro, a Xenopus homolog of the Drosophila Iroquois complex genes, controls development at the neural plate. *Embo J* **17**, 181-90.
- Goriely, A., Mollereau, B., Coffinier, C. and Desplan, C.** (1999). Munster, a novel paired-class homeobox gene specifically expressed in the Drosophila larval eye. *Mech Dev* **88**, 107-10.
- Goriely, A., Stella, M., Coffinier, C., Kessler, D., Mailhos, C., Dessain, S. and Desplan, C.** (1996). A functional homologue of gooseoid in Drosophila. *Development* **122**, 1641-50.
- Goulding, M. D., Lumsden, A. and Gruss, P.** (1993). Signals from the notochord and floor plate regulate the region-specific expression of two Pax genes in the developing spinal cord. *Development* **117**, 1001-16.
- Gribble, S. L., Nikolaus, O. B. and Dorsky, R. I.** (2007). Regulation and function of Dbx genes in the zebrafish spinal cord. *Dev Dyn* **236**, 3472-83.
- Griesel, G., Treichel, D., Collombat, P., Krull, J., Zembrzycki, A., van den Akker, W. M., Gruss, P., Simeone, A. and Mansouri, A.** (2006). Sp8 controls the anteroposterior patterning at the midbrain-hindbrain border. *Development* **133**, 1779-87.
- Gritsman, K., Talbot, W. S. and Schier, A. F.** (2000). Nodal signaling patterns the organizer. *Development* **127**, 921-32.
- Grossniklaus, U., Cadigan, K. M. and Gehring, W. J.** (1994). Three maternal coordinate systems cooperate in the patterning of the Drosophila head. *Development* **120**, 3155-71.
- Hafen, E., Levine, M. and Gehring, W. J.** (1984). Regulation of Antennapedia transcript distribution by the bithorax complex in Drosophila. *Nature* **307**, 287-9.
- Hahn, M. and Jackle, H.** (1996). Drosophila gooseoid participates in neural development but not in body axis formation. *Embo J* **15**, 3077-84.
- Hamada, F., Tomoyasu, Y., Takatsu, Y., Nakamura, M., Nagai, S., Suzuki, A., Fujita, F., Shibuya, H., Toyoshima, K., Ueno, N. et al.** (1999). Negative regulation of Wingless signaling by D-axin, a Drosophila homolog of axin. *Science* **283**, 1739-42.
- Hamburger, V. and Hamilton, H. L.** (1992). A series of normal stages in the development of the chick embryo. 1951. *Dev Dyn* **195**, 231-72.
- Handel, K., Basal, A., Fan, X. and Roth, S.** (2005). Tribolium castaneum twist: gastrulation and mesoderm formation in a short-germ beetle. *Dev Genes Evol* **215**, 13-31.
- Harland, R. M.** (1991). In situ hybridization: an improved whole-mount method for Xenopus embryos. *Methods Cell Biol* **36**, 685-95.
- Hartenstein, V.** (2006). The neuroendocrine system of invertebrates: a developmental and evolutionary perspective. *J Endocrinol* **190**, 555-70.
- Hartenstein, V., Rudloff, E. and Campos-Ortega, J. A.** (1987). The pattern of proliferation of the neuroblasts in the wild-type embryo of Drosophila melanogaster. *Roux Arch. dev. Biol.* **196**, 473-485.
- Hashimoto, H., Yabe, T., Hirata, T., Shimizu, T., Bae, Y., Yamanaka, Y., Hirano, T. and Hibi, M.** (2000). Expression of the zinc finger gene fez-like in zebrafish forebrain. *Mech Dev* **97**, 191-5.
- Hebert, J. M. and Fishell, G.** (2008). The genetics of early telencephalon patterning: some assembly required. *Nat Rev Neurosci.*
- Hein, H.** (2007). Identifizierung von Neuroblasten als Modell für die Regulierung ihrer Spezifizierung in Tribolium castaneum. *Diploma Thesis; Dpt. for Developmental Biology Georg-August-University Goettingen.*
- Heisenberg, C. P., Houart, C., Take-Uchi, M., Rauch, G. J., Young, N., Coutinho, P., Masai, I., Caneparo, L., Concha, M. L., Geisler, R. et al.** (2001). A mutation in the Gsk3-binding domain of zebrafish Masterblind/Axin1 leads to a fate transformation of telencephalon and eyes to diencephalon. *Genes Dev* **15**, 1427-34.

- Hidalgo-Sanchez, M., Millet, S., Bloch-Gallego, E. and Alvarado-Mallart, R. M.** (2005). Specification of the meso-isthmo-cerebellar region: the Otx2/Gbx2 boundary. *Brain Res Brain Res Rev* **49**, 134-49.
- Hidalgo-Sanchez, M., Millet, S., Simeone, A. and Alvarado-Mallart, R. M.** (1999). Comparative analysis of Otx2, Gbx2, Pax2, Fgf8 and Wnt1 gene expressions during the formation of the chick midbrain/hindbrain domain. *Mech Dev* **81**, 175-8.
- Hirata, T., Nakazawa, M., Muraoka, O., Nakayama, R., Suda, Y. and Hibi, M.** (2006). Zinc-finger genes Fez and Fez-like function in the establishment of diencephalon subdivisions. *Development* **133**, 3993-4004.
- Hirata, T., Suda, Y., Nakao, K., Narimatsu, M., Hirano, T. and Hibi, M.** (2004). Zinc finger gene fez-like functions in the formation of subplate neurons and thalamocortical axons. *Dev Dyn* **230**, 546-56.
- Hirth, F., Kammermeier, L., Frei, E., Walldorf, U., Noll, M. and Reichert, H.** (2003). An urbilaterian origin of the tripartite brain: developmental genetic insights from Drosophila. *Development* **130**, 2365-73.
- Hirth, F., Loop, T., Egger, B., Miller, D. F., Kaufman, T. C. and Reichert, H.** (2001). Functional equivalence of Hox gene products in the specification of the tritocerebrum during embryonic brain development of Drosophila. *Development* **128**, 4781-8.
- Hirth, F. and Reichert, H.** (1999). Conserved genetic programs in insect and mammalian brain development. *Bioessays* **21**, 677-84.
- Holland, L. Z. and Holland, N. D.** (1999). Chordate origins of the vertebrate central nervous system. *Curr Opin Neurobiol* **9**, 596-602.
- Holland, P., Ingham, P. and Krauss, S.** (1992). Development and evolution. Mice and flies head to head. *Nature* **358**, 627-8.
- Holleman, T., Bellefroid, E. and Pieler, T.** (1998). The Xenopus homologue of the Drosophila gene tailless has a function in early eye development. *Development* **125**, 2425-32.
- Houart, C., Caneparo, L., Heisenberg, C., Barth, K., Take-Uchi, M. and Wilson, S.** (2002). Establishment of the telencephalon during gastrulation by local antagonism of Wnt signaling. *Neuron* **35**, 255-65.
- Hughes, C. L. and Kaufman, T. C.** (2000). RNAi analysis of Deformed, proboscipedia and Sex combs reduced in the milkweed bug *Oncopeltus fasciatus*: novel roles for Hox genes in the hemipteran head. *Development* **127**, 3683-94.
- Hui Yong Loh, S. and Russell, S.** (2000). A Drosophila group E Sox gene is dynamically expressed in the embryonic alimentary canal. *Mech Dev* **93**, 185-8.
- Ingham, P. W.** (1988). The molecular genetics of embryonic pattern formation in Drosophila. *Nature* **335**, 25-34.
- Ishibashi, M.** (2004). Molecular mechanisms for morphogenesis of the central nervous system in mammals. *Anat Sci Int* **79**, 226-34.
- Isshiki, T., Takeichi, M. and Nose, A.** (1997). The role of the msh homeobox gene during Drosophila neurogenesis: implication for the dorsoventral specification of the neuroectoderm. *Development* **124**, 3099-109.
- Izpisua-Belmonte, J. C., De Robertis, E. M., Storey, K. G. and Stern, C. D.** (1993). The homeobox gene goosecoid and the origin of organizer cells in the early chick blastoderm. *Cell* **74**, 645-59.
- Janssen, R. and Damen, W. G.** (2006). The ten Hox genes of the millipede *Glomeris marginata*. *Dev Genes Evol* **216**, 451-65.
- Jean, D., Bernier, G. and Gruss, P.** (1999). Six6 (Optx2) is a novel murine Six3-related homeobox gene that demarcates the presumptive pituitary/hypothalamic axis and the ventral optic stalk. *Mech Dev* **84**, 31-40.

- Jeong, J. Y., Einhorn, Z., Mathur, P., Chen, L., Lee, S., Kawakami, K. and Guo, S.** (2007). Patterning the zebrafish diencephalon by the conserved zinc-finger protein Fezl. *Development* **134**, 127-36.
- Jürgens, G., Lehmann, R., Schardin, M. and Nusslein-Volhard, C.** (1986). Segmental organisation of the head in the embryo of *Drosophila melanogaster*. *Roux's Arch. Dev. Biol.* **195**, 359-377.
- Kardong, K. V.** (1998). *Vertebrates: Comparative Anatomy, Function, Evolution*. Boston: WCB/McGraw-Hill.
- Kerner, P., Ikmi, A., Coen, D. and Vervoort, M.** (2009). Evolutionary history of the iroquois/Irx genes in metazoans. *BMC Evol Biol* **9**, 74.
- Kessel, M.** (1992). Respecification of vertebral identities by retinoic acid. *Development* **115**, 487-501.
- Kessel, M. and Gruss, P.** (1991). Homeotic transformations of murine vertebrae and concomitant alteration of Hox codes induced by retinoic acid. *Cell* **67**, 89-104.
- Kiecker, C. and Lumsden, A.** (2004). Hedgehog signaling from the ZLI regulates diencephalic regional identity. *Nat Neurosci* **7**, 1242-9.
- Kiecker, C. and Niehrs, C.** (2001). A morphogen gradient of Wnt/beta-catenin signalling regulates anteroposterior neural patterning in *Xenopus*. *Development* **128**, 4189-201.
- Kitambi, S. S. and Hauptmann, G.** (2007). The zebrafish orphan nuclear receptor genes nr2e1 and nr2e3 are expressed in developing eye and forebrain. *Gene Expr Patterns* **7**, 521-8.
- Kobayashi, M., Nishikawa, K., Suzuki, T. and Yamamoto, M.** (2001). The homeobox protein Six3 interacts with the Groucho corepressor and acts as a transcriptional repressor in eye and forebrain formation. *Dev Biol* **232**, 315-26.
- Koster, R. W., Kuhnlein, R. P. and Wittbrodt, J.** (2000). Ectopic Sox3 activity elicits sensory placode formation. *Mech Dev* **95**, 175-87.
- Kumar, S., Nei, M., Dudley, J. and Tamura, K.** (2008). MEGA: a biologist-centric software for evolutionary analysis of DNA and protein sequences. *Brief Bioinform* **9**, 299-306.
- Kurusu, M., Maruyama, Y., Adachi, Y., Okabe, M., Suzuki, E. and Furukubo-Tokunaga, K.** (2009). A conserved nuclear receptor, Tailless, is required for efficient proliferation and prolonged maintenance of mushroom body progenitors in the *Drosophila* brain. *Dev Biol* **326**, 224-36.
- Lagutin, O. V., Zhu, C. C., Kobayashi, D., Topczewski, J., Shimamura, K., Puelles, L., Russell, H. R., McKinnon, P. J., Solnica-Krezel, L. and Oliver, G.** (2003). Six3 repression of Wnt signaling in the anterior neuroectoderm is essential for vertebrate forebrain development. *Genes Dev* **17**, 368-79.
- Lamonerie, T., Tremblay, J. J., Lanctot, C., Therrien, M., Gauthier, Y. and Drouin, J.** (1996). Ptx1, a bicoid-related homeo box transcription factor involved in transcription of the pro-opiomelanocortin gene. *Genes Dev* **10**, 1284-95.
- Lanctot, C., Lamolet, B. and Drouin, J.** (1997). The bicoid-related homeoprotein Ptx1 defines the most anterior domain of the embryo and differentiates posterior from anterior lateral mesoderm. *Development* **124**, 2807-17.
- Lavado, A., Lagutin, O. V. and Oliver, G.** (2008). Six3 inactivation causes progressive caudalization and aberrant patterning of the mammalian diencephalon. *Development* **135**, 441-50.
- Lawrence, P. A. and Morata, G.** (1994). Homeobox genes: their function in *Drosophila* segmentation and pattern formation. *Cell* **78**, 181-9.
- Lebel, M., Mo, R., Shimamura, K. and Hui, C. C.** (2007). Gli2 and Gli3 play distinct roles in the dorsoventral patterning of the mouse hindbrain. *Dev Biol* **302**, 345-55.

- Lemaire, L., Roeser, T., Izipisua-Belmonte, J. C. and Kessel, M.** (1997). Segregating expression domains of two goosecoid genes during the transition from gastrulation to neurulation in chick embryos. *Development* **124**, 1443-52.
- Lewis, E. B.** (1978). A gene complex controlling segmentation in *Drosophila*. *Nature* **276**, 565-70.
- Lichtneckert, R., Nobs, L. and Reichert, H.** (2008). Empty spiracles is required for the development of olfactory projection neuron circuitry in *Drosophila*. *Development* **135**, 2415-24.
- Lichtneckert, R. and Reichert, H.** (2005). Insights into the urbilaterian brain: conserved genetic patterning mechanisms in insect and vertebrate brain development. *Heredity* **94**, 465-77.
- Lilly, B., O'Keefe, D. D., Thomas, J. B. and Botas, J.** (1999). The LIM homeodomain protein dLim1 defines a subclass of neurons within the embryonic ventral nerve cord of *Drosophila*. *Mech Dev* **88**, 195-205.
- Liu, W., Lagutin, O. V., Mende, M., Streit, A. and Oliver, G.** (2006). Six3 activation of Pax6 expression is essential for mammalian lens induction and specification. *Embo J* **25**, 5383-95.
- Liu, Z. and Friedrich, M.** (2004). The *Tribolium* homologue of glass and the evolution of insect larval eyes. *Dev Biol* **269**, 36-54.
- Logan, C. Y. and Nusse, R.** (2004). The Wnt signaling pathway in development and disease. *Annu Rev Cell Dev Biol* **20**, 781-810.
- Loosli, F., Koster, R. W., Carl, M., Krone, A. and Wittbrodt, J.** (1998). Six3, a medaka homologue of the *Drosophila* homeobox gene *sine oculis* is expressed in the anterior embryonic shield and the developing eye. *Mech Dev* **74**, 159-64.
- Loosli, F., Winkler, S. and Wittbrodt, J.** (1999). Six3 overexpression initiates the formation of ectopic retina. *Genes Dev* **13**, 649-54.
- Lopez-Rios, J., Gallardo, M. E., Rodriguez de Cordoba, S. and Bovolenta, P.** (1999). Six9 (Optx2), a new member of the six gene family of transcription factors, is expressed at early stages of vertebrate ocular and pituitary development. *Mech Dev* **83**, 155-9.
- Lopez-Rios, J., Tessmar, K., Loosli, F., Wittbrodt, J. and Bovolenta, P.** (2003). Six3 and Six6 activity is modulated by members of the groucho family. *Development* **130**, 185-95.
- Lowe, C. J.** (2008). Molecular genetic insights into deuterostome evolution from the direct-developing hemichordate *Saccoglossus kowalevskii*. *Philos Trans R Soc Lond B Biol Sci* **363**, 1569-78.
- Lowe, C. J., Terasaki, M., Wu, M., Freeman, R. M., Jr., Runft, L., Kwan, K., Haigo, S., Aronowicz, J., Lander, E., Gruber, C. et al.** (2006). Dorsoventral patterning in hemichordates: insights into early chordate evolution. *PLoS Biol* **4**, e291.
- Lowe, C. J., Wu, M., Salic, A., Evans, L., Lander, E., Stange-Thomann, N., Gruber, C. E., Gerhart, J. and Kirschner, M.** (2003). Anteroposterior patterning in hemichordates and the origins of the chordate nervous system. *Cell* **113**, 853-65.
- Lu, S., Bogarad, L. D., Murtha, M. T. and Ruddle, F. H.** (1992). Expression pattern of a murine homeobox gene, *Dbx*, displays extreme spatial restriction in embryonic forebrain and spinal cord. *Proc Natl Acad Sci U S A* **89**, 8053-7.
- Lu, S., Wise, T. L. and Ruddle, F. H.** (1994). Mouse homeobox gene *Dbx*: sequence, gene structure and expression pattern during mid-gestation. *Mech Dev* **47**, 187-95.
- Lufkin, T., Dierich, A., LeMeur, M., Mark, M. and Chambon, P.** (1991). Disruption of the *Hox-1.6* homeobox gene results in defects in a region corresponding to its rostral domain of expression. *Cell* **66**, 1105-19.
- Luo, T., Matsuo-Takasaki, M., Lim, J. H. and Sargent, T. D.** (2001). Differential regulation of *Dlx* gene expression by a BMP morphogenetic gradient. *Int J Dev Biol* **45**, 681-4.

- Lynch, J. and Desplan, C.** (2003a). 'De-evolution' of *Drosophila* toward a more generic mode of axis patterning. *Int J Dev Biol* **47**, 497-503.
- Lynch, J. and Desplan, C.** (2003b). Evolution of development: beyond bicoid. *Curr Biol* **13**, R557-9.
- Lynch, J. A., Brent, A. E., Leaf, D. S., Pultz, M. A. and Desplan, C.** (2006). Localized maternal orthodenticle patterns anterior and posterior in the long germ wasp *Nasonia*. *Nature* **439**, 728-32.
- Maderspacher, F., Bucher, G. and Klingler, M.** (1998). Pair-rule and gap gene mutants in the flour beetle *Tribolium castaneum*. *Dev Genes Evol* **208**, 558-68.
- Mallamaci, A., Iannone, R., Briata, P., Pintonello, L., Mercurio, S., Boncinelli, E. and Corte, G.** (1998). EMX2 protein in the developing mouse brain and olfactory area. *Mech Dev* **77**, 165-72.
- Marques-Souza, H., Aranda, M. and Tautz, D.** (2008). Delimiting the conserved features of hunchback function for the trunk organization of insects. *Development* **135**, 881-8.
- Martin, B. L. and Kimelman, D.** (2009). Wnt signaling and the evolution of embryonic posterior development. *Curr Biol* **19**, R215-9.
- Martinez, S.** (2001). The isthmus organizer and brain regionalization. *Int J Dev Biol* **45**, 367-71.
- Mathers, P. H., Grinberg, A., Mahon, K. A. and Jamrich, M.** (1997). The Rx homeobox gene is essential for vertebrate eye development. *Nature* **387**, 603-7.
- Matsuo-Takasaki, M., Lim, J. H., Beanan, M. J., Sato, S. M. and Sargent, T. D.** (2000). Cloning and expression of a novel zinc finger gene, Fez, transcribed in the forebrain of *Xenopus* and mouse embryos. *Mech Dev* **93**, 201-4.
- Mazet, F., Hutt, J. A., Milloz, J., Millard, J., Graham, A. and Shimeld, S. M.** (2005). Molecular evidence from *Ciona intestinalis* for the evolutionary origin of vertebrate sensory placodes. *Dev Biol* **282**, 494-508.
- McGinnis, W. and Krumlauf, R.** (1992). Homeobox genes and axial patterning. *Cell* **68**, 283-302.
- McGregor, A. P.** (2006). Wasps, beetles and the beginning of the ends. *Bioessays* **28**, 683-6.
- McGregor, A. P., Pechmann, M., Schwager, E. E., Feitosa, N. M., Kruck, S., Aranda, M. and Damen, W. G.** (2008). Wnt8 is required for growth-zone establishment and development of opisthosomal segments in a spider. *Curr Biol* **18**, 1619-23.
- McGrew, L. L., Lai, C. J. and Moon, R. T.** (1995). Specification of the anteroposterior neural axis through synergistic interaction of the Wnt signaling cascade with noggin and follistatin. *Dev Biol* **172**, 337-42.
- McLarren, K. W., Litsiou, A. and Streit, A.** (2003). DLX5 positions the neural crest and preplacode region at the border of the neural plate. *Dev Biol* **259**, 34-47.
- McMahon, A. P., Joyner, A. L., Bradley, A. and McMahon, J. A.** (1992). The midbrain-hindbrain phenotype of Wnt-1-/- mice results from stepwise deletion of engrailed-expressing cells by 9.5 days postcoitum. *Cell* **69**, 581-95.
- McNeill, H., Yang, C. H., Brodsky, M., Ungos, J. and Simon, M. A.** (1997). mirror encodes a novel PBX-class homeoprotein that functions in the definition of the dorsal-ventral border in the *Drosophila* eye. *Genes Dev* **11**, 1073-82.
- McNulty, C. L., Peres, J. N., Bardine, N., van den Akker, W. M. and Durston, A. J.** (2005). Knockdown of the complete Hox paralogous group 1 leads to dramatic hindbrain and neural crest defects. *Development* **132**, 2861-71.
- Meijlink, F., Beverdam, A., Brouwer, A., Oosterveen, T. C. and Berge, D. T.** (1999). Vertebrate aristaless-related genes. *Int J Dev Biol* **43**, 651-63.
- Merrill, V. K., Diederich, R. J., Turner, F. R. and Kaufman, T. C.** (1989). A genetic and developmental analysis of mutations in labial, a gene necessary for proper head formation in *Drosophila melanogaster*. *Dev Biol* **135**, 376-91.

- Mizunami, M., Weibrecht, J. M. and Strausfeld, N. J.** (1998). Mushroom bodies of the cockroach: their participation in place memory. *J Comp Neurol* **402**, 520-37.
- Mizuseki, K., Kishi, M., Matsui, M., Nakanishi, S. and Sasai, Y.** (1998a). Xenopus Zic-related-1 and Sox-2, two factors induced by chordin, have distinct activities in the initiation of neural induction. *Development* **125**, 579-87.
- Mizuseki, K., Kishi, M., Shiota, K., Nakanishi, S. and Sasai, Y.** (1998b). SoxD: an essential mediator of induction of anterior neural tissues in Xenopus embryos. *Neuron* **21**, 77-85.
- Mo, R., Freer, A. M., Zinyk, D. L., Crackower, M. A., Michaud, J., Heng, H. H., Chik, K. W., Shi, X. M., Tsui, L. C., Cheng, S. H. et al.** (1997). Specific and redundant functions of Gli2 and Gli3 zinc finger genes in skeletal patterning and development. *Development* **124**, 113-23.
- Mohler, J., Mahaffey, J. W., Deutsch, E. and Vani, K.** (1995). Control of Drosophila head segment identity by the bZIP homeotic gene cnc. *Development* **121**, 237-47.
- Monaghan, A. P., Bock, D., Gass, P., Schwager, A., Wolfer, D. P., Lipp, H. P. and Schutz, G.** (1997). Defective limbic system in mice lacking the tailless gene. *Nature* **390**, 515-7.
- Monaghan, A. P., Grau, E., Bock, D. and Schutz, G.** (1995). The mouse homolog of the orphan nuclear receptor tailless is expressed in the developing forebrain. *Development* **121**, 839-53.
- Murphy, P. and Hill, R. E.** (1991). Expression of the mouse labial-like homeobox-containing genes, Hox 2.9 and Hox 1.6, during segmentation of the hindbrain. *Development* **111**, 61-74.
- Nagy, L. M. and Carroll, S.** (1994). Conservation of wingless patterning functions in the short-germ embryos of *Tribolium castaneum*. *Nature* **367**, 460-3.
- Nassel, D. R.** (2002). Neuropeptides in the nervous system of Drosophila and other insects: multiple roles as neuromodulators and neurohormones. *Prog Neurobiol* **68**, 1-84.
- Nie, W., Stronach, B., Panganiban, G., Shippy, T., Brown, S. and Denell, R.** (2001). Molecular characterization of Tclabial and the 3' end of the *Tribolium* homeotic complex. *Dev Genes Evol* **211**, 244-51.
- Niehrs, C.** (1999). Head in the WNT: the molecular nature of Spemann's head organizer. *Trends Genet* **15**, 314-9.
- Nieuwkoop, P. D.** (1997). Short historical survey of pattern formation in the endo-mesoderm and the neural anlage in the vertebrates: the role of vertical and planar inductive actions. *Cell Mol Life Sci* **53**, 305-18.
- Nieuwkoop, P. D.** (1999). The neural induction process; its morphogenetic aspects. *Int J Dev Biol* **43**, 615-23.
- Nieuwkoop, P. D. and Faber, J.** (1967). Normal table of *Xenopus laevis* (Daudin). Amsterdam: North Holland.
- Northcutt, R. G. and Gans, C.** (1983). The genesis of neural crest and epidermal placodes: a reinterpretation of vertebrate origins. *Q Rev Biol* **58**, 1-28.
- Ober, K. A. and Jockusch, E. L.** (2006). The roles of wingless and decapentaplegic in axis and appendage development in the red flour beetle, *Tribolium castaneum*. *Dev Biol* **294**, 391-405.
- Ohto, H., Kamada, S., Tago, K., Tominaga, S. I., Ozaki, H., Sato, S. and Kawakami, K.** (1999). Cooperation of six and eya in activation of their target genes through nuclear translocation of Eya. *Mol Cell Biol* **19**, 6815-24.
- Olesnický, E. C., Brent, A. E., Tonnes, L., Walker, M., Pultz, M. A., Leaf, D. and Desplan, C.** (2006). A caudal mRNA gradient controls posterior development in the wasp *Nasonia*. *Development* **133**, 3973-82.

- Oliver, G., Mailhos, A., Wehr, R., Copeland, N. G., Jenkins, N. A. and Gruss, P.** (1995). Six3, a murine homologue of the sine oculis gene, demarcates the most anterior border of the developing neural plate and is expressed during eye development. *Development* **121**, 4045-55.
- Oppenheimer, D. I., MacNicol, A. M. and Patel, N. H.** (1999). Functional conservation of the wingless-engrailed interaction as shown by a widely applicable baculovirus misexpression system. *Curr Biol* **9**, 1288-96.
- Overton, P. M., Meadows, L. A., Urban, J. and Russell, S.** (2002). Evidence for differential and redundant function of the Sox genes Dichaete and SoxN during CNS development in Drosophila. *Development* **129**, 4219-28.
- Panganiban, G. and Rubenstein, J. L.** (2002). Developmental functions of the Distal-less/Dlx homeobox genes. *Development* **129**, 4371-86.
- Pankratz, M. J. and Jackle, H.** (1990). Making stripes in the Drosophila embryo. *Trends Genet* **6**, 287-92.
- Peel, A. D., Chipman, A. D. and Akam, M.** (2005). Arthropod segmentation: beyond the Drosophila paradigm. *Nat Rev Genet* **6**, 905-16.
- Peng, G. and Westerfield, M.** (2006). Lhx5 promotes forebrain development and activates transcription of secreted Wnt antagonists. *Development* **133**, 3191-200.
- Pera, E. M. and Kessel, M.** (1997). Patterning of the chick forebrain anlage by the prechordal plate. *Development* **124**, 4153-62.
- Peterson, K. J. and Eernisse, D. J.** (2001). Animal phylogeny and the ancestry of bilaterians: inferences from morphology and 18S rDNA gene sequences. *Evol Dev* **3**, 170-205.
- Pierani, A., Brenner-Morton, S., Chiang, C. and Jessell, T. M.** (1999). A sonic hedgehog-independent, retinoid-activated pathway of neurogenesis in the ventral spinal cord. *Cell* **97**, 903-15.
- Pignoni, F., Baldarelli, R. M., Steingrimsson, E., Diaz, R. J., Patapoutian, A., Merriam, J. R. and Lengyel, J. A.** (1990). The Drosophila gene tailless is expressed at the embryonic termini and is a member of the steroid receptor superfamily. *Cell* **62**, 151-63.
- Pignoni, F., Hu, B., Zavitz, K. H., Xiao, J., Garrity, P. A. and Zipursky, S. L.** (1997). The eye-specification proteins So and Eya form a complex and regulate multiple steps in Drosophila eye development. *Cell* **91**, 881-91.
- Pillai, A., Mansouri, A., Behringer, R., Westphal, H. and Goulding, M.** (2007). Lhx1 and Lhx5 maintain the inhibitory-neurotransmitter status of interneurons in the dorsal spinal cord. *Development* **134**, 357-66.
- Pinson, K. I., Brennan, J., Monkley, S., Avery, B. J. and Skarnes, W. C.** (2000). An LDL-receptor-related protein mediates Wnt signalling in mice. *Nature* **407**, 535-8.
- Pommereit, D., Pieler, T. and Hollemann, T.** (2001). Xpitx3: a member of the Rieg/Pitx gene family expressed during pituitary and lens formation in *Xenopus laevis*. *Mech Dev* **102**, 255-7.
- Posnien, N., Bashasab, F. and Bucher, G.** (accepted for publication). The insect upper lip (labrum) is a non-segmental appendage-like structure.
- Posnien, N. and Bucher, G.** (submitted). The Hox1 ortholog Tc-labial is required for embryonic development of the intercalary segment giving rise to lateral parts of the head in *Tribolium*.
- Prince, V. E. and Pickett, F. B.** (2002). Splitting pairs: the diverging fates of duplicated genes. *Nat Rev Genet* **3**, 827-37.
- Qiu, M., Anderson, S., Chen, S., Meneses, J. J., Hevner, R., Kuwana, E., Pedersen, R. A. and Rubenstein, J. L.** (1996). Mutation of the Emx-1 homeobox gene disrupts the corpus callosum. *Dev Biol* **178**, 174-8.
- Reichert, H.** (2005). A tripartite organization of the urbilaterian brain: developmental genetic evidence from Drosophila. *Brain Res Bull* **66**, 491-4.

- Reichert, H. and Simeone, A.** (2001). Developmental genetic evidence for a monophyletic origin of the bilaterian brain. *Philos Trans R Soc Lond B Biol Sci* **356**, 1533-44.
- Reifers, F., Bohli, H., Walsh, E. C., Crossley, P. H., Stainier, D. Y. and Brand, M.** (1998). Fgf8 is mutated in zebrafish acerebellar (ace) mutants and is required for maintenance of midbrain-hindbrain boundary development and somitogenesis. *Development* **125**, 2381-95.
- Rhinn, M., Lun, K., Luz, M., Werner, M. and Brand, M.** (2005). Positioning of the midbrain-hindbrain boundary organizer through global posteriorization of the neuroectoderm mediated by Wnt8 signaling. *Development* **132**, 1261-72.
- Richards, S. Gibbs, R. A. Weinstock, G. M. Brown, S. J. Denell, R. Beeman, R. W. Gibbs, R. Beeman, R. W. Brown, S. J. Bucher, G. et al.** (2008). The genome of the model beetle and pest *Tribolium castaneum*. *Nature* **452**, 949-55.
- Rivera-Pomar, R., Niessing, D., Schmidt-Ott, U., Gehring, W. J. and Jackle, H.** (1996). RNA binding and translational suppression by bicoid. *Nature* **379**, 746-9.
- Rogers, B. T. and Kaufman, T. C.** (1996). Structure of the insect head as revealed by the EN protein pattern in developing embryos. *Development* **122**, 3419-32.
- Rogers, B. T. and Kaufman, T. C.** (1997). Structure of the insect head in ontogeny and phylogeny: a view from *Drosophila*. *Int Rev Cytol* **174**, 1-84.
- Rowitch, D. H. and McMahon, A. P.** (1995). Pax-2 expression in the murine neural plate precedes and encompasses the expression domains of Wnt-1 and En-1. *Mech Dev* **52**, 3-8.
- Roy, K., Thiels, E. and Monaghan, A. P.** (2002). Loss of the tailless gene affects forebrain development and emotional behavior. *Physiol Behav* **77**, 595-600.
- Rubenstein, J. L., Shimamura, K., Martinez, S. and Puelles, L.** (1998). Regionalization of the prosencephalic neural plate. *Annu Rev Neurosci* **21**, 445-77.
- Rubenstein, J. L. R. and Shimamura, K.** (1997). Regulation of patterning and differentiation in the embryonic vertebrate forebrain. In *Molecular and Cellular Approaches to Neural Development*, (ed. W. M. Cowan T. M. Jessell and S. L. Zipursky), pp. 356-390. New York Oxford: Oxford University Press.
- Ruiz i Altaba, A.** (1993). Induction and axial patterning of the neural plate: planar and vertical signals. *J Neurobiol* **24**, 1276-304.
- Saitou, N. and Nei, M.** (1987). The neighbor-joining method: a new method for reconstructing phylogenetic trees. *Mol Biol Evol* **4**, 406-25.
- Sasai, Y.** (2001a). Regulation of neural determination by evolutionarily conserved signals: anti-BMP factors and what next? *Curr Opin Neurobiol* **11**, 22-6.
- Sasai, Y.** (2001b). Roles of Sox factors in neural determination: conserved signaling in evolution? *Int J Dev Biol* **45**, 321-6.
- Schetelig, M. F., Schmid, B. G., Zimowska, G. and Wimmer, E. A.** (2008). Plasticity in mRNA expression and localization of orthodenticle within higher Diptera. *Evol Dev* **10**, 700-4.
- Schinko, J. B., Kreuzer, N., Offen, N., Posnien, N., Wimmer, E. A. and Bucher, G.** (2008). Divergent functions of orthodenticle, empty spiracles and buttonhead in early head patterning of the beetle *Tribolium castaneum* (Coleoptera). *Dev Biol* **317**, 600-13.
- Schlosser, G.** (2005). Evolutionary origins of vertebrate placodes: insights from developmental studies and from comparisons with other deuterostomes. *J Exp Zool B Mol Dev Evol* **304**, 347-99.
- Schlosser, G.** (2006). Induction and specification of cranial placodes. *Dev Biol* **294**, 303-51.
- Schlosser, G.** (2008). Do vertebrate neural crest and cranial placodes have a common evolutionary origin? *Bioessays* **30**, 659-72.
- Schlosser, G. and Ahrens, K.** (2004). Molecular anatomy of placode development in *Xenopus laevis*. *Dev Biol* **271**, 439-66.

- Schlosser, G., Awtry, T., Brugmann, S. A., Jensen, E. D., Neilson, K., Ruan, G., Stammler, A., Voelker, D., Yan, B., Zhang, C. et al.** (2008). *Eya1* and *Six1* promote neurogenesis in the cranial placodes in a *SoxB1*-dependent fashion. *Dev Biol* **320**, 199-214.
- Schmahl, W., Knoedlseder, M., Favor, J. and Davidson, D.** (1993). Defects of neuronal migration and the pathogenesis of cortical malformations are associated with *Small eye* (*Sey*) in the mouse, a point mutation at the *Pax-6*-locus. *Acta Neuropathol* **86**, 126-35.
- Schneider, V. A. and Mercola, M.** (1999). Spatially distinct head and heart inducers within the *Xenopus* organizer region. *Curr Biol* **9**, 800-9.
- Schoenwolf, G. C. and Smith, J. L.** (1990). Mechanisms of neurulation: traditional viewpoint and recent advances. *Development* **109**, 243-70.
- Scholpp, S., Lohs, C. and Brand, M.** (2003). *Engrailed* and *Fgf8* act synergistically to maintain the boundary between diencephalon and mesencephalon. *Development* **130**, 4881-93.
- Schroder, R.** (2003). The genes *orthodenticle* and *hunchback* substitute for *bicoid* in the beetle *Tribolium*. *Nature* **422**, 621-5.
- Schroder, R., Eckert, C., Wolff, C. and Tautz, D.** (2000). Conserved and divergent aspects of terminal patterning in the beetle *Tribolium castaneum*. *Proc Natl Acad Sci U S A* **97**, 6591-6.
- Schulte-Merker, S., Hammerschmidt, M., Beuchle, D., Cho, K. W., De Robertis, E. M. and Nusslein-Volhard, C.** (1994). Expression of zebrafish *gooseoid* and *no tail* gene products in wild-type and mutant *no tail* embryos. *Development* **120**, 843-52.
- Schulz, C., Schroder, R., Hausdorf, B., Wolff, C. and Tautz, D.** (1998). A caudal homologue in the short germ band beetle *Tribolium* shows similarities to both, the *Drosophila* and the vertebrate caudal expression patterns. *Dev Genes Evol* **208**, 283-9.
- Schweickert, A., Steinbeisser, H. and Blum, M.** (2001). Differential gene expression of *Xenopus* *Pitx1*, *Pitx2b* and *Pitx2c* during cement gland, stomodeum and pituitary development. *Mech Dev* **107**, 191-4.
- Seecoomar, M., Agarwal, S., Vani, K., Yang, G. and Mohler, J.** (2000). *knot* is required for the hypopharyngeal lobe and its derivatives in the *Drosophila* embryo. *Mech Dev* **91**, 209-15.
- Seufert, D. W., Prescott, N. L. and El-Hodiri, H. M.** (2005). *Xenopus* *aristaless*-related homeobox (*xARX*) gene product functions as both a transcriptional activator and repressor in forebrain development. *Dev Dyn* **232**, 313-24.
- Shawlot, W. and Behringer, R. R.** (1995). Requirement for *Lim1* in head-organizer function. *Nature* **374**, 425-30.
- Sheng, H. Z., Bertuzzi, S., Chiang, C., Shawlot, W., Taira, M., Dawid, I. and Westphal, H.** (1997). Expression of murine *Lhx5* suggests a role in specifying the forebrain. *Dev Dyn* **208**, 266-77.
- Shimamura, K., Hartigan, D. J., Martinez, S., Puellas, L. and Rubenstein, J. L.** (1995). Longitudinal organization of the anterior neural plate and neural tube. *Development* **121**, 3923-33.
- Shimamura, K. and Rubenstein, J. L.** (1997). Inductive interactions direct early regionalization of the mouse forebrain. *Development* **124**, 2709-18.
- Shimeld, S. M. and Holland, P. W.** (2000). Vertebrate innovations. *Proc Natl Acad Sci U S A* **97**, 4449-52.
- Shimizu, T. and Hibi, M.** (2009). Formation and patterning of the forebrain and olfactory system by zinc-finger genes *Fezf1* and *Fezf2*. *Dev Growth Differ* **51**, 221-31.
- Shinmyo, Y., Mito, T., Matsushita, T., Sarashina, I., Miyawaki, K., Ohuchi, H. and Noji, S.** (2005). *caudal* is required for gnathal and thoracic patterning and for posterior elongation in the intermediate-germband cricket *Gryllus bimaculatus*. *Mech Dev* **122**, 231-9.

- Shinozaki, K., Miyagi, T., Yoshida, M., Miyata, T., Ogawa, M., Aizawa, S. and Suda, Y.** (2002). Absence of Cajal-Retzius cells and subplate neurons associated with defects of tangential cell migration from ganglionic eminence in *Emx1/2* double mutant cerebral cortex. *Development* **129**, 3479-92.
- Shoji, H., Ito, T., Wakamatsu, Y., Hayasaka, N., Ohsaki, K., Oyanagi, M., Kominami, R., Kondoh, H. and Takahashi, N.** (1996). Regionalized expression of the *Dbx* family homeobox genes in the embryonic CNS of the mouse. *Mech Dev* **56**, 25-39.
- Simeone, A., Acampora, D., Gulisano, M., Stornaiuolo, A. and Boncinelli, E.** (1992a). Nested expression domains of four homeobox genes in developing rostral brain. *Nature* **358**, 687-90.
- Simeone, A., Gulisano, M., Acampora, D., Stornaiuolo, A., Rambaldi, M. and Boncinelli, E.** (1992b). Two vertebrate homeobox genes related to the *Drosophila* empty spiracles gene are expressed in the embryonic cerebral cortex. *Embo J* **11**, 2541-50.
- Skeath, J. B.** (1999). At the nexus between pattern formation and cell-type specification: the generation of individual neuroblast fates in the *Drosophila* embryonic central nervous system. *Bioessays* **21**, 922-31.
- Slack, J. M., Holland, P. W. and Graham, C. F.** (1993). The zootype and the phylotypic stage. *Nature* **361**, 490-2.
- Snodgrass, R. E.** (1935). Principles of Insect Morphology. New York: McGraw Hill.
- Sokoloff, A.** (1974). The Biology of *Tribolium*. Oxford: Clarendon Press.
- Solomon, K. S. and Fritz, A.** (2002). Concerted action of two *dlx* paralogs in sensory placode formation. *Development* **129**, 3127-36.
- St Johnston, D. and Nusslein-Volhard, C.** (1992). The origin of pattern and polarity in the *Drosophila* embryo. *Cell* **68**, 201-19.
- Stachel, S. E., Grunwald, D. J. and Myers, P. Z.** (1993). Lithium perturbation and goosecoid expression identify a dorsal specification pathway in the pregastrula zebrafish. *Development* **117**, 1261-74.
- Stauber, M., Prell, A. and Schmidt-Ott, U.** (2002). A single *Hox3* gene with composite bicoid and *zerknüllt* expression characteristics in non-Cyclorrhaphan flies. *Proc Natl Acad Sci U S A* **99**, 274-9.
- Steinbeisser, H. and De Robertis, E. M.** (1993). *Xenopus* goosecoid: a gene expressed in the prechordal plate that has dorsalizing activity. *C R Acad Sci III* **316**, 959-71.
- Stenman, J. M., Wang, B. and Campbell, K.** (2003). *Tlx* controls proliferation and patterning of lateral telencephalic progenitor domains. *J Neurosci* **23**, 10568-76.
- Stoykova, A., Fritsch, R., Walther, C. and Gruss, P.** (1996). Forebrain patterning defects in Small eye mutant mice. *Development* **122**, 3453-65.
- Strecker, T. R., Merriam, J. R. and Lengyel, J. A.** (1988). Graded requirement for the zygotic terminal gene, *tailless*, in the brain and tail region of the *Drosophila* embryo. *Development* **102**, 721-34.
- Streit, A.** (2004). Early development of the cranial sensory nervous system: from a common field to individual placodes. *Dev Biol* **276**, 1-15.
- Streit, A.** (2007). The preplacodal region: an ectodermal domain with multipotential progenitors that contribute to sense organs and cranial sensory ganglia. *Int J Dev Biol* **51**, 447-61.
- Struhl, G. and White, R. A.** (1985). Regulation of the *Ultrabithorax* gene of *Drosophila* by other bithorax complex genes. *Cell* **43**, 507-19.
- Sundin, O. H., Busse, H. G., Rogers, M. B., Gudas, L. J. and Eichele, G.** (1990). Region-specific expression in early chick and mouse embryos of *Ghox-lab* and *Hox 1.6*, vertebrate homeobox-containing genes related to *Drosophila labial*. *Development* **108**, 47-58.
- Szeto, D. P., Rodriguez-Esteban, C., Ryan, A. K., O'Connell, S. M., Liu, F., Kioussi, C., Gleiberman, A. S., Izpisua-Belmonte, J. C. and Rosenfeld, M. G.** (1999). Role of the

- Bicoid-related homeodomain factor Pitx1 in specifying hindlimb morphogenesis and pituitary development. *Genes Dev* **13**, 484-94.
- Takada, S., Stark, K. L., Shea, M. J., Vassileva, G., McMahon, J. A. and McMahon, A. P.** (1994). Wnt-3a regulates somite and tailbud formation in the mouse embryo. *Genes Dev* **8**, 174-89.
- Takahashi, M. and Osumi, N.** (2008). Expression study of cadherin7 and cadherin20 in the embryonic and adult rat central nervous system. *BMC Dev Biol* **8**, 87.
- Tallafuss, A., Wilm, T. P., Crozatier, M., Pfeffer, P., Wassef, M. and Bally-Cuif, L.** (2001). The zebrafish buttonhead-like factor Bts1 is an early regulator of pax2.1 expression during mid-hindbrain development. *Development* **128**, 4021-34.
- Tamura, K., Dudley, J., Nei, M. and Kumar, S.** (2007). MEGA4: Molecular Evolutionary Genetics Analysis (MEGA) software version 4.0. *Mol Biol Evol* **24**, 1596-9.
- Tao, W. and Lai, E.** (1992). Telencephalon-restricted expression of BF-1, a new member of the HNF-3/fork head gene family, in the developing rat brain. *Neuron* **8**, 957-66.
- Technau, G. M., Berger, C. and Urbach, R.** (2006). Generation of cell diversity and segmental pattern in the embryonic central nervous system of Drosophila. *Dev Dyn* **235**, 861-9.
- Tessmar-Raible, K.** (2007). The evolution of neurosecretory centers in bilaterian forebrains: insights from protostomes. *Semin Cell Dev Biol* **18**, 492-501.
- Tessmar-Raible, K., Raible, F., Christodoulou, F., Guy, K., Rembold, M., Hausen, H. and Arendt, D.** (2007). Conserved sensory-neurosecretory cell types in annelid and fish forebrain: insights into hypothalamus evolution. *Cell* **129**, 1389-400.
- Theil, T., Alvarez-Bolado, G., Walter, A. and Ruther, U.** (1999). Gli3 is required for Emx gene expression during dorsal telencephalon development. *Development* **126**, 3561-71.
- Thor, S., Andersson, S. G., Tomlinson, A. and Thomas, J. B.** (1999). A LIM-homeodomain combinatorial code for motor-neuron pathway selection. *Nature* **397**, 76-80.
- Tole, S., Ragsdale, C. W. and Grove, E. A.** (2000). Dorsoventral patterning of the telencephalon is disrupted in the mouse mutant extra-toes(J). *Dev Biol* **217**, 254-65.
- Tomoyasu, Y., Wheeler, S. R. and Denell, R. E.** (2005). Ultrabithorax is required for membranous wing identity in the beetle *Tribolium castaneum*. *Nature* **433**, 643-7.
- Toyama, R., Curtiss, P. E., Otani, H., Kimura, M., Dawid, I. B. and Taira, M.** (1995). The LIM class homeobox gene lim5: implied role in CNS patterning in *Xenopus* and zebrafish. *Dev Biol* **170**, 583-93.
- Tremblay, J. J., Lanctot, C. and Drouin, J.** (1998). The pan-pituitary activator of transcription, Ptx1 (pituitary homeobox 1), acts in synergy with SF-1 and Pit1 and is an upstream regulator of the Lim-homeodomain gene Lim3/Lhx3. *Mol Endocrinol* **12**, 428-41.
- Tsuchida, T., Ensini, M., Morton, S. B., Baldassare, M., Edlund, T., Jessell, T. M. and Pfaff, S. L.** (1994). Topographic organization of embryonic motor neurons defined by expression of LIM homeobox genes. *Cell* **79**, 957-70.
- Urbach, R.** (2007). A procephalic territory in Drosophila exhibiting similarities and dissimilarities compared to the vertebrate midbrain/hindbrain boundary region. *Neural Dev* **2**, 23.
- Urbach, R. and Technau, G. M.** (2003). Segment polarity and DV patterning gene expression reveals segmental organization of the Drosophila brain. *Development* **130**, 3607-20.
- Urbach, R. and Technau, G. M.** (2008). Dorsoventral patterning of the brain: a comparative approach. *Adv Exp Med Biol* **628**, 42-56.
- van der Zee, M., Berns, N. and Roth, S.** (2005). Distinct functions of the *Tribolium* zerknüllt genes in serosa specification and dorsal closure. *Curr Biol* **15**, 624-36.
- VanHook, A. and Letsou, A.** (2008). Head involution in Drosophila: genetic and morphogenetic connections to dorsal closure. *Dev Dyn* **237**, 28-38.

- Veelaert, D., Schoofs, L. and De Loof, A.** (1998). Peptidergic control of the corpus cardiacum-corpora allata complex of locusts. *Int Rev Cytol* **182**, 249-302.
- Vieira, C., Garda, A. L., Shimamura, K. and Martinez, S.** (2005). Thalamic development induced by Shh in the chick embryo. *Dev Biol* **284**, 351-63.
- Vincent, A., Blankenship, J. T. and Wieschaus, E.** (1997). Integration of the head and trunk segmentation systems controls cephalic furrow formation in *Drosophila*. *Development* **124**, 3747-54.
- Wada, H. and Satoh, N.** (2001). Patterning the protochordate neural tube. *Curr Opin Neurobiol* **11**, 16-21.
- Walterhouse, D., Ahmed, M., Slusarski, D., Kalamaras, J., Boucher, D., Holmgren, R. and Iannaccone, P.** (1993). gli, a zinc finger transcription factor and oncogene, is expressed during normal mouse development. *Dev Dyn* **196**, 91-102.
- Warren, N. and Price, D. J.** (1997). Roles of Pax-6 in murine diencephalic development. *Development* **124**, 1573-82.
- Weber, H.** (1966). Grundriss der Insektenkunde. Stuttgart: Gustav Fischer Verlag.
- Wei, Z., Yaguchi, J., Yaguchi, S., Angerer, R. C. and Angerer, L. M.** (2009). The sea urchin animal pole domain is a Six3-dependent neurogenic patterning center. *Development* **136**, 1179-89.
- Weiss, J. B., Von Ohlen, T., Mellerick, D. M., Dressler, G., Doe, C. Q. and Scott, M. P.** (1998). Dorsoventral patterning in the *Drosophila* central nervous system: the intermediate neuroblasts defective homeobox gene specifies intermediate column identity. *Genes Dev* **12**, 3591-602.
- Westheide, W. and Rieger, R.** (1996). Spezielle Zoologie; Teil 1: Einzeller und Wirbellose Tiere
Stuttgart-Jena-New York: Gustav Fischer Verlag.
- Wheeler, S. R., Carrico, M. L., Wilson, B. A., Brown, S. J. and Skeath, J. B.** (2003). The expression and function of the achaete-scute genes in *Tribolium castaneum* reveals conservation and variation in neural pattern formation and cell fate specification. *Development* **130**, 4373-81.
- Wieschaus, E., Nusslein-Volhard, C. and Jurgens, G.** (1984). Mutations affecting the pattern of the larval cuticle in *Drosophila melanogaster*. 3. Zygotic loci on the X-chromosome and 4th chromosome. *Wilhelm Roux's Arch. Dev. Biol.*, 296-307.
- Willert, K., Logan, C. Y., Arora, A., Fish, M. and Nusse, R.** (1999). A *Drosophila* Axin homolog, Daxin, inhibits Wnt signaling. *Development* **126**, 4165-73.
- Wilson, L. and Maden, M.** (2005). The mechanisms of dorsoventral patterning in the vertebrate neural tube. *Dev Biol* **282**, 1-13.
- Wimmer, E. A., Cohen, S. M., Jackle, H. and Desplan, C.** (1997). buttonhead does not contribute to a combinatorial code proposed for *Drosophila* head development. *Development* **124**, 1509-17.
- Wimmer, E. A., Jackle, H., Pfeifle, C. and Cohen, S. M.** (1993). A *Drosophila* homologue of human Sp1 is a head-specific segmentation gene. *Nature* **366**, 690-4.
- Woda, J. M., Pastagia, J., Mercola, M. and Artinger, K. B.** (2003). Dlx proteins position the neural plate border and determine adjacent cell fates. *Development* **130**, 331-42.
- Wodarz, A. and Huttner, W. B.** (2003). Asymmetric cell division during neurogenesis in *Drosophila* and vertebrates. *Mech Dev* **120**, 1297-309.
- Wohlfrom, H., Schinko, J. B., Klingler, M. and Bucher, G.** (2006). Maintenance of segment and appendage primordia by the *Tribolium* gene knodel. *Mech Dev* **123**, 430-9.
- Wurst, W., Auerbach, A. B. and Joyner, A. L.** (1994). Multiple developmental defects in Engrailed-1 mutant mice: an early mid-hindbrain deletion and patterning defects in forelimbs and sternum. *Development* **120**, 2065-75.

- Wurst, W. and Bally-Cuif, L.** (2001). Neural plate patterning: upstream and downstream of the isthmic organizer. *Nat Rev Neurosci* **2**, 99-108.
- Xu, P. X., Adams, J., Peters, H., Brown, M. C., Heaney, S. and Maas, R.** (1999). *Eya1*-deficient mice lack ears and kidneys and show abnormal apoptosis of organ primordia. *Nat Genet* **23**, 113-7.
- Yang, L., Zhang, H., Hu, G., Wang, H., Abate-Shen, C. and Shen, M. M.** (1998). An early phase of embryonic *Dlx5* expression defines the rostral boundary of the neural plate. *J Neurosci* **18**, 8322-30.
- Yang, X., Weber, M., Zarinkamar, N., Posnien, N., Friedrich, F., Wigand, B., Beutel, R., Damen, W. G., Bucher, G., Klingler, M. et al.** (2009a). Probing the *Drosophila* retinal determination gene network in *Tribolium* (II): the *Pax6* genes *eyeless* and *twin of eyeless*. *Dev Biol*.
- Yang, X., Zarinkamar, N., Bao, R. and Friedrich, M.** (2009b). Probing the *Drosophila* retinal determination gene network in *Tribolium* (I): The early retinal genes *dachshund*, *eyes absent* and *sine oculis*. *Dev Biol*.
- Yoshida, M., Suda, Y., Matsuo, I., Miyamoto, N., Takeda, N., Kuratani, S. and Aizawa, S.** (1997). *Emx1* and *Emx2* functions in development of dorsal telencephalon. *Development* **124**, 101-11.
- Younossi-Hartenstein, A., Green, P., Liaw, G. J., Rudolph, K., Lengyel, J. and Hartenstein, V.** (1997). Control of early neurogenesis of the *Drosophila* brain by the head gap genes *tll*, *otd*, *ems*, and *btd*. *Dev Biol* **182**, 270-83.
- Younossi-Hartenstein, A., Tepass, U. and Hartenstein, V.** (1993). Embryonic origin of the imaginal discs of the head of *Drosophila melanogaster*. *Roux's Arch. Devel. Biol.* **203**, 60-73.
- Yu, R. T., McKeown, M., Evans, R. M. and Umesono, K.** (1994). Relationship between *Drosophila* gap gene *tailless* and a vertebrate nuclear receptor *Tlx*. *Nature* **370**, 375-9.
- Zhang, C. L., Zou, Y., He, W., Gage, F. H. and Evans, R. M.** (2008). A role for adult *TLX*-positive neural stem cells in learning and behaviour. *Nature* **451**, 1004-7.
- Zheng, W., Huang, L., Wei, Z. B., Silvius, D., Tang, B. and Xu, P. X.** (2003). The role of *Six1* in mammalian auditory system development. *Development* **130**, 3989-4000.
- Zhu, C. C., Dyer, M. A., Uchikawa, M., Kondoh, H., Lagutin, O. V. and Oliver, G.** (2002). *Six3*-mediated auto repression and eye development requires its interaction with members of the Groucho-related family of co-repressors. *Development* **129**, 2835-49.
- Zilinski, C. A., Shah, R., Lane, M. E. and Jamrich, M.** (2005). Modulation of zebrafish *pitx3* expression in the primordia of the pituitary, lens, olfactory epithelium and cranial ganglia by hedgehog and nodal signaling. *Genesis* **41**, 33-40.
- Zuber, M. E., Gestri, G., Viczian, A. S., Barsacchi, G. and Harris, W. A.** (2003). Specification of the vertebrate eye by a network of eye field transcription factors. *Development* **130**, 5155-67.
- Zuber, M. E., Perron, M., Philpott, A., Bang, A. and Harris, W. A.** (1999). Giant eyes in *Xenopus laevis* by overexpression of *XOptx2*. *Cell* **98**, 341-52.
- Zuckerlandl, E. and Pauling, L.** (1965). Evolutionary divergence and convergence in proteins. In *Evolving Genes and Proteins*, (ed. V. Bryson and H. J. Vogel), pp. 97-166. New York: Academic Press.

7 Appendix

7.1 Supplementary Tables

Table S1 (part1): Vertebrate candidate genes.

	vertebrate gene	synonyms
expressed in the head of <i>Tribolium</i>		
1	orthodenticle homolog / otx	
2	sine oculis-related homeobox 3/6 homolog / six3/6	
3	Tlx	nuclear receptor subfamily 2, group E, member 1 (Nr2e1)
4	LIM homeobox protein 1/5 / lhx1/5	Lim1/5
5	NK2 homeobox 1 / nkx2.1	Nkx2-1, T/EBP, thyroid transcription factor-1, tinman, Titf1, Ttf-1
6	goosecoid / gsc	
7	retinal homeobox / rx	retina and anterior neural fold homeobox (rax),
8	Fez family zinc finger / fezf	forebrain embryonic zinc-finger
9	sonic hedgehog / shh	Hhg 1, Hx, Hxl3
10	wingless-related MMTV integration site 1 / wnt1	int-1
11	GLI-Kruppel family member / gli	brachyphalangy (bph)
12	Iroquois related homeobox / irx	
13	empty spiracles homolog / emx	
14	forkhead box G1 / foxg1	brain factor 1 (bfl, bf-1)
15	paired box gene 6 / pax6	Dey, small eye
16	developing brain homeobox 1 / dbx1	Mmx C
17	paired-like homeodomain transcription factor / pitx	pituitary homeobox
18	distal-less homeobox / Dlx	
19	eyes absent homolog / eya	
20	sine oculis-related homeobox 1 homolog / six1	
21	sine oculis-related homeobox 4 homolog / six4	AREC3, TrexBF
not expressed in the head of <i>Tribolium</i>		
22	aristaless related homeobox / arx	
23	wingless related MMTV integration site 11 / wnt11	
24	BarH like homeobox / Barx	
not in the <i>Tribolium</i> genome		
25	Hesx1	HES-1, Rpx, ANF
26	ventral anterior homeobox containing gene 1 / Vax1	
27	diencephalon/mesencephalon homeobox 1 / Dmbx1	Atx, Cdmx, Mbx, Otx3

Table S1 (part2): *Tribolium castaneum* orthologs and protein domains.

	Tribolium ortholog	synonyms	Protein domains
expressed in the head of <i>Tribolium</i>			
1	orthodenticle / otd1	ocelliless (oc)	homeobox
2	six3	optix	homeobox, SIX-domain
3	tailless / tll		VitaminD receptor, Zinc finger nuclear hormone receptor-type, Steroid hormone receptor
4	Lim1/5		LIM type zinc-finger, homeobox
5	scarecrow / scro		homeobox
6	goosecoid / gsc	PvuII-PstI homology 25 (Pph25)	homeobox
7	retinal homeobox / rx	bk50, wombat (wom)	homeobox, paired-like homeodomain
8	fez		zinc-finger, Engrailed homology 1 (Eh1) repressor motif
9	hedgehog / hh		Peptidase C46, Hedgehog/intein hint domain, Hedgehog amino-terminal signaling region, Intein splicing si
10	wingless / wg	wnt1, int1	Secreted growth factor Wnt protein
11	cunited interruptus / ci		zinc-finger
12	nirrot / mirr		homeobox, Iroquois-class homeodomain
13	empty spiracles / ems	antenna (ant)	homeobox, Helix-turn-helix motif
14	sloppy paired / slp	foxg, FD6, FD7	fork head box, Winged helix repressor DNA-binding domain
15	eyeless / ey & twin of eyeless / toy		homeobox, paired-like homeodomain, Winged helix repressor DNA-binding domain
16	dbx		homeobox, Helix-turn-helix motif
17	ptx		homeobox, paired-like homeodomain
18	Distalless / Dll		homeobox, Helix-turn-helix motif
19	eyes absent / eya	clift (cli)	Haloacid dehalogenase-like hydrolase
20	sine oculis / so		homeobox, SIX-domain
21	six4	myotonix	homeobox, SIX-domain
not expressed in the head of <i>Tribolium</i>			
22	munster / mun	PvuII-PstI homology 13 (Pph13)	homeobox, Paired-like homeodomain
23	wnt11		Secreted growth factor Wnt protein
24	BarH	B-H	homeobox, Helix-turn-helix motif
not in the <i>Tribolium</i> genome			
25			homeobox
26			homeobox, Helix-turn-helix motif
27			homeobox, Paired-like homeodomain

Table S2: Quantification of bristle pattern defects of the RNAi screen.

Gene	Beetles x2	bell row		vertex triplet						labrum quartet		gena triplet				maxilla escort			
		bells	bristle	vertex setae			vertex bristles			clypeus	labrum	post	dors	ant	bristle	ant	med	post	
				post	vent	ant	triplet	ant bas	median										ant
six4 detailed	16	0	2	2	1	1	1+2	7	0	2	0	0	0	0	1	3	0	0	0
six4	16	0	2	2	1	1	3	7	0	2	0	0	0	0	1	3	0	0	0
%		0	12,5	12,5	6,25	6,25	18,75	43,75	0	12,5	0	0	0	0	6,25	18,75	0	0	0
eya detailed	12	1	4+4	1	2+1	1	0	10	1	0	0	0	2+7	12	2+7	11	0	4	4
eya eRNAi	12	1	8	1	3	1	0	10	1	0	0	0	9	12	9	11	0	4	4
%		8,33	66,7	8,333	25	8,333	0	83,33	8,333	0	0	0	75	100	75	91,667	0	33,33	33,33
so detailed	20	1	1+3	0	1	0	2	17	0	2	0	0	1+1	16+2	14+2	16+1	0	1	0
so aRNAi	20	1	4	0	1	0	2	17	0	2	0	0	2	18	16	17	0	1	0
%		5	20	0	5	0	10	85	0	10	0	0	10	90	80	85	0	5	0
toy detailed	12	10	12	4	5	0	12	11	3	0	0	0	1	1+1	1	10	0	10	0
toy	12	10	12	4	5	0	12	11	3	0	0	0	1	2	1	10	0	10	0
%		83,3	100	33,33	41,67	0	100	91,67	25	0	0	0	8,333	16,67	8,3333	83,333	0	83,33	0
ey	10	2	1	0	1	0	0	0	1	0	0	0	0	2	0	4	1	2	2
%		20	10	0	10	0	0	0	10	0	0	0	0	20	0	40	10	20	20
toyley detailed	6	6	6	2+2	6	0	6	6	3	0	0	0	2	4	3	5	2	6	5
toyley	6	6	6	4	6	0	6	6	3	0	0	0	2	4	3	5	2	6	5
%		100	100	66,67	100	0	100	100	50	0	0	0	33,33	66,67	50	83,333	33,33	100	83,33
gsc	4	0	0	0	0	0	0	0	0	0	0	0	0	0	0	2	0	1	0
%		0	0	0	0	0	0	0	0	0	0	0	0	0	0	50	0	25	0
fez detailed	26	0	7	1	1	1+4	1	2	1+1	1	0	0	0	0	0	15	0	6	0
fez	26	0	7	1	1	5	1	2	2	1	0	0	0	0	0	15	0	6	0
%		0	26,9	3,846	3,846	19,23	3,846	7,692	7,692	3,85	0	0	0	0	0	57,692	0	23,08	0
ttl detailed	20	2	4	0	0	0	0	1	0	0	0	0	3	3	2	2+3	2	2+2	2
ttl	20	2	4	0	0	0	0	1	0	0	0	0	3	3	2	5	2	4	2
%		10	20	0	0	0	0	5	0	0	0	0	15	15	10	25	10	20	10
dbx detailed	22	0	0	0	1	0	0	2	0	0	0	0	7	7	7	6+7+1	0	3	0
dbx	22	0	0	0	1	0	0	2	0	0	0	0	7	7	7	14	0	3	0
%		0	0	0	4,545	0	0	9,091	0	0	0	0	31,82	31,82	31,818	63,636	0	13,64	0
lim1 detailed	24	0	5	1	1	0	1	2	1+1	2	0	0	2	2	2	16	6+1	9	0
lim1	24	0	5	1	1	0	1	2	2	2	0	0	2	2	2	16	7	9	0
%		0	20,8	4,167	4,167	0	4,167	8,333	8,333	8,33	0	0	8,333	8,333	8,3333	66,667	29,17	37,5	0
scro detailed	28	0	0	0	0	1	2	0	0	6	0	0	2	2	2	2	0	0	0
scro	28	0	0	0	0	1	2	0	0	6	0	0	2	2	2	2	0	0	0
%		0	0	0	0	3,571	7,143	0	0	21,4	0	0	7,143	7,143	7,1429	7,1429	0	0	0
rx	16	0	0	0	0	0	0	5	0	0	10	0	0	0	0	5	2	4	0
%		0	0	0	0	0	0	31,25	0	0	62,5	0	0	0	0	31,25	12,5	25	0
ci detailed	20	0	1	0	12	0	7+5	2+6	4+2	2+1	1	0	2	2	2	7	0	0	4
ci	20	0	1	0	12	0	12	8	6	3	1	0	2	2	2	7	0	0	4
%		0	5	0	60	0	60	40	30	15	5	0	10	10	10	35	0	0	20
slp2 detailed	20	0	4	16	0	8	16	2	13	8	8	0	0	0	0	1+8	2+10	2+10	6+7
slp2	20	0	4	16	0	8	16	2	13	8	8	0	0	0	0	9	12	12	13
%		0	20	80	0	40	80	10	65	40	40	0	0	0	0	45	60	60	65
ptx detailed	20	6	9	3+2	0	0	1	2	2	1	0	0	0	0	0	4	0	0	0
ptx	20	6	9	5	0	0	1	2	2	1	0	0	0	0	0	4	0	0	0
%		30	45	25	0	0	5	10	10	5	0	0	0	0	0	20	0	0	0
arx detailed	22	1	11	0	2	0	2	1+1	1	0	0	0	1+1	1+1	5+1+2	1+8	2	1+6	1+4
arx	22	1	11	0	2	0	2	2	1	0	0	0	2	2	8	9	2	7	5
%		4,55	50	0	9,091	0	9,091	9,091	4,545	0	0	0	9,091	9,091	36,364	40,909	9,091	31,82	22,73
irx aRNAi	18	14	15	6	0	0	6	1	1	1	0	0	0	1	0	2	0	1	0
%		77,8	83,3	33,33	0	0	33,33	5,556	5,556	5,56	0	0	0	5,556	0	11,111	0	5,556	0
DII detailed	24	1	0	0	4	0	0	0	0	0	0	0	2	2	2	0	0	0	0
DII	24	1	0	0	4	0	0	0	0	0	0	0	2	2	2	0	0	0	0
%		4,17	0	0	16,67	0	0	0	0	0	0	0	8,333	8,333	8,3333	0	0	0	0
six3 detailed	16	2	2	11+2	8+1	2+11	7+2	7	4+1	14	16	16	0	1	0	5	0	5	0
six3	16	2	2	13	9	13	9	7	5	14	16	16	0	1	0	5	0	5	0
%		12,5	12,5	81,25	56,25	81,25	56,25	43,75	31,25	87,5	100	100	0	6,25	0	31,25	0	31,25	0

 loss of bristle
 additional bristles
 misplaced bristles
 0%-14% = no phenotype
 15% - 24% = very likely a phenotype
 >25% = significant phenotype

Table S3: Quantification of synergy of *Tc-ey/pax6* and *Tc-toy/pax6*.

gene	n	bell row		vertex triplet							lr. quart.		gena triplet				maxilla escort			
		bells	bristle	vertex setae			vertex bristles				clypeus	labrum	post	dors	ant	bristle	ant	med	post	
				post	vent	ant	triplet	ant bas	median	ant										(post)
toy	12	10	12	4	5	0	12	11	3	0	8	0	0	1	2	1	10	0	10	0
%		83,3	100,0	33,3	41,7	0,0	100,0	91,7	25,0	0,0	66,7	0,0	0,0	8,3	16,7	8,3	83,3	0,0	83,3	0,0
ey	10	2	1	0	1	0	0	0	1	0	0	0	0	2	0	4	1	2	2	
%		20,0	10,0	0,0	10,0	0,0	0,0	0,0	10,0	0,0	0,0	0,0	0,0	20,0	0,0	40,0	10,0	20,0	20,0	
toy+ey	6	6	6	4	6	0	6	6	3	0	6	0	0	2	4	3	5	2	6	5
%		100,0	100,0	66,7	100,0	0,0	100,0	100,0	50,0	0,0	100,0	0,0	0,0	33,3	66,7	50,0	83,3	33,3	100,0	83,3
synergy*				2,0	1,9				1,4		1,5			4,0	1,8	6,0		3,3		4,2

* effect of double knockdown exceeds additive effect x-fold

Table S4: Quantification of bristle pattern defects of *Tc-axin* RNAi.

Gene	Beetles x2	bell row		vertex triplet							labrum quartet		gena triplet				maxilla escort			
		bells	bristle	vertex setae			vertex bristles				clypeus	labrum	post	dors	ant	bristle	ant	med	post	
				post	vent	ant	triplet	ant bas	median	ant										
axin detailed	16																			
axin	16	5	13	5	6	6	7	9	5	8	6	9	1	2	1	10	2	10	9	
%		31,25	81,25	31,25	37,5	37,5	43,75	56,25	31,25	50	37,5	56,25	6,25	12,5	6,25	62,5	12,5	62,5	56,25	

Table S5: Quantification of bristle pattern defects of *Tc-lab/Hox1* RNAi.

Gene	Beetles x2	bell row		vertex triplet							labrum quartet		gena triplet				maxilla escort			
		bells	bristle	vertex setae			vertex bristles				clypeus	labrum	post	dors	ant	bristle	ant	med	post	
				post	vent	ant	triplet	ant bas	median	ant										
lab	20	0	0	0	0	0	0	0	0	0	0	0	16	4	0	0	0	14	20	
%		0	0	0	0	0	0	0	0	0	0	0	80	20	0	0	0	70	100	

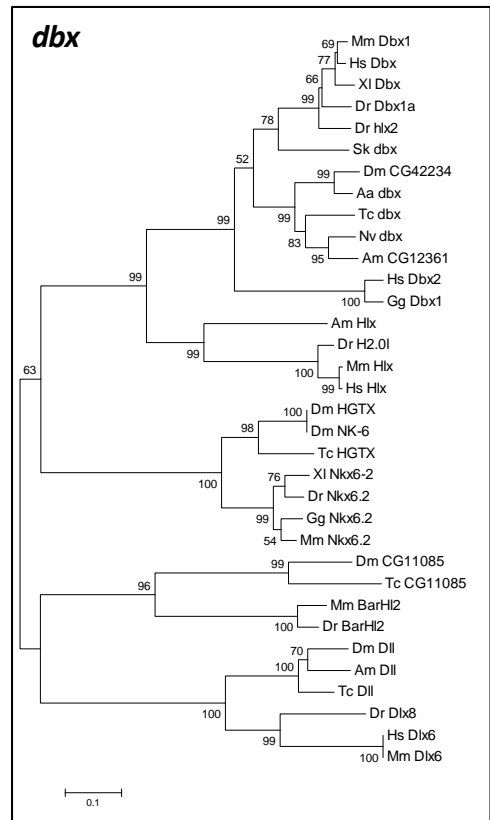
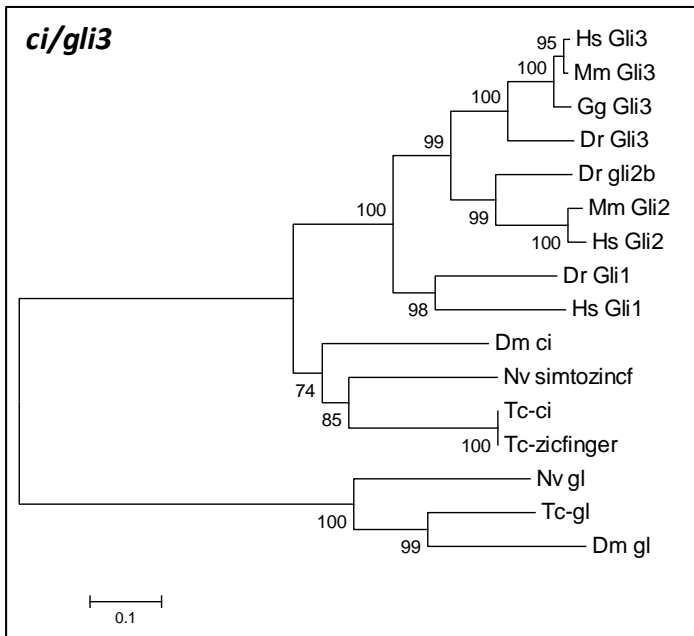
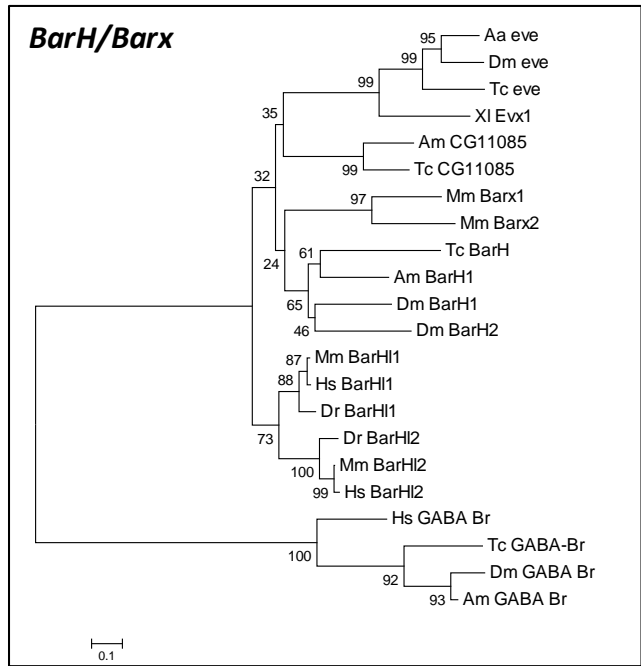
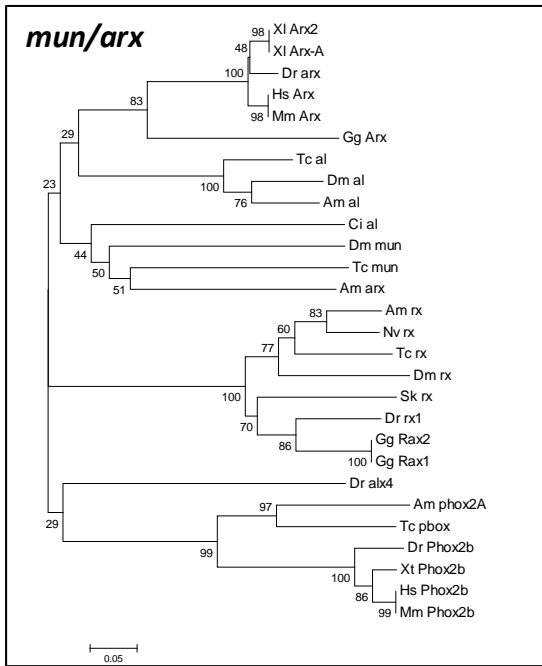
Table S6: Reference list for vertebrate gene expression patterns.

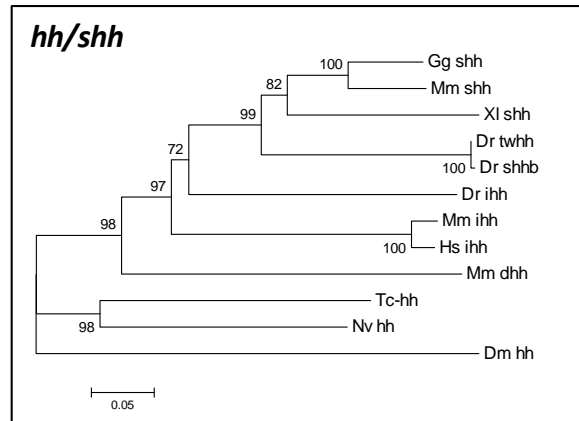
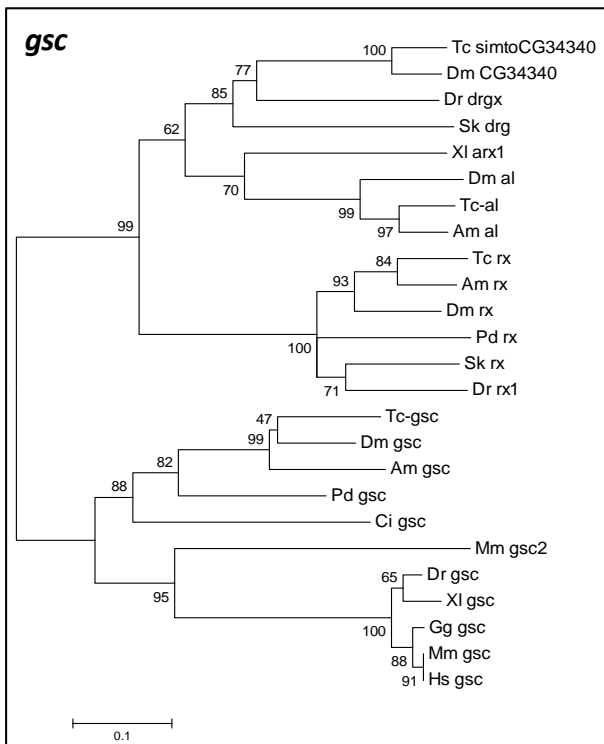
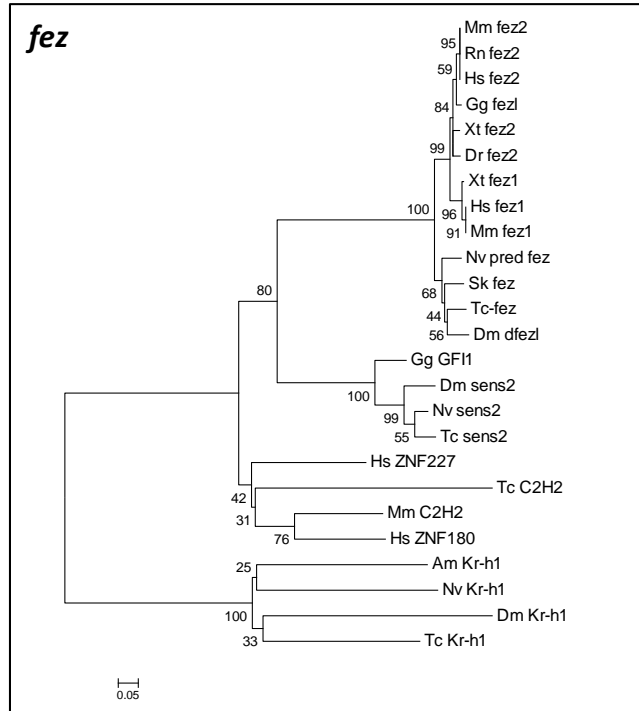
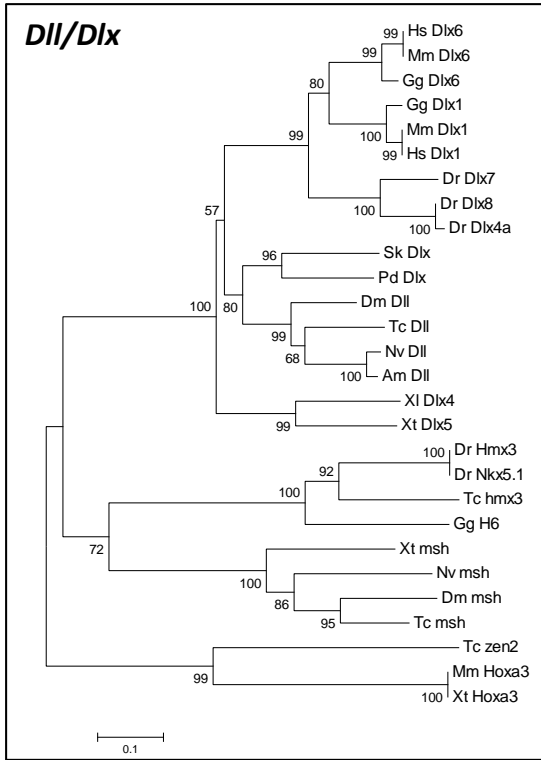
Gene	References
<i>Otx1/2</i>	(Boncinelli et al., 1993; Rubenstein et al., 1998; Rubenstein and Shimamura, 1997)
<i>Nkx 2.1</i>	(Rubenstein et al., 1998; Rubenstein and Shimamura, 1997)
<i>Emx1/2</i>	(Boncinelli et al., 1993; Rubenstein et al., 1998; Rubenstein and Shimamura, 1997)
<i>BF1</i>	(Hebert and Fishell, 2008; Rubenstein et al., 1998; Rubenstein and Shimamura, 1997)
<i>Pax6</i>	(Rubenstein and Shimamura, 1997; Scholpp et al., 2003; Shimamura and Rubenstein, 1997)
<i>gsc</i>	(Camus et al., 2000; Lemaire et al., 1997)
<i>FGF8</i>	(Rubenstein et al., 1998)
<i>Shh</i>	(Rubenstein et al., 1998)
<i>Wnt1</i>	(McMahon et al., 1992; Rubenstein et al., 1998)
<i>Gli3</i>	(Aoto et al., 2002; Hebert and Fishell, 2008)
<i>Six1</i>	(Schlosser, 2006; Schlosser and Ahrens, 2004)
<i>Six4</i>	(Schlosser, 2006; Schlosser and Ahrens, 2004)
<i>Eya</i>	(Schlosser, 2006; Schlosser and Ahrens, 2004)
<i>Dbx1/2</i>	(Fjose et al., 1994 for <i>hlx-1/dbx1a</i> , prechordal plate, mesoderm) (Gershon et al., 2000 for <i>Xdbx</i> , diencephalon) (Lu et al., 1992; Lu et al., 1994; Shoji et al., 1996 for late expression in the spinal chord)
<i>En2/3</i>	(Rowitch and McMahon, 1995; Scholpp et al., 2003)
<i>Rx1/2/3</i>	(Chuang et al., 1999; Mathers et al., 1997; Meijlink et al., 1999) (Deschet et al., 1999 late in diencephalon)
<i>Tlx</i>	(Arendt and Nubler-Jung, 1996; Hollemann et al., 1998; Kitambi and Hauptmann, 2007; Monaghan et al., 1995; Yu et al., 1994)

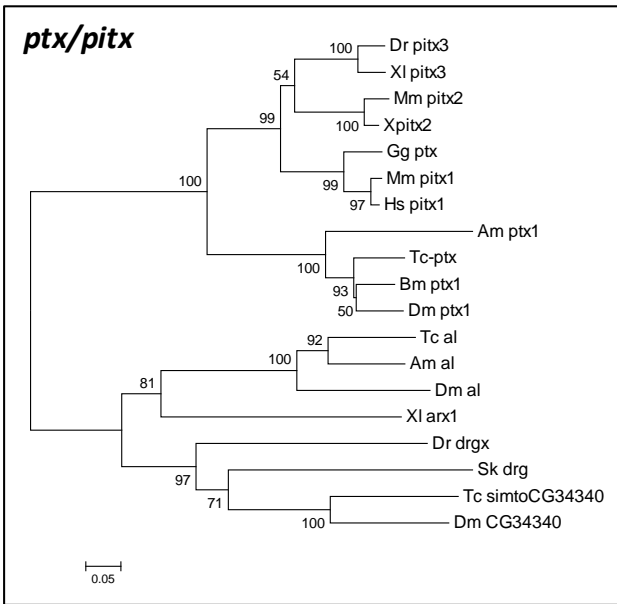
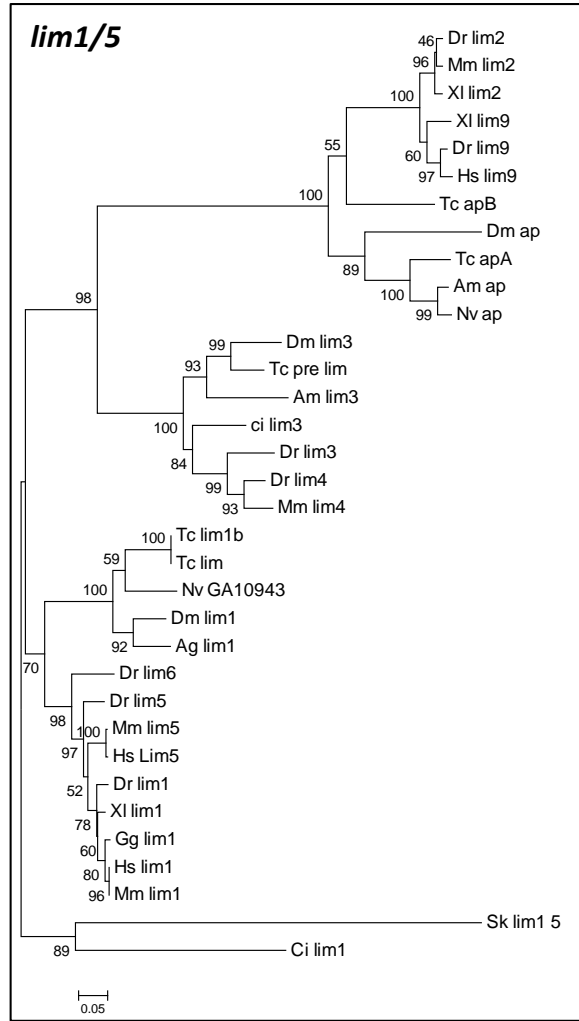
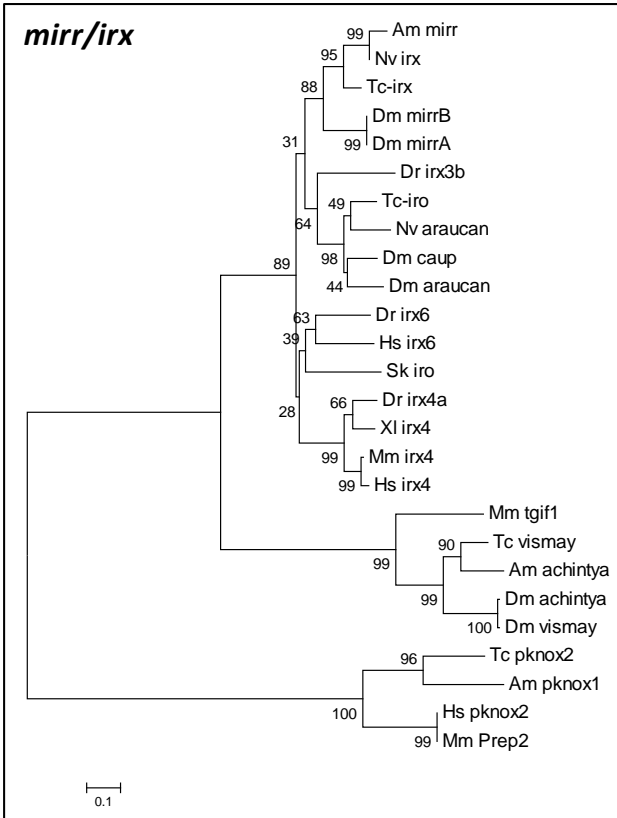
Appendix

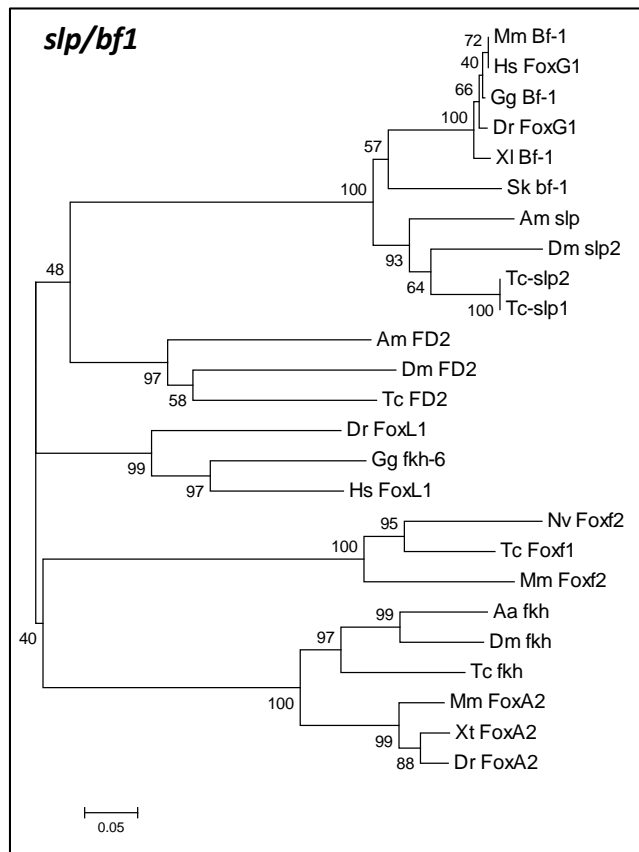
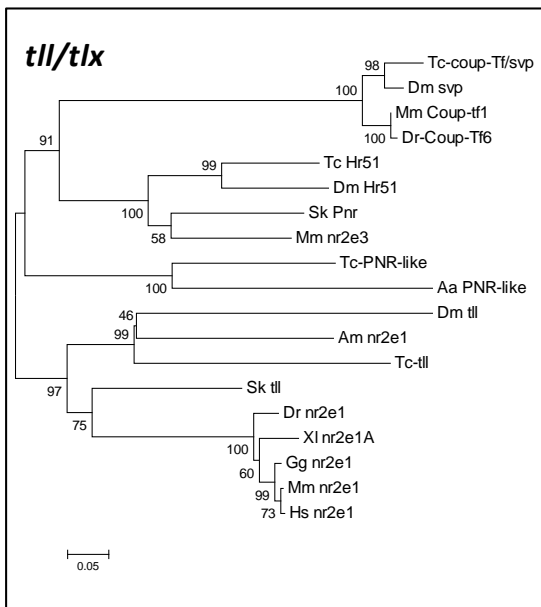
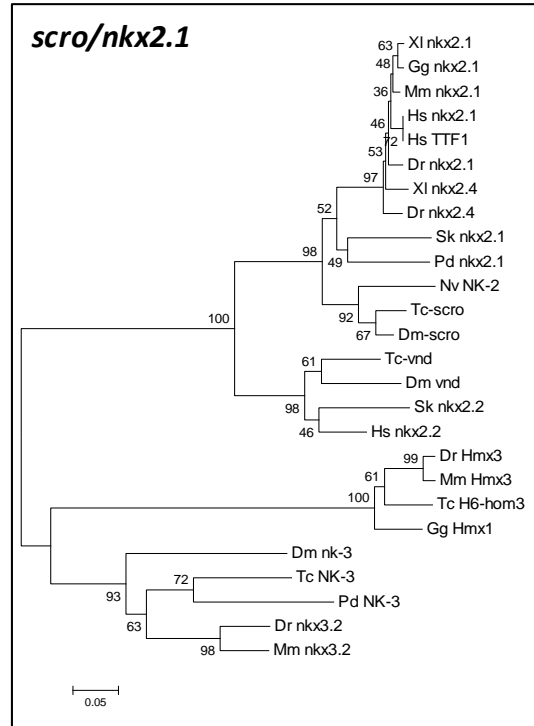
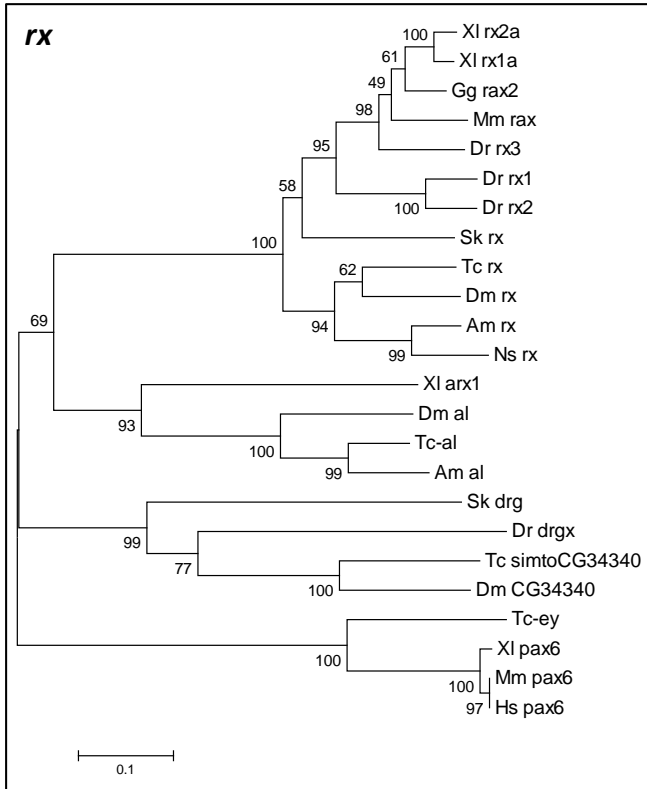
<i>Six3</i>	(Loosli et al., 1998; Oliver et al., 1995; Takahashi and Osumi, 2008)
<i>Dlx</i>	(Panganiban and Rubenstein, 2002) (Luo et al., 2001 for Dlx3, Dlx5, Dlx6) (Yang et al., 1998 for Dlx5)
<i>Irx2/3</i>	(Cavodeassi et al., 2001; Glavic et al., 2002; Gomez-Skarmeta et al., 1998; Takahashi and Osumi, 2008)
<i>Fez</i>	(Hashimoto et al., 2000; Hirata et al., 2006; Hirata et al., 2004; Jeong et al., 2007; Matsuo-Takasaki et al., 2000)
<i>Pitx</i>	(Dickinson and Sive, 2007; Dutta et al., 2005; Meijlink et al., 1999; Schweickert et al., 2001; Zilinski et al., 2005)
<i>Arx</i>	(Colombo et al., 2004; El-Hodiri et al., 2003; Friocourt et al., 2006; Seufert et al., 2005)
<i>Lhx5</i>	(Sheng et al., 1997)

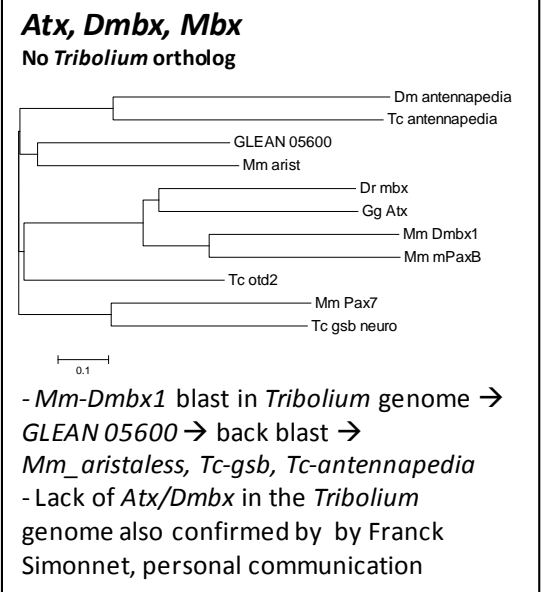
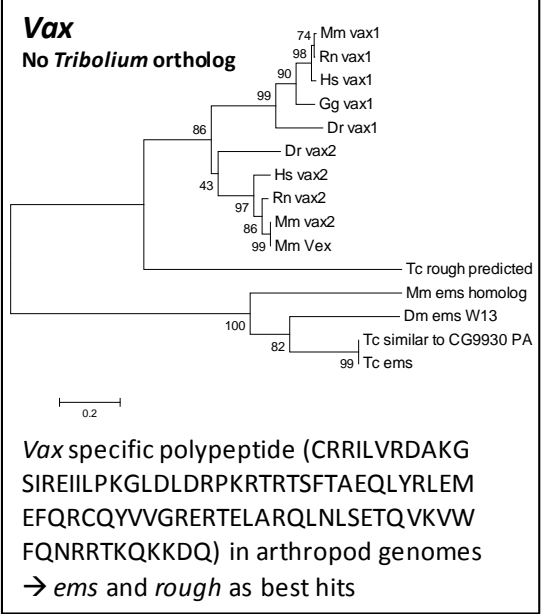
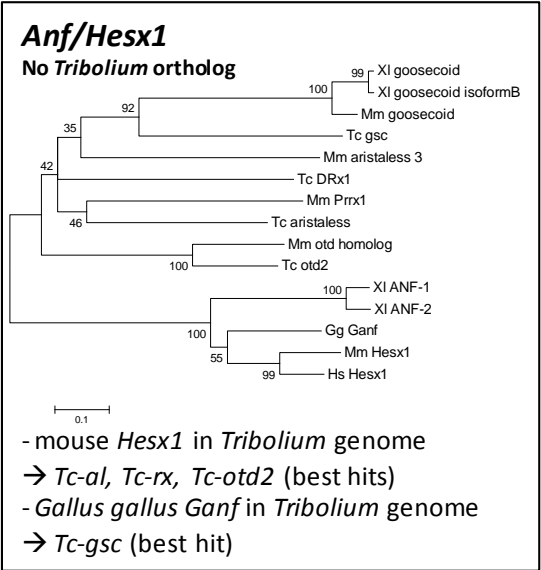
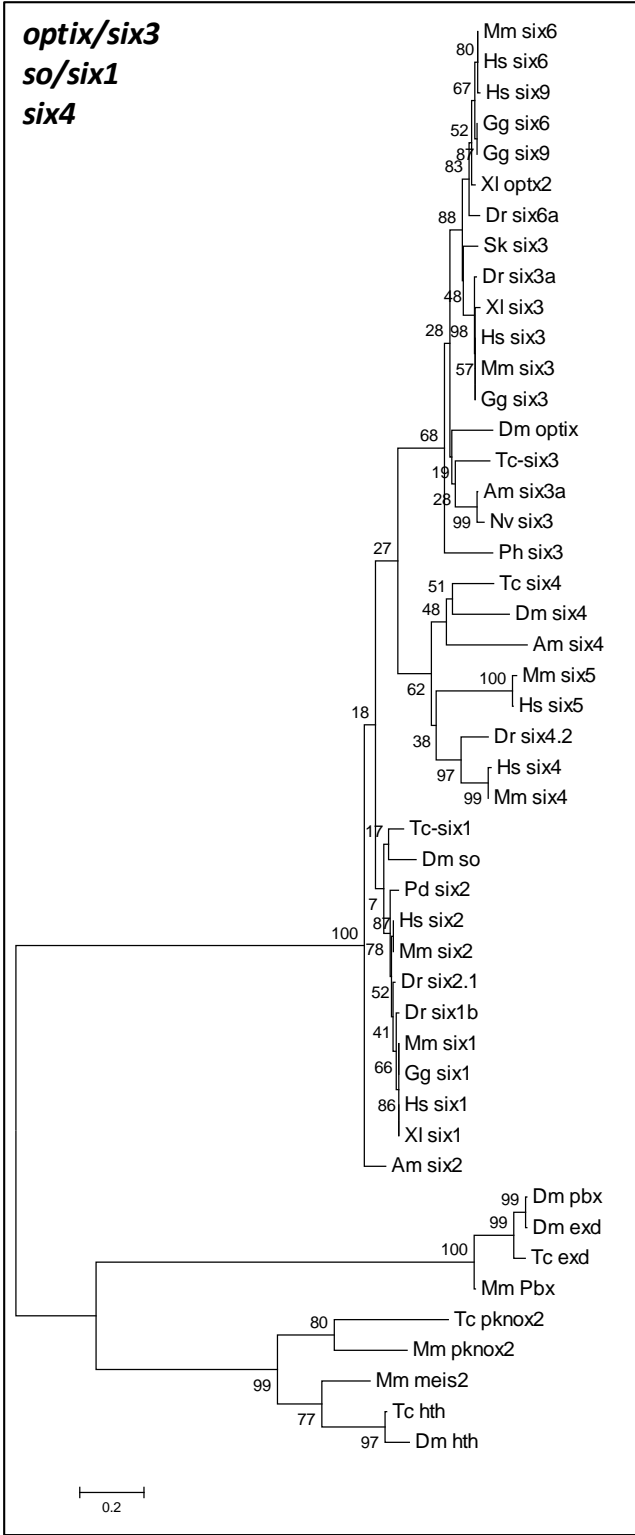
7.2 Supplementary Figures (phylogenetic trees).











7.3 Abbreviations

general:

aRNAi	adult RNAi
cDNA	complementary DNA
dsRNAi	double-stranded RNA
eRNAi	embryonic RNAi
mRNA	messenger RNA
pRNAi	pupal RNAi
RNAi	RNA interference
tGFP	turbo green fluorescent protein
WT	wild type

organisms:

<i>Aa</i>	<i>Aedes aegypti</i>
<i>Ag</i>	<i>Anopheles gambiae</i>
<i>Am</i>	<i>Apis mellifera</i>
<i>Bm</i>	<i>Bombyx mori</i>
<i>Ci</i>	<i>Ciona intestinalis</i>
<i>Dm</i>	<i>Drosophila melanogaster</i>
<i>Dr</i>	<i>Danio rerio</i>
<i>Gg</i>	<i>Gallus gallus</i>
<i>Hs</i>	<i>Homo sapiens</i>
<i>Mm</i>	<i>Mus musculus</i>
<i>Ns</i>	<i>Nasonia vitripennis</i>
<i>Pd</i>	<i>Platynereis dumerilii</i>
<i>Ph</i>	<i>Parhyale hawaiiensis</i>
<i>Rn</i>	<i>Rattus norvegicus</i>
<i>Sk</i>	<i>Saccoglossus kowalevskii</i>
<i>Tc</i>	<i>Tribolium castaneum</i>
<i>Xl</i>	<i>Xenopus laevis</i>
<i>Xt</i>	<i>Xenopus tropicalis</i>

8 Curriculum vitae

Personal Details

Name: Nico Posnien
Nationality: german
Date of birth: 01.10.1981
Place of birth: 37308 Heiligenstadt

Address of Current Place of Work

University: Georg-August-University Göttingen
Institute: Johann-Friedrich-Blumenbach-Institute of Zoology and Anthropology
Department: Dpt. for Developmental Biology
Supervisor: Prof. Dr. Gregor Bucher
Street: Justus-von-Liebig-Weg-11
Town: 37077 Göttingen
Country: Germany
Telephone: +49-551-3910124
E-mail for contact: Nico.Posnien@biologie.uni-goettingen.de

University studies

University: Georg-August-University Göttingen
Country: Germany
Subjects: Developmental Biology, Human Genetics, Zoology
From: 10/2001
To: 07/2006
Degree: Diploma
Thesis: "The *Tribolium castaneum* gene *Tc-optix/six3* and the evolution of the labrum"
Supervisor of the thesis: Prof. Dr. Gregor Bucher

PhD thesis

University: Georg-August-University Göttingen
Country: Germany
From: 07/2006
Thesis: „Function and Evolution of highly conserved head genes in the red flour beetle *Tribolium castaneum*”
Supervisor of the thesis: Prof. Dr. Gregor Bucher

Teaching experience

Teaching Assistant: EMBO/Zoonet Course “Molecular approaches to Evolution and Development”, 30 June - 12 July 2008 in Fiskebäckskil/Sweden

Publications (published & in prep)

Richards, S., R. A. Gibbs (including **Posnien, N.**), et al. (2008). "The genome of the model beetle and pest *Tribolium castaneum*." Nature 452(7190): 949-55.

Schinko, J.B., Kreuzer, N., Offen, N., **Posnien, N.**, Wimmer, E., Bucher, G. (2008) Diverged function of *Tribolium orthodenticle*, *empty-spiracles* and *buttonhead* in head patterning. Dev Biol 317, 600-613

Yang, X., Weber, M., Zarinkamar, N., **Posnien, N.**, Friedrich, F., Wigand, B., Beutel, R., Damen,

W. G., Bucher, G., Klingler, M. et al. (2009). Probing the *Drosophila* retinal determination gene network in *Tribolium* (II): the Pax6 genes *eyeless* and *twin of eyeless*. Dev Biol.

Posnien, N., Bashasab, F. and Bucher, G. (accepted for publication). The insect upper lip (labrum) is a non-segmental appendage-like structure.

Posnien, N., Schinko, J., Grossmann, D., Shippy, T. D., Konopova, B., Bucher, G. (accepted for publication). RNAi in the Red Flour Beetle (*Tribolium*). CSH Protocols, Cold Spring Harbor Laboratory Press

Posnien, N. and Bucher, G. (submitted). The *Hox1* ortholog *Tc-labial* is required for embryonic development of the intercalary segment giving rise to lateral parts of the head in *Tribolium*.

Patrick R. H. Steinmetz*, **Nico Posnien***, Rolf Urbach, Joakim Eriksson, Roman Kostyuchenko, Carlo Brena, Michael Akam, Gregor Bucher & Detlev Arendt (in preparation) „Evolution of the head in annelids and arthropods”

* equal contribution